EFFECTS OF ADAXIAL-ABAXIAL SIGNALLING ON LEAF POLARITY

by

Julia S. Nowak

M.Sc., University of Guelph, 2007

A THESIS SUBMITTED IN PARTIAL FULFILLMENT OF

THE REQUIREMENTS FOR THE DEGREE OF

DOCTOR OF PHILOSOPHY

in

THE FACULTY OF GRADUATE STUDIES

(Botany)

THE UNIVERSITY OF BRITISH COLUMBIA

(Vancouver)

August 2012

Abstract

The unifying theme of this thesis is adaxial-abaxial or dorsiventral patterning in leaves. The adaxial-abaxial axis sets the thickness of a leaf and without the appropriate juxtaposition of the adaxial and abaxial domains, radialized leaves develop. The underlying genetic mechanisms of the development of these polarity defects started to be elucidated only over the past 20 years in the model *Arabidopsis*, in particular. I investigated this patterning in a variety of non-model species. Firstly, I investigated the variability of dorsiventral polarity in plants with naturally occurring radialized leaves including *Allium, Nepenthes,* Krishna fig, *Pelargonium*, several Cactaceae species, and *popREVOLUTA* mutant of a poplar hybrid. Subsequent chapters aimed to incorporate morphology and anatomy with molecular genetics in order to elucidate the underlying basis of the phenotype of interest in species that have not been used as model systems for leaf development, including canola and poplar. A novel mutant (*lamina epiphylla, lip*) was identified in canola, which has adaxialized leaves and leaf-derived organs. Some of the *HD-ZIPIII* candidate genes were sequenced in canola, but I was unable to determine the location of the *LIP* mutation. The rest of this thesis focuses on the abaxial greening and unifacial petiole phenotypes seen in some species of poplar that have isobilateral leaves (others in the genus have bifacial leaves). *YABBY, KANADI*, and *HD-ZIPIII* genes are some of the major contributors to setting proper adaxial-abaxial polarity and I investigated the relationships of these genes by identifying the orthologs in *Arabidopsis*, poplar, and eucalyptus (a genus that shares the abaxial greening phenotype with poplar). Further, I studied the species relationships within the genus *Populus* in order to establish the ancestral state of leaf type. I determined that bifacial leaves are likely derived within the

genus. Finally, two poplar species (black cottonwood with bifacial leaves and hybrid aspen with isobilateral leaves) were compared on the basis of morphology, anatomy, and molecular genetics in order to determine the underlying basis of the abaxial greening and unifacial petiole phenotypes in hybrid aspen. I identified a subset of genes that may be involved in determining these phenotypes, but further investigation is needed.

Preface

Dr. Quentin Cronk collected all of the material presented in Chapter 1, except poplar. The *popREVOLUTA* mutant and wild type plants were kindly provided by Dr. Andrew Groover (UC Davis). I performed all of the analyses presented in this chapter.

Work presented in Chapter 2 was done in collaboration with Dr. Erin Gilchrist, Dr. George Haughn (UBC Botany), and Dr. Isobel Parkin (Agriculture and Agri-Food Canada; AAFC). Dr. Gilchrist did the mutagenesis screen, discovered the mutant, and determined the segregation pattern of the mutation. I planted and grew the plants used in this study and also did all of the morphological and anatomical analyses. Dr. Gilchrist designed the primers and analyzed the sequences. I did the molecular work, including DNA extraction and PCR. Dr. Parkin provided *Brassica rapa* and *Brassica oleracea* sequences that I used in further phylogenetic analysis. Saemundur Sveinsson determined the best model for the phylogenetic analysis. This study was, in part, supported by Genome Canada/Genome Alberta funding to Dr. Haughn. A version of this chapter has been submitted for publication.

Work in Chapter 3 was done in collaboration with Dr. Armando Geraldes, Saemundur Sveinsson, Dr. Carl Douglas, Dr. Shawn Mansfield (UBC Botany), Dr. Charles Hefer (University of Pretoria/UBC Botany), and Dr. Zander Myburg (University of Pretoria). I analyzed the transcriptome data as I received it (as RPKM or FPKM expression) from Dr. Geraldes and Dr. Hefer, who were involved in mapping and annotating the original transcriptome data. I aligned the sequences with MUSCLE and manually. S. Sveinsson ran

SATé and some phylogenetic analyses on the sequences that I obtained from Phytozome. I ran ML and MP analyses on the alignments. Poplar and eucalyptus transcriptome results were generated and funded through Dr. Douglas and Dr. Mansfield labs and Dr. Myburg lab, respectively.

Work in Chapter 4 was done in collaboration with Dr. Athena McKown and Dr. Rob Guy (UBC Forestry). Other students in Dr. Cronk's lab collected some of the poplar leaf material used here. I collected the remaining material for DNA extraction and anatomical analysis. I extracted some DNA along with Linda Quamme (UBC Forestry) and Dr. Nyssa Temmel (UBC Botany). Some plant material and photos for Figure 4.8 were provided by Carole Ann Lacroix (University of Guelph), Linda Jennings (UBC Herbarium), Tom Wendt (University of Texas at Austin), and Jim Solomon (Missouri Botanical Garden Herbarium). Dr. Geraldes and Dr. Raju Soolanayakanahally provided some primers for this study. I performed all of the work including PCR, sequence analysis, and all of the phylogenetic analysis. Dr. Guy provided part of the funding for this project and Dr. McKown provided helpful discussions.

Transcriptome results presented in Chapter 5 were provided by Dr. Geraldes, from the project done in collaboration with Dr. Carl Douglas and Dr. Shawn Mansfield. I analyzed the transcriptome data provided, as in Chapter 3. I performed all of the analyses presented in this chapter, including RNA and DNA extractions, RT-PCR, and qRT-PCR.

Table of Contents

List of Tables

List of Figures

List of Abbreviations

AE7 – ASYMMETRIC LEAVES ENHANCER 7

AFO – ABNORMAL FLOWER ORGAN

AGO – ARGONAUTE

AS1/AS2 – ASYMMERTIC LEAVES 1/2

ATHB8 – ARABIDOPSIS THALIANA HOMEOBOX 8

ATS – ABERRANT TESTA SHAPE

Cad – cinnamyl-alcohol dehydrogenase

CNA – CORONA

CRC – CRABS CLAW

DCL4 – DICER-LIKE 4

Eg – *Eucalyptus grandis*

EMS – ethylmethane sulphonate

ETT/ARF4 – ETTIN/AUXIN RESPONSE FACTOR 4

FAA – formalin acetic acid alcohol

FPKM – fragments per kilobase of exon model per million mapped fragments

Gly – glycoside hydrolase family 19 protein

GOF – gain-of-function mutation

HD-ZIPIII – HOMEODOMAIN LEUCINE ZIPPER class III

INO – INNER NO OUTER

ITS – internal transcribed spacer

KAN – KANADI

KNOX – KNOTTED-LIKE HOMEOBOX

LIP – LAMINA EPIPHYLLA

LOF – loss-of-function mutation

LRW – LR White

Mip – major intrinsic protein

miRNA – micro RNA

ML – maximum likelihood

MP – maximum parsimony

Pcs – phytochelatin synthetase-like protein

PGY3 – PIGGYBACK 3

PHAN – PHANTASTICA

PHB – PHABULOSA

PHV – PHAVOLUTA

PRE – popREVOLUTA mutant

Pt – *Populus trichocarpa*

qRT-PCR – quantitative reverse transcriptase polymerase chain reaction

RDR6 – RNA-DEPENDENT RNA POLYMERASE 6

REV – REVOLUTA

RPKM – reads per kilobase of exon model per million mapped reads

RT-PCR – reverse transcriptase polymerase chain reaction

Sad – S-adenosyl-L-homocysteine hydrolase

SAM – shoot apical meristem

Sect. – section

SGS3 – SUPRESSOR OF SILENCING 3

SPL – SQUAMOSA PROTEIN BINDING-LIKE

tasi-RNA – trans-acting small interfering RNA

YAB – YABBY

ZPR – LITTLE ZIPPER

Acknowledgements

I would like to first thank my supervisor, Dr. Quentin Cronk, for his guidance and support during my Ph.D. I am grateful for having the opportunity to work in his lab and to learn molecular methods, while incorporating my interest in morphology and anatomy into my work. I also thank my co-supervisor, Dr. Sean Graham, my committee member, Dr. Keith Adams, for their support and guidance throughout my graduate studies, the exam committee: Dr. Sean Graham, Dr. Xin Li (UBC Botany), Dr. Patricia Schulte (UBC Zoology), Dr. Rodger Evans (Acadia University) for their time and helpful suggestions, and Dr. Sally Aitken (UBC Forestry) for chairing. I thank Natural Sciences and Engineering Research Council of Canada for funding me for three years during my Ph.D.

There are many others who have helped me with my Ph.D. progress. I would like to thank Dr. Armando Geraldes, Dr. Athena McKown, Saemundur Sveinsson, Dr. Erin Gilchrist, Dr. Charles Hefer, Dr. Isidro Ojeda, and Dorothy Cheung, who have all contributed to my work presented in this thesis. And I would also like to thank Linda Jennings and Amber Saundry (UBC Herbarium) for the microscope use and help, Garnet Martens (UBC BioImaging Facility) for the microtome use, and David Kaplan (UBC) for greenhouse use. Also, the all of the staff, faculty, and graduate students made the Botany Department a fantastic place to work.

I am thankful to my parents for inspiring me to go to graduate school. And finally, I am very grateful to my husband, Adam, and my two boys for their support and always reminding me to enjoy life!

Chapter 1: Adaxial-abaxial polarity in leaves: integration of genetics and morphology

1.1 Synopsis

This introductory chapter aims to incorporate the current molecular genetic knowledge of dorsiventral leaf polarity patterning with previous morphological studies on species that show either adaxialized or abaxialized leaf phenotypes. As most of our current understanding regarding adaxial-abaxial patterning comes from experiments in the model plant *Arabidopsis*, it is not clear whether these results can be generalized to other non-model systems found in nature. Here, I discuss the differences in anatomy of previously described mutants of *Arabidopsis* with affected dorsiventral leaf polarity and show that species with such variations found in nature are much more complex due basic anatomical differences compared to *Arabidopsis* (e.g., vascular patterning). Hypotheses, as to which genes may be involved in generating such phenotypes as abaxialization or adaxialization of leaves, are also discussed.

1.2 Introduction

The diversity of leaf shapes and sizes among angiosperms is great, but a typical angiosperm leaf is flat with identifiable top and bottom sides. The top or adaxial side functions in light capture, while the bottom or abaxial side generally acts in gas exchange. The evolution of this megaphyll flat lamina from a photosynthetic stem has occurred on several occasions within the euphyllophytes (e.g., ferns, gymnosperms, and angiosperms) (Tomescu 2009) and has been a long-standing topic of interest in plant biology (e.g., Floyd

and Bowman 2010), but the relatively recent elucidation of gene networks in leaf development (e.g., Waites and Hudson 1995) has been a major contributor to getting us closer to answering the question of how this structure has evolved.

1.2.1 Leaf initiation

The vegetative shoot apical meristem (SAM) is an indeterminate structure, reflecting continual formation of stem cells, the production of which is controlled by the *WUSCHEL* and *CLAVATA* (*WUS/CLV*) negative feedback loop (Schoof et al. 2000). *KNOTTED-LIKE HOMEOBOX* (*KNOX*) genes (*SHOOTMERISTEMLESS* or *STM* in *Arabidopsis*) maintain indeterminacy in the meristem, and the absence of *KNOX* expression marks the sites of initiation of leaf primordia in lateral positions (Long et al. 1996, Sinha 1999, Hake and Ori 2002, Hake et al. 2004, Hay and Tsiantis 2010).

A leaf is defined as a determinate structure that develops on the flanks of the SAM generally having three axes of polarity (all relative to SAM): proximodistal, dorsiventral or adaxial-abaxial, and mediolateral (Kaplan 1997, Cronk 2009). The proximodistal axis sets the length of the leaf, with the proximal side closer to the SAM, while the distal side is further away, at the tip of the leaf. The dorsiventral or adaxial-abaxial axis sets the thickness of a leaf, with the adaxial side closer to the SAM, and the abaxial side away from the shoot axis. Finally, the mediolateral axis sets the width of the leaf, and its growth is considered to be dependent on the juxtaposition of the adaxial and the abaxial leaf surfaces (Waites and Hudson 1995, Kidner and Timmermans 2010).

Incision experiments were performed by Sussex (1951, 1954), in which the side proximal to the SAM (adaxial side) was separated from the meristem. The primordium

development was not arrested, but mostly radial abaxialized leaves developed, completely lacking the adaxial surface. Some variability among leaves was observed, with some forming a distal blade portion with adaxial and abaxial surfaces. Fifty years later, Reinhardt et al. (2005) repeated a similar experiment using laser ablation and microdissection experiments, with similar results. Their contribution showed that only the single outermost layer (L1) of the meristem needs to be disrupted, at the region of primordium development, in order for the lamina not to develop and for no blade outgrowth to occur.

Subsequent studies important to dorsiventral polarity were done using *Antirrhinum majus* (referred to as *Antirrhinum* below) (Waites and Hudson 1995, Waites et al. 1998). Waites and colleagues discovered the *phantastica* (*phan*) mutant, which developed radial or abaxialized leaves in extreme cases, or leaves with ectopic outgrowths of abaxial tissues on the adaxial side of the blade. The *Arabidopsis* and maize orthologs of this locus (*ASYMMETRIC LEAVES1* and *ROUGH SHEATH2*, respectively) do not show dorsiventral polarity defects (Byrne et al. 2000, Hay and Tsiantis 2010), but the phenomenon of *KNOX* repression and therefore the promotion of a determinant state or the development of a primordium is conserved across seed plants (Ori et al. 2000, Kidner and Timmermans 2010).

These sets of discoveries and experiments were significant for understanding adaxial-abaxial polarity development. A resulting discovery is the "Sussex" signal, which is necessary for proper dorsiventral development. Without this sustained signal from the meristem, the adaxial surface is unable to develop, and therefore radialized or abaxialized organs form. The abaxial cell fate therefore can be considered as the "default state" (e.g., Townsley and Sinha 2012). Since the resulting organs will be radial, the lack of juxtaposition of adaxial and abaxial surfaces will prevent blade outgrowth, in most cases.

1.2.2 Acquisition of the adaxial-abaxial cell fate

The dorsiventral axis distinguishes the ancestral stem system from the derived lamina structure of a leaf (Cronk 2009). Since 1995, when Waites and Hudson first published their work on the *phantastica* mutant in *Antirrhinum*, there was a surge of research done on the developmental pathways involved in adaxial-abaxial polarity determination in leaves, and on the elucidation of the underlying gene networks. The accurate development of the adaxial-abaxial axis is determined by the mutually antagonistic action of an array of transcription factors and corresponding small RNA molecules (Figure 1.1). The three major groups of genes and regulators contributing to the dorsiventral development in leaves include: 1) AS1/AS2–KANADI, 2) HD-ZIPIII–miR165/166, and 3) ETT/ARF4–tasiR-ARF (e.g., Chitwood et al. 2007, Husbands et al. 2009, Kidner and Timmermans 2010).

1.2.3 AS/KANADI complex

The genes in the AS1/AS2–KANADI pathway are *ASYMMETRIC LEAVES1* and *2* (*AS1/AS2*) and genes belonging to the *KANADI* family (*KAN* or *KAN1*, *KAN2*, *KAN3*, and *KAN4* or *ABERRANT TESTA SHAPE* or *ATS*). The interaction of these genes is conserved in vascular plants (Kidner and Timmermans 2010). *AS1* is expressed throughout the leaf, while *AS2* is restricted by *KANADI* genes to the adaxial domain. *KANADI* gene expression is constrained to the abaxial domain and associated phloem tissues (Eshed et al. 2001, Kerstetter et al. 2001), complementary to *HD-ZIPIII* expression.

In *Arabidopsis*, single gene *KANADI* mutations produce only mild polarity defects such as the upward curling of leaves and the production of abaxial trichomes (Eshed et al.

2001, Kerstetter et al. 2001) Multiple loss-of-function (LOF) mutations (e.g., *kan1 kan2 kan3*) in *KANADI* genes produce an enlarged meristem and adaxialized leaves (Eshed et al. 2004). Izhaki and Bowman (2007) showed that *kan1 kan2 kan4* triple mutants produce ectopic adaxialized leaves from the hypocotyl in association with *PIN1*-mediated auxin maxima, necessary for primordia initiation (Szakonyi et al. 2010). This is in contrast to gain-of-function (GOF) mutants, which show a lack of meristem and produce narrow abaxialized cotyledons (Eshed et al. 2001). While the GOF mutations in *AS2* produce similar phenotypes to *kan1* LOF mutations, with the production of adaxial lamina outgrowths on the abaxial side (Lin et al. 2003), LOF mutations in *AS1* do not produce visible polarity defects (Byrne et al. 2000).

1.2.4 HD-ZIPIII/miRNA complex

Within the HD-ZIPIII/miRNA complex, found in land plants, the major contributors to the pathways are *class III homeodomain leucine zipper* (*HD-ZIPIII*) genes and interacting microRNAs (miR165/166) (Townsley and Sinha 2012). *HD-ZIPIII* gene family consists of five members, including *PHABULOSA* (*PHB*), *PHAVOLUTA* (*PHV*), *REVOLUTA* (*REV*), *ARABIDOPSIS THALIANA HOMEOBOX 8* (*ATHB8*), and *CORONA* (*CNA*). Complementary to *KANADI* expression, *HD-ZIPIII* genes are highly expressed in xylem and are restricted to the leaf adaxial domain (Baima et al. 1995, Zhong and Ye 1999, Otsuga et al. 2001, Prigge et al. 2005) via the miRNA165/166-mediated pathway in the abaxial domain. *LITTLE ZIPPER* (*ZPR1-4*) genes also directly restrict *HD-ZIPIII* expression via a negative feedback loop. An indirect interaction between *HD-ZIPIII* and *KANADI* genes allows the limitation of each gene family to the appropriate domain.

Most single gene mutations in most *HD-ZIPIII* genes do not result in significant polarity defects, apart from *rev* mutants that have defects in lateral meristem function (Talbert et al. 1995, Zhong and Ye 1999, Otsuga et al. 2001, Emery et al. 2003, Prigge et al. 2005; see Chapter 2 for a more detailed discussion). In *Arabidopsis*, *phb phv rev* triple mutants produce a single abaxialized cotyledon and therefore experience complete loss of the adaxial or central domain (Emery et al. 2003, Prigge et al. 2005). Alternatively, GOF mutations, for example in *PHB* (or *PHV* or *REV* or *CNA*), produce an enlarged SAM and adaxialized leaves (McConnell and Barton 1998, Zhong and Ye 1999, McConnell et al. 2001, Emery et al. 2003, Ochando et al. 2006). Overall, LOF mutations in *HD-ZIPIII* genes show a similar phenotype to *KANADI* GOF mutations, while *HD-ZIPIII* GOF mutations have a similar phenotype to *KANADI* LOF mutations.

1.2.5 ARF/ta-siRNA complex

The third pathway within the dorsiventral polarity network, which is highly conserved in land plants, includes *ETTIN* (*AUXIN RESPONSE FACTOR3* or *ARF3*) and *ARF4* genes and the corresponding trans-acting small interfering RNAs (tasiR-ARF) (Kidner and Timmermans 2010). The initial upregulation of *ETT/ARF4* is initiated with auxin (Pekker et al. 2005). These genes are restricted to the abaxial domain by the related tasiR-ARF siRNAs, which form a concentration gradient across the dorsiventral axis of the leaf, with highest expression in the adaxial domain and declining expression towards the abaxial-most side (Townsley and Sinha 2012). The boundary between adaxial and abaxial identity is therefore attained when the concentration of tasiR-ARF is not high enough to suppress *ETT/ARF4* expression (Pekker et al. 2005). The tasiR-ARFs in the miR390/*TAS3* pathway are derived

from non-coding *TAS3*, from miR390, via *ARGONAUTE7* (*AGO7*) gene action (Hunter et al. 2003, 2006, Adenot et al. 2006, Fahlgren et al. 2006). Further processing of tasiR-ARFs occurs through a set of genes, including *SUPRESSOR OF GENE SILENCING3* (*SGS3*), *RNA-DEPENDENT RNA POLYMERASE6* (*RDR6*), and *DICER-LIKE4* (*DCL4*) (Allen et al. 2005, Yoshikawa et al. 2005). tasiR-ARFs also indirectly restrict miR165/166 expression in the adaxial domain.

In a similar manner to genes involved in the other complexes within the network, single *arf* LOF mutants do not have an obvious effect on leaf polarity. LOF *arf3 arf4* double mutants, on the other hand, cause abaxialization of leaves (Pekker et al. 2005). The GOF mutation in *ARF3* accelerates vegetative phase change transition, contributing to the development of morphologically adult leaves.

1.2.6 *YABBY* gene family

Until recently, *YABBY* genes have been thought of as major contributors to abaxial cell fate in eudicotyledonous angiosperms (Sawa et al. 1999, Seigfried et al. 1999, Bowman 2000, Eshed et al. 2004, Sarojam et al. 2010), along with *KANADI* genes. Recent literature (e.g., Kidner and Timmermans 2011, Townsley and Sinha 2012) has de-emphasized the importance of *YABBY* genes suggesting that they primarily contribute to mediolateral outgrowth of the blade in the presence of properly juxtaposed adaxial and abaxial domains.

Although not a major contributor to dorsiventral polarity signalling network, the *YABBY* gene family has important effects in setting adaxial-abaxial polarity in leaves. This gene family, thought to be unique to seed plants, has been implicated in the evolution of the seed plant lamina (Floyd and Bowman 2007, 2010), although a recent discovery of a *YABBY*

gene in *Micromonas*, which requires further investigation, may invalidate this hypothesis (Worden et al. 2009, Townsley and Sinha 2012).

The *YABBY* gene family consists of six members, including *ABNORMAL FLOWER ORGAN* (*AFO*) or *FILAMENTOUS FLOWER* (*FIL*), *YAB2*, *YAB3*, *INO*, *YAB5*, and *CRABS CLAW* (*CRC*). *YABBY* expression is restricted to the abaxial domain in eudicots, such as *Arabidopsis* and *Tropaeolum majus* (Sawa et al. 1999, Seigfried et al. 1999, Gleissberg et al. 2005). This is contrary to what is seen in monocots (e.g., maize and rice) and basal angiosperms (e.g., *Amborella*), where *YABBY* gene expression is limited to the adaxial domain (Juarez et al. 2004, Townsley and Sinha 2012). The evolution of different functions or the lack of conservation of function and expression in different groups of plants is reflected in a reduced emphasis on the importance of *YABBY* genes in overall adaxial-abaxial polarity establishment, in the recent literature.

Generally, a reduction in *YABBY* expression leads to a reduction in lamina development (Floyd and Bowman 2010). Single or double *YABBY* mutants in *Arabidopsis* do not show strong phenotypes, as *fil yab3* mutants show only a reduction in the lamina (Siegfried et al. 1999, Golz et al. 2004). This *fil yab3* phenotype is the same as that observed in the *gram* (*GRAMINIFOLIA*; *AFO* or *FIL* ortholog) mutant of *Antirrhinum*. The LOF *gram prolongata* mutation produces plants with leaves that virtually lack lamina development (Floyd and Bowman 2010). GOF mutations in *YABBY* genes cause the abaxialization of leaves (Chitwood et al. 2007).

1.2.7 Examples of polarity related leaf variation in nature

There is a large amount of leaf variation among angiosperms, including filamentous or radialized leaves (e.g., Cactaceae), pitcher-shaped leaves (e.g., *Nepenthes* spp.), trumpet-shaped leaves (e.g., *Ficus benghalensis* var. *krishnae*), and peltate leaves (e.g., *Tropaeolum majus*), all of which have morphological similarities to the described dorsiventral polarity mutants seen in model systems such as *Arabidopsis* or *Antirrhinum*. Here, I used anatomical analyses to survey the extent of similarities of several non-model plant species that have been previously described as containing abaxialized or adaxialized leaves or leaf parts, solely based on morphological or anatomical evidence.

The objective here is to determine whether the conceptual models about leaf dorsiventral polarity variation, derived from the genes and mutants described above, can be related to the plant biodiversity found in nature.

1.3 Materials and methods

1.3.1 Plant material

Several plant species were chosen for anatomical analysis based on previous descriptions regarding unifaciality of the leaf or leaf-derived organ. Abaxialized-leaved species that were studied included *Allium cepa* and *Nepenthes ventricosa* (Arber 1918, 1941, Traub 1968, Kaplan 1997), while the species that contained possibly adaxialized leaves included *Ficus benghalensis* var. *krishnae* (De Candolle 1897, 1901, 1902, Prain 1906, Biswas 1932, 1935, Puri 1946)*, Pelargonium* x *hortorum* (with adaxialized and dorsiventrally flat bracts) (Dupuy and Guédès 1979), *Maihuenia poeppigii*, and *Opuntia* sp. (the latter two belonging to the Cactaceae) (Bailey 1967, Mauseth 2007, Ogburn and

Edwards 2009). Two Cactaceae species that contain dorsiventrally flat leaves, *Pereskia grandiflora* and *Pereskia aculeata*, were also analyzed for comparison. Finally, leaves of *popREVOLUTA* (*PRE*) mutant (and *Populus tremula* x *alba* hybrid, clone INRA 717-IB4, wild type plants) were analyzed, as previous work on this mutant was only done on stem tissues (Robischon et al. 2011).

1.3.2 Sample preparation

Whole plant photographs were taken to document the morphological features of leaves or leaf-derived organs. Whole leaves/bracts or leaf pieces, cut from the centre of leaf blade or midpoint of the petiole, were fixed in 70% formalin acetic acid alcohol (FAA) for resin embedding. Following a graded dehydration series, tissues were embedded into LR White Resin according to methods previously described by Nowak et al. (2007). The embedded tissues were sectioned with glass knives using an OmU3 C Reichert microtome (Reichert, Vienna) and the resulting approximately 6 µm-thick sections were mounted onto SuperFrost slides (Fisher Scientific), stained with 0.05% aq Toluidine Blue O, and further mounted with Permount. The slides were photographed using a Nikon Eclipse 80i microscope with a DS-Ri1 digital camera (Nikon Corp.; UBC Herbarium).

1.4 Results

1.4.1 Allium

The green onion (*Allium cepa*) leaf is awl-shaped and, in transection, the leaf tissue is in the shape of a ring (Figure 1.2A). The vascular bundles, found throughout the

circumference of the leaf, are arranged in a collateral pattern where the phloem is towards the outside of the leaf and xylem towards the inside (Figure 1.2B).

1.4.2 Nepenthes

Nepenthes ventricosa leaf consists of a proximal dorsiventrally flat petiole, a radial petiole, and a distal pitcher-shaped blade (Figure 1.2C). The flat petiole portion exhibits conventional dorsiventral polarity where the top surface of the petiole contains a double layer of palisade mesophyll cells, while the bottom surface consists of compact spongy mesophyll cells (Figure 1.2D). The vascular bundles also exhibit adaxial-abaxial polarity where the xylem is towards the top and phloem towards the bottom of the petiole, in cross-section.

Unlike the flat petiole, the radial petiole is round in transverse section with a ring of sclerified tissue or fibres (Figure 1.2E). The vascular bundles are embedded in the fibres within the petiole. The radial petiole cross-section typically contains several larger vascular bundles that have an amphicribral-like arrangement (Figure 1.2F). A single large bundle is positioned along the adaxial-abaxial axis with the xylem at the centre of the bundle with phloem capping the xylem on either side in a bicollateral arrangement (Figure 1.2E). The remaining large bundles have the same xylem-phloem arrangement, but are positioned laterally, along the circumference of the petiole. There are also several smaller bundles located within the radial petiole, not capped with phloem on either side of the xylem, but which instead contain a collateral arrangement. These smaller bundles either have an arrangement where the phloem is towards the outside and xylem is towards the inside of the petiole or are positioned laterally around the circumference of the petiole.

1.4.3 Ficus

The wild type Banyan tree (*Ficus benghalensis*) leaves have a typical bifacial morphology where the adaxial leaf surface on the top is shiny and the bottom or abaxial surface is dull (Figure 1.3A). In transverse section, the adaxial leaf surface is associated with double palisade mesophyll tissue, a smooth epidermis, and a large subepidermal hypodermis layer (Figure 1.3C). The abaxial surface, in contrast, consists of spongy mesophyll cells, a single palisade mesophyll cell layer, and a rougher epidermal layer (Figure 1.3C), compared to the adaxial surface. The petiole is subradial or slightly flattened in the dorsiventral plane in transverse section (Figure 1.3E). The petiole is abaxialized and the vascular bundles are in a collateral arrangement where the xylem is closer to the centre while the phloem, arranged in groups, is closer to the outside (Figure 1.3G).

The *Ficus benghalensis* var. *krishnae* (Krishna fig) was discovered in the wild and originally named *Ficus krishnae* (de Candolle 1897, 1901, 1902). Its leaf blade is cup-like, with the shiny adaxial surface comprising the outside while the duller abaxial surface makes up the inside of the cup (Figure 1.3B). The anatomy of the leaf blade is virtually identical to the Banyan blade. As in the Banyan tree, in transverse section, the adaxial side of the leaf consists of a smooth epidermal layer, associated with the adaxial side, as well as the hypodermis and a double palisade mesophyll layer of cells, while the abaxial surface is associated with a rougher epidermal layer and spongy and palisade mesophyll tissues (Figure 1.3D). The petiole is radial in transverse section (Figure 1.3F) and the vascular bundles are sometimes amphivasal, where the xylem surrounds the phloem tissue, but collateral and amphicribral bundles are also seen within petioles (Figure 1.3H).

1.4.4 Pelargonuim

The flowers of *Pelargonium* x *hortorum* are surrounded by morphologically distinct bracts (Figure 1.4A). The bracts, which enclose individual flowers, are flattened in the dorsiventral plane. The bracts surrounding the flower buds can either be dorsiventrally flattened (Figures 1.4B, 1.4C) or trumpet-shaped (Figure 1.4D), and occasionally filamentous. All flat *Pelargonium* bracts contain large trichomes on the outside or abaxial surface, while these trichomes are present within the distal blade portion in trumpet-shaped bracts. The vascular arrangement is collateral within flat bracts, with phloem towards the outside or abaxial side of the bract and xylem towards the inside or adaxial side (Figures 1.4E, 1.4F). The proximal portion of the trumpet-shaped bract is petiole-like and radial in cross-section while the distal portion is blade-like in the shape of a trumpet (Figure 1.4D). Trumpet-shaped bracts exhibit a similarly collateral vascular arrangement within the petiole-like region (with xylem towards the adaxial side and phloem on the opposite side away from the inflorescence axis) and within the distal blade region that is circular in transverse section, with xylem towards the outside of the blade-like tissue and phloem towards the inside (Figures 1.4G-1.4I).

1.4.5 Cactaceae

1.4.5.1 Maihuenia

The leaves of *Maihuenia poeppigii* are awl-shaped and radial in transverse section (Figure 1.5A). Within the leaf cross-section, there are many small vascular bundles arranged in a circle within the circumference of the leaf, and a single large bundle located almost at the centre (Figure 1.5B). The small bundles are collateral in arrangement, with xylem located

towards the outside and phloem towards the inside of the leaf (Figure 1.5C). The large bundle is partially amphicribral with phloem toward the inside of the leaf, partially surrounding the xylem on the outside.

1.4.5.2 Opuntia

Similar to *Maihuenia*, *Opuntia* sp. leaves are awl-shaped and radial to subradial in transverse section (Figure 1.5D). Within the leaf, there are a few small vascular bundles arranged in a row, and a single larger bundle at the centre of the leaf (Figures 1.5E, 1.5F). All of the bundles are arranged in a collateral pattern with xylem towards the outside and phloem towards the inside of the leaf.

1.4.5.3 Pereskia

Pereskia aculeata contains vegetative leaves and leaves that are smaller in size and associated with fruits. Vegetative leaves consist of a short petiole and a large simple leaf blade (Figure 1.5G). The leaf blade contains several layers of palisade mesophyll on the adaxial side and spongy mesophyll on the abaxial side (Figure 1.5H). As in conventional dorsiventrally flattened leaves, here, the vascular bundles are collateral with xylem towards the top and phloem towards the bottom surface. Within the petiole, which is almost radial in cross-section, but slightly flattened on the adaxial side, there is a single vascular bundle that is generally collateral in arrangement, with xylem towards the adaxial side and phloem partially surrounding the xylem on the abaxial side (Figure 1.5I).

Pereskia grandiflora anatomy and vascular arrangement is nearly identical to that of *P. aculeata* (results not shown).

1.4.6 popREVOLUTA

Mature wild type hybrid *P. tremula* x *alba* (referred to as hybrid aspen below) leaves consist of a long mediolaterally flattened petiole and a flat isobilateral leaf blade (Figure 1.6A). The leaf blade transverse section shows double palisade mesophyll cells on the adaxial side and a spongy mesophyll to "green-compact mesophyll" cells (see Chapter 4 for a more detailed discussion). The vascular bundles are in a collateral pattern within the leaf blade with xylem towards the top and phloem towards the bottom surface (Figure 1.6B). In cross-section, the petiole usually contains three major vascular bundles that may separate into two, arranged in a row along the adaxial-abaxial axis, with the phloem completely surrounding the xylem within each bundle, arranged in an amphicribral manner (Figure 1.6C).

The two leaf types that are observed in *popREVOLUTA* plants include wild type-like leaves and trumpet-like leaves that are curled towards the adaxial side (Figure 1.6A). The *PRE* wild type-like leaves are virtually identical to wild type leaves, both morphologically and anatomically. Wild type-like leaves are associated with mediolaterally flattened petioles and isobilateral leaf blades with the same cell type and vascular bundle distributions as wild type leaves (Figures 1.6D, 1.6E). The trumpet-like leaves, on the other hand, are morphologically distinct and are smaller in size compared to wild type and wild type-like leaves. The petiole of trumpet-like leaves is radial or adaxially flattened in cross-section, with several vascular bundles arranged in a ring-like pattern, but they are sometimes scattered throughout the centre of the petiole (Figure 1.6G). The vascular bundle arrangement is similar to wild type with phloem to the outside and xylem towards the inside of the petiole.

The major difference between trumpet-like leaf petioles and wild type is the presence of discontinuity of parenchyma within the vascular bundles. Unlike in wild type, the vascular bundles of trumpet-like leaf petioles are not fully amphicribral but contain regions of discontinuity between the bundles that appear more collateral, but arranged in a ring-like pattern forming a larger bundle.

1.5 Discussion

Although a conventional angiosperm leaf is dorsiventrally flattened, there is a large amount of natural leaf diversity, including leaves that exhibit adaxial-abaxial polarity defects (termed as such for model plant mutants). Unifacial or radialized leaves can be thought of as "natural mutants" and show the most striking difference from dorsiventrally flattened leaves. The outer surface of these leaves consists of a single surface where the blade can either be filamentous or petiole-like, funnel or trumpet-shaped, or the leaf can be peltate. In trumpet-shaped or peltate leaves, the inner surface of the funnel or the upper surface of the peltate leaf consists of another surface from that of the petiole. For example, garden nasturtium (*Tropaeolum majus*) has peltate leaves with an abaxialized (consisting of bottom surface) petiole and the top of the leaf consists of the adaxial (top) surface. Funnel or trumpet-shaped leaves are simply topological variations of this type of peltate leaf where the leaf blade simply continues to grow upward along the margins, creating a cup (Franck 1976). These types of leaf shape variation are most common among eudicotyledonous species. In monocots, on the other hand, unifacial leaves are of two types in transection: radial and mediolaterally flattened (Kaplan 1997). Radial leaves contain a distal unifacial blade and a

bifacial proximal leaf base. Mediolaterally flattened leaf blades are also attached to a bifacial leaf base, but the flattening of the blade occurs secondarily along the adaxial-abaxial axis.

The majority of plants with radialized or unifacial leaves are of the abaxial type, as in the petiole of *T. majus*. Some other examples of plants with abaxialized leaves include members of Nepenthaceae (*Nepenthes*), Cephalotaceae (*Cephalotus*), Sarraceniaceae (*Sarracenia*, *Darlingtonia*, *Heliamphora*), Lentibulariaceae (*Utricularia*, *Polypompholyx*, *Biovularia*, *Ganlisia*), most of which are associated with a carnivorous habit (Franck 1976). Abaxialized unifacial leaves are also quite common among the monocots including among the members of the Iridaceae (*Iris*, *Morea*, *Sisyrhynchium*, *Tigridia*), Tofieldiaceae (*Tofieldia*), Nartheciaceae (*Narthecium*), Juncaceae (*Juncus*), Orchidaceae (*Epidendrum*, *Maxillaria*), Haemodoraceae (*Wachendorfia*, *Lachnanthes*, *Dilatris*), and Acoraceae (*Acorus*) (Rudall 1990, Kaplan 1997, Rudall and Buzgo 2002, Yamaguchi and Tsukaya 2010, Yamaguchi et al. 2010). Although abaxialized leaves are much more common in nature, plants with adaxialized leaves or leaf-derived organs have been described among members of the following families: Asclepiadaeceae (*Dischidia*), Asteraceae (*Celmisia*), Ericaceae (*Cassiope*), Melastomaceae (*Tococa*, *Maieta*), Asteraceae (upper leaves of *Calycadenia truncata*), Moraceae (*Ficus benghalensis* var. *krishnae*), Geraniaceae (*Pelargonium*), bracts of certain Marcgraviaceae, sepals of some Violaceae (*Viola*) and Fumariacaceae, petals of Rosaceae (*Malus prunifolia*), and leaves of leaf-bearing Cactaceae (*Opuntia*, *Maihuenia*) (Franck 1976, Dupuy and Guédès 1979).

1.5.1 Vascular patterning

There are several factors that can be used to identify the type of surface present (i.e., adaxial or abaxial) including epidermal cell types, stomatal distribution, and cell types associated with the particular surface (i.e., palisade vs. spongy mesophyll). But the most obvious indicator of surface identity is the location and arrangement of the vasculature. In conventional flat leaves, xylem is always associated with the adaxial surface while phloem is toward the abaxial surface (Kaplan 1997, Cronk 2009). As vasculature is followed through the petiole and consequently into the stem, this arrangement is generally maintained, but phloem becomes situated to the outside or peripheral (abaxial) domain of the petiole or stem while xylem becomes associated with the central (adaxial) domain. The genetic mechanisms of this linkage are also conserved in that *HD-ZIPIII* genes are highly expressed in the xylem, but also are among those responsible for adaxial cell identity with which xylem is associated (Green et al. 2003, Kang et al. 2003, Ariel et al. 2007, Chitwood et al. 2007). Conversely, *KANADI* genes are expressed in the phloem as well as in the abaxial domain (Emery et al. 2003, Byrne 2005, Moon and Hake 2011).

Although *Arabidopsis* mutants have given us a great amount of information about adaxial-abaxial patterning in leaves, it is necessary to study other systems due to differences in vascular patterning. The general impression acquired from the study of *Arabidopsis* mutants is that the radialization of leaves causes the vasculature to be similarly radialized. If the leaf becomes abaxialized, the single vascular strand within the leaf becomes amphicribral in arrangement with phloem surrounding the xylem. Similarly, if the leaf is adaxialized, the strand becomes amphivasal where xylem surrounds the phloem (e.g., Zhong and Ye 2004). This is not the case when the anatomy of naturally radialized plants is observed.

One might speculate that if the petiole or a portion of a leaf is radialized, but a distal lamina is maintained, the vasculature within the proximal portion would not be completely radialized. In other words, if there is a distal blade (e.g., *Ficus benghalensis* var. *krishnae*), the vasculature within maintains collateral arrangement, as in a typical flat leaf. But if the flat blade portion is absent and the leaf is completely radialized (e.g., *Opuntia* and *Maihuenia*), it is possible to assume the radialization of the vasculature may occur (Kaplan 1997). This is not observed in plants investigated here, as they generally have more than one single vascular strand, as seen in *Arabidopsis*.

How then would the vasculature be rearranged to account for the differences in polarity? *Allium cepa*, other monocots, and *Nepenthes* have the collateral bundles in a ring along the circumference of the unifacial leaf (in cross-section) with phloem towards the outside and xylem towards the inside (i.e., abaxialized) (Kaplan 1997). The other species investigated with adaxialized leaves or bracts are eudicots and have developed a similar mechanism for vascular rearrangement. But here, the collateral bundles are "inverted" (Arber 1918) or arranged in such a way that xylem is towards the outside of the leaf (or bract) and phloem is towards the inside. Even the very small trumpet-shaped bracts of *Pelargonium* x *hortorum*, similar in size to *Arabidopsis* leaves, do not contain radialized vasculature (although reported as such by Dupuy and Guédès 1979), but rather contain a single collateral vascular bundle. Amphicribral (abaxialized) arrangement of the petiolar vascular bundles in hybrid aspen is observed in both wild type and mutant sections (as well as in other poplar species; see Chapter 4) and is not uncommon to occur in other species (Dupuy and Guédès 1979). Some partially radialized vascular bundles are observed in *F. benghalensis* var. *krishnae*, but as are collateral bundles, which are most common throughout the petiole

sections. Fully amphivasal bundles are not observed in any of the adaxialized species, as may be expected from descriptions of *Arabidopsis* mutants (e.g., *rev*). Amphicribral-like vascular bundles have been described for some monocot species with mediolaterally flattened blades (e.g., *Freesia refracta*) (Troll 1939). Kaplan (1997) challenged this observation by suggesting that these bundles are in fact two collateral bundles that have been fused due to the compression of the blade, and therefore are not radialized.

The presence of a single vascular bundle within the petiole of an *Arabidopsis* leaf is generally not representative of most plants. As the vasculature passes from the blade through the petiole, it continues on through the stem of the plant. In general, only lateral organs are affected by dorsiventral polarity gene mutations and the stem is unaffected, with a few exceptions (e.g., *PRE* affects secondary growth within the stem; Robischon et al. 2011). Therefore, the stem maintains the typical collateral vascular arrangement where phloem is associated with the outside or periphery of the stem and xylem is located towards the centre or pith. It is necessary to maintain some sort of continuity between the stem vasculature and the leaf vasculature, which is achieved through a bifacial leaf base, particularly in monocots with unifacial leaves (Kaplan 1997). But when the leaf is abaxialized, it is fairly easy to develop amphicribral bundles by encircling the central xylem with the peripheral phloem. Adaxialized leaves, on the other hand, are more difficult to develop as they would require the central xylem to completely encircle the outer phloem in order to form amphivasal vascular bundles, therefore removing the abaxial identity from the outside of the leaf. This is a possible reason for abaxialization to be more common in nature, compared to adaxialization. But adaxialized leaves, whether fully or partially adaxialized, have developed a intriguing way of avoiding radialization of bundles by "inverting" the arrangement and placing xylem

to the outside of the leaf and phloem to the inside. Simple *Arabidopsis* mutants therefore imply a simple conceptual model where polarity affects surface and vasculature in the same predictable way. But these naturally radialized leaves suggest that dorsiventral polarity establishment is more complex and that vascular polarity and surface polarity are developmentally separate, although related.

1.5.2 Genetic mechanisms

From *Arabidopsis*, a general model for leaf polarity can be developed. Downregulation of adaxial cell fate specifying genes or overexpression of abaxial cell fate genes causes the abaxialization of organs. The same holds true for the reverse mode, adaxialization where adaxial cell fate genes are upregulated and the adaxial genes are downregulated. The major contributors in the network include *AS1/AS2*, *KANADI*, *HD-ZIPIII*, and *ETT/ARF4* genes, as well as their corresponding small RNA molecules and other genes, which regulate or are regulated within the three major pathways. Single gene mutations can cause severe dorsiventral polarity defects (e.g., *rev* mutation in *Arabidopsis*), but a combination of genes usually has a more extreme effect on the phenotype (e.g., *phb phv rev* triple mutants in *Arabidopsis*). *Arabidopsis* contains single gene copies of each of the representatives within the dorsiventral polarity network, but other plants may have multiple copies. Poplar, for example, underwent a whole genome duplication event following the split from *Arabidopsis* (Tuskan et al. 2006), and there are two or occasionally several more representatives of each of the genes found in *Arabidopsis* (see Chapter 3).

Apart from the number of genes that an individual species would contain, the specific plant may have acquired a novel or different function to that found in *Arabidopsis*. The most

obvious example is that of the *PHANTASTICA* gene in *Antirrhinum*. While LOF mutants in *Antirrhinum* develop abaxialized leaves, this phenotype is absent in *Arabidopsis* when *AS* is downregulated (Iwakawa et al. 2002, Lin et al. 2003). The *AS* ortholog of tomato (*SlPHAN*) has also been recruited for a novel function not present in *Arabidopsis*. In tomato, this gene acts mutually with *KNOX* to develop leaflets. If *SlPHAN* is downregulated, abaxialized leaves with no leaflets develop (Kim et al. 2003, Zoulias et al. 2012).

Here, I investigated several species found in nature, previously described as abaxialized or adaxialized. The abaxialized species studied included *Allium cepa* and *Nepenthes ventricosa*, while samples of adaxialized leaves (or leaf-derived organs) were from *Ficus benghalensis* var. *krishnae*, *Pelargonium* x *hortorum*, and several Cactaceae species (*Opuntia* sp. and *Maihuenia poepiggii*). These can be further subdivided into four groups to aid in the discussion of possible genetic mechanisms underlying the observed leaf phenotypes: 1) *Allium*, 2) *Nepenthes* and *Ficus*, 3) Cactaceae, and 4) *Pelargonium*.

Allium is a monocot and has patterns of gene expression that are likely more similar to maize or rice rather than *Arabidopsis*. This would be most evident with expression of *YABBY* genes, which are likely expressed in the adaxial or central domain of the leaf. As with other radialized monocot species, *Allium* leaves are abaxialized (Arber 1918, Traub 1968, Kaplan 1997). The genetic mechanisms responsible for this phenotype in *Allium* are very likely similar to those of other monocots. Species within the genus *Juncus* are either radial or mediolaterally flattened, in transection (Yamaguchi and Tsukaya 2010, Yamaguchi et al. 2010). Although the genetic basis of the radial leaf has not been fully investigated in this system, Yamaguchi et al. (2010) showed the importance of *DROOPING LEAF* (*DL*; *CRC* ortholog) in the flattening of the blade. *DL* functions in midrib formation only in monocots,

while in *Arabidopsis CRC* is involved in nectary development (Alvarez and Smyth 1999, Bowman and Smyth 1999, Baum et al. 2001, Ishikawa et al. 2009). In the radial *Juncus* leaf, *ETT* is expressed in the outer region of the leaf, while *PHB* is restricted to the xylem (Yamaguchi et al. 2010). In rice, for example, the *leafbladeless1* (*lbl1*; *AS/PHAN* ortholog) mutation causes abaxialized leaves (Timmermans et al. 1998). This evidence, therefore, suggests that there are numerous possibilities of gene expression patterns that can contribute to abaxialized leaves in *Allium*. These can include overexpression of *KANADI*, *ETT/ARF4*, and *YABBY* orthologs or the downregulation of *AS* and *HD-ZIPIII* orthologs, either as single genes or likely in combination with each other and other interacting genes and small RNAs.

Although *Nepenthes* and *Ficus* contain leaves that are abaxialized and adaxialized, respectively, the leaf types show similarities. Both species contain a unifacial petiole and a distal (and also proximal, in the case of *Nepenthes*) blade portion that contains both adaxial and abaxial surface identities. These two species, therefore, can be considered to have a moderate leaf phenotype, particularly in relation to the severe phenotype of the unifacial Cactaceae leaves. Leaves of *Opuntia* and *Maihuenia* are fully adaxialized and therefore do not develop a distal flat or trumpet-shaped lamina. These species are eudicots and therefore will likely have more similarities in gene expression to *Arabidopsis* and other eudicots, rather than the previously discussed monocot species.

Nepenthes and *Ficus* retain a respectively distally located pitcher and trumpet-shaped, leaf blade that should contain adaxial-abaxial polarity gene expression comparable to a conventional bifacial flat leaf. Only the proximal petiole region is unifacial. This is contrary to the two Cactaceae species investigated where the entire leaf blade is unifacial. This, therefore, suggests that the Cactaceae species have a more severe unifacial phenotype,

compared to *Nepenthes* and *Ficus*, and do not contain the abaxial surface identity. Similar to *Nepenthes*, the *T. majus* (garden nasturtium) petiole is abaxialized while the distal peltate leaf in garden nasturtium is flattened (Kaplan 1997). The *AFO* ortholog (*TmFIL*) is upregulated in the unifacial petiole, causing its abaxialization (Gleissberg et al. 2005). Adaxial-abaxial patterning is not affected in the peltate blade. A similar pattern of expression is expected in *Nepenthes*. Conversely, there may be a down regulation of the *AFO* orthologue in *Ficus* petiole and no change in dorsiventral patterning in the distal blade. The adaxialized petiole of *Ficus* and leaves of the Cactaceae likely contain overexpression of *AS* and *HD-ZIPIII* and/or downregulation of *KANADI*, *ETT/ARF4*, *YABBY* genes with a combination of other genes and small RNAs in the network. Similarly, the converse gene expression pattern can be expected for the abaxialized petiole of *Nepenthes*, although probably not upregulation of *ETT*, as this causes accelerated vegetative phase change in eudicots rather than abaxialization (Pekker et al. 2005).

Pelargonium bracts are adaxialized and have morphological similarities to both *Ficus* and unifacial Cactaceae leaves. Although most of the unifacial bracts are trumpet-shaped, some are also fully adaxialized. Bracts are considered to be homologous to leaves (Hagemann 1984) and will likely have similarities in gene expression patterns to other adaxialized-leaved eudicots, such as *Ficus* and Cactaceae species.

The final plant investigated was a hybrid aspen *REVOLUTA* mutant, which has adaxializing characteristics due to the mutation in one of the *REV* genes (*Pt-HB1.7*; see Chapter 3). Robischon et al. (2011) have described the variability of the phenotypes including moderate and severe, which produce wild type-like leaves, upwardly curling leaves, leaves with adaxial outgrowths (on the abaxial surface), and partially radialized

leaves. The two leaf types are mostly observed for moderate mutant plants investigated here, which are wild type-like and trumpet-like. Generally, the leaf phenotypes observed were similar to the *REV* GOF mutants in *Arabidopsis* (Talbert et al. 1995, Emery et al. 2003) and phenotypic variability is also observed depending on the genetic background used (Prigge et al. 2005). Complete adaxialization of leaves would not be expected, since only a single *REV* gene copy is upregulated, but poplar contains two copies (see Chapter 3; Robischon et al. 2011). Since the genus *Populus* has undergone whole genome duplication (Tuskan et al. 2006), there are usually at least twice as many genes in the dorsiventral polarity network as there are for *Arabidopsis* and in some cases more (e.g., *KANADI* genes; see Chapter 3). This duplication creates many more numerous gene combinations that would need to interact in order to fully radialize a leaf, either in the adaxial or abaxial direction. Some of these new (compared to *Arabidopsis*) copies can attain novel or different functions, which are not present or necessary in *Arabidopsis* (e.g., role of *PRE* in secondary thickening [Robischon et al. 2011]).

1.6 Conclusions

The majority of our knowledge about the genetic and developmental basis of adaxial-abaxial polarity patterning is based on the model eudicot, *Arabidopsis*, although this field of dorsiventral patterning was started with the findings in *Antirrhinum* (Waites and Hudson 1995). Monocotyledonous species have also contributed to broadening this field as well as highlighting differences in genetic mechanisms between different clades (i.e., eudicots vs. monocots) (e.g., Juarez et al. 2004). These differences are important for synthesizing gene expression patterns from model systems and being able to extrapolate these results to other

non-model species. Every species will have some degree of variability due to number of gene copies or gene evolution, but overall functions are likely conserved, except possibly for *YABBY* or *AS* genes. Currently, the genomic resources are lacking for all of the species discussed here (with the exception of poplar), but similarities in phenotypes can be the initial starting point for determining the genetic basis of these "natural unifacial mutants", aiding in the search for the factor(s) that contribute to leaf evolution.

1.7 Aims of thesis

The aim of this thesis is to investigate adaxial-abaxial polarity patterns in a variety of plants. Here, I began my study with a literature review of molecular genetic controls of dorsiventral polarity in model systems. My interest was to determine the relevance of the conceptual models that are based on model systems through the investigation of non-model species with leaves that show variability in the development of the dorsiventral axis. Other species that are not considered to be model systems for leaf development that are further investigated here include *Brassica napus* (Chapter 2) and poplar (Chapters 3-5).

This introductory chapter sets up the importance of linking morphological and anatomical investigations in non-model system with molecular genetic evidence in order to have a complete picture of dorsiventral leaf polarity, as *Arabidopsis* cannot provide a complete representation of the diversity observed in nature. The integration of genetics and morphology of non-model systems with regard to dorsiventral polarity has not been previously investigated, with the exception of *Juncus* (e.g., Yamaguchi et al. 2010). *Brassica napus* adaxialized leaf mutant is newly discovered and is studied on an anatomical and molecular genetic level in a subsequent chapter, with the intention to show an example of

linking morphological and anatomical studies with molecular biology in order to determine the underlying genotypic cause for the phenotype of interest.

The remaining portion of the thesis focuses on morphological and molecular genetic differences between poplar species that contain phenotypes that are related to dorsiventral polarity in leaves. Orthologs of *HD-ZIPIII* genes in poplar have been previously identified (e.g., Coté et al. 2010), but the full set of *YABBY* and *KANADI* genes in poplar has not been published before. As eucalyptus genome has only recently become publicly available (i.e., January 2011), determination of dorsiventral polarity orthologs has not been done to date. Further, transcript levels in all of the poplar and eucalyptus adaxial-abaxial polarity genes have not been previously investigated.

The abaxial greening phenotype in poplar has not been extensively investigated. One study (Wu et al. 1997) mapped this phenotype and the associated petiole to two quantitative trait loci, but the underlying genetic differences between bifacial- and isobilateral-leaved species of *Populus* has not been studied further. Phylogenetic analysis of the genus *Populus*, done in Chapter 4, provides a framework for determining the ancestral leaf character (bifacial vs. isobilateral), which is currently not known. Finally, in Chapter 5, I investigated the underlying molecular genetic mechanisms between black cottonwood and hybrid aspen or bifacial- and isobilateral-leaved species. Although further work is needed to conclusively determine gene(s) responsible for abaxial greening and unifacial petiole phenotypes in isobilateral leaves of hybrid aspen, I identified a subset of genes that may be contributing to these phenotypes.

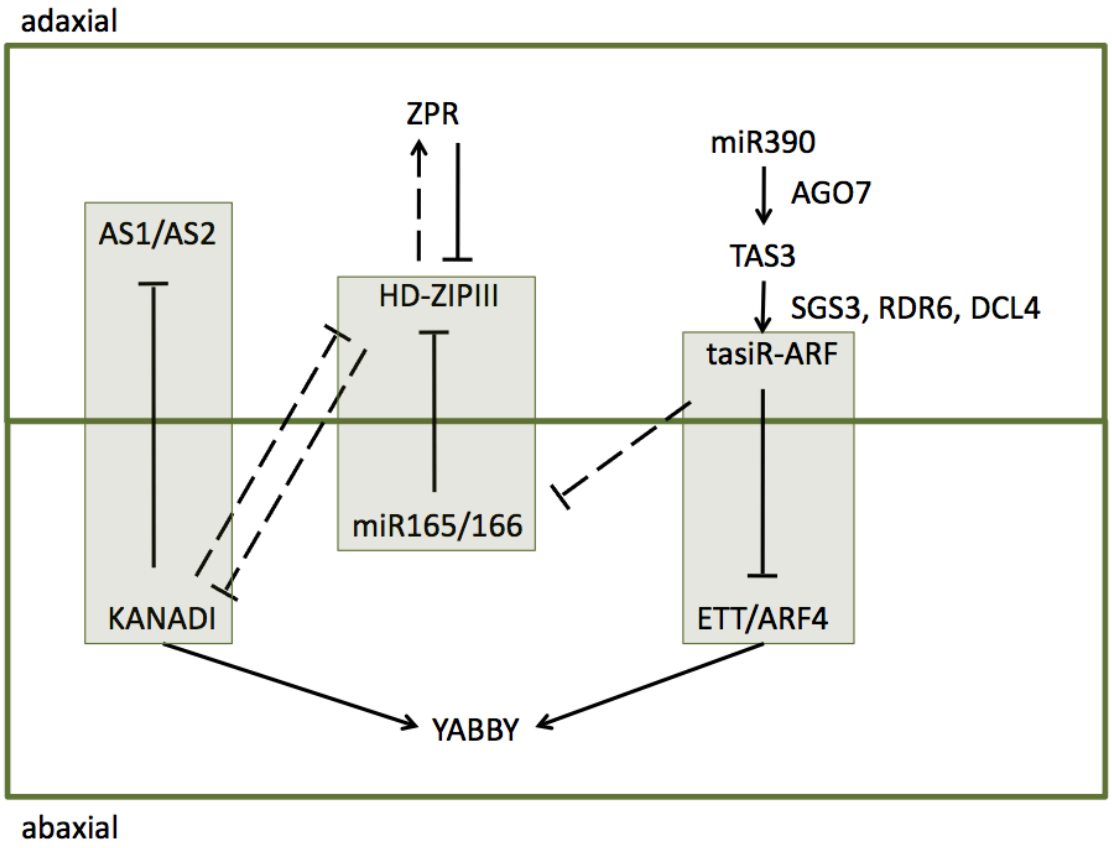

Figure 1.1 Adaxial-abaxial patterning in leaves is controlled by an array of transcription factors and corresponding small RNAs. Gene pathways enclosed with boxes specify the major complexes setting dorsiventral polarity: 1) AS1/AS2–KANADI, 2) HD-ZIPIII–miR165/166, and 3) ETT/ARF4–tasiR-ARF. Solid lines indicate direct interactions while dashed lines indicate interactions that are indirect.

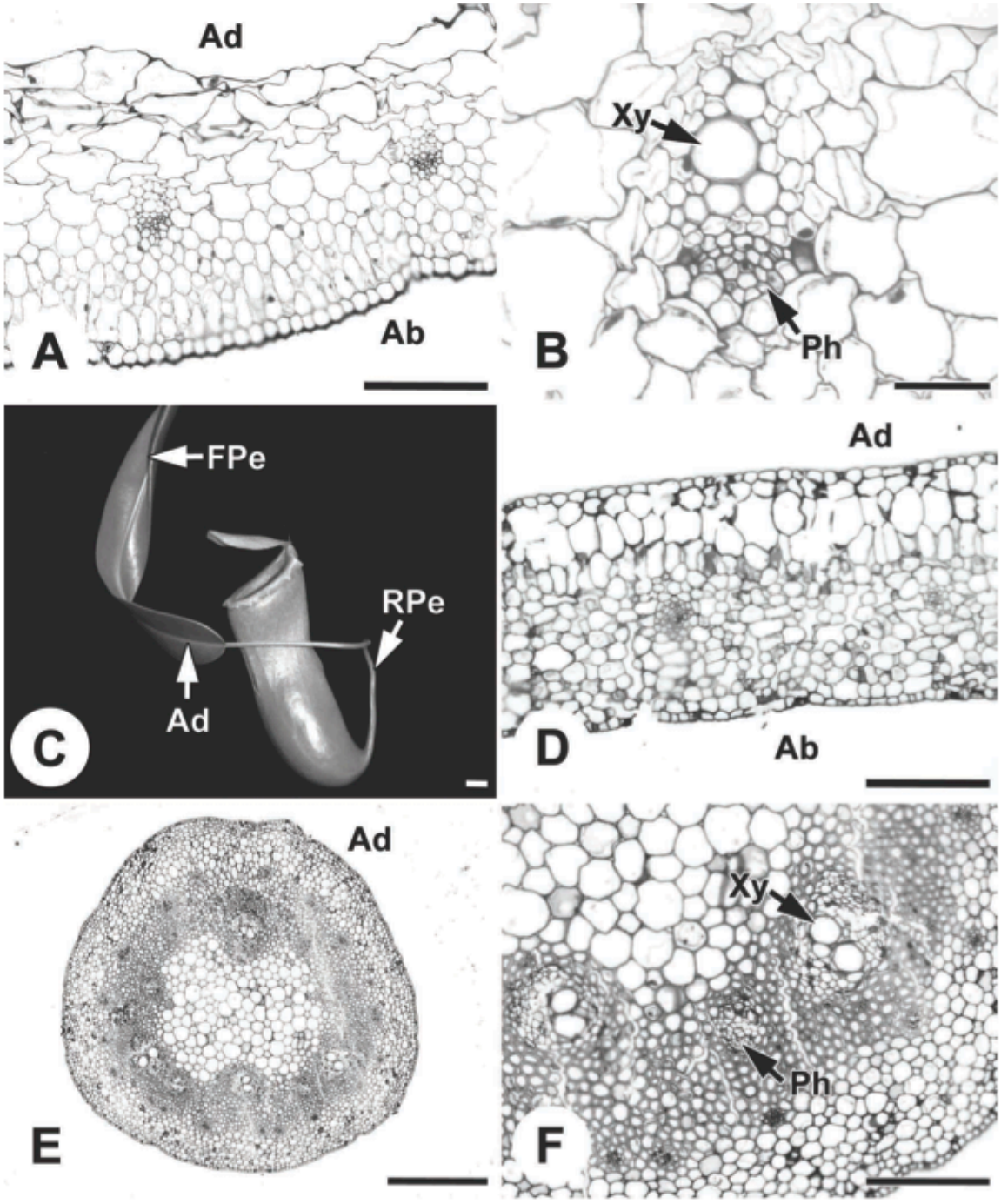

Figure 1.2 Morphology and anatomy of abaxialized leaves: *Allium* (A, B) and *Nepenthes* (C-F). A. High magnification of *Allium* leaf transverse section, which is in the shape of a ring. B. Higher magnification of vascular bundles (in A) that are collateral in arrangement with xylem towards the inside and phloem towards the outside. C. Morphology of *Nepenthes* pitcher, which is attached to the plant with a radial and a proximal flat petiole. D. The flat petiole is dorsiventrally flattened in cross-section with collateral

vascular bundles. E. Transverse section of the radial petiole with vascular bundles arranged in a ring within. F. Higher magnification of vascular bundles in E. Major vascular bundles have an amphicribral-like arrangement, with phloem capping the central xylem on either side, and are positioned laterally within the petiole. Minor vascular bundles are collateral in arrangement with phloem towards the outside and xylem towards the inside of the petiole. Ad – adaxial side, Ab – abaxial side, FPe – flat petiole, RPe – radial petiole, Ph – phloem, Xy – xylem. Scale bars = 100µm (A, D, F), 50µm (B), 1cm (C), 500µm (E).

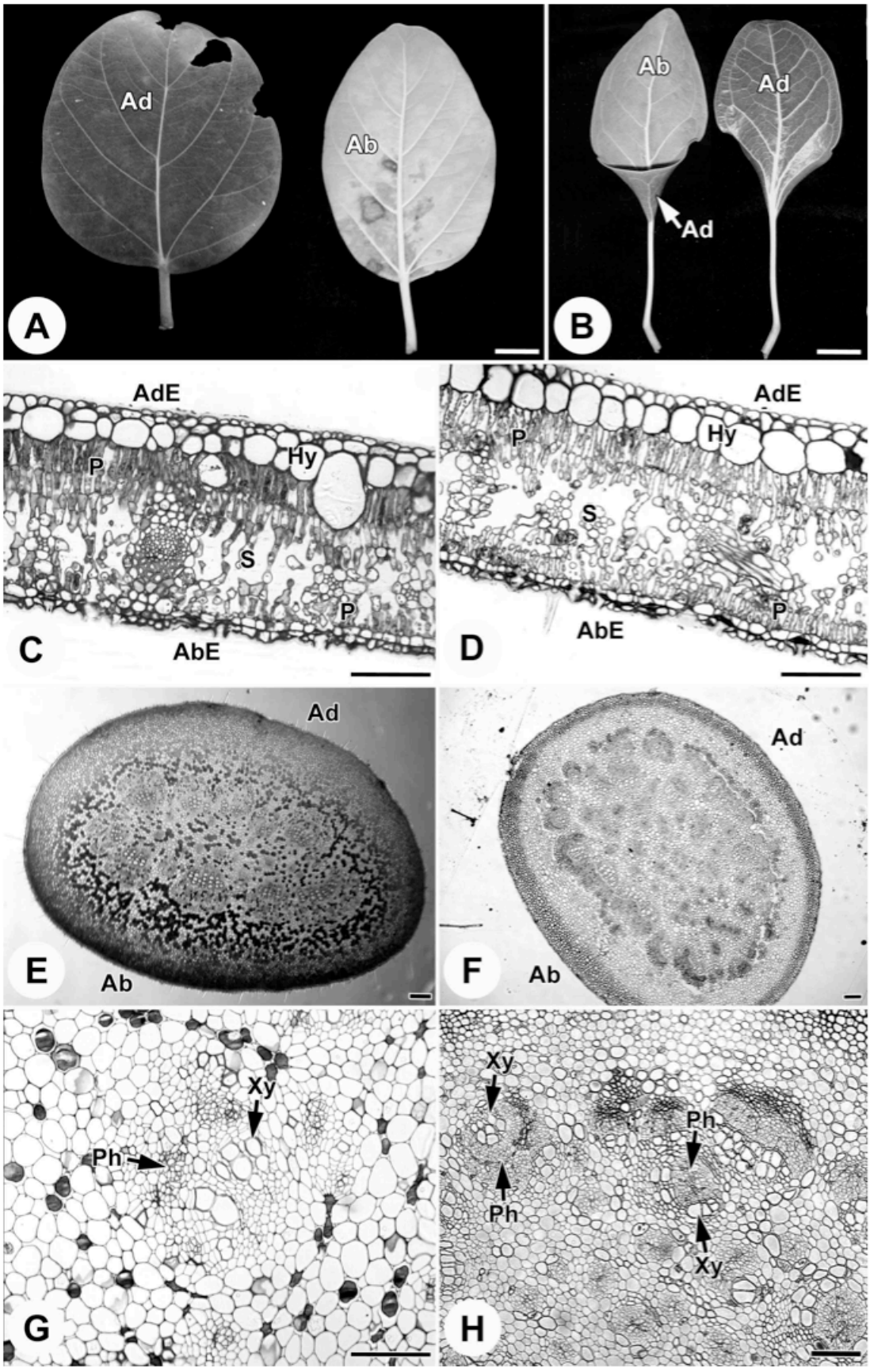
Ad
Ab
A
Ab
Ad
Ad
B
AdE
P
Hy
S
P
C
AbE
AdE
P
Hy
S
P
AbE
D
Ad
E
Ab
Ad
F
Ab
Xy
Ph
G
Xy
Ph
Ph
Xy
H

Figure 1.3 Morphology and anatomy of *Ficus benghalensis* (A, C, E, G) and *Ficus benghalensis* var. *krishnae* (B, D, F, H) leaves. A. *F. benghalensis* bifacial leaf with a shiny adaxial surface and a duller abaxial surface. B. *F. benghalensis* var. *krishnae* cup-shaped leaf with the shiny adaxial surface on the outside and the duller abaxial surface on the inside of the cup. C. Transverse section of the bifacial leaf blade consists of an adaxial epidermal layer, hypodermis, double palisade mesophyll, spongy mesophyll, abaxial palisade mesophyll, and an abaxial epidermal layer. D. Transverse section of the bifacial leaf blade, of the cup-shaped leaf, consists of an adaxial epidermal layer, hypodermis, double palisade mesophyll, spongy mesophyll, abaxial palisade mesophyll, and an abaxial epidermal layer. E. Transverse section of the subradial petiole that is slightly flattened in the adaxial-abaxial plane. F. Transverse section of the subradial petiole. G. Higher magnification of a petiolar vascular bundle with a collateral arrangement where the phloem is located to the outside, or closer to the periphery, of the more centrally-located xylem. H. Higher magnification of petiolar vascular bundles with amphicribral (with phloem surrounding the xylem; labeled on the left), amphivasal (with xylem surrounding the phloem; labeled on the right) or collateral arrangements. Ad – adaxial side/surface, Ab – abaxial side/surface, AdE – adaxial epidermis, AbE – abaxial epidermis, Hy – hypodermis, P – palisade mesophyll, S – spongy mesophyll, Ph – phloem, Xy – xylem. Scale bars = 2cm (A, B), 100µm (C, D, F-H), 200µm (E).

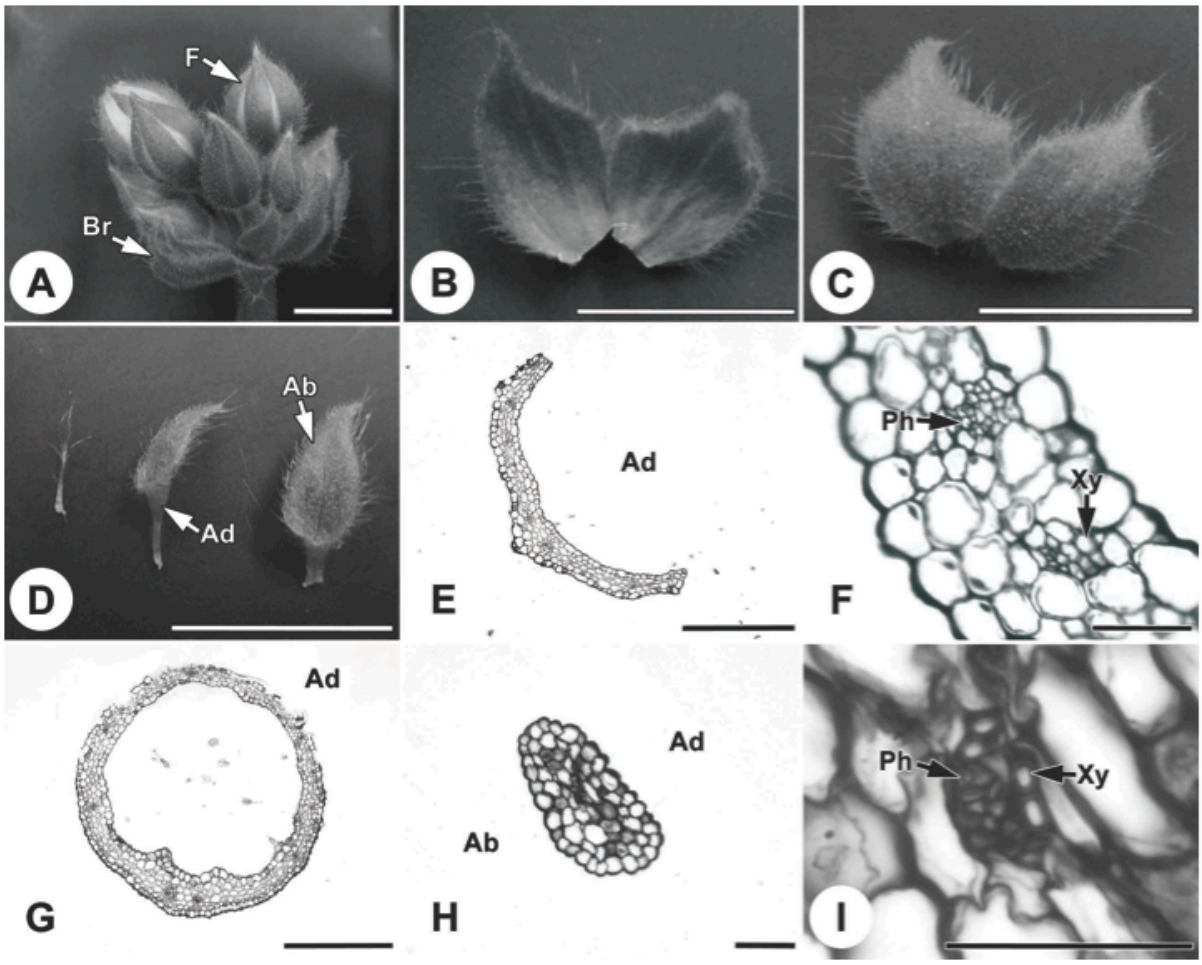

Figure 1.4 ***Pelargonium*** **x** ***hortorum*** **bract morphology and anatomy. A. Morphology of the flower buds with dorsiventrally flattened bracts surrounding the flower buds and a set of bracts below, which are either dorsiventrally flattened or trumpet-shaped. B. Adaxial view of the dorsiventrally flattened bracts. C. Abaxial view of the dorsiventrally flattened bracts, with many trichomes present. D. Filamentous (left) and trumpet-shaped bracts. Adaxial surface is on the outside of the bracts and abaxial surface, identifiable by the presence of trichomes, is on the inside of the distal trumpet blade portion of the bract. E. Transverse section of a dorsiventrally flattened bract with adaxial side labeled. F. Higher magnification of vascular bundles in E. The bundles are arranged in a collateral pattern with xylem towards the adaxial and phloem towards the abaxial sides. G. Transverse section of trumpet-shaped blade portion of the bract, with the abaxial surface internal within the circle. H. Transverse section of the petiole-like proximal portion of the bract, which is radial to slightly dorsiventrally flattened. I. Higher magnification of the single vascular bundle that is arranged in a collateral pattern. Ad – axial side, Ab –**

abaxial side, Br – bract, F – flower bud, Ph – phloem, Xy – xylem. Scale bars = 1cm (A-D), 500µm (E, G), 100µm (H), 50µm (F, I).

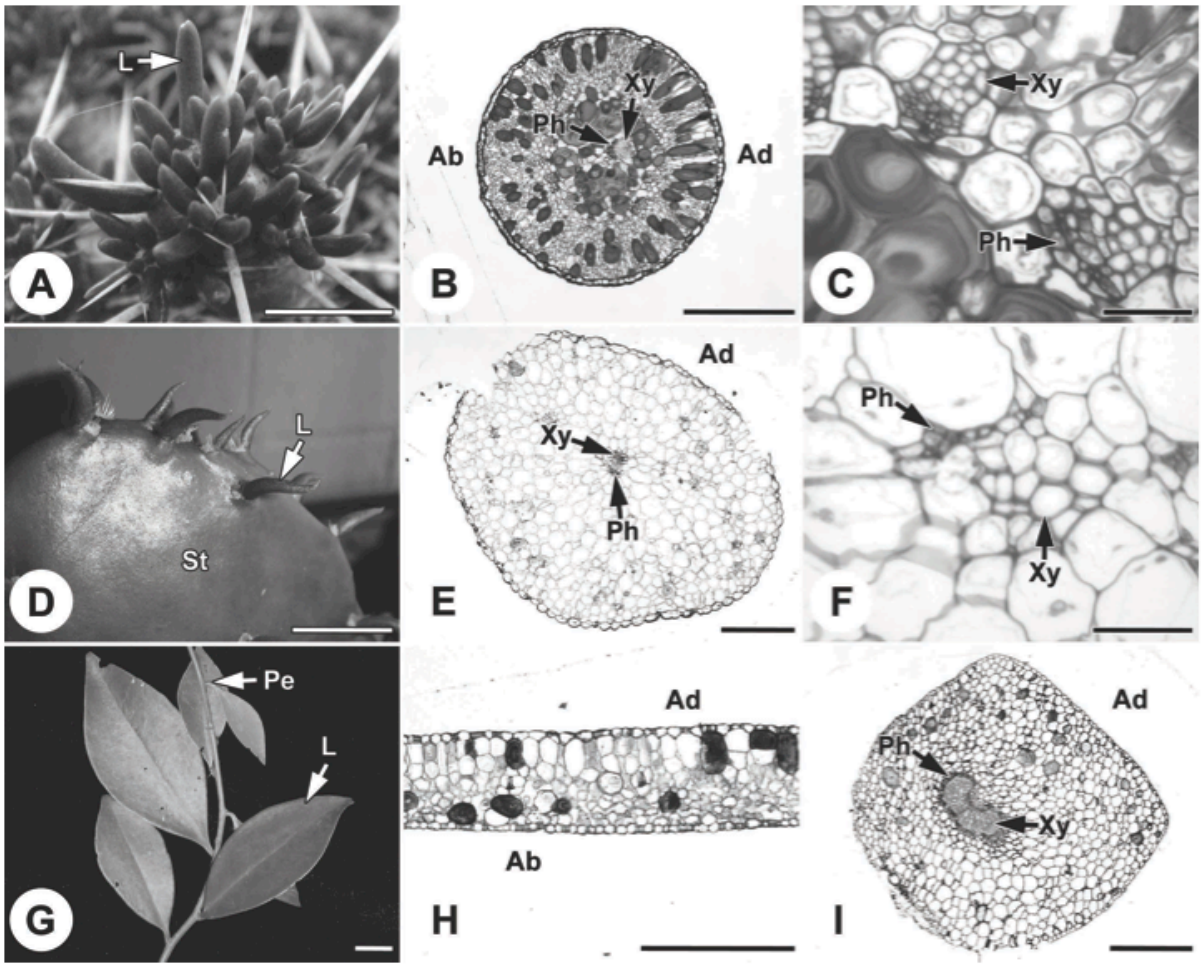

Figure 1.5 Morphology and anatomy of Cactaceae species: *Maihuenia poepigii* (A-C), *Opuntia* sp. (D-F), *Pereskia aculeata* (G-I). A. Leaves of *Maihuenia* are awl-shaped. B. Leaves are radial in transverse section with a major central bundle, partially amphicribral in arrangement with xylem towards the adaxial side and phloem towards the abaxial side. C. Higher magnification of collateral minor vascular bundles in B with xylem towards the outside of the leaf and phloem towards the inside. D. Leaves of *Opuntia* are awl-shaped and develop on the photosynthetic stem. E. Leaves are radial to subradial in transverse section with a major central bundle, which is collateral in arrangement. F. Higher magnification of collateral minor vascular bundles in E with xylem towards the outside of the leaf and phloem towards the inside. G. Top or adaxial view of the flat, petiolate leaves of *Pereskia* aculeata. H.

Leaf blades are flat with identifiable adaxial and abaxial sides, in transverse section. I. Petiole is almost radial, but slightly flattened on the adaxial side, with a single major central bundle, which is collateral to almost amphicribral in arrangement. L – leaf (blade), Ad – adaxial side, Ab – abaxial side, Xy – xylem, Ph – phloem, St – stem, Pe – petiole. Scale bars = 1cm (A, D, G), 500µm (B, E, H-I), 50µm (C, F).

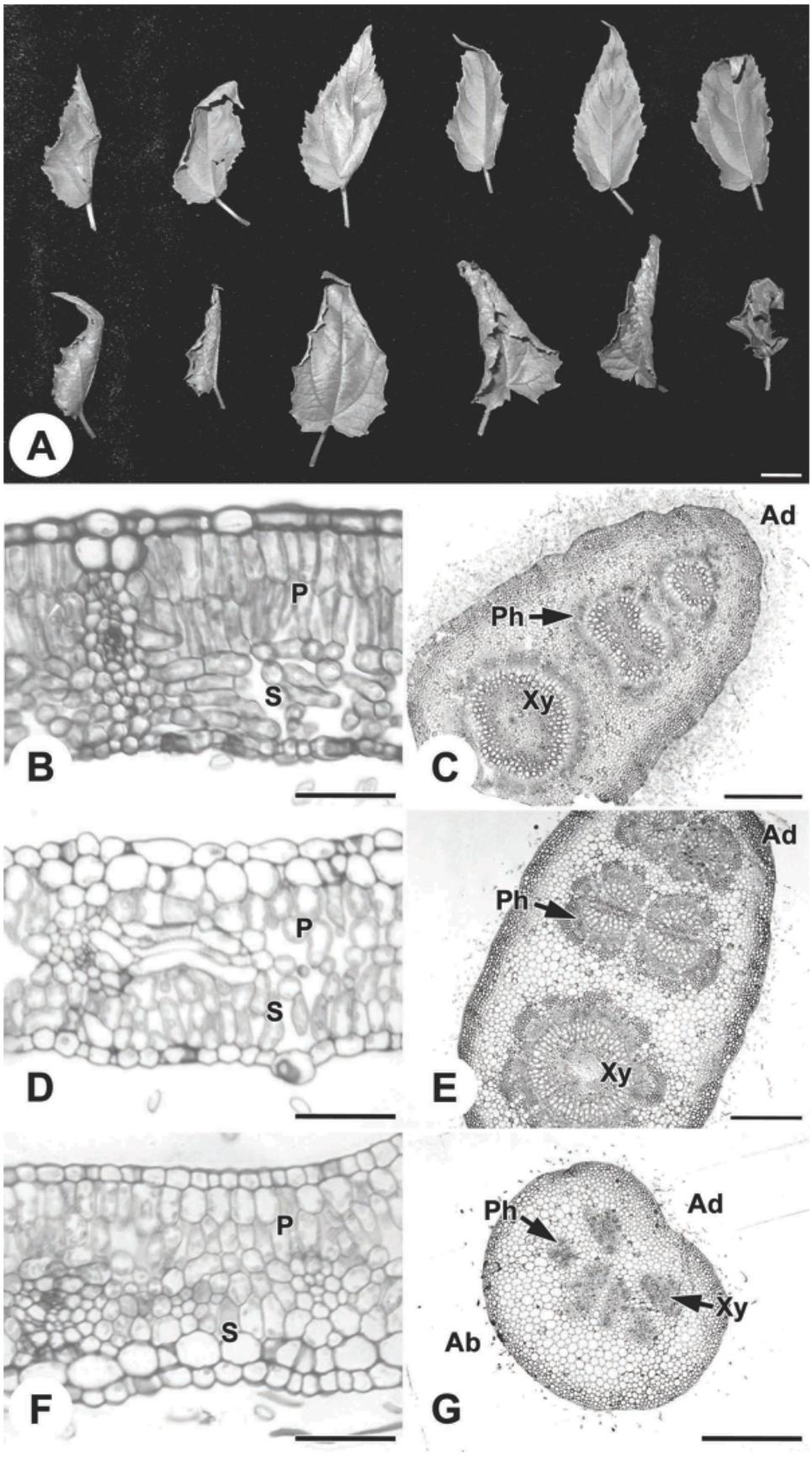
A
B
P
S
C
Ad
Ph
Xy
D
P
S
E
Ad
Ph
Xy
F
P
S
G
Ph
Ad
Xy
Ab

Figure 1.6 Morphology and anatomy of *Populus tremula* x *alba* wild type (top row in A; B, C) and *popREVOLUTA* (bottom row in A; D-G). A. Variability among young leaves of wild type (top row) and *PRE* mutant (bottom row) plants. The leaves of *PRE* are generally curled upwards towards the adaxial side. B. Wild type leaf blade with palisade mesophyll on the adaxial side and spongy mesophyll on the abaxial. The vascular bundles have a collateral arrangement with xylem towards the adaxial side and phloem towards the abaxial. C. Mediolaterally flattened petiole of wild type plant, which typically contains several vascular bundles arranged in a row along the adaxial-abaxial axis. Vascular bundles have an amphicribral arrangement with phloem surrounding the central xylem. D. Wild type-like leaf blade of *popREVOLUTA* plants with palisade mesophyll on the adaxial side and spongy mesophyll on the abaxial. The vascular bundles have a collateral arrangement. E. Mediolaterally flattened petiole of wild type-like leaves, which typically contains several vascular bundles arranged in a row, depending on leaf size, along the adaxial-abaxial axis. Vascular bundles have an amphicribral arrangement. F. Trumpet-like leaf blade of *PRE* plants with palisade mesophyll on the adaxial side and spongy mesophyll on the abaxial. The vascular bundles have a collateral arrangement. G. A radial petiole of trumpet-like leaves with several vascular bundles scattered in almost a ring-like pattern throughout the petiole. Some vascular bundles have an amphicribral arrangement, but mostly are collateral. Ad – adaxial side, Ab – abaxial side, P – palisade mesophyll, S – spongy mesophyll, Ph – phloem, Xy – xylem. Scale bars = 1cm (A), 50µm (B, D, F), 500µm (C, E, G).

Chapter 2: *Lamina epiphylla*: a novel adaxialized mutant of canola

2.1 Synopsis

A novel mutant was discovered during an EMS (ethylmethane sulphonate) mutagenesis screen, which exhibited a dorsiventral polarity phenotype in leaves and leaf-derived organs. This mutant was named *lip* for the adaxial epiphyllous outgrowths on the abaxial surface of the leaf lamina of some leaves. Leaves and other plant parts were analyzed on both morphological and anatomical levels. The leaves were adaxialized where the top surface comprised the periphery of trumpet-shaped or filamentous leaves, while the abaxial surface was greatly reduced to the inside of the cup in trumpet-shaped leaves. The observed phenotype was similar to previously described gain-of-function mutations in *Arabidopsis HD-ZIPIII* genes (e.g., *REV*, in particular). I determined some of the orthologs of *HD-ZIPIII* genes in canola and its two parent species (*Brassica rapa* and *Brassica oleracea*). Of the canola orthologs sequenced, none of them showed a difference between wild type and mutant sequences. It is, therefore, not clear as to whether one of the *HD-ZIPIII* genes is responsible for the observed mutation in the *lip* mutant.

2.2 Introduction

2.2.1 Polarity in leaf development

A conventional leaf is flat with identifiable adaxial (top) and abaxial (bottom) sides. The adaxial surface is generally designed for optimal light capture while the abaxial surface is where transpiration usually takes place. The juxtaposition of cells with adaxial and abaxial identity has been proposed to be essential in developing the mediolateral axis which sets the

width of the leaf (Waites and Hudson 1995). This hypothesis originated from dissection experiments performed by Sussex (1951, 1954) where the developing primordium was cut on the adaxial side, separating it from the meristem. These primordia developed into radialized leaves with the abaxial surface comprising the periphery, unable to develop proper adaxial and abaxial surfaces and therefore unable to expand in the mediolateral plane.

There are many variations to the conventional bifacial leaf, but the most striking difference is seen in leaves that are unifacial or that contain unifacial petioles (discussed in detail in Chapter 1). Unifacial leaves or organs can be of two types: abaxialized or adaxialized. While the former represents majority of plants with radialized leaves, there are many species that exhibit the latter unifacial leaf type (Franck 1976, Dupuy and Guédès 1979; see Chapter 1).

Along with the morphological characteristics, the anatomy of a radialized (adaxialized or abaxialized) leaf differs from a typical flat leaf. In a conventional leaf, a vascular bundle has a collateral arrangement where the xylem is located closest to the adaxial surface while phloem is closer to the abaxial surface. This tissue type (xylem and phloem) association is retained when a leaf becomes unifacial. In other words, xylem remains associated with the adaxial surface and phloem with the abaxial. Consequently, in adaxialized leaves vascular bundles are typically amphivasal (with xylem surrounding the phloem) versus amphicribral in abaxialized leaves (where phloem surrounds the xylem tissues) (Dupuy and Guédès 1979, Dengler and Kang 2001, Cronk 2009).

2.2.2 Molecular controls of dorsiventral polarity

Dorsiventrality in leaves is determined by a complex network of transcription factors and associated microRNAs (miRNAs) acting in a mutually antagonistic manner (e.g., Chitwood et al. 2007, Husbands et al. 2009, Kidner and Timmermans 2010). The major transcription factor families that are responsible for setting abaxial surface polarity are *YABBY* and *KANADI*, while the adaxial surface is determined by the action of homeodomain leucine zipper class III (HD-ZIPIII) proteins (Ariel et al. 2007). *YABBY* and *KANADI* expression is restricted to the abaxial domain in wild type leaves, while *HD-ZIPIII* expression is complementarily constrained to the adaxial domain. In *Arabidopsis*, the six *YABBY* (*YAB*) gene family members include *AFO/FIL* (*ABNORMAL FLOWER ORGAN/FILAMENTOUS FLOWER*), *YAB2, YAB3, INO* (*INNER NO OUTER*), and *CRC* (*CRABS CLAW*), while the *KANADI* (*KAN*) gene family consists of four members: *KAN1, KAN2, KAN3,* and *ATS/KAN4* (*ABERRANT TESTA SHAPE*). The *HD-ZIPIII* family consists of five genes: *PHB* (*PHABULOSA*), *PHV* (*PHAVOLUTA*), *REV* (*REVOLUTA*), *ARABIDOPSIS THALIANA HOMEBOX 8 (ATHB8)*, and *CNA/ATHB15* (*CORONA*).

Adaxialization of organs can occur due either to loss-of-function of *YABBY* or *KANADI* genes or due to a gain-of-function of *HD-ZIPIII* genes. The opposite holds for abaxialized organs which is caused by a gain-of-function of *YABBY* or *KANADI* genes or loss-of-function of *HD-ZIPIII* genes. For example, gain-of-function mutations in some *HD-ZIPIII* genes produce an enlarged shoot apical meristem (SAM) with adaxialized lateral organs, showing that these genes are sufficient to specify adaxial cell fate (McConnell et al. 2001, Emery et al. 2003, Chitwood et al. 2007, Husbands et al. 2009).

Several semi-dominant mutations affecting leaf polarity have previously been reported in the *Arabidopsis REV*, *PHB*, and *PHV* genes. These are the only semi-dominant mutations in *Arabidopsis* that are known to cause complete adaxialization of lateral organs (McConnell and Barton 1998, McConnell et al. 2001, Zhong and Ye 2004) and they are all caused by a single nucleotide change in their specific target miRNA binding sequence (Emery et al. 2003, Zhong and Ye 2004). The miR166/165 binds to HDZIP messenger RNA through complementary base pairing (Jung and Park 2007) and even a single base pair change in this sequence can prevent efficient miRNA binding to the target site, thus preventing targeted degradation of the gene product, resulting in increased levels of full-length *HD-ZIPIII* mRNA and hence an overexpression of the HD-ZIPIII protein(s) (Juarez et al. 2004, Townsley and Sinha 2012).

2.2.3 Objectives

An intriguing mutant phenotype was observed during the generation of an EMS mutagenized population of *B. napus* cv. DH12075 (E. Gilchrist, R. Dalta, G. Selvaraj, G. Haughn, UBC, unpublished data). This mutant phenotype contained epiphyllous outgrowths on leaves. Epiphylly is defined as "the occurrence of structures (organs, organs systems, or other constituents) upon a leaf or leaf homologue, in any position (e.g., adaxially, abaxially, apically, marginally, etc.)" (Dickinson 1978). The focus of this chapter was to examine this mutant phenotype in the context of current views of leaf development. Morphological and anatomical analyses indicated that this novel canola *lip* (*lamina epiphylla*) mutant resembled mutants seen in *Arabidopsis* and *Antirrhinum* that were caused by over-expression of one of

the *HD-ZIPIII* genes. Several of these genes were therefore sequenced in this mutant and wild type *B. napus* in an attempt to identify the gene responsible for this mutation.

2.3 Materials and methods

2.3.1 Identification of the *lip* mutant

In the process of generating an EMS (ethylmethane sulphonate) mutagenized population (E. Gilchrist et al., unpublished data), a mutant was identified and was named *lamina epiphylla* or *lip* because of the abnormal "lips" or epiphyllous outgrowths present on the abaxial surface of the leaves. The accession number for this line is CT0229-2. For wild type comparison, the parent genotype (DH12075) was used.

2.3.2 Morphological and anatomical analyses

Photographs were taken of both *lip* and wild type canola plants to document their overall morphology (macroscopically as well as with the aid of a stereomicroscope). Plant parts were collected and either hand-sectioned fresh or fixed in 70% formalin acetic acid alcohol (FAA) for resin embedding. Petioles were sectioned by hand and photographed using a Nikon Coolpix 4500 digital camera (Nikon Corp., Tokyo, Japan) mounted onto a Motic stereomicroscope (Ted Pella Inc., Redding, CA, USA). The hand-sectioned tissues were stained with 0.1% phloroglucinol in ethanol and hydrochloric acid (HCl). Some petiole hand-sections were stained with potassium iodide (IKI) following the method of Mano et al. (2006), to identify starch deposition, and some sections were photographed unstained. Small leaves were cleared using modified method No. 1 described by Fuchs (1963), mounted onto slides with Permount mounting medium (Fisher Scientific, Whitby, Ontario, Canada), and

photographed with a stereomicroscope. Tissues not used for hand-sectioning were embedded into LR White Resin according to methods previously described (see Chapter 1). The embedded tissues were sectioned and sections were mounted onto slides, which were further mounted and photographed using methods described in Chapter 1.

2.3.3 Molecular analysis

DNA was extracted from both *lip* mutant and wild-type canola leaves using Plant DNAzol Reagent (Invitrogen, Burlington, Ontario, Canada). Quality and concentrations of DNA were measured with a NanoDrop ND-1000 spectrophotometer (Thermo Scientific, Wilmington, DE, USA). Primers were designed, using Primer3 (http://frodo.wi.mit.edu/primer3/; Rozen and Skatletsky 2000), to amplify the region surrounding the miRNA165/166 binding site (Juarez et al. 2004, Jung and Park 2007, Zhong and Ye 2004) of each of the five genes in the *HD-ZIPIII* family: *PHB*, *PHV*, *REV*, *ATHB8*, and *CNA* (Appendix A.1). PCR reactions were run using varying conditions (LIP or LIP2 PCR program: 94°C 4min, (94°C 40sec, 55°C or 50°C 30sec, 72°C 90sec) x35, 72°C 10min, 4°C hold). Actin (ACT-7) primers, previously used in Degenhardt and Bonham-Smith (2008), were used as positive controls while the negative control lacked template DNA. PCR samples were run on 1% agarose gel at 100V for 1-1.5 hours. Further, PCR samples or gel extracts (using MinElute Gel Extraction Kit, Qiagen) from samples that contained at least 20ng of product were sent for sequencing (between 50 and 60 samples for 8 *B. napus* genes) to a commercial sequencing service (DNA Landmarks, Saint-Jean-sur-Richelieu, QC).

2.3.4 Sequence analysis

Sequences were edited with Sequencher version 4.5 (Gene Codes Corporation, Ann Arbor, MI). The resultant sequences were deposited to NCBI GenBank (http://www.ncbi.nlm.nih.gov/genbank/), via BankIt, with the following nucleotide sequence names and accession numbers: *BnPHB.1* (JN975041), *BnPHV.1* (JN975040), *BnPHV.2* (JN975039), *BnREV.1* (JN975038), *BnATHB8.11* (JN975045), *BnATHB8.12* (JN975044), *BnCNA.1* (JN975043), and *BnCNA.2* (JN975042) (Appendix A.2).

2.3.5 Phylogenetic analysis

Genomic *HD-ZIPIII* sequences of *Arabidopsis thaliana* (*PHB* - AT2G34710, *PHV* - AT2G34710, *REV* - AT5G60690, *ATHB8* - AT4G32880, and *CNA* - AT1G52150) were downloaded from TAIR (http://www.*Arabidopsis*.org) (Table 2.1). *Brassica rapa* and *B. oleracea* (*B. napus* parent species) homologous sequences were obtained using BLASTN alignment with *Arabidopsis* gene sequences (including UTR and introns) using an E-value cut off of E-10, with default parameters (Appendix A.3). Along with the partial *B. napus* gene sequences (produced in this study), the *HD-ZIPIII* nucleotide sequences from the above three species were aligned with MUSCLE Multiple Sequence Alignment (EMBL-EBI; www.ebi.ac.uk) (Appendix A.4, available on attached CD). The resulting alignment was inspected but not manually readjusted due to a lack of variability of the final tree in the initial sensitivity test. The *B. rapa* and *B. oleracea* orthologs were chosen by filtering out sequences that did not align well or that produced unusually long branches in an initial maximum likelihood (ML) run.

In order to determine the optimal DNA substitution model for the sequences, the alignment file was run using jModelTest 2.0 (Guindon and Gascuel 2003, Posada 2008). The generalized time-reversible (GTR) model (with gamma correction for site-to-site variation and estimate of invariable sites) has the best fit to the data. Using this model, standard ML analysis was run with RAxML (Stamatakis et al. 2005) using default settings with 100 replicates. Bootstrap support values (calculated also with RAxML using default settings and 100 replicates) that had a value of 50% or greater, were reported on the resulting optimal ML tree.

2.4 Results

2.4.1 Discovery of *LIP* in EMS screen and segregation

In order to determine the nature of the allele causing the *lip* phenotype, the CT0229-2 mutant (M_2) was allowed to self and M_3 seeds were collected. The M_3 plants grown from these seeds showed three different phenotypes: wild type, moderate mutant, and severe mutant in a ratio of 21:44:22. This 1:2:1 ratio is typical of the segregation pattern seen from a single locus in which one allele has a semi-dominant mutation. Progeny testing of the M_3 plants identified only phenotypically wild type progeny (scored at four weeks; Appendix A.5) confirming that they were homozygous wild type and that the M_2 parent had been heterozygous for this mutation. M_3 plants with a moderate mutant phenotype similar to the parent were also allowed to self and the progeny scored for the *lip* phenotype at four weeks of age. All segregated with both wild type and mutant progeny in the M_4 generation consistent with the hypothesis that each was heterozygous. The phenotypic ratios seen in the M_4 varied from line to line, with an overall lower than expected number of moderately

mutant phenotypes relative to wild type and severely mutant phenotypes (Appendix A.5) indicating heterozygosity for this locus in the M_3 generation. Such segregation distortion could have occurred through mis-scoring of moderate mutant plants or other phenotypes. Mis-scoring of the highly variable phenotype (see below) could have been enhanced by the fact that the plants were scored at a relatively young (four weeks) age. Unfortunately, all of the severe mutant M_3 plants were sterile and the progeny could not be tested, although the segregation ratio suggests that these plants were homozygous for the *LIP* mutation. There were no fertile M_3 plants that were homozygous for the *LIP* mutation, indicating that either this mutation causes sterility or lethality when homozygous, or that there is a second mutation in this line that segregates with the *LIP* mutation and causes sterility when homozygous.

2.4.2 Overall plant morphology

Mature wild type *B. napus* (Figure 2.1A) plants are typically ~50 cm in height with flat leaves, full internode extension, and fully developed and elongated inflorescences. Putative heterozygous *lip* mutant plants (Figure 2.1B) having a moderate phenotype are similarly identifiable by flat leaves, but are shorter in stature (~20 cm in height) and have reduced stem and internode elongation, compared to wild type. Putative homozygous *lip* mutant plants (Figure 2.1C) showing a severe phenotype, are characterized by the presence of mostly trumpet-shaped and filamentous leaves with very contorted petioles, shorter stature (~10 cm in height), and an almost complete lack of internodal stem elongation.

2.4.3 Leaf variants

The wild type leaf (typically ~15 cm in length) is flat, bifacial with distinctly coloured adaxial (Figure 2.2A) and abaxial (Figure 2.2B) surfaces, and is typically ovate to pinnately lobed, with the deepest lobes occurring at the base of the lamina and extending down the petiole. Plants with a moderate *lip* phenotype typically produce leaves that are bifacial and flat (Figures 2.2C, 2.2D), but also contain adaxial ectopic epilaminar outgrowths on the abaxial leaf surface (Figure 2.2D), and develop trumpet-shaped and/or filamentous outgrowths along the petiole (Figures 2.2C, 2.2D). The severe *lip* phenotype, however, is characterized by trumpet-shaped leaves, which vary in size and shape (Figure 2.2E). A trumpet-shaped leaf consists of an adaxialized cup- or funnel-shaped blade (bracket in Figure 2.2E) and a long rounded unifacial petiole (arrowhead in Figure 2.2E). The lighter abaxial surface is located inside the cup while the darker-coloured adaxial surface is on the outside. The contorted petiole (Figures 2.2E, 2.2F) is unifacial, adaxialized, and generally does not contain lobes or outgrowths along its length.

Wild type transverse sections reveal that the adaxial side of the leaf consists of double palisade mesophyll cells while the abaxial side consists of spongy mesophyll (Figure 2.3A). Transverse sections through the trumpet-shaped blade show double palisade mesophyll cells marking the outside (adaxial) side of the trumpet or cup, while spongy mesophyll is present on the abaxial side (inside of the cup) (Figure 2.3B). Darker-coloured epiphyllous laminar outgrowths are occasionally present on the internal abaxial surface of trumpet-shaped leaves and commonly on the abaxial surface of flat leaves (Figure 2.3C). In section, the darker surface of the outgrowths (Figure 2.3C) clearly consists of palisade mesophyll and corresponds to adaxial surface (Figure 2.3D). The abrupt transition on the margins of the

epiphyllous outgrowth between the adaxial surface of the outgrowth and the abaxial surface of the blade is clearly visible. Occasionally, plants exhibiting a severe phenotype produce filamentous leaves and consist almost entirely of a unifacial petiole with some blade remnants at the distal portion of the leaf (Figure 2.2E).

2.4.4 Petiole anatomy

Flat wild type and flat moderate *lip* mutant leaves are very similar in their vascular arrangement and usually have three vascular traces entering the leaf blade through the petiole (Figures 2.4A, 2.4B). In the severe *lip* mutant phenotype, however, a single vascular trace enters through the petiole into a trumpet-shaped leaf blade (Figure 2.4C). Although stem anatomy is similar in wild type and *lip* plants, the petiole anatomy is not. Transverse sections through wild type petiole show distinct abaxial and adaxial surfaces where the former comprises about three-quarters of the circumference and the latter comprises the remaining one-quarter (Figure 2.4D). Sections through petioles of plants showing a moderate phenotype show increased adaxial surface and reduced abaxial surface, with similar distribution of each surface along the circumference (Figure 2.4E). Finally, the petiole of a trumpet-shaped leaf (severe phenotype) is unifacial, circular in transverse section, and consists entirely of adaxial surface (Figure 2.4F).

The amount of adaxial and abaxial surface is closely correlated with the arrangement of the vascular traces in the petiole. Only collateral vascular bundles are found in sections of wild type petioles (Figure 2.4G), where the xylem is located in a central position while the phloem is adjacent but closer to the outside (abaxial) part. Most vascular bundles in moderate *lip* phenotype mutant leaves are collateral as well, but some are almost amphivasal with

xylem tissue partially surrounding the phloem (Figure 2.4H). The vascular bundles of severe *lip* mutant petioles are almost always completely amphivasal (Figure 2.4I), where xylem entirely surrounds the centralized phloem.

Petioles, particularly in putative homozygous plants with a severe phenotype, are very contorted and appear to have lost gravisensing ability. Recently, Mano et al. (2006) have indicated that starch-storing plastids (amyloplasts) tend to accumulate in cells on the abaxial surface of the petiole in *Arabidopsis*. The sedimentation of these amyloplasts under gravity is implicated in gravisensing. Sections of canola petioles show that there is starch deposition in wild type petioles on the abaxial surface adjacent to the margin between abaxial and adaxial surfaces while amyloplasts were not found in adaxialized *lip* petioles as the relevant tissues were not present (results not shown).

2.4.5 Characteristics of other plant organs

Transverse sections of wild type and severe *lip* phenotype stems (Appendix A.6A, A.6B) are very similar, although the wild type stem contains white spongy pith in the centre. The vasculature in both wild type and *lip* stem sections has a collateral arrangement. The primary difference in the stem anatomy of *lip* plants is the presence of amphivasal vascular bundles in the leaf traces around the periphery (Appendix A.6D), but these traces are collateral in wild type (Appendix A.6C). No obvious phenotype was observed in the roots of the *lip* mutant plants (Appendix A.6E, A.6F).

In *lip* flowers, dorsiventral polarity is affected in some leaf-derived organs, such as petals and sepals, while the external appearance of the stamens and pistils appears to indicate that these are more or less equivalent to wild type (Appendix A.7). Elongation of the

contorted and somewhat fasciated inflorescence stem, which appears to consist of fused pedicels, is impeded due to the tight packing of flowers. The overall size of flowers does not seem to be affected by this mutation.

2.4.6 Ortholog determination

Compared to five *Arabidopsis HD-ZIPIII* genes, ten *B. rapa* and nine *B. oleracea HD-ZIPIII* sequences were identified (Table 2.1). Along with eight *B. napus* sequences, these were used in ML phylogenetic reconstruction. Five distinct clades were observed in the resulting tree, corresponding to each of the five *Arabidopsis* genes (*PHB*, *PHV*, *REV*, *ATHB8*, and *CNA*), all with high bootstrap support (Figure 2.5). In each of the clades, the *Arabidopsis* gene is the sister group of the *Brassica* genes in all cases except where *B. rapa* and *B. oleracea REV* genes (*BrREV.3* and *BoREV.3*) fall outside of the clade, as the sister group of *Arabidopsis REV* and other *Brassica* genes, with high bootstrap support. There are generally two copies of each *B. rapa* and *B. oleracea* genes per single *Arabidopsis* gene, except in the cases of (1) *PHV*, where each *Brassica* has a single copy of the gene, (2) *ATHB8*, where only a single *B. oleracea* ortholog has been identified, and (3) *REV*, where three *B. rapa* and three *B. oleracea* orthologs have been determined (although *BrREV.3* and *BoREV.3* group together and appear to be less closely related to the rest of the clade).

Since *Arabidopsis* genes defined the deepest splits in each clade, in most cases, each clade was further divided into subclades, corresponding to two distinct gene copies in the *Brassica* species. The grouping of each of the PHB subclades was moderately well supported where each of the subclades contained one *B. rapa* and one *B. oleracea* gene copies. The

sequenced *B. napus PHB* gene was most closely related to the *PHB* genes in subclade 1 (*BrPHB.1* and *BoPHB.2*), with 99% bootstrap support.

Each of the sequenced *PHV* genes in *B. napus* grouped with each of the parental copies with high and low support (*BnPHV.1* and *BnPHV.2*, respectively). The grouping of the REV subclades was supported with 100% bootstrap value. *Brassica napus* sequence was most closely related to *B. rapa REV* gene in subclade 1 (*BrREV.1*).

The grouping of ATHB8 subclades or *BrATHB8.1* (the only gene in subclade 2) as sister to the rest of the subclade was supported with high bootstrap value. Both *B. napus ATHB8* sequences fall into subclade 1, with *BnATHB8.11* grouping with *BoATHB8.1* (64% bootstrap support). *BrATHB8.2* and *BnATHB8.12* placed as sister to this grouping with 71% and 100% bootstrap support, respectively.

Finally, two CNA subclades were grouped with low bootstrap support. *BnCNA.1* sequence was sister to *BoCNA.1* in subclade 1 with 78% bootstrap support, while *BnCNA.2* fell into subclade 2, sister to the *B. oleracea* and *B. rapa* grouping, with 81% bootstrap support.

2.4.7 Testing for genetic change in miRNA binding site

The *lip* phenotype is suggestive of previously described *HD-ZIPIII* mutants. Because the genome sequence of *B. napus* is not publically available, genomic or EST sequences predicted to be homologous to the *Arabidopsis HD-ZIPIII* genes were downloaded from GenBank or the Brassica BLAST Server (http://brassica.bbsrc.ac.uk/). Primers were designed to amplify segments of *B. napus HD-ZIPIII* genes (that flanked the miR165/166 binding site) for each identified locus. At least one putative homolog from each of the five *Arabidopsis*

genes (*PHB*, *PHV*, *REV*, *ATHB8*, and *CNA*) was amplified and sequenced (Appendix A.2) but no mutations were identified in the miRNA binding site in any of the loci sequenced. The *LIP* mutation is expected to be heterozygous in this mutant, so if the mutation had been located in one of the sequenced genes, a double peak (wild type and mutant alleles) in the chromatogram at the site of the mutation would have been observed.

2.5 Discussion

2.5.1 Background to discovery of the *lip* mutant

Brassica napus is an important oilseed crop that has been the subject of a reverse genetics project by the Canadian Tilling Facility (CAN-TILL: http://www.botany.ubc.ca/can-till/CAN-TILL.html). As part of the CAN-TILL project (E. Gilchrist et al., unpublished) a population of more than 4000 lines of *B. napus* cv. DH12075 was developed for screening for mutations in genes of interest to requesting researchers and the public.

Chemical mutagenesis using EMS or ethyl nitrosourea (ENU) induces point mutations in DNA in all species in which it has been tested. Induced mutations can be divided into either loss-of-function, causing null or hypomorphic phenotypes or modification/gain-of-function mutations, causing neomorphic or hypermorphic phenotypes (Wilkie 1994). While hypomorphic, or loss-of-function alleles may be most useful for determining wild type gene function, neomorphic or hypermorphic alleles are more likely to be dominant and so typically are more likely to cause an observable phenotype in genes with a high degree of redundancy, such as duplicated genes. The frequency of missense alleles (i.e., mutations resulting in a change of amino acid) is on average three times higher than that of nonsense alleles (e.g., premature stop codons) (Greene et al. 2003), but it is difficult to

predict how many of the former mutations will have an effect on gene function since many of the missense mutations may not alter the gene product significantly. Examples of dominant point mutations that do have an effect on gene function have, however, been well documented in several cases, for example in plant hormone responses (Wang et al. 2006, Biswas et al. 2009), host-pathogen defense (Eckardt 2007), and adaxial-abaxial leaf polarity (Juarez et al. 2004, Byrne 2006).

2.5.2 Why is the *lip* mutant special?

Adaxialized mutants have intrinsic interest as adaxialized organs are rare in nature. The question of why adaxialized leaves are much less common in nature than abaxialized leaves has not been fully resolved. However, it may be that the adaxialized phenotype is more extreme and therefore less likely to survive in nature. Stems have a single, abaxial, surface due to the orientation of the vasculature, and therefore an abaxialized leaf tends to become stem-like (Cronk 2009). In an evolutionary context this may have considerable advantages. However, an adaxialized leaf is neither stem-like nor leaf-like.

The stem can be thought of as a unifacial organ in which the periphery consists of abaxial surface, with which phloem is associated, while xylem is created toward the centre (axis) of the stem (comprising the adaxial domain). The bottom of a leaf or any lateral organ is, therefore, continuous with the abaxial surface of the outside of the stem while the adaxial surface or domain on top of the lateral organ has to develop independently (Cronk 2001). In order to form the adaxial surface on a leaf, expression of abaxial identity genes (primarily *YABBY* and *KANADI* genes) is required in that region allowing for the juxtaposition of adaxial and abaxial domains and hence lateral outgrowth (Waites and Hudson 1995).

The *lip* mutant phenotype of *B. napus* is certainly a dramatic one. The plant has shorter stature due to the lack of internode elongation, and also exhibits aberrant leaf development. The wild type plant displays flat bifacial leaves, while *lip* plants with severe phenotype develop strikingly adaxialized and trumpet-shaped leaves, where the adaxial surface is on the outside of the trumpet and the abaxial surface comprises the inner surface of the blade. The petiole of such plants is unifacial, long, contorted, and also has a strongly adaxialized internal anatomy, with radialized or amphivasal vascular bundles.
Mutant plants with a moderate phenotype provide an intriguing "intermediate" state between the wild type and severely mutant plants. These generally have flat bifacial leaves, much like wild type, but also develop areas of ectopic epilaminar outgrowths of adaxial lamina on the abaxial surface of leaves. Such leaves may be useful as developmental models for studies seeking to determine the origin and maintenance of abaxial and adaxial identity.

2.5.3 Comparison of *lip* to known *Arabidopsis* mutants

The *lip* mutant is in many respects similar to *Arabidopsis* gain-of-function mutants in *HD-ZIPIII* genes. This raises the intriguing question of whether they are caused by a comparable mutation in the same gene family. Unlike, *Arabidopsis*, *B. napus* is much woodier, contains lobed leaves (rather than simple), and so phenotypes in *B. napus* are unlikely to exactly reflect those in *Arabidopsis*.

Mutations in the *REV* gene have been well documented in *Arabidopsis* producing a few mutants including *avb1* (*amphivasal vascular bundle 1*; Zhong and Ye 1999, Zhong and Ye, 2004), *ifl1* (*interfascicular fibreless 1*; Otsuga et al. 2001, Zhong and Ye 1999), and several other allelic mutations including *rev-1, rev-6, rev-9, rev-10d* (Emery et al. 2003,

Otsuga et al. 2001, Talbert et al. 1995). *avb1* is the only mutation in the *REV* gene which clearly affects the polarity of leaves within the plant. This semi-dominant mutation, within the miRNA binding site, appears to have the effect of transforming the vasculature into the amphivasal pattern and forming adaxialized leaf and flower organs (Zhong and Ye 2004), as seen in *B. napus lip* mutant. Unlike *lip*, however, the *avb1* mutation causes quite an extreme phenotype, transforming all vasculature into the amphivasal pattern, including in the stele and in all leaf variants (i.e., flat, trumpet-shaped, and filamentous) (Zhong and Ye 2004).

The dominant *phb-1d* mutation, which occurs in the START domain, of *Arabidopsis PHB* gene produces a similar mutant phenotype to *lip* and the stele vasculature is not obviously affected, with amphivasal bundles only occurring as leaf traces and in the petiole (McConnell and Barton 1998, McConnell et al. 2001). These mutations were found to affect the miR165/166 binding site in these genes, thus explaining their dominant effects (Rhoades et al. 2002). There is variation in the degree of vascularization in these mutants, where the severe mutant phenotype has leaves without a vascular strand, while plants with the moderate mutant phenotype can develop a single xylem strand in the place of normal/full vasculature (McConnell and Barton 1998). The canola *lip* mutation was not observed to cause an extreme phenotype (such as reducing the vasculature to a single strand or eliminating it altogether), at least in heterozygous plants, nor was the vascular arrangement within the stele obviously affected. But the possibility of the *lip* mutation being located within the *B. napus PHB* or *REV* genes cannot be ruled out, due to the morphological and genetic difference between *B. napus* and *Arabidopsis*. It is also possible that the reason for the more severe phenotype in *Arabidopsis* might be because of its dominance, as there is only a single *PHB* gene in this species, but likely more than one in *B. napus*.

2.5.4 Possible molecular explanations for the *lip* mutation

The similarity of phenotypes suggests that *HD-ZIPIII* genes are possible candidates for the *B. napus lip* mutation. How then might changes in *HD-ZIPIII* genes at the molecular level be responsible for the *lip* phenotype? Preliminary segregation analysis indicates that the *LIP* mutation behaves as a single locus and is semi-dominant. This dominance suggests that it may be due to a gain-of-function mutation rather than a loss-of function, which would normally cause a recessive phenotype. This hypothesis is consistent with gain-of-function mutations that have been found in other plants in *HD-ZIPIII* gene(s) that also exhibit dominant or semi-dominant phenotypes (e.g., *avb1* and *phb-1d*) rather than loss-of-function mutation in other genes in this pathway such as *KANADI* or *YABBY* that cause a similar phenotype (Chitwood et al. 2007).

Another piece of evidence that is consistent with the hypothesis that one of the *HD-ZIPIII* genes may be responsible for the *lip* phenotype is the fact that *lip* mutants appear to lack normal gravitropism in their petioles, as evidenced by the extremely contorted petioles observed mainly in plants with severe phenotype. *HD-ZIPIII* genes play a role in auxin transport (Ariel et al. 2007), and this hormone has been shown to be involved in gravitropism. However, the mutant plants also lack amyloplast-containing tissue, which may instead explain the lack of normal gravitropism, since sedimentation of amyloplasts in typical leaf petioles is a major mechanism for controlling gravitropism (Mano et al. 2006).

2.5.5 How many *HD-ZIPIII* genes are found in *Brassica*?

The *HD-ZIPIII* gene family consists of five members in *Arabidopsis* (*PHB, PHV, REV*, *ATHB8*, and *CNA*). *PHB* and *PHV* genes are very closely related to each other and have many overlapping functions such as leaf polarity determination and development (Ariel et al. 2007). *ATHB8* and *CNA* genes are more closely related to each other than to the other *HD-ZIPIII* genes. *ATHB8* is the primary molecular marker for xylem development in early developmental stages (Kang et al. 2003). *CNA* is important in vascular development, but it also functions as a meristem regulator, along with *PHB* and *PHV* (Green et al. 2005, Ariel et al. 2007). The *REV* gene, like *PHB* and *PHV*, has functions in maintaining the adaxial domain, and functions to maintain and develop xylem, similar to *ATHB8* and *CNA* (Zhong and Ye 2004).

While the *Arabidopsis HD-ZIPIII* gene family consists of five members, *B. napus* should likely contain twice as many copies since it is a tetraploid species originating from a cross between the two of the diploid *Brassica* species (*B. oleracea* and *B. rapa*) (U 1935). This study identified, on average, only two genes in *B. oleracea* and two in *B. rapa*, for every *Arabidopsis HD-ZIPIII* ortholog. Previous studies have indicated that there is strong evidence for the diploid *Brassica* species having a triplicated genome compared to *Arabidopsis* (Lagercrantz 1998, Lukens et al. 2004, Lysak et al. 2005, Town et al. 2006, Lysak et al. 2007, Hong et al. 2008, Mun et al. 2009, Carlier et al. 2011, Wang et al. 2011b). Therefore, *B. rapa* and *B. oleracea* might be expected to contain as many as three copies of each gene for each *Arabidopsis* ortholog. *Brassica napus*, with its relatively recent origin (~500 years; Gomez-Campo and Parakash 1999), should contain twice the number of genes

of its diploid progenitors since it has likely undergone relatively limited rearrangements (Parkin et al. 2003). It is possible, therefore, that *B. napus* may carry up to six copies of each *Arabidopsis* ortholog. When looking at the five *Arabidopsis* genes of interest, it would appear possible that *B. napus* might carry up to 30 loci. However, the *HD-ZIPIII* gene family in *B. rapa* and *B. oleracea* have been identified from the complete genome sequences of these species and consist of ten and nine known genes, respectively. This represents an overall duplication rather than a triplication of this gene family and so it may be that a likely estimate of the size of the *B. napus HD-ZIPIII* gene family is fewer than 20 members.

Whatever the precise number, the degree of potential redundancy is enormous. Therefore if a mutation occurs in a single *B. napus* gene, while the other paralogs remain unchanged and retain their normal function, the resultant phenotypes are likely to be less severe than if all of the paralogous genes were altered. The significance of this for mutagenesis screens in polyploid species such as *Brassica napus* is considerable: not only are phenotypes likely to be less extreme, but also, because dominant mutations (such as *lip*) are more likely to cause a phenotype than recessive mutations, they will be detected at a higher relative frequency compared to similar screens in *Arabidopsis*.

2.6 Conclusions

This study characterized the novel phenotype of *Brassica napus lip* mutant using anatomical and morphological methods. The mutant exhibits a strongly adaxialized phenotype and is shown to be similar to known phenotypes in *Arabidopsis* resulting from gain-of-function mutations in *HD-ZIPIII* genes. In other plant species, many of these mutations are caused by a point mutation that has occurred in the miR166/165 binding site of

one of the *HD-ZIPIII* genes. Currently available genomic resources allowed us to characterize eight of the putative 20 *HD-ZIPIII B. napus* genes. These have been sequenced and placed into a phylogeny along with the currently known *B. rapa* and *B. oleracea* orthologs. None of the sequenced *B. napus HD-ZIPIII* genes have been shown to carry a mutation in the *lip* mutant. As further genomic resources become available, it will be easier to examine additional *HD-ZIPIII* genes in this species, and the analyses given here should facilitate that process.

Table 2.1 *HD-ZIPIII* gene names of *Arabidopsis thaliana* and the identified orthologs of *Brassica rapa*, *Brassica oleracea*, and *Brassica napus*.

A. thaliana **gene name**	***B. rapa*** **ortholog names**	***B. oleracea*** **ortholog names**	***B. napus*** **ortholog names**
PHABULOSA (PHB)	*BrPHB.1* *BrPHB.2*	*BoPHB.1* *BoPHB.2*	*BnPHB.1*
PHAVOLUTA (PHV)	*BrPHV.1*	*BoPHV.1*	*BnPHV.1* *BnPHV.2*
REVOLUTA (REV)	*BrREV.1* *BrREV.2* *BrREV.3*	*BoREV.1* *BoREV.2* *BoREV.3*	*BnREV.1*
ARABIDOPSIS THALIANA HOMEOBOX 8 (ATHB8)	*BrATHB8.1* *BrATHB8.2*	*BoATHB8.1*	*BnATHB8.11* *BnATHB8.12*
CORONA (CNA)	*BrCNA.1* *BrCNA.2*	*BoCNA.1* *BoCNA.2*	*BnCNA.1* *BnCNA.2*

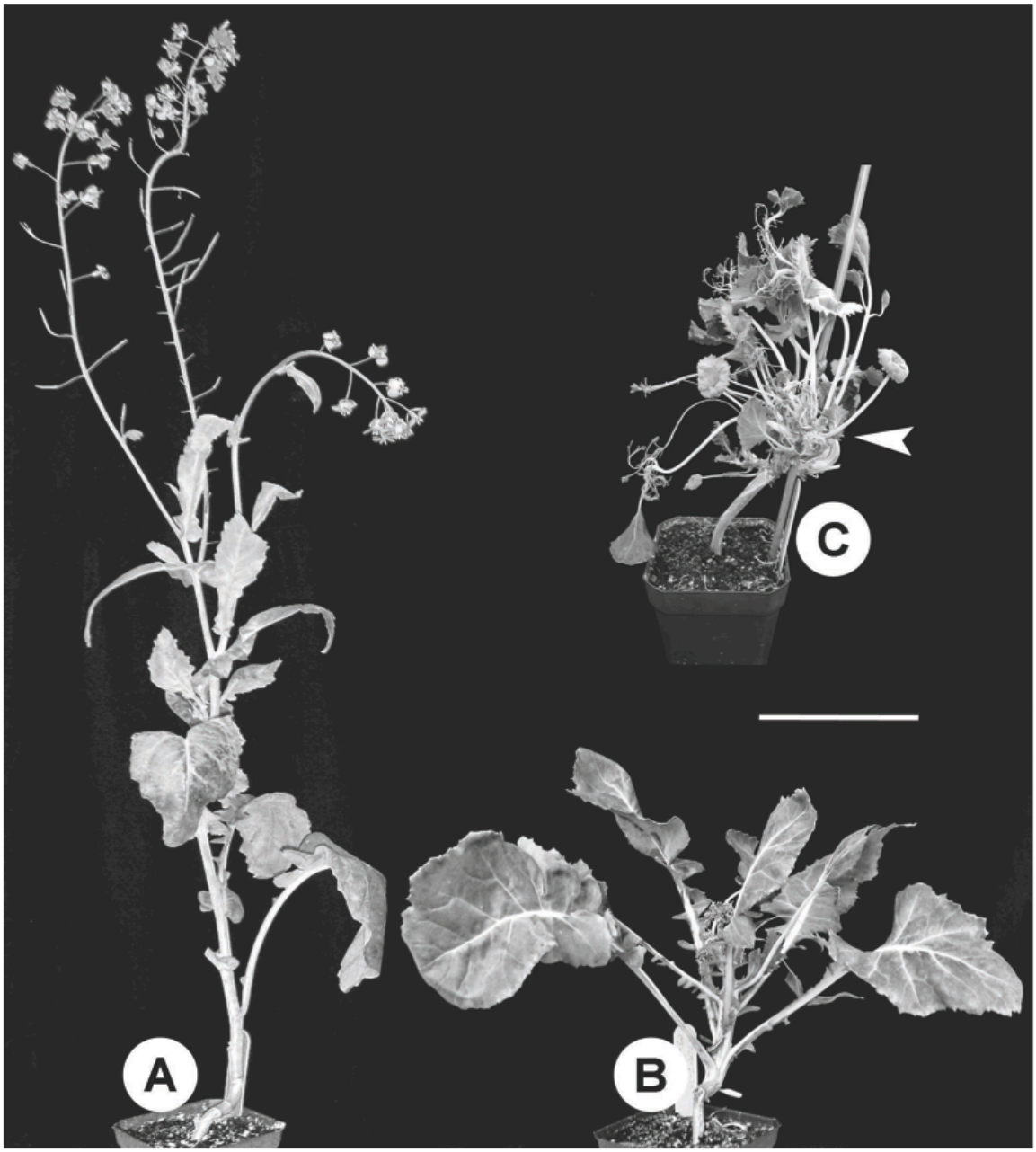

Figure 2.1 Whole plant morphology. A. Mature wild type *B. napus* plant (~50cm in height), ~1.5 months old, with flat leaves and full internode extension. B. Heterozygous *lip* mutant plant, ~1.5 months old, is identifiable by flat leaves, shorter stature (~20 cm in height), and reduced stem/internode elongation. C. Homozygous *lip* mutant plant, ~3.5 months old, is characterized by the presence of mostly trumpet-shaped and filamentous leaves with very contorted petioles, shorter stature (~10cm in height), and a nearly complete lack of stem elongation (arrowhead). Scale bars = 10cm.

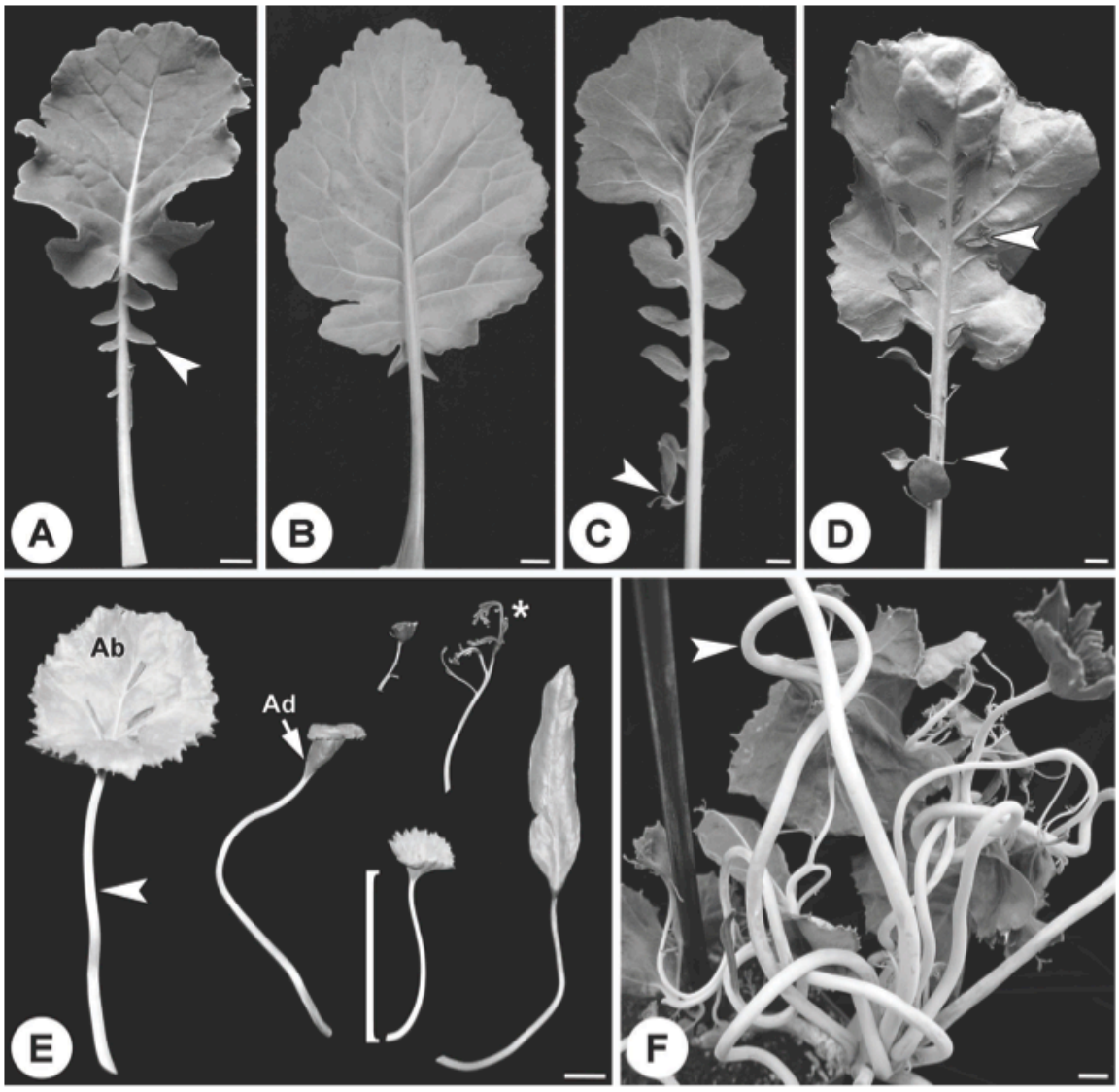

Figure 2.2 Whole leaf morphology. A. The wild type leaf (~15cm in length) is flat, bifacial with distinct adaxial (darker colouration, shown here) and (B) abaxial (lighter) surfaces, and typically ovate, with lobes (arrowhead in A) extending down the petiole. C. Plants with a moderate *lip* phenotype typically produce leaves that are bifacial and flat, but also contain adaxial ectopic epilaminar outgrowths on the (D) abaxial leaf surface (top arrowhead), and the development of trumpet-shaped and/or filamentous outgrowths along the petiole (bottom arrowhead and arrowhead in C). E. The severe *lip* phenotype is characterized by various sizes and shapes of trumpet leaves. A trumpet-shaped leaf consists of an adaxialized cup-shaped blade (bracket) and a long unifacial petiole (arrowhead). The lighter abaxial surface is located inside the cup while the darker-coloured adaxial surface is on the outside. Occasionally, plants exhibiting severe phenotype produce filamentous leaves (asterisk) that consist almost entirely of a

unifacial petiole with some blade remnants at the distal portion of the leaf. F. The leaf petioles of severe phenotype *lip* mutants have very contorted petioles (arrowhead) and appear to lack gravisensing ability. Ad – adaxial surface, Ab – abaxial surface. Scale bars = 1cm.

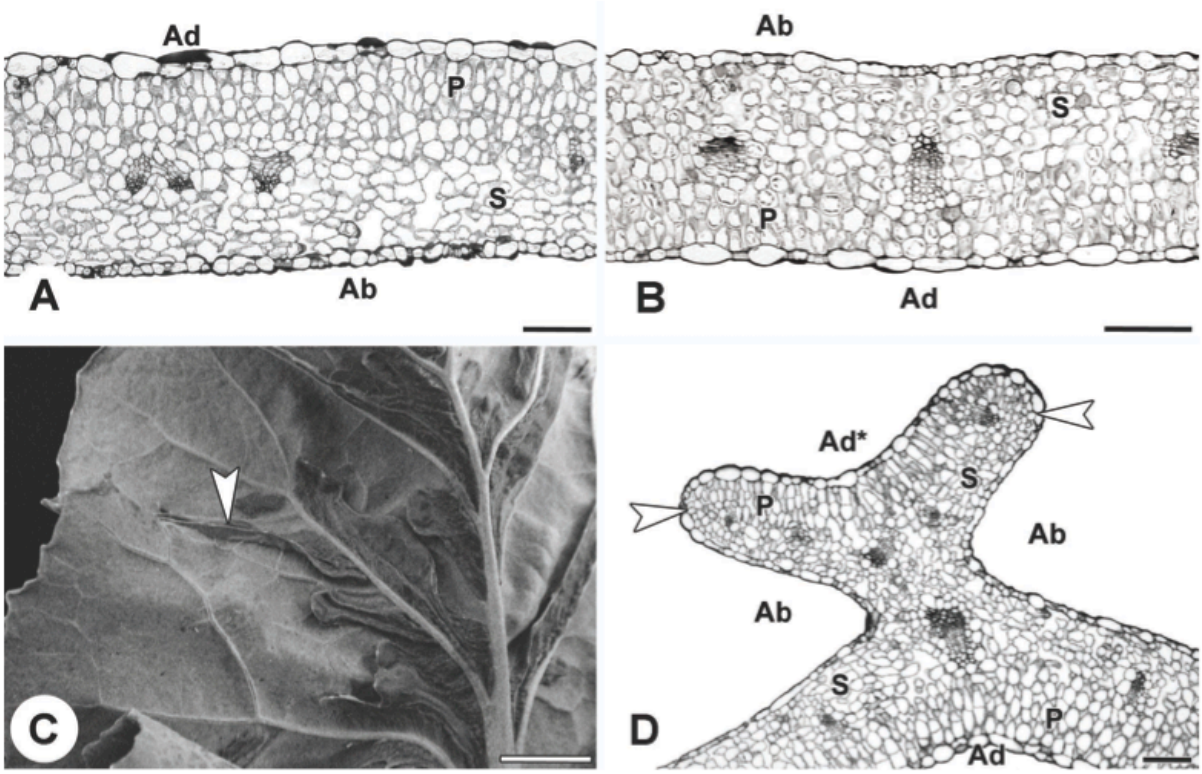

Figure 2.3 Leaf blade anatomy. A. The bifaciality of the wild type leaf blade is indicated in transverse section by the presence of double palisade mesophyll cells in the upper adaxial surface and spongy mesophyll cells in the lower abaxial surface. B. Transverse section through the trumpet-shaped blade shows double palisade mesophyll cells in the outside adaxial surface and spongy mesophyll in the abaxial on top or inside. C. Darker-coloured ectopic epilaminar outgrowths are occasionally present on the abaxial surface of leaves (arrowhead). D. In section, the darker surface of the outgrowths clearly consists of palisade mesophyll cells. Arrowheads indicate the abrupt transition between the adaxial surface of the ectopic epilaminar outgrowth and the abaxial surface (consisting of spongy mesophyll cells) of the internal surface of the trumpet-shaped blade. Ad – adaxial surface, Ab – abaxial surface, P – palisade mesophyll, S – spongy mesophyll, Ad* – ectopic adaxial surface. Scale bars = 100 µm (A, B, D) and 1cm (C).

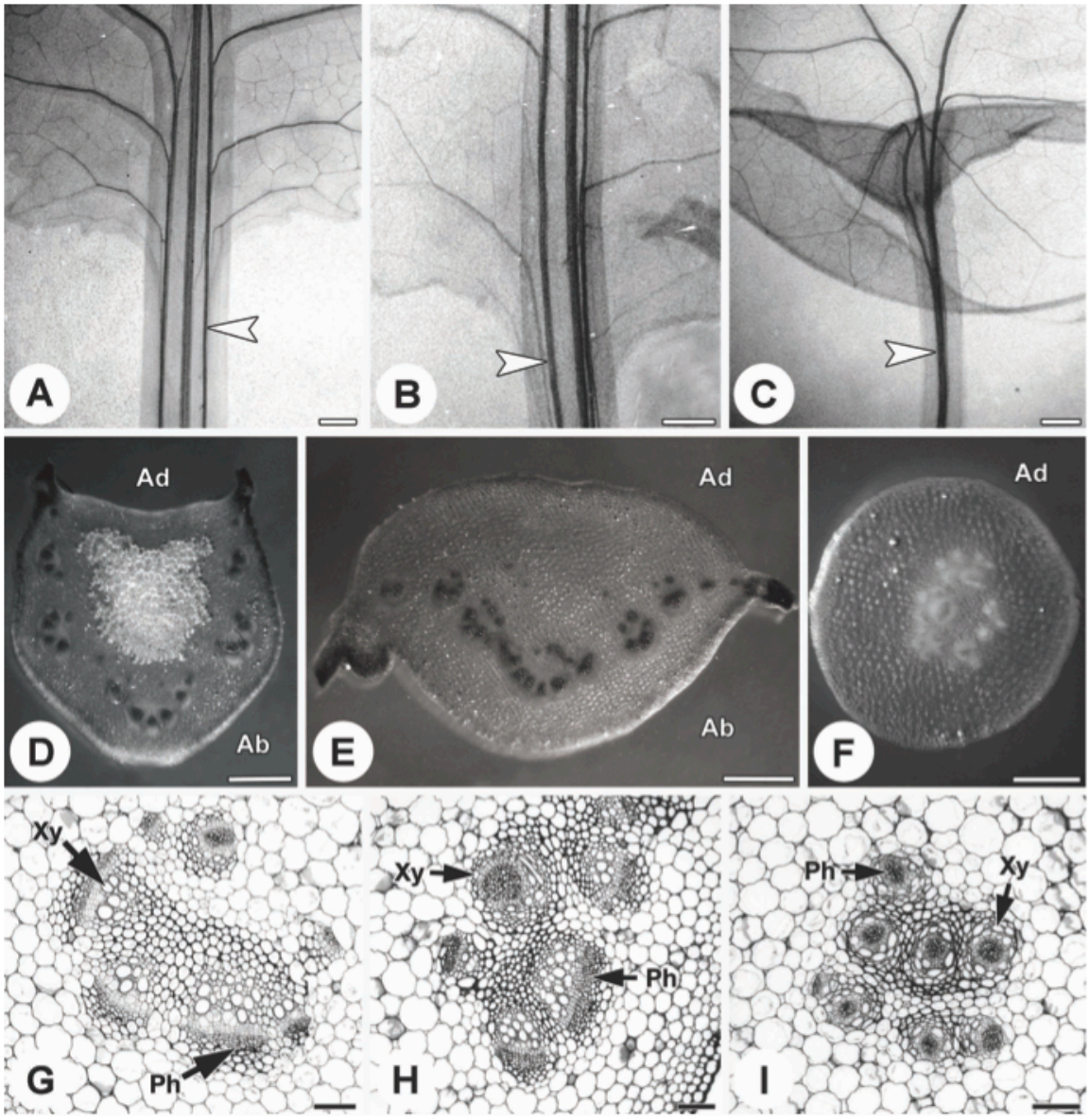

Figure 2.4 Petiole anatomy. A-C. Abaxial view of small cleared leaves: A. Wild type leaf with three vascular traces (arrowhead) entering through the petiole into the blade. B. Moderate *lip* mutant leaf with about two to three vascular traces (arrowhead) entering through the petiole into the blade. C. Trumpet-shaped leaf of severe *lip* mutant phenotype with a single vascular trace (arrowhead) entering through the petiole into the blade. D-F. Petiole transverse sections. D. Wild type petiole has distinct abaxial and adaxial surfaces. E. Moderate mutant petiole with an increased adaxial surface and a reduction of abaxial surface. F. Petiole of unifacial trumpet-shaped leaf (severe phenotype), which consists solely of

adaxial surface. G-I. High magnification of petiolar vascular bundles. G. A set of collateral vascular bundles found in wild type petioles. H. A set of vascular bundles, mostly collateral with some partially amphivasal, found in moderate phenotype plant petioles. I. A set of amphivasal vascular bundles found in severe *lip* mutant petioles. Ab – abaxial surface, Ad – adaxial surface, Xy – xylem, Ph – phloem. Scale bars = 1mm (A-F), 100µm (G-I).

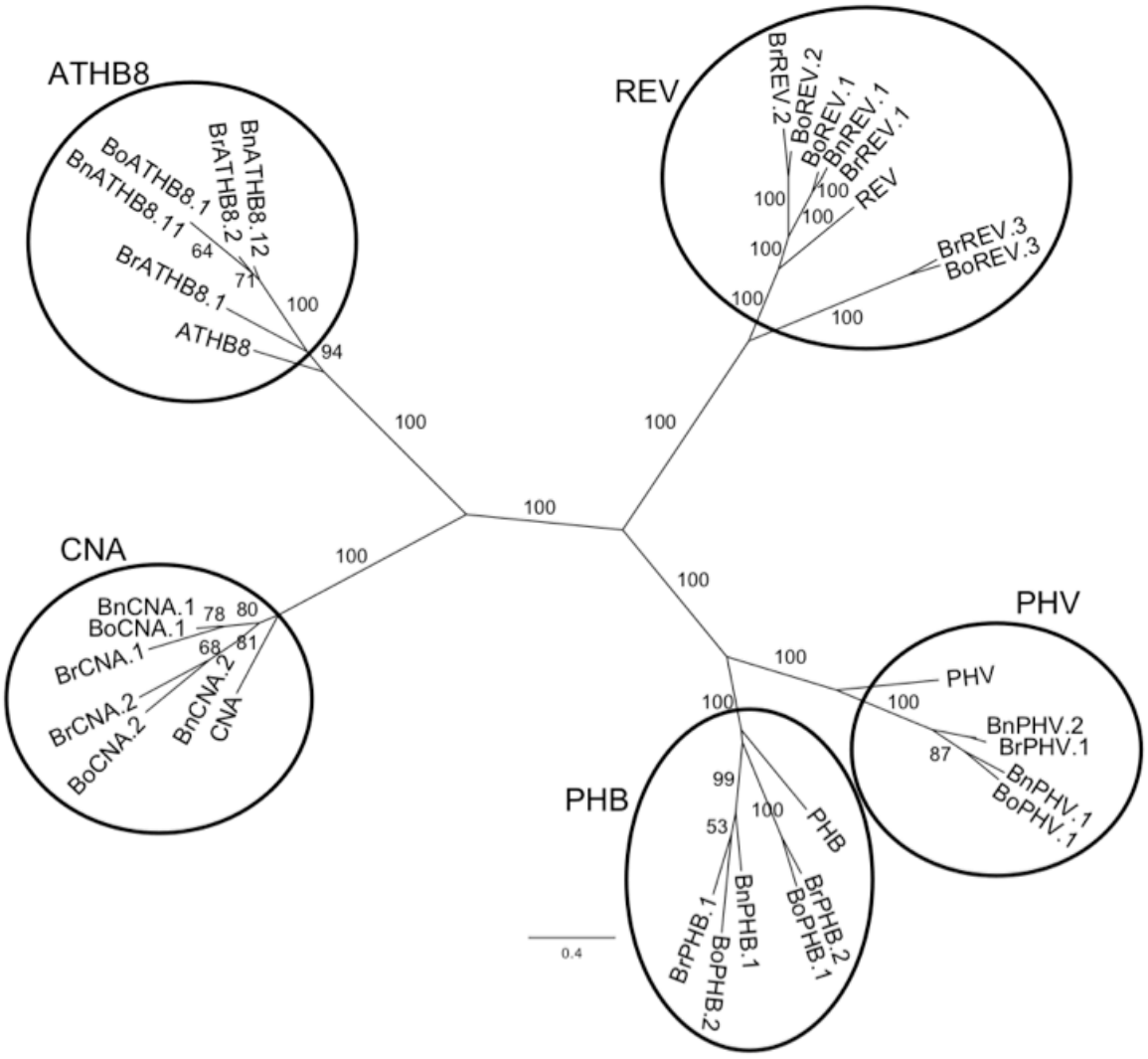

Figure 2.5 Maximum likelihood reconstruction of nucleotide sequences of *HD-ZIPIII* homologs from *Arabidopsis thaliana* (*PHB, PHV, REV, ATHB8, CNA*), *Brassica rapa* (Br), *Brassica oleracea* (Bo), and partial *Brassica napus* (Bn) sequences, with each major clade of genes identified (PHB, PHV, REV, ATHB8, and CNA). Only bootstrap support values greater than 50% are indicated.

Chapter 3: Phylogenomics and expression of dorsiventral polarity genes in leaves of forest trees

3.1 Synopsis

Populus and *Eucalyptus* are two genera that exhibit leaf heteromorphism, where leaf variants are present between species or within a single individual. The two types of leaf variants present are bifacial and isobilateral leaves that are also associated with a radial or a unifacial petiole, respectively. Due to the presence of the unifacial petiole in isobilateral leaves, leaf dorsiventral polarity genes are primary candidates for the underlying phenotype. I identified poplar and eucalyptus orthologs, belonging to three major gene families (i.e., *YABBY*, *KANADI*, and *HD-ZIPIII*). Generally, there were 2:1 and 1:1 ratios of poplar and eucalyptus genes for every *Arabidopsis* ortholog. I also analyzed the transcript levels from mRNA-seq data in order to determine genes that contribute to leaf and not xylem development and/or maintenance in these species. Similar patterns were observed in poplar and eucalyptus with primary expression of *YABBY* and *KANADI* genes found in leaves. *HD-ZIPIII* genes, however, were expressed in both xylem and leaf tissues. Two genes (*Pt-YAB2.1* and *Pt-ATS.2*) were of particular interest as they showed high levels of expression in poplar leaves, while their function in *Arabidopsis* does not appear to be fully conserved.

3.2 Introduction

Leaves are the primary photosynthetic organs contributing to increase in plant biomass. Their shape and diversity are determined by differentiation along the three axes of polarity: proximodistal, mediolateral, and adaxial-abaxial (dorsiventral). Dorsiventral

polarity in leaves is set by a complex gene network, including the mutually antagonistic actions of three gene families and their regulation by small RNA molecules (Kidner and Timmermans 2007). These are the *YABBY*, *KANADI*, and *HD-ZIPIII* gene families, all containing key genes contributing to the establishment and development of dorsiventral polarity in leaves.

3.2.1 Dorsiventral polarity genes

Genes of the *YABBY* family of seed-plant specific transcription factors maintain abaxial surface identity in lateral organs (Bowman 2000). The six members of the *YABBY* gene family in *Arabidopsis* include: *AFO/FIL* (*ABNORMAL FLOWER ORGAN/FILAMENTOUS FLOWER*), *YAB2*, *YAB3*, *INO* (*INNER NO OUTER*), *YAB5*, *CRC* (*CRABS CLAW*) (Bowman 2000). *AFO, YAB2, YAB3*, and *YAB5* are expressed to various degrees in the abaxial domain of all lateral organs (Siegfried et al. 1999, Bowman 2000). *AFO* and *YAB3*, in particular, can promote abaxial cell fate when ectopically expressed in the adaxial domain (Seigfried et al. 1999). Some *YABBY* genes are restricted to floral organs, particularly those with likely homology to leaves. The expression of *INO* is generally restricted to the inner ovule integument while *CRC* is expressed in nectaries and carpels (Bowman 2000).

KANADI genes are members of the GARP family of transcription factors, and as with the *YABBY* genes, their primary role is to establish the formation of the abaxial and peripheral domain (e.g., phloem in the vasculature) in lateral organs (Emery et al. 2003, Byrne 2005, Moon and Hake 2011). In *Arabidopsis*, there are four members belonging to the *KANADI* gene family: *KAN*, *KAN2*, *KAN3*, and *ATS/KAN4* (*ABERRANT TESTA SHAPE*).

They all control the abaxial domain of lateral organs (Emery et al. 2003), with *ATS* having a primary role in carpel development (McAbee et al. 2006, Kelley et al. 2009).

The *HD-ZIP* class *III* family is responsible for many important developmental mechanisms in plants. These primary functions include the establishment of the adaxial leaf surface and vasculature (primarily associated with xylem and the central domain), lateral meristem (Chitwood et al. 2007, Kidner and Timmermans 2007), and carpel development (Kelley et al. 2009). *HD-ZIPIII* family consists of five genes in *Arabidopsis*: *PHB* (*PHABULOSA*), *PHV* (*PHAVOLUTA*), *REV* (*REVOLUTA*), *ARABIDOPSIS THALIANA HOMEOBOX 8* (*ATHB8*), and *CNA/ATHB15* (*CORONA*) (Green et al. 2003, Kang et al. 2003, Ariel et al. 2007). *PHB, PHV*, and *REV* are developmental regulators of the leaf adaxial domain, and of vascular bundles, while the main function of *ATHB8* and *CNA* is the regulation of vascular development (Green et al. 2003, Kang et al. 2003, Ariel et al. 2007).

3.2.2 Why study poplar and eucalyptus?

Poplar and eucalyptus are important trees for the bioenergy and pulp and paper industries due to their rapid growth and wood production (Jansson and Douglas 2007, Hinchee et al. 2009, Lev-Yadun 2010), and because of the availability of genomic resources for both organisms (Tuskan et al. 2006, Myburg et al. 2008, 2012) they can be used as models for wood development. This has led to recent interest in the *HD-ZIPIII* genes in poplar (Ko et al. 2006, Coté et al. 2010, Du et al. 2011, Robischon et al. 2011). There are many leaf traits that are important for high photosynthetic rate and therefore an increase in biomass. Determining homologous sequences in *Arabidopsis* is the first step to dissecting out

the genetic controls of these desired traits in forest trees, including poplar and eucalyptus, because *Arabidopsis* is a well understood model plant system.

Both poplar and eucalyptus are known to exhibit leaf heteromorphism (King 1997, Cronk 2005, Wang et al. 2011a) that occurs between species in poplar and within a single individual in both poplar and eucalyptus. Some species of poplar (e.g., black cottonwood or *P. trichocarpa*) have bifacial leaves, where the adaxial surface consists of palisade mesophyll cells while the abaxial surface consists of spongy mesophyll cells (Kaplan 1997). Alternatively, leaves that contain palisade parenchyma on both the adaxial and abaxial sides are called isobilateral (e.g., aspen or *P. tremuloides*). Juvenile leaves in many eucalyptus species are bifacial while the mature adult phase leaf is isobilateral (e.g., *E. globulus* ssp. *globulus*; James and Bell 2001). The same is true for poplar where leaves that are isobilateral at vegetative maturity can have a bifacial phenotype while in the juvenile stage (as in *P.* x *canadensis*, for example; Wang et al. 2011a). This vegetative phase change from juvenile to mature leaves, an example of heteroblasty affects the leaf blade and petiole polarity, and variation in leaf phenotype between mature leaves of different poplar species also involves similar leaf polarity phenotypes.

3.2.3 Adaptive significance of leaf heteromorphism

The genus *Populus* is native to the Northern Hemisphere, and species with isobilateral leaves are usually associated with a long mediolaterally flattened petiole contributing to the "leaf flutter" syndrome (Cronk 2005). In a series of papers, Roden and Pearcy (1993a, b, c) have shown that leaf flutter syndrome contributes to overall carbon gain through the following mechanisms: 1) an increase in mean photon flux density in the lower

canopy allowing for a more even distribution of light throughout the tree (Roden and Pearcy 1993a); 2) an improvement in post-illumination CO_2 fixation, achieved by short sunflecks through the canopy (Roden and Pearcy 1993b); and 3) decrease in leaf temperature through an increase in boundary-layer conductance to convective heat exchange, significant to aspens growing in warmer climates (e.g., California), also increasing water use efficiency (Roden and Pearcy 1993c). A recent study by Yamazaki (2011) has suggested that leaf flutter can also deter herbivory. It is not clear how many of the 29 *Populus* species exhibit such heteroblastic development, but it is likely that species with isobilateral leaves at maturity belonging to sections *Abaso*, *Turanga*, *Aigeiros*, and *Populus,* corresponding to approximately half of the species within the genus, undergo vegetative phase change (Eckenwalder 1996b).

The genus *Eucalyptus* is native almost exclusively to Australia, which has a broad range of climactic regions ranging from arid to high rainfall zones. Approximately 12% of the 504 species in the genus have leaves that are bifacial at the adult stage (primarily in subgenus *Corymbia*), while the remaining 88% have isobilateral leaves (King 1997). The leaf angle in eucalyptus is an important feature associated with the leaf type where bifacial leaves are generally horizontally oriented, while isobilateral leaves typically hang in the vertical orientation. Vertically oriented or isobilateral leaves of eucalyptus species growing in arid regions allow a reduction in leaf temperatures and thus increase water use efficiency and carbon gain (King 1997). This is not as critical in regions where rainfall is more frequent. The benefit of isobilateral leaves in these regions can instead be attributed to efficiency of light interception at low sun angles that are common at high altitudes and decreasing cold-associated photoinhibition at low leaf temperatures (King 1997).

3.2.4 Objectives

The underlying genetic basis of the variation between bifacial and isobilateral leaves has not been investigated, although a recent study (Wang et al. 2011a) showed the importance of *squamosa protein binding-like* (*SPL*) genes and their interacting miRNAs during vegetative phase change or heteroblastic development in various plant species (including poplar and eucalyptus), transitioning from juvenile to mature leaf stages. There are clear morphological and anatomical differences between bifacial and isobilateral leaves that can be indicative of vegetative phase change, but the genetic basis of these traits may be rooted in dorsiventral polarity or may be controlled by other factors (Poethig 2010). Primary candidates for genes contributing to this difference in leaf morphology are members of *YABBY*, *KANADI*, and *HD-ZIPIII* gene families due to their effects on dorsiventral polarity in leaves.

Here I aimed to determine the orthology relations of the leaf polarity genes in the *YABBY*, *KANADI*, and *HD-ZIPIII* gene families in poplar and eucalyptus in relation to *Arabidopsis* and examine the levels of expression of these in leaf tissues in order to elucidate genes important in leaf development of these trees, using orthology to predict functional similarity.

3.3 Materials and methods

3.3.1 Ortholog identification

Arabidopsis thaliana amino acid sequences (six *YABBY*, four *KANADI*, and five *HD-ZIPIII*) were obtained from TAIR (http://www.arabidopsis.org/) and NCBI GenBank

(http://www.ncbi.nlm.nih.gov/genbank/). The sequences were BLASTed (tBLASTn) using Phytozome (http://www.phytozome.net; Goodstein et al. 2011) against *Populus trichocarpa* v2.2 (done in November 2010) and *Eucalyptus grandis* v1.0 (done in November 2011) genomes. All of the homologous sequences were selected based on maximum likelihood tree reconstructions. Larger data sets, which included all of the available amino acid sequences for Viridiplantae for each of the gene families (data not shown), were consistent with the results shown.

3.3.2 Phylogenetic analysis

The selected sequences were initially aligned using MUSCLE (Edgar 2004) and then using SATé (Simultaneous Alignment and Tree estimation) (Liu et al. 2009, Yu et al. 2011). Alignment with only MUSCLE, with SATé, and manually adjusted SATé alignment were all compared in a sensitivity analysis. Although some of the nodes had highest bootstrap support from simply aligning using MUSCLE, this program aligned the first amino acid (methionine) quite poorly. This was mostly corrected by SATé, although adjustments with manual alignment, particularly of the start and end of each sequence, were necessary to produce the final alignment used in this study (Appendix B.1, B.2, B.3).

According to ProtTest (http://darwin.uvigo.es/software/prottest_server.html; Abascal et al. 2005), the James Taylor Thornton (JTT) substitution model including parameters correcting for site-to-site variation (gamma and a separate parameter for invariable sites), and empirical base frequency estimates, had the best fit for all data sets. Maximum likelihood (ML) analysis, including 1000 bootstrap replicates, was run with RAxML (Stamatakis et al. 2005) and distance analysis was performed with PHYLIP (Felsenstein 1989, 2005), both

using default settings with 1000 replicates. ML and distance bootstrap support values were applied to ML trees and categorized based on high (greater than or equal to 80%), moderate (50-79%), and low (less than 50%) support. ML results are primarily presented here, with distance results discussed only where major differences from ML were observed.

3.3.3 Illumina mRNA-seq data and tissue preparation

The transcriptomes for *P. trichocarpa* and *E. grandis* were generated as part of larger projects (Geraldes et al. 2011 and Myburg et al. 2012, respectively). Three leaf and three xylem (from the main stem) samples were obtained from three separate individuals of poplar and eucalyptus, allowing for a direct comparison of transcript expression between leaf and xylem in each taxon. Poplar tissue preparation and sequencing followed the protocols reported previously by Geraldes et al. (2011) except that the mapping here was done onto v2.2 of the *P. trichocarpa* genome, while eucalyptus tissue was prepared and sequenced according to Mizrachi et al. (2010).

3.3.4 Poplar expression data analysis

Transcript expression levels were calculated as reads per kilobase of exon model per million mapped reads (RPKM) (Mortazavi et al. 2008) using scripts kindly provided by the Genome Sciences Centre (GSC; UBC). Mean and standard deviation values of the normalized coverage or RPKM expression levels of each of the *P. trichocarpa* orthologs were calculated for three young expanding leaf and three developing stem xylem sample replicates.

Paralogous gene pairs were compared using a paired t-test (significant p-value <0.05) to determine whether one of the genes had a significantly higher expression in leaf tissue compared to stem xylem, helping to elucidate genes important in leaf and not xylem function.

3.3.5 Eucalyptus expression data analysis

Gene models from the *E. grandis* (v1.0, Phytozome) genome sequence were used as input to TopHat (Trapnell and Salzberg 2009), to align the short reads to the genome sequence (C. Hefer, pers. comm.). Cufflinks was then used to calculate the fragments per kilobase of transcript per million fragments mapped (FPKM) values of transcript expression levels for each gene model in the annotated TopHat output file (Trapnell et al. 2010). Mean and standard deviation values of the FPKM expression levels of each of the *E. grandis* orthologs were calculated for three young expanding leaf and three developing stem xylem replicates. Paralogous pairs, when present, were compared using a two-paired t-test ($p \leq 0.05$), as in poplar.

Eucspresso (http://eucspresso.bi.up.ac.za) is a publicly available resource of assembled contigs from *Eucalyptus grandis* x *urophylla* hybrid (Mizrachi et al. 2010). The FPKM expression values were obtained for only some eucalyptus hybrid contigs corresponding to *E. grandis* orthologs because assembly of full-length genes did not occur in all cases (Mizrachi et al. 2010). Sequence similarity between *E. grandis* and eucalyptus hybrid contigs were determined with a MUSCLE alignment (Edgar 2004). The eucalyptus hybrid data were compared with *E. grandis* to determine similarities in levels and overall patterns of expression, and to determine patterns of expression in tissues other than young leaf and developing xylem, including mature xylem, mature leaf, phloem, and the shoot tip.

3.3.6 Characterization of expression levels

In order to describe the overall expression levels in poplar tissues, four categories were assigned to the mean resulting RPKM values: category I (no detectable expression) contains values less than 0.001 RPKM; category II (low expression) contains values ranging from 0.001 to 10 RPKM; category III (moderate expression) contains values ranging from 10.001 to 20 RPKM; and category IV (high expression) contains values greater than 20 RPKM.

The expression values for eucalyptus were categorized into the same types of groups as in poplar: category I (FPKM = 0), category II (FPKM between 0.001 and 10), category III (FPKM between 10.001 and 20), category IV (FPKM > 20). Expression values for poplar and eucalyptus were not directly compared, as they are measured in different units (RPKM for poplar and FPKM for eucalyptus), but instead the overall relative expression patterns were evaluated. However, it should be noted that a comparison of RPKM (v2.2) and FPKM (v2.0) values was made and these can in fact be directly compared (results not shown). Overall expression levels were also compared to the ranking of each gene in the genome in relation to all of genes with detectable expression or values greater than 0 RPKM or 0 FPKM, for poplar and eucalyptus, respectively, expressed as quartiles.

3.4 Results

3.4.1 Ortholog identification

The *Arabidopsis* genome contains six *YABBY*, four *KANADI*, and five *HD-ZIPIII* genes. Orthologous sequences from poplar and eucalyptus were identified with the general

pattern of gene number being two poplar genes and one eucalyptus gene for every one *Arabidopsis* gene (Table 3.1) with 13 and six *YABBY*, eight and six *KANADI*, and eight and four *HD-ZIPIII* genes found in the genomes of poplar and eucalyptus, respectively. Exceptions within the poplar genome are seen with *YAB2*, which has three poplar orthologs (*Pt-YAB2.1, Pt-YAB2.2, Pt-YAB2.3*), *KAN* that has four poplar orthologs (*Pt-KAN.1, Pt-KAN.2, Pt-KAN.3, Pt-KAN.4*), *KAN2* and *KAN3* that together have two orthologs (*Pt-KAN2/3.1, Pt-KAN2/3.2*), and *PHB* and *PHV* together also have two orthologs (*Pt-PHB.1, Pt-PHB.2*). In eucalyptus, on the other hand, a single gene corresponding to each of the *Arabidopsis* orthologs was determined (Table 3.1) with several exceptions: *KAN2* and *KAN3* have three orthologous genes (*Eg-KAN2/3.1, Eg-KAN2/3.2, Eg-KAN2/3.3*), *KAN* has two (*Eg-KAN.1, Eg-KAN.2*), and *PHB* and *PHV* have a single eucalyptus ortholog (*Eg-PHB/PHV.1*).

3.4.2 Phylogenetic analysis

ML tree reconstructions separate *YABBY* genes into five major groups (Figure 3.1A): *AFO/YAB3* with moderate bootstrap support, *YAB2* with low bootstrap support, *INO, YAB5*, and *CRC*, all with high support values (100%, 99%, and 100%, respectively). *AFO/YAB3* and *INO* clades are more closely related to each other, while *YAB2*, *YAB5*, and *CRC* clades group together, with high bootstrap support (81%). The position of the *YAB2* clade is variable and highly dependent on the alignment, as it can either group with *YAB5* (as presented here, with low bootstrap support), *INO* or *CRC* (when using other alignment variations, as described in Methods section). The grouping into five clades was found with distance analysis, although there were slight differences in ortholog arrangement within each clade and a major

difference in the placement of *Pt-YAB2.3* (results not shown). In distance analysis, the eucalyptus ortholog was sister to the two poplar paralogs with low support (56%) while *Arabidopsis YAB2* was sister to the rest of the clade, supported with high bootstrap value (84%) (results not shown).

The *KANADI* genes are grouped into two clear clades (Figure 3.1B): *KAN* and *ATS* with high support (100%, in both cases). *KAN2, KAN3*, and their orthologs are not monophyletic. However, the grouping of *KAN3* and *ATS* clade is supported with high bootstrap values (92%). Based on this grouping, it appears that *KAN3* does not have orthologous sequences in poplar and eucalyptus, and the orthologs that are present are more closely related to *KAN2*. As with *YAB2* genes, the positions of *KAN2* and *KAN3* within the ML tree are alignment-dependent and can group as sister to the rest of the clade (as presented here) or sister to the eucalyptus paralogs, or *KAN2* and *KAN3* group together as sister to the rest of clade (when using other alignment variations, as described in Methods section). In contrast to ML analysis, distance analysis groups *KANADI* genes into three distinct clades: *KAN* and *ATS* with high support (100% and 99%, respectively) and *KAN2/3* with low support (54%) (results not shown). The arrangement of the genes generally differs within each clade in distance analysis compared to ML.

The *HD-ZIPIII* genes are grouped into four clades (Figure 3.1C): *PHB/PHV*, *REV, ATHB8*, and *CNA*, all with high bootstrap support (100%, 100%, 95%, and 99%, respectively). *PHB/PHV* and *REV* clades are more closely related to each other, with high bootstrap support (100%) while *ATHB8* and *CNA* clades are more closely related to each other. The overall bootstrap support values are high with only three branches having bootstrap support below 80%. The same overall grouping into four clades was recovered with

distance analysis, although *REV* and *ATHB8* clades showed differences in arrangement within each clade.

3.4.3 Overall patterns of gene expression in poplar leaves

Of the total 40,668 genes in v2.2 of the *P. trichocarpa* genome (Tuskan et al. 2006), there are approximately 3,000 more genes expressed (RPKM > 0) in the leaf tissue (33,102±405.33) compared to xylem (30,270±250.05; p = 0.0023). From these numbers, 81.40% (±1.00%) and 74.33% (±0.58%) of the total genes in the genome have detectable expression levels (RPKM > 0) in leaf and xylem tissues, respectively.

3.4.4 Expression of dorsiventral polarity genes in poplar

YABBY and *KANADI* genes have overall higher expression levels in the leaf tissue compared to xylem (Figures 3.2A, 3.2B). On average, the *YABBY* genes show ~300 times higher expression in leaves compared to xylem, while *KANADI* genes are expressed in the leaf only ~30 times higher compared to xylem (Appendix B.4). Most of the *YABBY* genes show a significant difference in level of expression between leaf and xylem samples except *Pt-INO.1* and both *Pt-CRC* paralogs, which have no detectable expression (Appendix B.5). Similar to *YABBY* genes, most of the *KANADI* genes show a significant difference in levels of expression between leaf and xylem except *Pt-KAN.3* and *Pt-KAN.4* (Appendix B.5). *HD-ZIPIII* genes, on the other hand, show the opposite pattern with approximately four times higher expression levels in the xylem compared to leaves (Figure 3.2C, Appendix B.4). Only one *HD-ZIPIII* gene, *Pt-HB1.8*, does not show a significant difference between leaf and

xylem expression levels, with mean xylem expression only twice the mean level of leaf expression (Appendix B.5).

Most of the *YABBY* orthologs have no detectable expression (RPKM = 0) in the xylem (Figure 3.2A, Appendix B.4). The highest RPKM value for xylem expression was in *Pt-YAB2.1* (Appendix B.4), an expression level so low it may not be associated with functional activity, ranking in the third quartile (Appendix B.6). The rest of the *YABBY* genes ranked in the fourth quartile and had very low expression in the xylem with lowest observed in *Pt-AFO.2*, followed by *Pt-AFO.1*, *Pt-YAB3.1, Pt-YAB3.2*, and *Pt-YAB2.2* (Appendix B.6).

The two *Pt-CRC* paralogs did not have any detectable expression in leaves (Figure 3.2A, Appendix B.4). The lowest detected expression was observed in *Pt-INO* paralogs (Figure 3.2A, Appendix B.4), ranking in category I (low expression) (Table 3.1). These two genes were also ranked in the fourth quartile, with expression in only one leaf sample (*Pt-INO.1* = 98.9% and *Pt-INO.2* = 97.6% from the total genes with detectable expression) and showed no detectable expression in the other two leaf samples (Appendix B.6). *Pt-YAB3.2* and *Pt-YAB2.2* had moderate leaf expression (category II) (Table 3.1) and ranked in the second quartile (Appendix B.6). All of the other *YABBY* genes were highly expressed in leaves and ranked in the first quartile (Appendix B.6), with the highest expression seen in *Pt-YAB5.2*, followed by *Pt-AFO.2, Pt-YAB2.1, Pt-AFO.1, Pt-YAB2.3, Pt-YAB3.1*, and *Pt-YAB2.3* (Figure 3.2A, Appendix B.4).

The highest RPKM value for xylem expression observed within *KANADI* genes was in *Pt-KAN.4* (Figure 3.2B, Appendix B.4), ranking in the third quartile (Appendix B.6). All of the other *KANADI* orthologs had low expression values and ranked in the fourth quartile (Appendix B.6). The lowest level of expression in the xylem was observed in *Pt-KAN.1*,

followed by *Pt-KAN2/3.2, Pt-KAN.2, Pt-ATS.2, Pt-KAN2/3.1, Pt-KAN.3*, and *Pt-ATS.1* (Figure 3.2B, Appendix B.4).

Most *KANADI* genes showed detectable expression in leaves, with the highest seen in *Pt-KAN.2* and *Pt-ATS.2* (Figure 3.2B, Appendix B.4). Both of these genes ranked in the second quartile (Appendix B.6). The remaining genes ranked in the third quartile (Appendix B.6) and showed low expression, with the next highest in *Pt-KAN2/3.1*, followed by *Pt-ATS.1, Pt-KAN2/3.2, Pt-KAN.1*, and *Pt-KAN.4*. *Pt-KAN.3* had the lowest expression value (Figure 3.2B, Appendix B.4).

The overall expression of *HD-ZIPIII* genes in xylem was relatively high although *Pt-HB1.7* showed only moderate xylem expression (Figure 3.2C, Appendix B.4), being ranked in the second quartile (Appendix B.6). The other *HD-ZIPIII* genes ranked in the first quartile (Appendix B.6) and showed high expression, with the highest seen in *Pt-ATHB.12,* followed by *Pt-PHB.2, Pt-HB1.6, Pt-ATHB.11, Pt-PHB.1*, and *Pt-HB1.8* (Figure 3.2C, Appendix B.4).

The highest level of expression in the leaves was seen for *Pt-HB1.6*, followed by *Pt-PHB.1, Pt-HB1.7,* and *Pt-HB1.8* (ranking in the first quartile). *Pt-ATHB.12* and *Pt-ATHB.11*, both in the second quartile, showed moderate leaf expression while *Pt-HB1.5* and *Pt-HB1.7* had low expression values and ranked in the third quartile (Figure 3.2C, Appendix B.4, B.6).

3.4.5 Poplar paralog comparison

The majority of poplar *YABBY* paralog pairs that showed a significant difference in levels of expression in leaves included *Pt-AFO* ($p = 0.0305$), *Pt-YAB2.1* and *Pt-YAB2.2* ($p = 0.0169$), *Pt-YAB2.2* and *Pt-YAB2.3* ($p = 0.0167$), *Pt-YAB3* ($p = 0.0112$), and *Pt-YAB5* paralogs ($p = 0.0054$). *Pt-YAB2.1* and *Pt-YAB2.3* as well as *Pt-INO* paralogs did not show a

significant difference in expression in leaves (Appendix B.7). No significant differences were seen between any *YABBY* gene pairs in the xylem due to very low expression levels. *Pt-INO* and *Pt-YAB5* paralogs were not compared due to undetectable expression levels in the xylem and *Pt-CRC* paralogs, due to lack of detectable expression in both xylem and leaf tissues.

In leaf tissue, a significant difference in the level of expression was observed between *Pt-KAN.1* and *Pt-KAN.2* paralogs ($p = 0.0081$), *Pt-KAN.2* and *Pt-KAN.3* ($p = 0.0085$), *Pt-KAN.2* and *Pt-KAN*.4 ($p = 0.0155$), and between *Pt-ATS* paralogs ($p = 0.0295$) (Appendix B.7). Significant differences in levels of expression in the xylem were not observed with *KANADI* genes, except between *Pt-KAN.1* and *Pt-KAN.2* ($p = 0.0169$).

Within the *HD-ZIPIII* genes, all of the paralog pairs showed a significant difference in level of expression in xylem: *Pt-PHB* ($p = 0.0105$), *Pt-HB1.5* and *Pt-HB1.6* ($p = 0.0407$), *Pt-HB1.7* and *Pt-HB1.8* ($p = 0.0180$), and *Pt-ATHB.11* and *Pt-ATHB.12* ($p = 0.0256$) (Appendix B.7). In leaves, a significant difference in levels of expression was only detected between *Pt-HB1.7* and *Pt-HB1.8* ($p = 0.0356$) as well as between *Pt-HB1.5* and *Pt-HB1.6* ($p = 0.0168$).

3.4.6 Overall patterns of gene expression in eucalyptus leaves

Of the total of 44,977 sequenced genes (Myburg et al. 2012) (44,974 available on Phytozome v7.0), there are approximately 3,500 more genes expressed (FPKM > 0) in the leaf tissue (27,971±93.18) compared to xylem (24,453±370.21; $p = 0.0021$). From all of the genes, those that have detectable expression (FPKM > 0) comprise 62.19% (±0.20%) and 54.37% (±0.82%) in leaf and xylem tissues, respectively.

3.4.7 Expression of dorsiventral polarity genes in eucalyptus

On average, *YABBY* genes were ~1,200 times more highly expressed in leaves compared to xylem (Figure 3.3A). Similarly, *KANADI* genes showed ~150 times higher expression in leaves as compared to xylem (Figure 3.3B). The *HD-ZIPIII* genes, however, were five times more highly expressed in xylem compared to leaves (Figure 3.3C).

There was no detectable expression of *Eg-INO.1* or *Eg-CRC.1* genes in xylem tissue while *Eg-AFO/YAB3* paralogs, *Eg-YAB2.1*, and *Eg-YAB5.1* had low expression (Figure 3.3A, Appendix B.8), which ranked in the fourth quartile (Appendix B.9). Among the three gene families, most of the *YABBY* genes had high expression in the leaf (Figure 3.3A, Appendix B.8), all ranking in the first quartile (Appendix B.9), except *Eg-INO.1* and *Eg-CRC.1*, which were not detected. The highest expression level among *YABBY* genes was seen in *Eg-AFO/YAB3.1*, followed by *Eg-AFO/YAB3.2*, *Eg-YAB2.1*, and *Eg-YAB5.1* (Figure 3.3A, Appendix B.8).

Eg-KAN.1 and *Eg-ATS.1* were not detected in xylem, while the rest of the *KANADI* genes had low expression (Figure 3.3B, Appendix B.8) and ranked in the fourth quartile (Appendix B.9). The most highly expressed *KANADI* gene was *Eg-KAN2/3.1* (Figure 3.3B, Appendix B.8), the only *KANADI* gene ranking in the first quartile (Appendix B.9). The rest of the *KANADI* genes were expressed at low levels: *Eg-KAN.1* (ranking in the second quartile), *Eg-ATS.1, Eg-KAN2/3.3, Eg-KAN2/3.2*, and lowest expression was seen in *Eg-KAN.2* (ranking in the third quartile).

All of the *HD-ZIPIII* genes had high expression in the xylem (Figure 3.3C, Appendix B.8) where they all ranked in the first quartile (Appendix B.9). In leaves, *Eg-PHB/PHV.1* had high expression along with *Eg-CNA.1*, followed by *Eg-REV.1*, all ranking in the first quartile,

and *Eg-ATHB8.1* with moderate expression, ranking in the second quartile (Figure 3.3C, Appendix B.8, B.9).

3.4.8 Eucalyptus paralog comparison

Eg-AFO/YAB3 paralogs did not show a significant difference in expression in either leaf or xylem tissues (Appendix B.10). Similarly, *Eg-KAN* and *Eg-KAN2/3* paralogs were not differentially expressed in xylem due to low expression levels. There was, however, a significant difference in levels of expression in leaf tissues of *Eg-KAN* paralogs ($p = 0.0012$), *Eg-KAN2/3.1* and *Eg-KAN2/3.2* ($p = 0.0042$), *Eg-KAN2/3.1* and *Eg-KAN2/3.2* ($p = 0.0037$), and *Eg-KAN2/3.2* and *Eg-KAN2/3.3* ($p = 0.0205$) (Appendix B.10).

3.4.9 Gene expression in eucalyptus hybrid

Expression data from *E. grandis* x *urophylla* hybrid assembled contigs were only available for the following *E. grandis* orthologs: *Eg-AFO/YAB3.2* (contig_82502), *Eg-YAB2.1* (contig_94705), *Eg-YAB5.1* (contig_92866), and all of the *HD-ZIPIII* genes (*Eg-PHB/PHV.1* (contig_3301), *Eg-REV.1* (contig_22876), *Eg-ATHB8.1* (contig_8660), *Eg-CNA.1* (contig_2647) (Appendix B.11). All, but two contigs (contig_92866 and contig_8660), showed some variation in amino acid sequence from the corresponding *E. grandis* gene. BLAST showed similarity of contig_94293 to *Eg-AFO/YAB3.1*, but was not included here due to high sequence divergence, lack of a fully conserved *YABBY* and zinc finger domains, and inconsistency in expression levels compared with the other putative eucalyptus *YABBY* genes.

Similarity between *E. grandis* and eucalyptus hybrid expression data sets was determined using a scatter plot (Figure 3.4, Appendix B.11), which showed more similarity between xylem data, compared to leaf, particularly in *YABBY* and *KANADI*, likely due to low or undetectable levels of expression. Overall gene expression patterns in *E. grandis* and *E. grandis* x *urophylla* were expected to be quite similar, but surprisingly, this was not the case.

Among the three gene families, all of the *YABBY* genes had high expression in the leaf and, as expected, all of the *YABBY* orthologs had no detectable expression in the xylem (Appendix B.11). The only *KANADI* gene with information for an available contig was *Eg-KAN2/3.1*, which had no detectable expression in the xylem and moderate expression in leaf (Appendix B.11). The expression of *HD-ZIPIII* genes in the xylem was about five times higher than in the leaf tissues. The highest value for expression in the leaf was observed in *Eg-CNA.1*, while a similar trend was observed in xylem expression levels of the eucalyptus *HD-ZIPIII* genes for which highest expression was observed for the *ATHB8* ortholog, followed by *CNA* ortholog (Appendix B.11).

There was no change between levels of expression in young compared to mature xylem of any *YABBY* or *KANADI* genes, as in both tissues, expression was undetectable. In young xylem, all of the *HD-ZIPIII* genes had high expression levels, but in mature xylem, the expression level of *Eg-PHB/PHV.1* was reduced over time to moderate, while the rest of the genes maintained high expression levels (Figure 3.5, Appendix B.12). The overall pattern of gene expression is maintained, however, with the highest expression in mature xylem observed for the *ATHB8* ortholog (as in developing xylem).

There was no detectable *YABBY* and *KANADI* gene expression found in the phloem tissue (Figure 3.5, Appendix B.12). *HD-ZIPIII* genes, on the other hand, all showed high

expression levels in the phloem (Figure 3.5, Appendix B.12). The highest level of expression in the phloem was observed in the *ATHB8* ortholog. Surprisingly, expression of *Eg-PHB/PHV.1* and *Eg-REV.1* was higher in the phloem compared to either young or mature xylem.

In mature leaves, the pattern of gene expression of *YABBY* genes was similar to that seen in young leaves, but with reduced expression levels overall. The highest expression in mature leaves was observed for the eucalyptus *AFO/YAB3* and *YAB5* orthologs. *YAB2*, on the other hand, had no detectable expression, a reduction from high expression in young leaves (Figure 3.5, Appendix B.12). There was less expression of the eucalyptus *KAN2/3* ortholog in mature leaves compared to young leaves (Figure 3.5, Appendix B.12). The highest level of expression of *HD-ZIPIII* genes in mature leaves was observed in *Eg-CNA.1* (similar to young leaves), while *Eg-ATHB8.1* had low expression (a reduction compared to young leaves) (Figure 3.5, Appendix B.12). Similar to *Eg-YAB2.1*, *Eg-PHB/PHV.1* expression was undetectable in mature leaves.

Overall, *YABBY* gene expression was higher in the shoot tip compared to mature leaves, but lower than young leaves. The pattern of expression, however, was maintained in both leaf tissues with the highest expression observed in *Eg-AFO/YAB3.1* (Figure 3.5, Appendix B.12). Shoot tips showed highest expression of *Eg-KAN2/3.1* gene compared to young or mature leaves. Expression pattern of *HD-ZIPIII* genes in the shoot tip was similar to that of young leaf, with highest expression observed in *Eg-CNA.1* gene.

3.5 Discussion

3.5.1 Organismal phylogeny

The relationships of eurosid I (including poplar), eurosid II (including *Arabidopsis*), with Myrtales (including eucalyptus) are not very well established at present. These three taxa are often represented as a trichotomy (APG, Stevens 2010), which, depending on the analysis, can be resolved in any of the three possible ways (Figure 3.6). Unsurprisingly, different genes in this study suggest different organismal phylogenies. ML analysis of *CRC, REV, ATHB8* suggest one putative scenario of resolution, while *INO, ATS, CNA* and *AFO/YAB3, YAB5, KAN, PHB/PHV* suggest the two others, respectively, with only two of these clades (i.e., ATS and PHB/PHV) showing moderate support. Distance analysis of *YAB2* and *REV* arranges the taxa in the form of the third scenario while the *KAN* paralogs follow the second scenario where poplar is also sister to the second grouping (poplar and *Arabidopsis* with sister to this grouping eucalyptus).

From these overall results, poplar (eurosid I) and eucalyptus (Myrtales) are more closely related to each other than to *Arabidopsis*. It is also clear that it is difficult to resolve this problematic branch using other genes. Recently published studies (Zhu et al. 2007, Shulaev et al. 2011) have resolved these groups in different ways. For instance, one study places poplar in the Malvidae (eurosid II) based on 154 protein-coding genes (Shulaev et al. 2011). Poplar would therefore be more closely related to *Arabidopsis* (Bell et al. 2010). This is contrary to many other studies, which place *Arabidopsis* (Brassicales) and eucalyptus (Myrtales) in the Malvidae, with poplar as sister to most of the Fabidae (eurosid I) based on many genes derived from complete plastid genome sequences (Moore et al. 2010, Soltis et al.

2010). The lack of resolution here, however, is not critical to ortholog determination and the grouping into clades is more important in this study.

3.5.2 Gene family number

The three taxa investigated here all belong to the rosid clade that, along with an early diverging lineage *Vitis*, experienced an ancient hexaploidization event (Jaillon et al. 2007) (Figure 3.6). Further, unlike *Vitis*, poplar underwent another whole genome duplication (WGD) event following its divergence from its common ancestor with *Arabidopsis* (Sterck et al. 2005, Tuskan et al. 2006). This is consistent with my results, which typically show two poplar genes for every *Arabidopsis* gene. It has been suggested that the rosid order Myrtales, to which eucalyptus belongs, may have undergone one or more duplication events along with the ancient hexaploidization, an independent duplication to that in poplar (Myburg et al. 2012). This hypothesis is not supported by the data presented here, as the eucalyptus gene number generally shows an approximately 1:1 ratio of orthologs compared to *Arabidopsis*. If a WGD event had taken place in eucalyptus, it may be expected to produce gene number results more similar to poplar.

There are, however, a few exceptions to the 2:1 and 1:1 ratios of poplar and eucalyptus genes in relation to *Arabidopsis*. There are three *YAB2* orthologs and four *KAN* orthologs in the poplar genome. All of the poplar *YAB2* orthologs are annotated as *YABBY* proteins in Phytozome (accessed via Pfam: http://pfam.sanger.ac.uk/) and it is possible that these genes in poplar may have some function that is not present in *Arabidopsis*, or that an ortholog of *Pt-YAB2* genes was lost in *Arabidopsis*. WGD in poplar is likely responsible for the paralogs in *YABBY*, *KANADI*, and *HD-ZIPIII* gene families, as gene paralogs are located

on chromosome segments corresponding to those that have duplicated (Tuskan et al. 2006). This holds true for all of the poplar dorsiventral polarity genes except *YAB2*, which may have duplicated by means other than WGD as its paralogs are on scaffolds (corresponding to chromosomes or genes arranged in a group, but not mapped onto a chromosome to date) 1, 127 (this gene was not present in the poplar annotation version 2.0), and 16. *Pt-YAB2.1* and *Pt-YAB2.3* had significantly higher expression in the leaf compared to their paralog (*Pt-YAB2.2*), possibly suggesting neofunctionalization (Moore and Purugganaan 2005, Flagel and Wendel 2009). A similar pattern is observed with *Pt-KAN.1*, which has significantly higher expression than its three paralogs. There are two *KAN* orthologs in eucalyptus, suggesting diversification of these genes in both poplar and eucalyptus after their splits from *Arabidopsis*. Another possibility is that there were two copies of *KAN* prior to the diversification of the rosid clade, with the loss of a paralogous gene in *Arabidopsis*, leaving only a single *KAN* copy.

There are also cases where for two *Arabidopsis* genes there are only two poplar genes and either three or one eucalyptus gene. *KAN2* and *KAN3* appear to have diverged following the splits of rosids into Myrtales, eurosid I, and eurosid II. The two copies in poplar likely correspond to the *Populus* WGD. Alternatively, the eucalyptus and *Arabidopsis* split likely occurred following *KAN2* and *KAN3* divergence, and one of the genes later became duplicated. *PHB* and *PHV* both have two orthologs in poplar due to the *Populus* WGD, suggesting divergence following the rosid splits. But unlike with *KAN2/KAN3*, the divergence of *PHB* and *PHV* occurred following the split of rosids, since the eucalyptus genome has a single copy of *PHB/PHV*. Both *KAN2/3* and *PHB/PHV* paralogs in poplar do not show a significantly differential expression in leaves, which is suggestive of redundancy.

But one should be cautious when making these comparisons due to low divergence between paralogs, as some "incorrect" mapping of short reads occurring across paralogs cannot be ruled out.

Low bootstrap support values for some of the branches are likely reflective of the challenges in aligning *YABBY* and *KANADI* sequences, particularly with respect to eucalyptus genes and those belonging to the poplar *YAB2* group, **or a simple lack of variation**. This variation among domains that are usually conserved in well-annotated genomes, such as *Arabidopsis*, is likely exacerbated by incompleteness of the poplar (Geraldes et al. 2011) and eucalyptus genomes.

3.5.3 Overall expression patterns

Dorsiventral leaf polarity genes are expressed in localized domains within the leaf, with *YABBY* and *KANADI* genes restricted to the abaxial domain, and *HD-ZIPIII* genes expressed in the adaxial domain (Ariel et al. 2007). Due to differences in spatial expression within a leaf, higher or lower gene expression can mean a variety of things. Higher expression of a specific gene can mean that: 1) this is occurring in all the cells of the organ; 2) this is occurring only in some portion of the cells (i.e., abaxial or adaxial domain) suggesting differential patterning of expression, or 3) there is no increase or change in gene expression, but there is an increase in "cell types" (i.e., abaxial or adaxial surface identity cells) and expression of this gene per cell remains the same. The second scenario of differential patterning of expression is more plausible here due to the expected dorsiventral genes expression, but functional experiments such as *in situ* hybridization would be needed to confirm this.

This study showed that there are more leaf-expressed genes in both poplar and eucalyptus transcriptomes compared to xylem. This is expected since leaves are complex organs while xylem tissues consist of only a small number of cell types and it can be predicted that there is a greater number of genes required to form and maintain a leaf compared to xylem. The poplar and eucalyptus results both showed that *YABBY* genes have the highest overall expression in the leaves compared with *KANADI* and *HD-ZIPIII* genes, consistent with the importance of *YABBY* genes in leaf function (Street et al. 2008). Despite the low levels of expression of *HD-ZIPIII* genes in the leaf tissue, due to their predominant expression in the xylem, the overall expression is still ~2.5 and ~4.5 times higher than that of the *KANADI* genes in poplar and eucalyptus, respectively. This low expression of *KANADI* genes suggests that low amounts of the genes are sufficient for their normal function or that RNA was not extracted at the peak of its expression. Overall, most of the genes under study had a detectable level of expression in leaf tissue, except *Pt-INO* and *Pt-CRC* genes, which are known to have functions in flower development (Alvarez and Smyth 1999, Bowman and Smyth 1999, Bowman 2000, Baum et al. 2001).

3.5.4 Expression patterns of *YABBY* genes

The results for *YABBY* gene expression are fairly consistent with the available data in previously published microarray studies of young leaves in a closely related balsam poplar, *Populus balsamifera*, (Wilkins et al. 2009) and *Arabidopsis* (Schmid et al. 2005). There were no comparable data for *YAB2* in *Arabidopsis*. It is known to have similar expression patterns, but very low expression level compared to *AFO* (or *FIL*) and *YAB3* (Seigfried et al. 1999). The highest levels of *YABBY* gene expression in *Arabidopsis* young leaves are seen in *YAB5*,

followed by *YAB3* and *AFO* (Schmid et al. 2005). Expression values for poplar showed a similar pattern to *Arabidopsis*, with *Pt-AFO.1* and *Pt-YAB2.1* being highly expressed, and *Pt-YAB5.1* having the highest expression level. *Populus balsamifera* microarray results showed a similar expression pattern in comparable paralogs from poplar genome version 1.1 (Appendix B.13) of *Pt-YAB5.1* and *Pt-AFO.1*. The next highest level was detected in *Pt-YAB2.2* in balsam poplar where I found this gene to have second lowest detectable level of expression in black cottonwood. This discrepancy could come from the lack of information about *Pt-YAB2.1* in the balsam poplar microarray data and the absence of this gene in version 1.1 of the poplar genome. A significant difference was seen between *Pt-YAB2.1* and *Pt-YAB2.2*, suggesting one of these has a more important function over its respective paralog.

With little or no published data on dorsiventral polarity genes and their expression levels in eucalyptus, comparisons can only be made to the poplar data presented here, and to data obtained from Eucspresso for the eucalyptus hybrid. As with poplar expression results, *INO* and *CRC* orthologs in eucalyptus had no detectable expression in leaf or xylem tissues. The highest levels of gene expression in eucalyptus leaves were seen for the *Eg-AFO/YAB3.1* paralog, followed by *Eg-AFO/YAB3.2*, *YAB2* and *YAB5* orthologs. The eucalyptus hybrid data also showed highest expression in *Eg-AFO/YAB3.2* gene, but the next highest expression was seen for *YAB2* followed by the *YAB5* orthologs. These expression patterns show a similar trend to the genes similarly highly expressed in leaves of poplar, but cannot be directly compared due to variability of expression levels in poplar paralogs and the general lack of paralogous *YABBY* genes in eucalyptus. The two *AFO/YAB3* paralogs in eucalyptus did not have a significant difference in expression, suggesting that their diversification may be fairly recent, and so these genes may be undergoing positive selection:

> "It has since become apparent that positive selection does play a key role in preserving some gene copies, and indeed can act at a very early stage of the gene duplication process. For example, a population genetic analysis of three unlinked duplicate gene pairs in A. thaliana that originated less than 1.2 million years ago (mya) revealed significantly reduced levels of nucleotide polymorphism in the progenitor locus, the duplicate locus or both. This reduced nucleotide variation, which is associated with a recent selective sweep, is evidence that positive selection plays a prominent role in the establishment of duplicate loci" (Moore and Purugganan 2005).

3.5.5 Expression patterns of *KANADI* genes

Arabidopsis microarray results show that *ATS* has the lowest leaf expression and that *KAN* has the highest expression levels (Schmid et al. 2005). This is contrary to Wilkins et al. (2009) findings for poplar leaf expression, where *Pt-ATS.2* showed the highest expression. My results were similar to both Schmid et al. (2005) and Wilkins et al. (2009) in that *Pt-KAN.1* had its highest expression in the leaf followed by *Pt-ATS.2*. However, *Pt-KAN.1* had the lowest expression of available orthologs. These data point to high variability of *KANADI* genes expression between species and between different analyses. Although low levels of *ATS* were detected in young leaves of *Arabidopsis* (Schmid et al. 2005) there is very little evidence documenting the functional significance of this gene in *Arabidopsis* leaves, possibly suggesting that it has a background level of expression. The primary function of *ATS* is in promoting integument outgrowth (Kelley et al. 2009) and in the regulation of the flavonoid pathway in developing seeds (Gao et al. 2010). A comparison of expression of *Pt-KAN.2* to any of its three paralogs and between *Pt-ATS* paralogs suggests a possible role for *Pt-KAN.2* and *Pt-ATS.2* in leaf function.

Each of the representative *KANADI* genes showed variability in expression levels, but as with poplar, the *ATS* ortholog is among the highest expressed *KANADI* genes, in eucalyptus. The high expression of *ATS* in both poplar and eucalyptus suggests a possible

functional significance in leaves of these trees compared to the lack of expression in leaves of *Arabidopsis*.

3.5.6 Expression patterns of *HD-ZIPIII* genes

All of the *HD-ZIPIII* genes are expressed in young *Arabidopsis* leaves, with *ATHB8* expressed at a low level (Schmid et al. 2005). Wilkins et al. (2009) found very low levels of hybridization of poplar *ATHB8* paralogs compared to the other *HD-ZIPIII* genes in leaves. This is partly inconsistent with my findings, in that *Pt-HB1.6* showed highest and *Pt-HB1.5* showed the second lowest expression levels (both *ATHB8* orthologs). All of the *HD-ZIPIII* genes showed a significant difference in expression between their respective paralogs in xylem, where their function is well documented (Chitwood et al. 2007, Kidner and Timmermans 2007), while significant differences were observed between each respective *REV* and *ATHB8* paralog pair in leaves. This possibly suggests that one or both genes in the pair may have evolved a different function, likely with respect to secondary growth, which is not present in *Arabidopsis*. This may be similar to the functional divergence of *FLOWERING LOCUS* (*FT1* and *FT2*) paralogs in poplar, which have temporally divergent expression, and are involved in coordinating cycles of vegetative and reproductive growth (Hsu et al. 2011), a function that is not present in *Arabidopsis*.

The acquisition of a novel function or functional divergence cannot be conclusively determined without functional studies, as Du et al. (2011) and Robischon et al. (2011) have done for the *PCN* (*Pt-HB1.8*) and *PRE* (*Pt-ATHB.12*) genes in poplar, respectively. Du et al. (2011) have shown the significance of *PCN* to secondary vascular tissue development using *in situ* hybridization. *PCN* is highly expressed in secondary vasculature but not in leaf

primary vascular tissue (Du et al. 2011). As with *PCN*, *PRE* is important in patterning secondary vasculature and cambium initiation (Robischon et al. 2011), which is lost in *Arabidopsis*. This similarity in function of *REV* is retained in the promotion of adaxial surface identity (Robischon et al. 2011). These studies demonstrate the importance of studying the function of the identified orthologs in trees, which may very likely have evolved different functions critical to proper development.

In eucalyptus, *PHB/PHV* and *CNA* orthologs have their highest expression in leaves while *ATHB8* and *REV* show the lowest expression. This trend is reversed in xylem tissues, where *ATHB8* and *REV* have highest expression, and *PHB/PHV* and *CNA* the lowest expression levels. The gene expression trend was generally also found in the eucalyptus hybrid data.

3.5.7 Neofunctionalization and subfunctionalization of duplicate genes in poplar

In this study, ortholog relations between *Arabidopsis*, poplar, and eucalyptus were elucidated. Overall, I found an almost 1:1 ratio of eucalyptus to *Arabidopsis* genes, while the duplication of genes in poplar due to an ancient whole genome duplication event is reflected in a 2:1 ratio of poplar to *Arabidopsis* genes. My results show that many of the poplar paralogs have significantly different expression in leaf tissues, possibly suggesting the acquisition of a novel function (neofunctionalization) or at least the division of an ancestral function (subfunctionalization) (Moore and Purugganan 2005, Rogers-Melnick et al. 2012). Of particular interest are *Pt-ATS.2* and *Pt-YAB2.1*. In *Arabidopsis*, *ATS* is expressed as two alternatively spliced transcripts that are differentially expressed at low levels in siliques (Gao et al. 2010). In poplar, the *Pt-ATS.2* paralog, on the other hand, has moderate expression in

young leaves, but overall is one of the most highly expressed *KANADI* gene in *P. trichocarpa*. *Pt-YAB2.1* showed third highest expression level in leaves. *YAB2* is expressed in a similar pattern as *AFO* and *YAB3* in *Arabidopsis*, but has the lowest expression level among these three genes, and likely acts in a pathway that is not redundant with these genes, reflected in its high sequence divergence from *AFO* and *YAB3* (Seigfried et al. 1999).

3.6 Conclusion

The presence of WGD duplication was confirmed with usually double the number of genes present in poplar compared to *Arabidopsis*. Eucalyptus, on the other hand, mostly showed the absence of duplication in the dorsiventral leaf polarity genes. The observed general trend of gene expression in poplar and eucalyptus was quite similar, where *YABBY* and *KANADI* genes were exclusively expressed in the leaves and *HD-ZIPIII* genes were expressed in both leaf and xylem tissues. One of each of the *YAB2* and *ATS* paralogs showed significant expression in poplar leaves, which has not been reported in *Arabidopsis*. Future functional analyses of the identified dorsiventral polarity gene orthologs in *Populus* and *Eucalyptus* will aid in answering questions about gene function as well as roles in development, which will likely differ from their functional role in the herbaceous *Arabidopsis*.

Table 3.1 Ortholog names with categorized levels of expression of *YABBY*, *KANADI*, and *HD-ZIPIII* genes (left columns) for *Arabidopsis thaliana*, *Populus trichocarpa* (v2.2), and *Eucalyptus grandis* (v1.0) with corresponding transcript name (right columns) are shown. *Italics* indicate previously annotated genes.

Gene family	*Arabidopsis thaliana*		*Populus trichocarpa*		*Eucalyptus grandis*	
	Gene name	**Accession number**	**Gene name**	**Accession number**	**Gene name**	**Accession number**
YABBY	*AFO* *YAB3*	AT2G45190 AT4G00180	*Pt-AFO.1* [IV] Pt-AFO.2 [III] Pt-YAB3.1 [IV] Pt-YAB3.2 [IV]	POPTR_0014s 06210 POPTR_0002s 14600 POPTR_0003s 11230 POPTR_0001s 00240	Eg-AFO/YAB3.1 [IV] Eg-AFO/YAB3.2 [IV]	Egrandis_v1_0 .025894m Egrandis_v1_0 .021658m
YABBY	*YAB2*	AT1G08465	Pt-YAB2.1 [III] Pt-YAB2.2 [IV] Pt-YAB2.3 [IV]	POPTR_0001s 22180 POPTR_0127s 00201 POPTR_0016s 06760	Eg-YAB2.1 [IV]	Egrandis_v1_0 .027818m
	INO	AT4G00180	Pt-INO.1 [I] *Pt-INO.2* [II]	POPTR_0008s 19330 POPTR_0010s 05220	Eg-INO.1 [I]	Egrandis_v1_0 .049262m
	YAB5	AT1G23420	Pt-YAB5.1 [IV] Pt-YAB5.2 [IV]	POPTR_0006s 06700 POPTR_0018s 12990	Eg-YAB5.1 [IV]	Egrandis_v1_0 .028251m
	CRC	AT2G26580	*Pt-CRC.1* [I] *Pt-CRC.2* [II]	POPTR_0008s 09740 POPTR_0010s 16410	Eg-CRC.1 [I]	Egrandis_v1_0 .029168m
KANADI	*KAN*	AT5G16560	Pt-KAN.1 [III] Pt-KAN.2 [II] Pt-KAN.3 [II] Pt-KAN.4 [II]	POPTR_0017s 02220.1 POPTR_0004s 08070.1 POPTR_0015s 05340.1 POPTR_0012s 03900.1	Eg-KAN.1 [II] Eg-KAN.2 [II]	Egrandis_v1_0 .012339m Egrandis_v1_0 .048318m
	KAN2 *KAN3*	AT1G32240 AT4G17695	Pt-KAN2/3.1 [II] Pt-KAN2/3.2 [II]	POPTR_0003s 09490.1 POPTR_0001s 02010.1	Eg-KAN2/3.1 [IV] Eg-KAN2/3.2 [II] Eg-KAN2/3.3 [II]	Egrandis_v1_0 .016255m Egrandis_v1_0 .018107m Egrandis_v1_0 .015464m

Gene family	*Arabidopsis thaliana*		*Populus trichocarpa*		*Eucalyptus grandis*	
	Gene name	**Accession number**	**Gene name**	**Accession number**	**Gene name**	**Accession number**
	ATS	AT5G42630	Pt-ATS.1 [II] Pt-ATS.2 [III]	POPTR_0002s13170.1 POPTR_0014s03650.1	Eg-ATS.1 [II]	Egrandis_v1_0.018962m
HD-ZIP III	*PHB* *PHV*	AT2G34710 AT1G30490	*Pt-PHB.1* [II] *Pt-PHB.2* [III]	POPTR_0011s10070 POPTR_0001s38120	Eg-PHB/PHV.1 [IV]	Egrandis_v1_0.002659m
	REV	AT5G60690	*Pt-HB1.7* [IV] *Pt-HB1.8* (*PRE*) [IV]	POPTR_0004s22090 POPTR_0009s01990	Eg-REV.1 [III]	Egrandis_v1_0.002715m
	ATHB8	AT4G32880	*Pt-HB1.5* [IV] *Pt-HB1.6* [IV]	POPTR_0018s08110 POPTR_0006s25390	Eg-ATHB8.1 [III]	Egrandis_v1_0.041842m
	CNA	AT1G52150	*Pt-ATHB.11* [II] *Pt-ATHB.12* (*PCN*) [III]	POPTR_0003s04860 POPTR_0001s18930	Eg-CNA.1 [IV]	Egrandis_v1_0.002702m

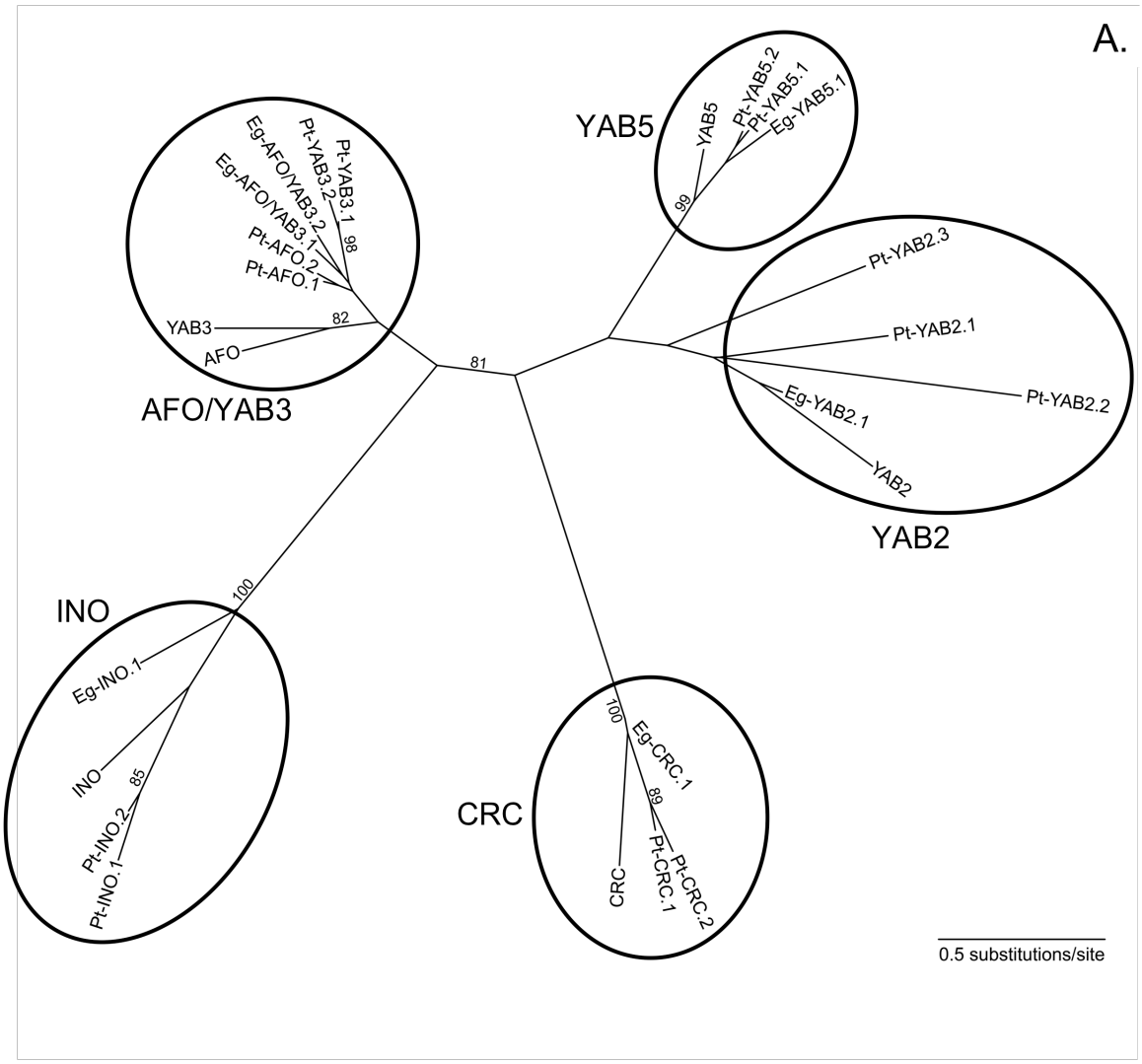
A.
YAB5
YAB5
Pt-YAB5.2
Pt-YAB5.1
Eg-YAB5.1
99
Eg-AFO/YAB3.3
Pt-YAB3.2
Pt-YAB3.1
98
Eg-AFO/YAB3.2
Eg-AFO/YAB3.1
Pt-AFO.2
Pt-AFO.1
YAB3
82
AFO
AFO/YAB3
81
Pt-YAB2.3
Pt-YAB2.1
Pt-YAB2.2
Eg-YAB2.1
YAB2
YAB2
100
INO
Eg-INO.1
INO
85
Pt-INO.2
Pt-INO.1
100
Eg-CRC.1
89
Pt-CRC.1
Pt-CRC.2
CRC
CRC
0.5 substitutions/site

B.

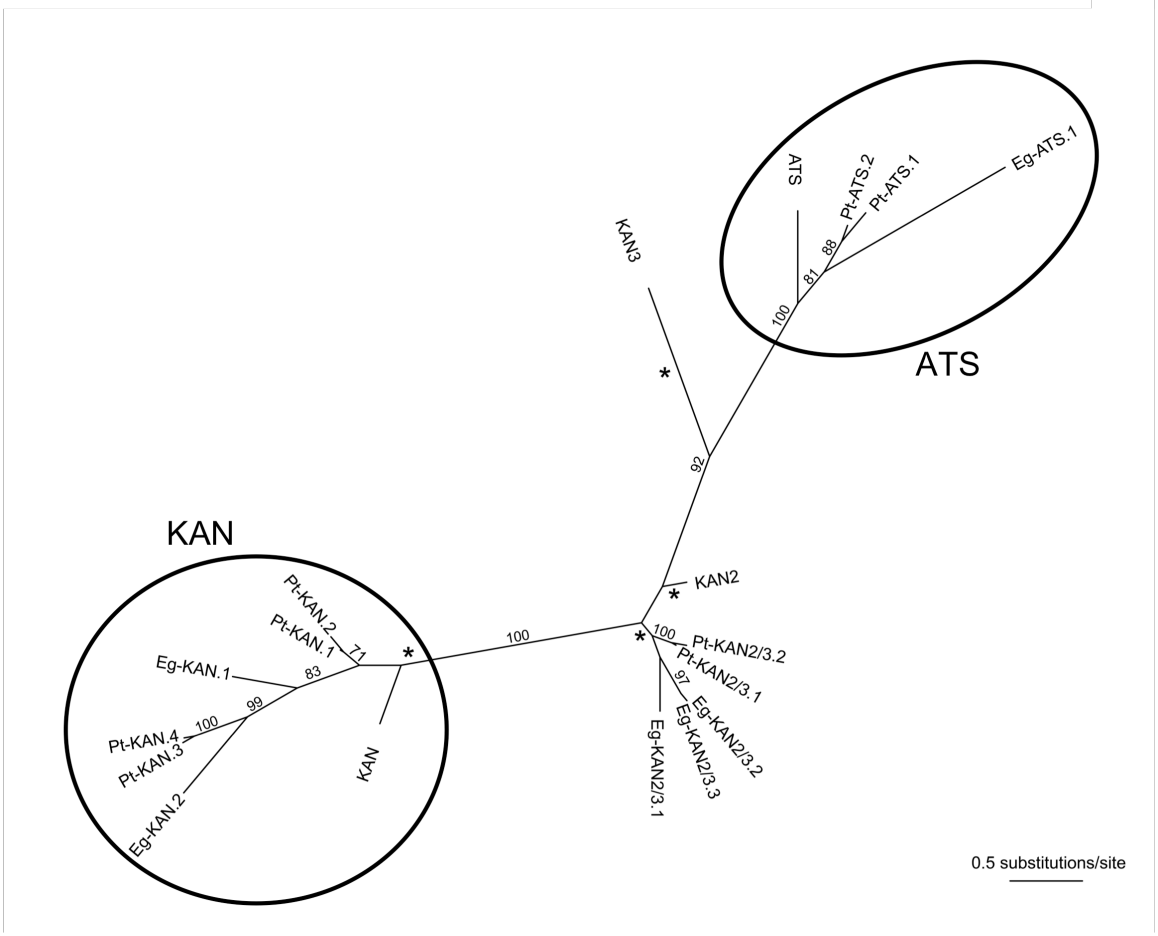
ATS
Pt-ATS.2
Pt-ATS.1
Eg-ATS.1
88
81
100
ATS
KAN3
*
29
KAN2
*
100
Pt-KAN2/3.2
Pt-KAN2/3.1
97
Eg-KAN2/3.2
Eg-KAN2/3.3
Eg-KAN2/3.1
100
*
KAN
Pt-KAN.2
Pt-KAN.1
71
*
Eg-KAN.1
83
99
100
Pt-KAN.4
Pt-KAN.3
Eg-KAN.2
KAN
0.5 substitutions/site

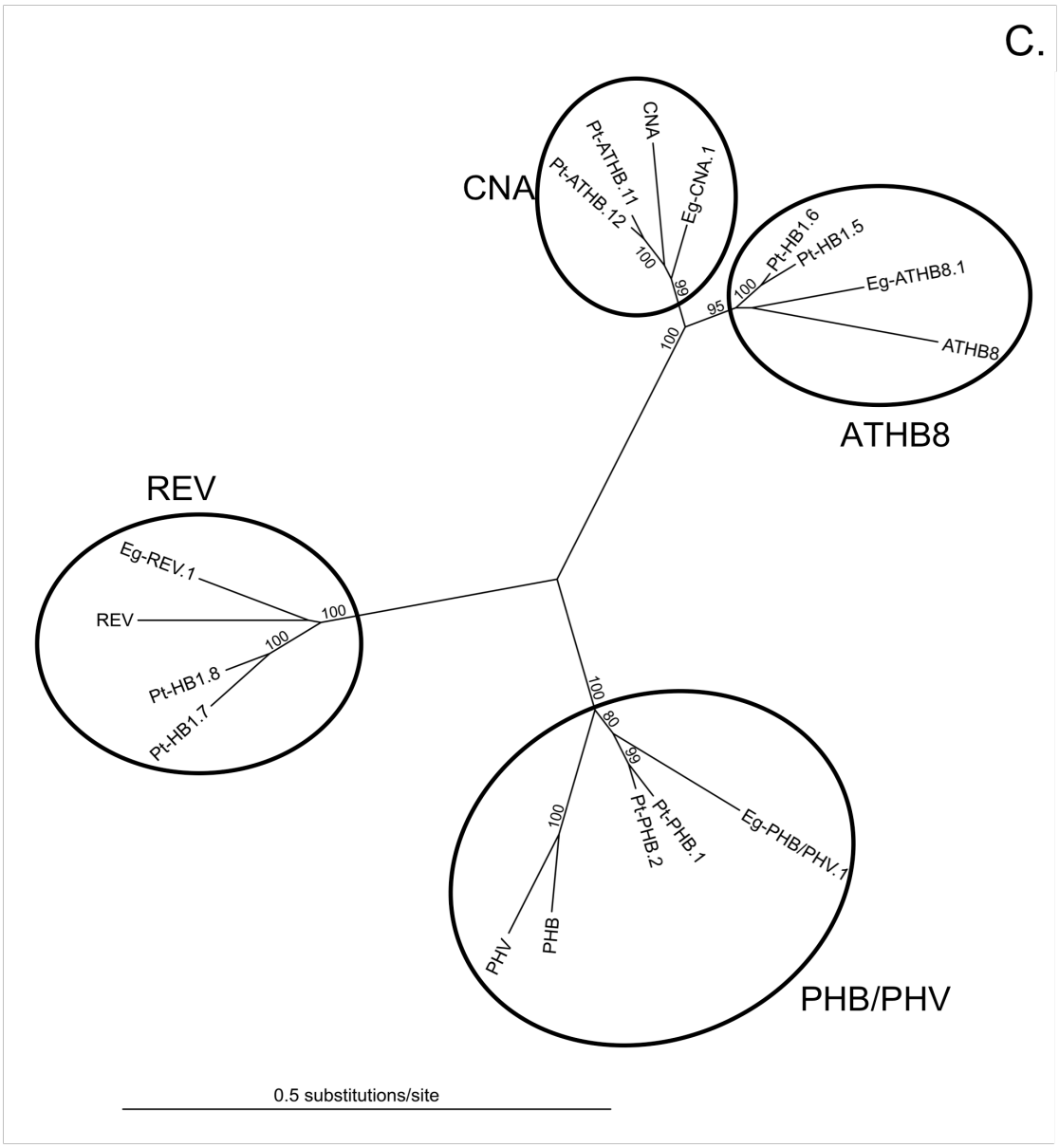

Figure 3.1 Maximum likelihood tree reconstructions for *A. thaliana*, *P. trichocarpa*, and *E. grandis* orthologs. Bootstrap support values (greater than and equal to 70%) are indicated on the branches. A. ***YABBY*** **phylogenic tree shows the separation of the family into five clades: AFO/YAB3, YAB2, INO, YAB5, and CRC.** B. ***KANADI*** **phylogenic tree shows the separation of the family into two main clades: KAN and ATS. KAN2/KAN3 genes are sister to the ATS clade and are not monophyletic.** C. ***HD-ZIPIII*** **phylogenic tree shows the separation of the family into four clades: PHB/PHV, REV, ATHB8, and CNA. Asterisks indicate clades or groups, which have a different topology according to distance analysis.**

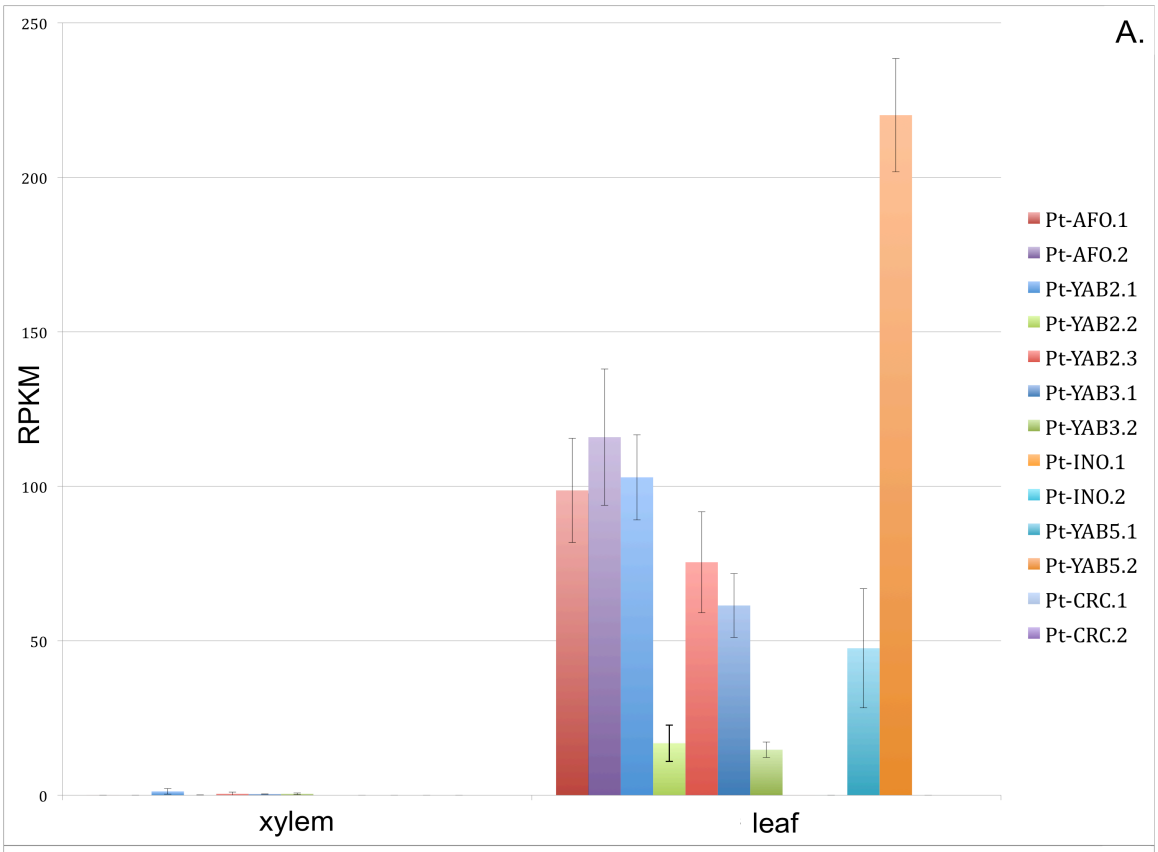
A.
250
200
150
100
50
0
RPKM
xylem
leaf
Pt-AFO.1
Pt-AFO.2
Pt-YAB2.1
Pt-YAB2.2
Pt-YAB2.3
Pt-YAB3.1
Pt-YAB3.2
Pt-INO.1
Pt-INO.2
Pt-YAB5.1
Pt-YAB5.2
Pt-CRC.1
Pt-CRC.2

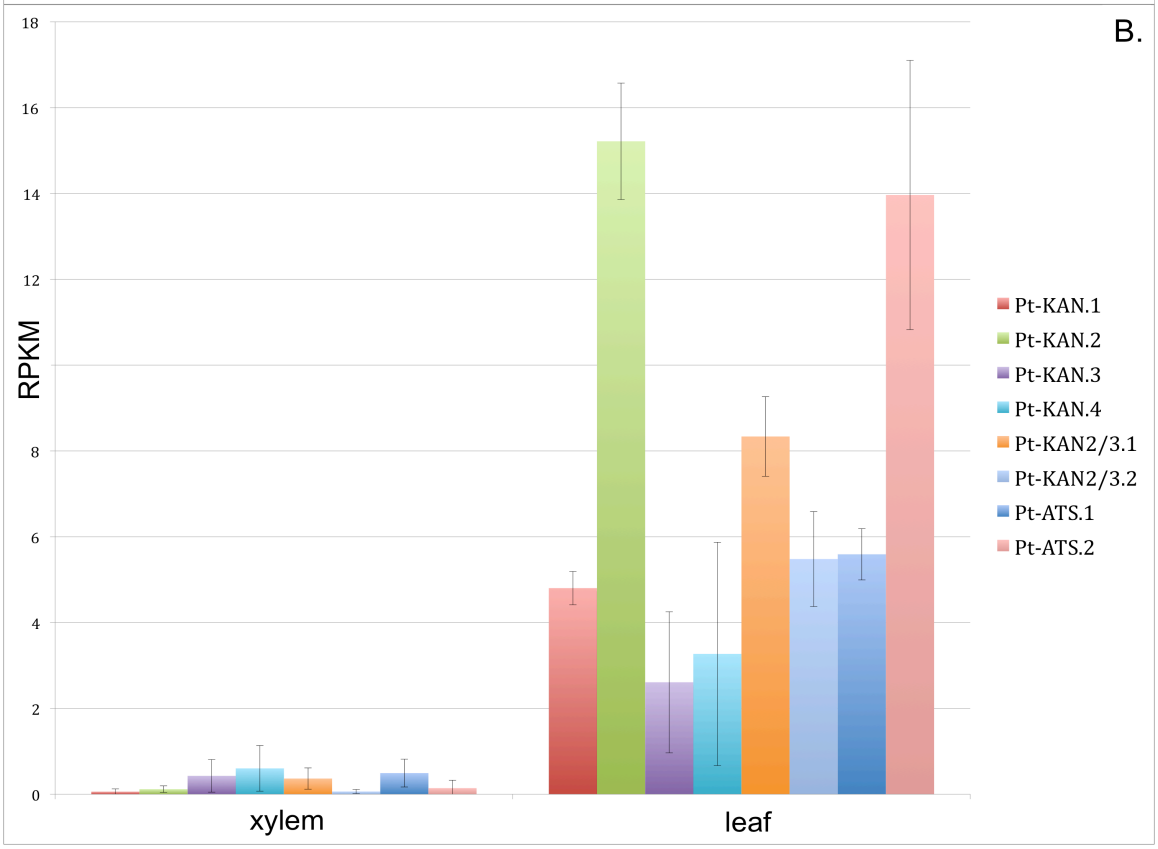
B.
18
16
14
12
10
8
6
4
2
0
RPKM
xylem
leaf
Pt-KAN.1
Pt-KAN.2
Pt-KAN.3
Pt-KAN.4
Pt-KAN2/3.1
Pt-KAN2/3.2
Pt-ATS.1
Pt-ATS.2

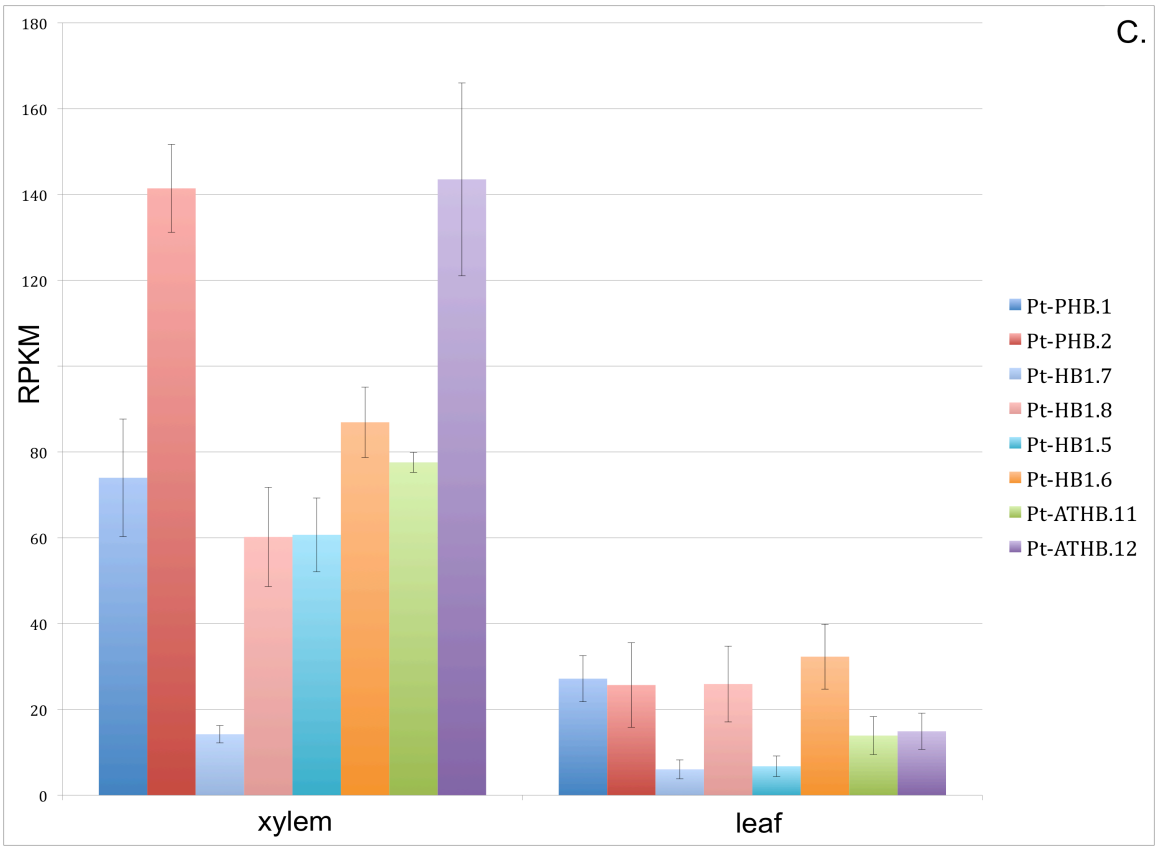

Figure 3.2 RPKM expression levels of three gene families in *P. trichocarpa* involved in determining abaxial-adaxial polarity (*YABBY, KANADI*, and *HD-ZIPIII*). A. ***YABBY*** **orthologs are primarily leaf expressed with low amounts expressed in the xylem.** B. ***KANADI*** **orthologs are expressed in the leaf with little expression in the xylem.** C. ***HD-ZIPIII*** **orthologs are more highly expressed in the xylem, but are also expressed in the leaf.**

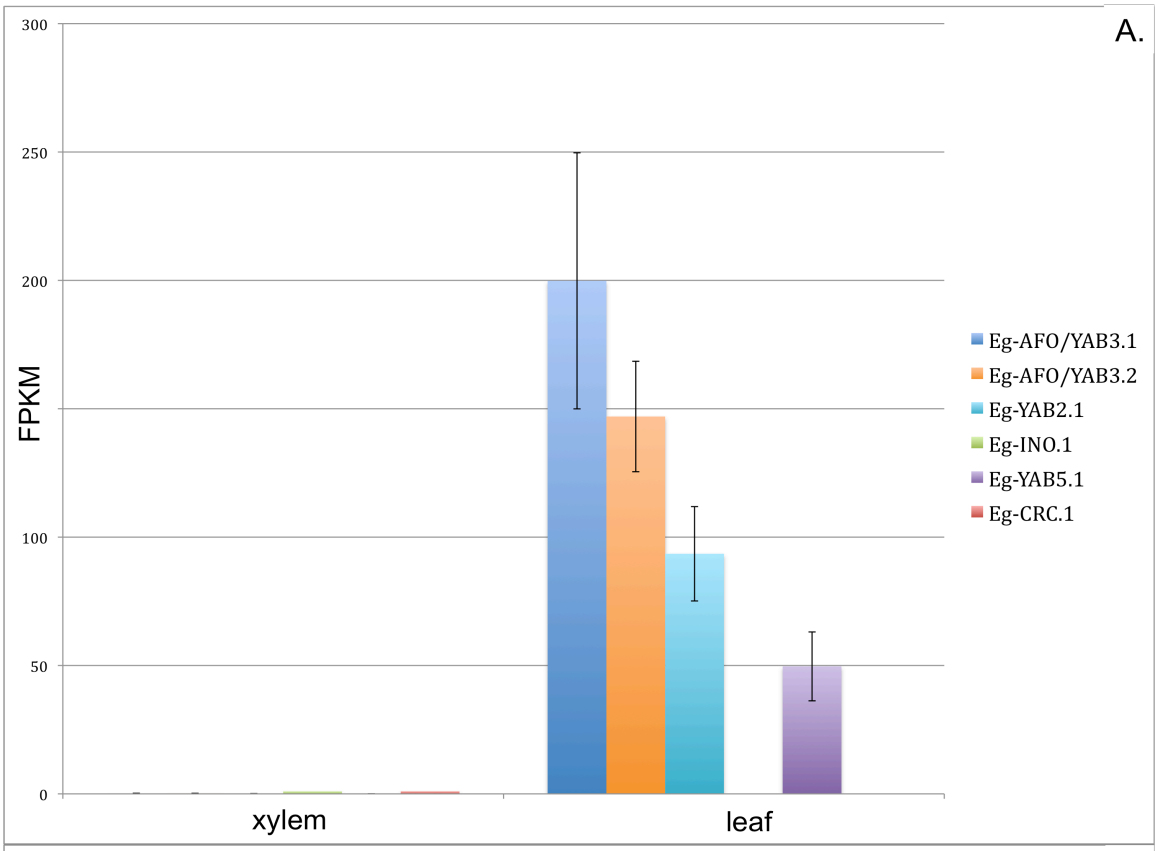
A.
300
250
200
100
50
0
FPKM
xylem
leaf
Eg-AFO/YAB3.1
Eg-AFO/YAB3.2
Eg-YAB2.1
Eg-INO.1
Eg-YAB5.1
Eg-CRC.1

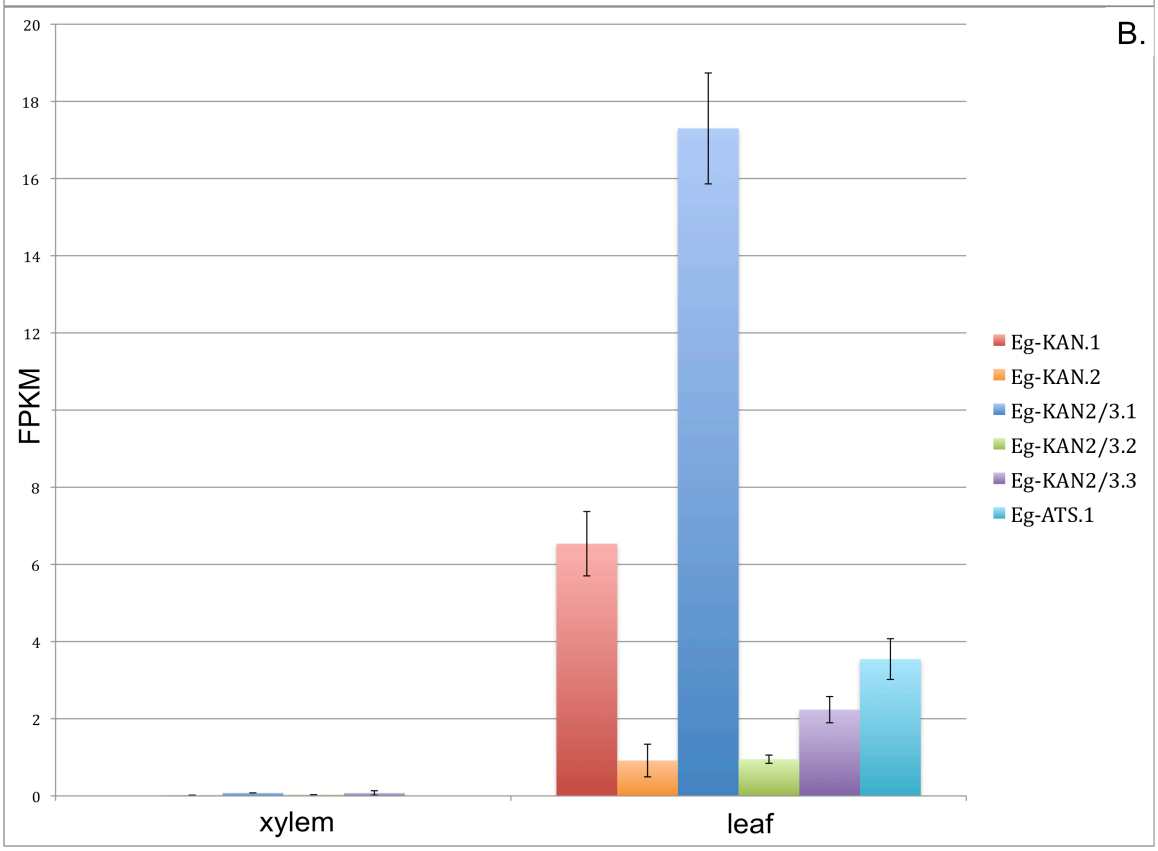
B.
20
18
16
14
12
8
6
4
2
0
FPKM
xylem
leaf
Eg-KAN.1
Eg-KAN.2
Eg-KAN2/3.1
Eg-KAN2/3.2
Eg-KAN2/3.3
Eg-ATS.1

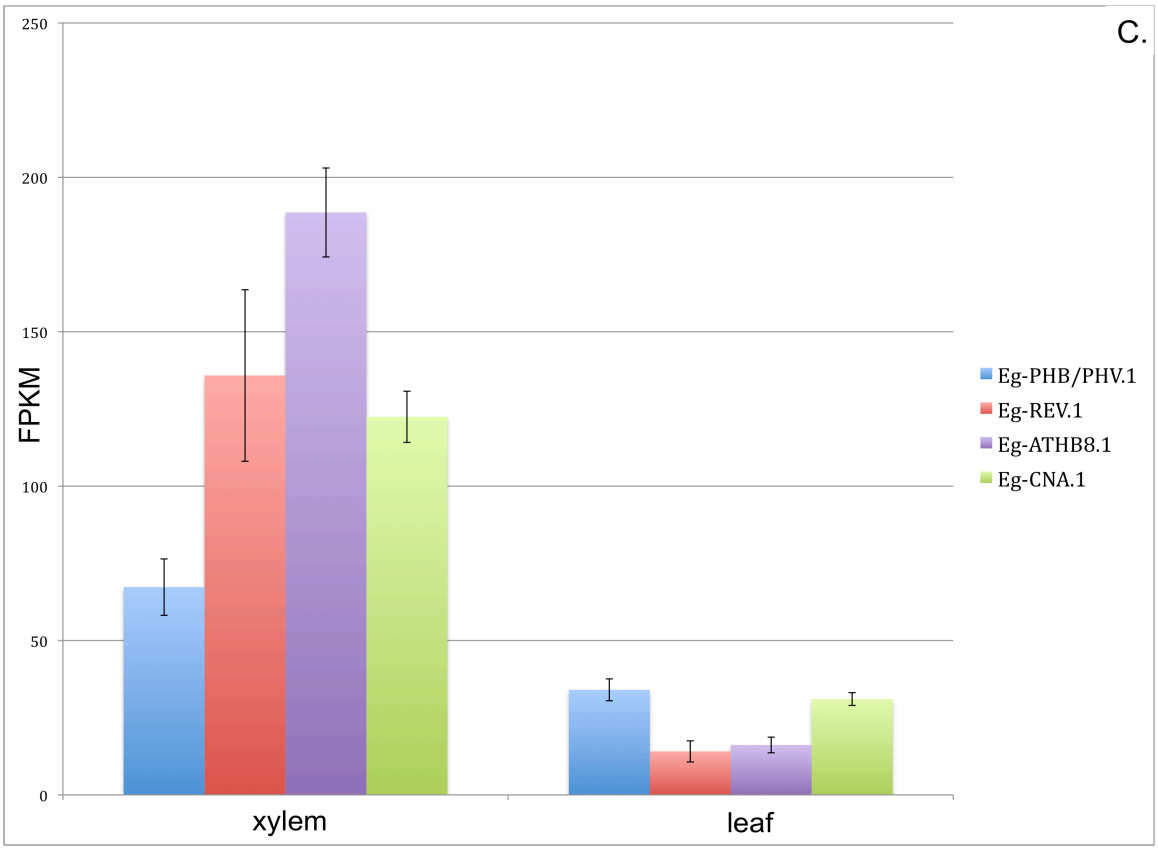

Figure 3.3 FPKM expression levels of three gene families in *E. grandis* involved in determining abaxial-adaxial polarity (*YABBY, KANADI*, and *HD-ZIPIII*). A. ***YABBY*** **orthologs are primarily leaf expressed with low amounts expressed in the xylem.** B. ***KANADI*** **orthologs are expressed in the leaf with little expression in the xylem.** C. ***HD-ZIPIII*** **orthologs are more highly expressed in the xylem, but are also expressed in the leaf.**

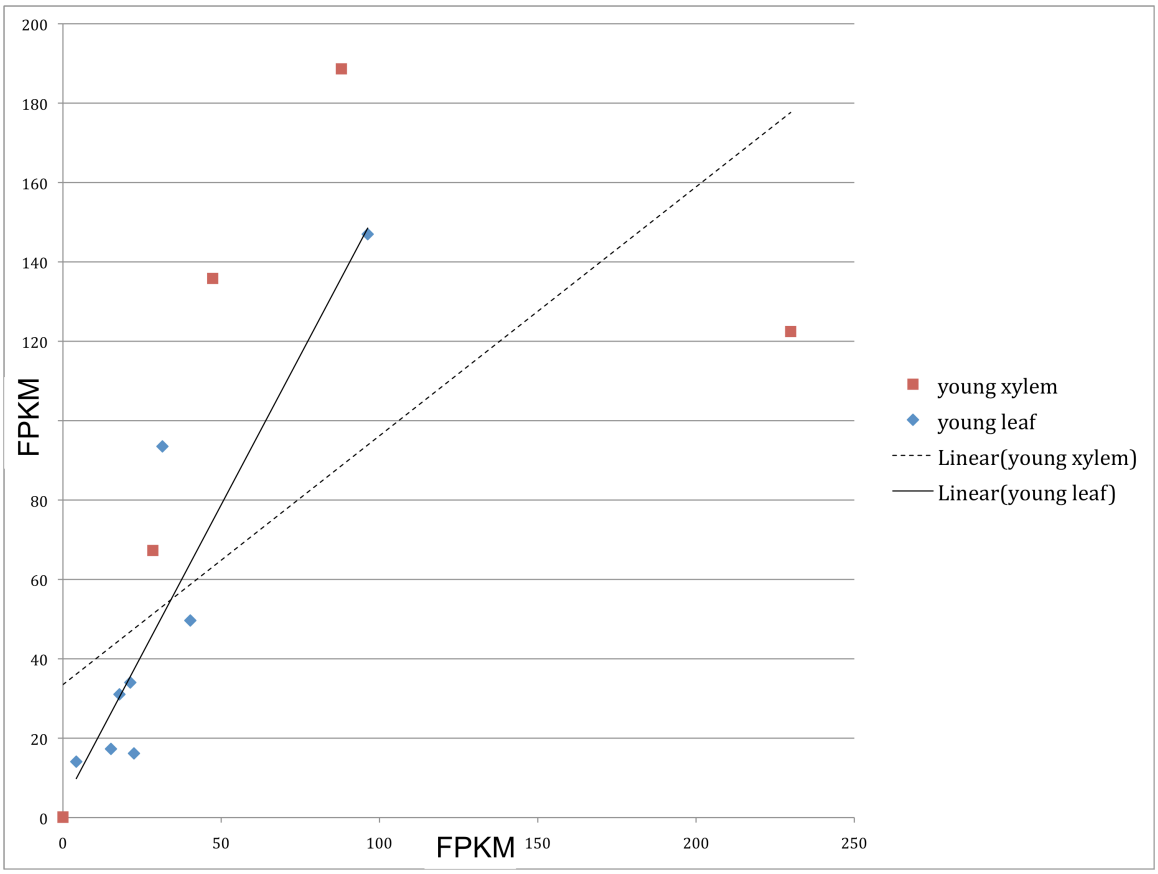

Figure 3.4 Correlation between eucalyptus hybrid (x-axis) and *E. grandis* (y-axis) FPKM expression values for xylem and leaf tissues, showing similarity between the two data sets.

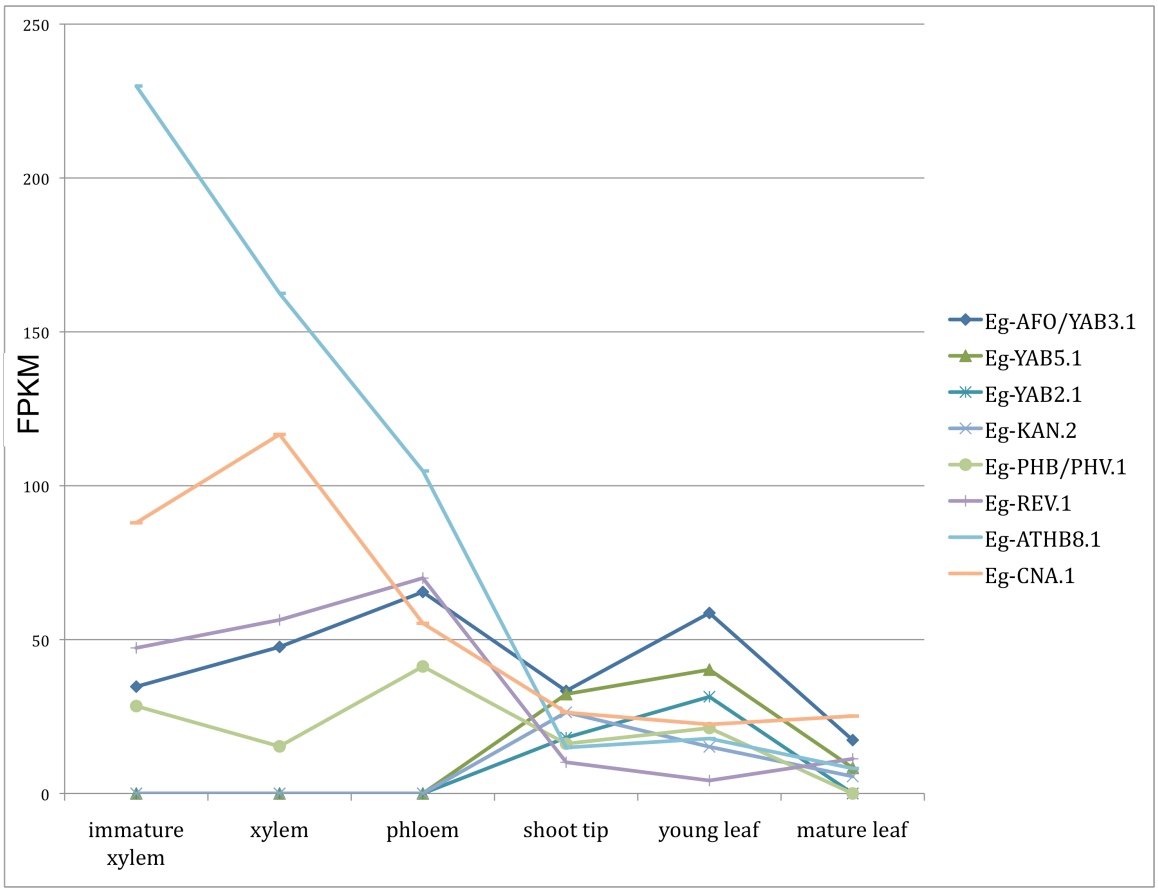

Figure 3.5 FPKM expression levels of all of the available gene contigs (for *Eg-AFO/YAB3.2, Eg-YAB2.1, Eg-YAB5.1, Eg-KAN2/3.1, Eg-PHB/PHV.1, Eg-REV.1, Eg-ATHB8.1,* and *Eg-CNA.1*) in immature xylem, xylem, phloem, shoot tip, young leaf, and mature leaf.

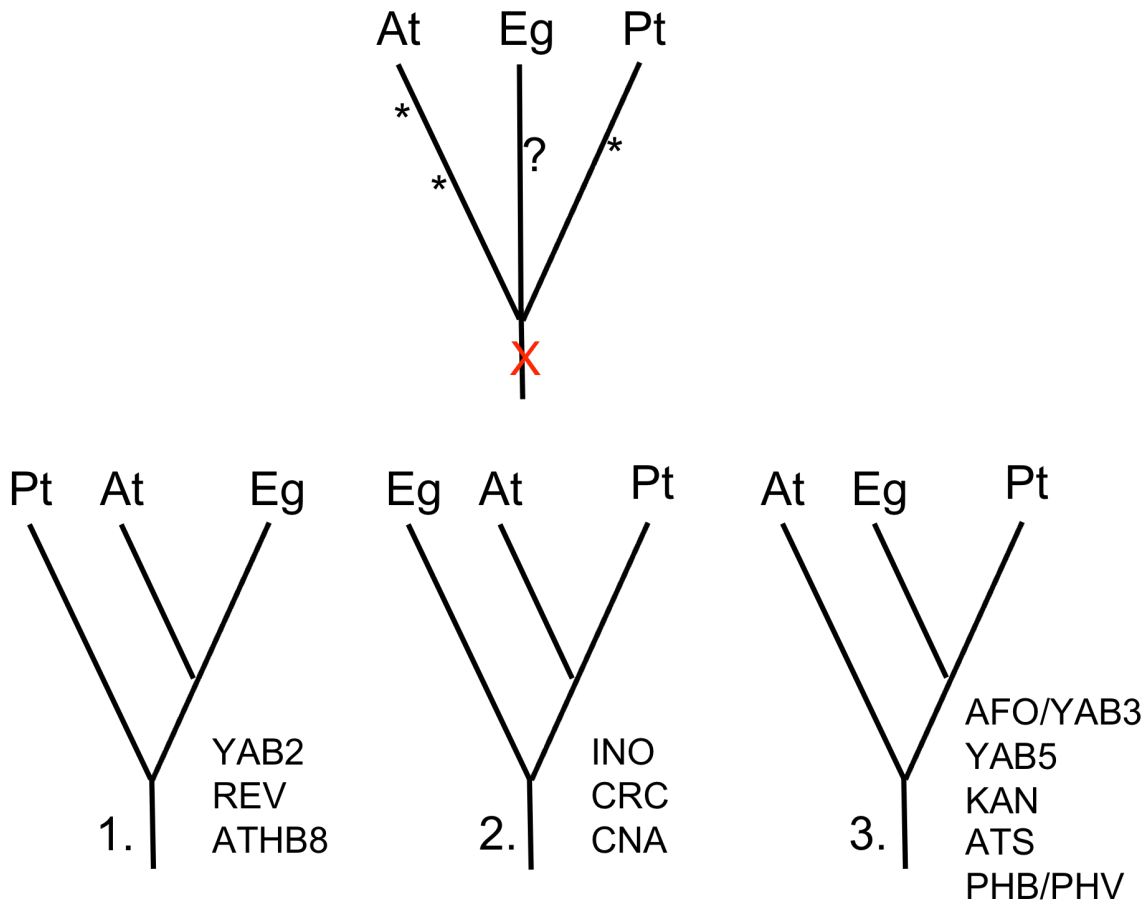

Figure 3.6 Phylogenetic relationship of *Arabidopsis thaliana*, *Eucalyptus grandis*, and *Populus trichocarpa* is represented as a trichotomy (top). Below, are three ways to resolve the trichotomy with #3 being most representative of dorsiventrality genes (using ML analysis), in particular: *AFO/YAB3, YAB5*, all *KANADI* genes, and *PHB/PHV* genes. At – *Arabidopsis*, Eg – eucalyptus, Pt – poplar, X – denotes ancient hexaploidy event, * – denote whole genome duplication (WGD), ? – denotes hypothesized WGD in eucalyptus (according to Myburg et al. 2012).

Chapter 4: North American *Populus* phylogeny and leaf analysis

4.1 Synopsis

The genus *Populus* has proven to cause difficulty in resolution, primarily due to extensive hybridization. I used six nuclear genes in a phylogenetic analysis of North American representatives of the genus in order to resolve their phylogenetic relationships and determine whether the assigned sections are maintained. There was variability in arrangement of the sections depending on the gene, but the overall grouping of the species within the appropriate sections was generally conserved with the exception of *P. guzmantlensis*. This species, belonging to the section *Aigeiros*, consistently grouped with its Mexican relative, *P. mexicana* (section *Abaso*). Further, I analyzed the anatomy of most of the species used in the phylogeny in order to elucidate the ancestral leaf character (bifacial vs. isobilateral) in *Populus*. Based on morphological and anatomical observations of leaves of North American species, only sections *Tacamahaca* and *Leucoides* consist of species with bifacial leaves. As none of the species belonging to either of these sections grouped sister to the rest of the poplars, it can therefore be concluded that bifacial leaves are probably derived within the genus *Populus*.

4.2 Introduction

Many of the species belonging to the genus *Populus*, collectively known as poplars, have a wide native range and can be found throughout the world, including Europe, Asia, Africa, and North America. It is generally accepted that there are 29 species within the genus (Eckenwalder 1996b), although some recognize as few as 22 or as many as 85 species. Some

of these may be varieties or hybrids that may be difficult to differentiate. Eckenwalder (1996) divided the genus into six sections: *Abaso*, *Aigeiros*, *Leucoides*, *Populus* (or *Leuce* in some studies), *Tacamahaca*, and *Turanga*. He based this on morphological characters of the flowers and inflorescences (including carpels, seeds, stamens, bracts) as well as leaves and buds (Eckenwalder 1996b). All of the sections, except *Turanga*, are represented in North America, with the following species: *Aigeiros* (*P. deltoides*, *P. fremontii*), *Abaso* (*P. mexicana*), *Leucoides* (*P. heterophylla*), *Populus* (*P. grandidentata, P. guzmantlensis, P. monticola, P. simaroa, P. tremuloides*), *Tacamahaca* (*P. angustifolia*, *P. balsamifera*, *P. trichocarpa*) (Eckenwalder 1996b). *Populus monticola* has been suggested to be an introduced variety of *P. alba* (var. *subintegerrima*) and *P. simaroa* a variety of the very closely-related *P. guzmantlensis* (Dickmann 2001). Therefore, it is reasonable to consider ten species to be native to North America, rather than the previously described 12.

4.2.1 Phylogenetics of the genus

The majority of the taxonomic inferences and placement of species into sections was based on morphological evidence (Eckenwalder 1996b). Recent studies have used DNA evidence to determine species relationships within the genus (Leskinen and Alstrom-Rapaport 1999, Hamzeh and Dayanandan 2004, Cervera et al. 2005, Hamzeh et al. 2006). Although these molecular studies provide more insight in comparison to the more traditional systematic studies, some issues have yet to be resolved. The phylogenetic relationships of the species within the genus *Populus* are not completely clear and are only partially resolved due to high variability in morphological characters and the possibility of widespread interspecific hybridization (Slavov and Zhelev 2010).

Hamzeh and Dayanandan (2004) included 21 species in their study, but omitted *P. mexicana* and other Mexican species. This makes it unclear which species or group of species is in fact sister to the rest of the poplars, as Eckenwalder (1977a) placed *P. mexicana* into its own section, *Abaso*, based on its close resemblance to the earliest known *Populus* fossils and putatively most primitive floral characteristics (Manchester et al. 1986, Eckenwalder 1996b), although the latter are not identical to the extant species. Cervera et al. (2005) included this species in their analysis, but even suggested that *P. mexicana* may belong to an entirely different genus, due to its dissimilarity to the remaining poplars.

Other molecular studies have produced conflicting results regarding the placement of certain sections. For example, using chloroplast RFLP (restriction fragments length polymorphism) DNA analysis, Smith (1988) showed that section (sect.) *Populus* appeared as a highly nested clade grouping with other sections, while Leskinen and Alstrom-Rapaport (1999) and Cervera et al. (2005) placed *Populus* as the sister group to the rest of the poplars using nuclear ITS (internal transcribed spacer) sequences and AFLPs (amplified fragment length polymorphims), respectively. Using nuclear and chloroplast evidence has also led to conflicting results concerning relationships of the species. For example, nuclear phylogenies place *P. nigra* within a clade that otherwise comprises *Aigeiros* species, while *P. nigra* plastid-based phylogenies placed it more closely to species within sect. *Populus* (Smith and Sytsma 1990, Hamzeh and Dayanandan 2004).

4.2.2 *Populus* leaf variation

There is a large amount of variability of leaf, bud, and twig morphology (i.e., tooth number, leaf shape, and bud and shoot pubescence) even within a single species of *Populus*

(e.g., *P. tremuloides*; Barnes 1975). A typical *Populus* leaf is simple in shape, has grandular teeth along the blade margins, often has glands at the blade/petiole junction, and has a petiole that is often mediolaterally flattened (Eckenwalder 1977b, 1996a). Variations among these characters have been important in species classification in the genus. Poplars contain two major types of leaf blades: bifacial and isobilateral, where the latter is more typical of the genus (Van Volkenburgh and Taylor 1996). Bifacial leaves have palisade mesophyll cells on the adaxial side of the leaf, while the abaxial surface has spongy mesophyll cells. In contrast, isobilateral leaves have palisade mesophyll cells on both adaxial and abaxial sides of the leaf. This phenomenon has been termed "abaxial greening", a phenotype that contributes to the "flutter syndrome" or the movement of leaves due to a slight breeze, described by Cronk (2005). Isobilateral leaves are known to be associated with a mediolaterally flattened petiole, which is also typical of the genus. Alternatively, a radial or rounded petiole has been described as being associated with a bifacial leaf within the genus. According to Eckenwalder (1996a), the following sections contain leaves that are bifacial: *Aigeiros* (but this also contains species with isobilateral leaves), *Leucoides*, *Populus*, and *Tacamahaca*. The remaining sections (*Abaso* and *Turanga*) contain only the typical isobilateral leaves. Morphological and anatomical observations of leaves are necessary in order to be able to determine which species, particularly within the sect. *Aigeiros*, are in fact isobilateral and have the abaxial greening phenotype or not.

4.2.3 Objectives

The literature suggests difficulty in resolving the phylogeny of the genus *Populus* as a whole due to hybridization (Slavov and Zhelev 2010, for example). This study was focused

on only the species that are native to North America, which is representative of about one third of the genus, in order to first elucidate relationships of a smaller number of species.

The main objective of this study was to attempt to resolve the phylogenetic relationships of ten North American *Populus* species in relation to the assigned sections and to determine the species/section/clade that is sister to the rest of the poplars, previously suggested to be *P. mexicana* (sect. *Abaso*) on the basis of morphology (Eckenwalder 1977a, 1996a). This information can be used to make inferences about which leaf characters (abaxial greening phenotype or the distribution of isobilateral and bifacial leaves) are ancestral. The second objective of this study was to characterize the North American species based on their leaf morphology and anatomy.

4.3 Materials and methods

4.3.1 Species selection

Ten *Populus* species were used in this study, representing five *Populus* sections native to North America: *Abaso* (*P. mexicana*), *Aigeiros* (*P. deltoides*, *P. fremontii*), *Leucoides* (*P. heterophylla*), *Populus* (*P. grandidentata*, *P. guzmantlensis*, *P. tremuloides*), *Tacamahaca* (*P. angustifolia*, *P. balsamifera*, *P. trichocarpa*). The genus *Salix* (willow) is sister to *Populus*, in the family Salicaceae (Leskinen and Alstrom-Rapaport 1999, Azuma et al. 2000). Five *Salix* species were used as outgroups in this analysis: *S. arctica*, *S. eleagnos*, *S. lapponum*, *S. reticulata*, and *S. sitchensis*.

At least three replicate samples for each of the ten *Populus* species were collected either from herbarium or fresh material, while a single sample of each of the *Salix* outgroup species was included (Table 4.1).

4.3.2 Gene selection

In addition to nuclear ribosomal ITS, an array of genes was selected based on primer availability, interest in function, presence as a single copy in the genome, and/or previous use in phylogenetic analyses. An initial test of primer specificity was performed on three distantly related *Populus* species (*P. mexicana*, *P. tremuloides*, and *P. trichocarpa*), including *Salix eleagnos* as an outgroup species. A total of 14 genes were initially tested. Six of these genes were successfully amplified and sequenced in the four species initially tested. These genes included ITS (Hamzeh and Dayanandan 2004), *glycoside hydrolase family 19 protein* (chitinase class I) (*Gly*), *major intrinsic protein* (*Mip*), *cinnamyl-alcohol dehydrogenase* (*Cad*), *phytochelatin synthetase-like protein* (*Pcs*), *S-adenosyl-L-homocysteine hydrolase* (*Sad*).

ITS primer sequences were the same as those used by Hamzeh and Dayanandan (2004) to amplify the 5.8S rDNA region and the surrounding ITS1 and ITS2 regions. The primers for the remaining five genes were supplied by A. Geraldes and R. Soolanayakanahally (UBC), which they created based on version 2.0 of the *Populus* genome (Phytozome; see Chapter 3) (Table 4.2). Sequence data for *P. deltoides* and *P. tremula* (Geraldes et al. 2011) showed that there was variation in the original primer sequences of two genes. Therefore, I redesigned the reverse primers for *Mip* and *Sad* using Primer3 (Rozen and Skatletsky 2000; see Chapter 2). The sequences, sizes of these genes, and locations of where the primers bind are shown in Figure 4.1 and Appendix C.1.

4.3.3 Sample preparation and sequencing

Genomic DNA was extracted from all of the *Populus* leaf samples using a modified version of the CTAB protocol of Doyle and Doyle (1987). The appropriate gene sequence was amplified using polymerase chain reaction (PCR) on an Eppendorf Mastercycler gradient thermocycler with varying conditions depending on the primers: 1) *Mip*, *Sad*, and ITS: SSU50/55 [95°C 3min, (94°C 1 min, 50/55°C 1min, 72°C 2min) x36, 72°C 5min, 4°C hold]; and 2) *Gly*, *Cad*, and *Pcs*: GFP2 [94°C 4min, (94°C 40 sec, 60°C 1min, 72°C 90 sec) x36, 72°C 10min, 4°C hold]. PCR samples were run on 1% agarose gel at 100V for 30min and samples that contained at least 20ng of product were sent out for purification and sequencing (Macrogen USA, Rockville, Maryland, USA).

4.3.4 Phylogenetic analysis

Sequences were edited and base-called with universal ambiguity codes using Sequencher v4.5 (Gene Codes Corporation, Ann Arbor, Michigan). Consensus contig sequences were initially aligned using MUSCLE (Edgar 2004) and then manually adjusted using MacClade 4.05 (Maddison and Maddison, released 22 September 2002). Sequences that were very short in length were removed. The final alignment (see Appendix C.2-C.7) was run with JModelTest v0.1.1 (see Chapter 2; Guindon and Gascuel 2003, Posada 2008) to determine the optimal substitution model of DNA evolution fitting the particular data set. The generalized time-reversible (GTR) model fit all of the data sets, but a gamma correction (*Pcs*) or estimate of invariable sites (ITS, *Gly*, and *Mip*) or a gamma correction and estimate of invariable sites (*Cad* and *Sad*) was also applied to the appropriate sequence alignment during further maximum likelihood (ML) analysis. An ML analysis, including 1000

bootstrap reiterations, was run with RAxML (Stamatakis et al. 2005) and maximum parsimony (MP) analysis (DNAPARS) was performed with PHYLIP (Felsenstein 1989, 2005), both using default settings with 1000 replicates. ML and MP bootstrap support values, equal to or greater than 50% are included on ML tree figures. The resulting phylogenetic trees were rooted with *Salix* species as the outgroup.

4.3.5 Morphological and anatomical analyses

Fresh leaf material of six out of the ten North American *Populus* species (*P. balsamifera*, *P. deltoides*, *P. fremontii*, *P. grandidentata*, *P. tremuloides*, and *P. trichocarpa*) (Table 4.3) was collected into 70% FAA (see Chapter 1). Pieces of leaf tissue from the middle of the blade, on either side of the midvein, and from the midpoint of the petiole were cut and taken through an ethanol dehydration series. Following complete dehydration with 100% ethanol, tissues were infiltrated with LR White resin and embedded in the resin (see Chapter 1).

Leaf tissues from *P. angustifolia* and *P. heterophylla* were collected from UBC Herbarium material (Table 4.3). Leaf blade and petiole pieces, sampled as above, were initially rehydrated by boiling in 50% ethanol for about 5 min and then cleared with 10M NaOH at 55°C for about 48 hours using a modified protocol from Welsh (2009). The cleared tissues were then taken through an ethanol dehydration series and subsequently embedded in LR White, as described for fresh leaf material above. The resin blocks were sectioned with glass knives on an ultramicrotome, stained and mounted with Permount mounting medium and photographed as described in Chapter 1. Samples of *P. mexicana* and *P. guzmantlensis* were unavailable for anatomical analysis.

4.4 Results

4.4.1 Phylogeny

Not all regions were amplified for each species or sample (Appendix C.8). The sequences in the final alignment were truncated to correspond to the longest sequence available for all of the taxa per gene amplified (Appendix C.2-C.7). The retained amplified regions corresponded to the following percentages of each gene in *P. trichocarpa* gene models (obtained from Phytozome): 354bp or 68.7% of the region amplified by *Cad* primers, 500bp or 76.1% of amplified *Gly* region, 602bp or 60.2% of amplified ITS region, 564bp or 76.9% of amplified *Mip* region, 594bp or 77.4% of amplified *Pcs* region, and 392bp or 44.6% of amplified *Sad* region (Figure 4.1).

4.4.1.1 Cinnamyl-alcohol dehydrogenase (Cad)

The region amplified, 354bp in length (based on the *P. trichocarpa* gene model from Phytozome), in all of the species for the *Cad* phylogeny corresponds to the intron between exons three and four (Figure 4.1). The alignment included 28 samples, was 441bp in length, and contained some variability between the species, with many species-specific indels (Appendix C.2).

The overall grouping of the species within sections are as expected, except for the placement of *Leucoides* within *Tacamahaca* with low bootstrap support (Figure 4.2). The rest of the sections (excluding *Tacamahaca*) with more than one representative, are monophyletic within this gene tree with high bootstrap support. While *Leucoides* is nested within

Tacamahaca, Tacamahaca is sister to *Aigeiros*. Section *Populus* is sister to the rest of the poplars in this gene tree.

The majority of species, at the current taxon sampling, are monophyletic with the exception of *P. balsamifera*, *P. deltoides*, and *P. fremontii*. The *P. trichocarpa* samples within the clade all group together, with high bootstrap support, sister to *P. heterophylla*, with little support, and the rest of the *P. balsamifera* samples group together with the exception of CAR5, which is present on the backbone of this clade. The monophyly of the *Aigeiros* clade is supported with high bootstrap support. Within this clade, three *P. deltoides* samples (UGA, 125-3, 125-6) group together while the placement of the rest of the *Aigeiros* samples within the clade has little support with all support values much lower than 50%.

4.4.1.2 Glycoside hydrolase family 19 protein (Gly)

The region amplified corresponds to 500bp (based on the *P. trichocarpa Gly* gene model, from Phytozome) and is located in the intergenic region between exons three and four (Figure 4.1). There was some variability among all of the 28 sequences used in the alignment, which was 526bp in length (Appendix C.3).

The general topology of the phylogenetic trees produced by ML and MP was similar, with the exception of the placement of *P. grandidentata* (UGA) (Figure 4.3). This gene tree grouped the poplars into three clades consisting of *Tacamahaca*, and *Abaso* (including *P. guzmantlensis*) nested within sect. *Populus*, as sister to each other, and *Aigeiros* as sister to the rest of the poplars. The *Populus/Abaso* clade was not similarly supported with MP analysis, which placed *P. grandidentata* species as sister to the rest of the poplars with 81% bootstrap support. Although the grouping of *Aigeiros* (with little variation between the

species) had high support with MP, grouping of the rest of the poplars had very low support of 14%.

Several species within this gene tree were not monophyletic. Within *Tacamahaca* clade, there were three *P. trichocarpa* individuals that clustered together (QCI, 34, 101-1) with moderate support, while the rest of the *P. trichocarpa* samples (33, Ptr2) grouped with *P. angustifolia* individuals with no branch length. *Populus trichocarpa* and *P. angustifolia* species grouped together in a clade with high support, as did the three *P. balsamifera* individuals.

Within the *Populus/Abaso* clade, not supported with MP, *Abaso* and *P. guzmantlensis* were nested sister to *P. tremuloides* individuals with poor bootstrap support. In MP analysis, the *P. tremuloides* individuals, supported with 100%, were sister to the rest of the species (with the exception of *Aigeiros* clade and *P. grandidentata*) with high support. The clade comprising *Abaso* and *P. guzmantlensis*, for MP analysis, had 100% bootstrap support and grouped sister to the *Tacamahaca* group with 100% bootstrap support.

4.4.1.3 Internal transcribed spacer (ITS)

The ITS primers amplified the rDNA regions and the surrounding ITS1 and ITS2 regions, which corresponds to 1000bp. The region used in the alignment in all 23 sequences was 607bp allowing for a minimal amount of gaps due to lack of sequence information (from our sequencing) (Appendix C.4). The unaligned *P. trichocarpa* sequence corresponded to 602bp.

The ITS phylogenetic tree is separated into five major clades (Figure 4.4): the *Salix* outgroup, *Abaso* and *P. guzmantlensis*, sect. *Populus* (excluding *P. guzmantlensis*), *Aigeiros*

(represented here only by *P. deltoides*), and *Tacamahaca*. The position of *Abaso/P. guzmantlensis* group as sister to the rest of the poplar species has high bootstrap support from MP, and moderate ML support. *Populus balsamifera* and *P. trichocarpa* are not monophyletic species (of those with more than one representative). These two species lack variation between each other and in comparison to *P. angustifolia*.

Both of the *P. mexicana* samples and the *P. guzmantlensis* group together, and show substantial sequence variability from the rest of the taxa. The entire sequence is generally continuous among all the species, with little sequence variation, except that the *Abaso* and *P. guzmantlensis* group have a TTCT indel at bases 22 to 25 and another indel of GAA at 424 to 426 bases that are absent in the rest of the species, including the *Salix* outgroup. Section *Populus* is not monophyletic due to the placement of *P. guzmantlensis* within *Abaso*. Within this grouping, *P. guzmantlensis* (372) is sister to *P. mexicana* (371) with high bootstrap support.

4.4.1.4 Major intrinsic protein (Mip)

The region amplified with the *Mip* primers and used in the alignment corresponds to 564bp of the *P. trichocarpa* sequence, based on the gene model from Phytozome. This region spans a portion of the first exon as well as part of the following intron (located between exons one and two) (Figure 4.1). The final alignment is 666bp in length and contains 22 individuals (Appendix C.5).

The species within this tree are separated into the expected sections (with ML and MP), which are all monophyletic (Figure 4.5). Sections *Tacamahaca* and *Populus* are sister to each other and *Abaso* is sister to this grouping although this is poorly supported. The

Aigeiros group is sister to the rest of the poplars. Within *Tacamahaca*, *P. balsamifera* and *P. trichocarpa* are not monophyletic and show, along with *P. angustifolia*, high sequence similarity. Within sect. *Aigeiros*, *P. deltoides* is also not monophyletic and shows little sequence variability from the single sampled *P. fremontii* individual.

4.4.1.5 Phytochelatin synthetase-like protein (Pcs)

The region of the *Pcs* gene that was amplified and used in the alignment corresponds to 594bp located in the intron between exons two and three as well as a portion of exon three (Figure 4.1), based on the *P. trichocarpa* gene model from Phytozome. The alignment used in the phylogenetic analysis consisted of 612bp in 26 individuals (Appendix C.6).

The overall arrangement of species is consistent between ML and MP analyses, with slight variation in the placement of the some of the individuals (Figure 4.6). None of the sections are monophyletic in this gene tree. Section *Aigeiros* is nested within *Tacamahaca* species, with sect. *Populus* (without *P. guzmantlensis*) sister to that grouping. The clade comprising *Abaso* and *P. guzmantlensis* is sister to the rest of the poplars.

Several species within this gene tree are also not monophyletic. These include *P. balsamifera, P. deltoides, P. mexicana,* and *P. trichocarpa.* The majority of the *P. balsamifera* individuals (with the exception 11-1-3) are grouped with *P. angustifolia*, with little variability, but high bootstrap support. Further, both *P. fremontii* individuals are nested within a *P. deltoides* group. With ML, the other *P. deltoides* individual (125-3) is located at the backbone with *P. trichocarpa* individuals (Ptr2, 11-1-6), which with MP analysis is sister to the *Aigeiros* group with low bootstrap support. In the MP analysis, two *P. trichocarpa* individuals (Ptr2, 11-1-6) are similarly located at the backbone with little sequence

variability. The remaining *P. trichocarpa* individuals (QCI, 34) group with one *P. balsamifera* individual (11-1-3), with moderate bootstrap support.

4.4.1.6 S-adenosyl-L-homocysteine hydrolase (Sad)

The region used in the alignment corresponds to 392bp within the intron located between first and last exons within the *Sad* gene (Figure 4.1), based on the *P. trichocarpa* gene model from Phytozome. The *Sad* alignment consists of 398bp and 15 individuals (Appendix C.7).

The phylogenetic trees for *Sad* with ML and MP analyses vary in the positions of the general groups of species, although the species belonging to the previously described sections are mostly monophyletic (Figure 4.7). In this gene tree, sect. *Tacamahaca* is the only one that is not monophyletic. Section *Populus* individuals are nested within *Tacamahaca*, and the resulting clade is sister to *Aigeiros*. Section *Abaso* is sister to the rest of the poplars. For MP analysis, sect. *Populus* individuals are sister to the rest of the poplar species, but with low support.

4.4.2 Leaf analysis

4.4.2.1 Leaf morphology

Leaf blades and petioles were analyzed morphologically (Figure 4.8). The two types of leaves present in the ten species studied are isobilateral and bifacial. Isobilateral leaves were determined based on similar colouration of the adaxial and abaxial surfaces of the leaf blades and mediolateral flattening of the petiole. In contrast, bifacial leaves have a darker adaxial surface and a lighter abaxial surface, which was sometimes a challenge to determine

as some of the leaf tissues were faded on the herbarium sheets, and the petiole appeared to be more rounded and shorter compared to the length of the blade. Based on morphological observations here, *P. fremontii*, *P. grandidentata*, *P. guzmantlensis*, *P. mexicana*, and *P. tremuloides* have isobilateral leaves. These correspond to sections *Abaso, Aigeiros,* and *Populus*. The remaining four species, from this analysis, that have bifacial leaves include *P. angustifolia*, *P. balsamifera*, *P. heterophylla*, and *P. trichocarpa*, corresponding to sections *Leucoides* and *Tacamahaca*.

4.4.2.2 Leaf anatomy

Both the adaxial and abaxial surfaces of isobilateral leaves consist of palisade mesophyll cells within the blade, while bifacial leaves contain this tissue only on the adaxial side, while its abaxial surface consists of spongy mesophyll cells. In transverse section, the petiole is mediolaterally flattened in isobilateral leaves and radial in bifacial leaves. Similarly, the anatomical observations of leaf blade and petiole revealed that *P. fremontii*, *P. grandidentata*, and *P. tremuloides* have isobilateral leaves while *P. angustifolia*, *P. balsamifera*, *P. heterophylla*, and *P. trichocarpa* have leaf blades that are bifacial (Figure 4.9), with the vascular bundles in a collateral arrangement (xylem towards the adaxial side and phloem towards the abaxial side). Within the petioles, the vascular bundles in all of the species are fully or almost amphicribral, where the phloem fully or partially surrounds the xylem.

A few exceptions in petiole anatomy were observed in *P. angustifolia*, *P. fremontii*, and *P. grandidentata* (Figures 4.9B, 4.9H, 4.9J). The vascular bundles were either arranged in a row (in a flattened petiole) or a ring-like pattern (in a radial petiole). The species that

contain petioles with vascular bundles arranged in a row include *P. angustifolia* (three major and two minor bundles), *P. deltoides* (two major bundles), and *P. tremuloides* (three major and one minor bundles). A ring-like pattern of the vascular bundles is seen in petioles of *P. balsamifera* (one major and two minor bundles), *P. fremontii* (about three major bundles), *P. heterophylla* (seven major bundles), and *P. trichocarpa* (one major and about two minor bundles). Although the vascular bundles are arranged in a row in *P. angustifolia*, the petiole is not mediolaterally-flattened, but rather flattened in the dorsiventral plane. The radial petiole of the *P. fremontii* is unusual in that it is associated with an isobilateral leaf blade. *Populus grandidentata* was shown to be an exception in containing a single horseshoe-shaped vascular bundle, with phloem towards the outside and xylem located towards the inside of the petiole.

4.5 Discussion

Phylogenetic relationships within the genus *Populus* were investigated and the overall species groupings were generally consistent with the currently accepted sections (Eckenwalder 1996b), with one major exception concerning the placement of *P. guzmantlensis*. There was variability among the gene trees as to which species/section was sister to the rest of the poplars which may reflect limited resolving power of individual genes. Half of the genes showed that *Abaso* or the grouping of *P. mexicana* and *P. guzmantlensis* was sister to the rest of the poplars. The placement of sect. *Abaso* as sister to the rest of the genus is consistent with previous morphological (Eckenwalder 1977a, 1996a) and molecular evidence (Cervera et al. 2005). The other gene trees, on the other hand, showed that *Aigeiros* (with *Gly* and *Mip*) or sect. *Populus* (with *Cad*) might be sister to the rest of the poplars.

Not all of the individual phylogenetic trees produced the same species arrangements, and therefore may be more representative of gene rather than species trees. Section *Tacamahaca* was not monophyletic in most gene trees. The single North American representative of sect. *Leucoides* (*P. heterophylla*) was sister to most of the *P. trichocarpa* individuals, nested within *Tacamahaca*. This placement was based on a single gene phylogeny (*Cad*) of a single *P. heterophylla* individual. Therefore a more thorough investigation of the relationship of *Leucoides* to the rest of the sections is still necessary. *Pcs* and *Sad* also showed a grouping of sect. *Aigeiros* and sect. *Populus* species, respectively, within *Tacamahaca*. A non-monophyletic origin of *Tacamahaca* is consistent with other studies (i.e., Eckenwalder 1996b, Hamzeh and Dayanandan 2004).

The placement of *P. angustifolia* is intriguing, as it does not place in a separate clade, apart from the balsam poplars (*P. balsamifera* and *P. trichocarpa*). *Populus angustifolia* is placed within *Tacamahaca*, between *P. trichocarpa* and *P. balsamifera*. Although some consider these as subspecies (i.e., *P. balsamifera* subsp. *trichocarpa* and *P. balsamifera* subsp. *balsamifera*), a recent study clearly showed that *P. trichocarpa* and *P. balsamifera* are sister species (Levsen et al. 2012). Therefore, it would be expected that these two species are more closely related to each other than to *P. angustifolia*. Only one phylogeny (*Gly*) shows the grouping of *P. angustifolia* and *P. trichocarpa* with high bootstrap support, while another (*Sad*) shows this grouping but with very little support. The sequence of *Sad* used to make the phylogeny was quite short, corresponding to only ~15% of the whole gene, and therefore may not provide a reliable representation of the species groupings. Another phylogeny (*Pcs*) showed the grouping of *P. angustifolia* with *P. balsamifera* with high support, but the overall resolution within sections *Tacamahaca* and *Aigeiros* was quite low. Therefore, a greater

number of individuals, more genes, longer gene sequences, and/or a "coalescence" perspective (Degnan and Rosenberg 2009) would be required to fully resolve the placement of *P. angustifolia*, which is likely not with *P. trichocarpa* but rather as sister to the two balsam poplars.

The exception to the expected placement of species within the appropriate sections is that of *P. guzmantlensis*, which did not group within sect. *Populus* (with *P. grandidentata* and *P. tremuloides*), but instead consistently placed within sect. *Abaso* with *P. mexicana*, with high bootstrap support. This was observed in all of the gene phylogenies in this study in which *P. guzmantlensis* was sampled. The only currently available phylogeny including this species is based on morphological characters (Eckenwalder 1996b), and no molecular studies regarding the placement of *P. guzmantlensis* have been done to date. The initial grouping of *P. guzmantlensis* within sect. *Populus* is exclusively based on morphology, in particular similarities among flower, inflorescence, leaf, and other vegetative characters. My results would suggest that either sect. *Populus* is not monophyletic, as the case for *P. nigra* chloroplast sequences (Hamzeh and Dayanandan 2004, Smith and Sytsma 1990) and results for *Gly*, or that *P. guzmantlensis* should be placed into sect. *Abaso*, along with the other Mexican species (*P. mexicana*). Although I have presented results for a single *P. guzmantlensis* individual, two were sampled and grouped together with *P. mexicana* consistently (results not shown), but one sample was removed due to the short length of the sequences. The gene trees with *Abaso* and *P. guzmantlensis* representatives show little variation between these two species. It is possible that *P. guzmantlensis* samples were misidentified, and are actually *P. mexicana*. However, the leaf morphology is quite different

between the two species, and therefore it is unlikely that the collectors of *P. guzmantlensis* made that mistake.

Two individual phylogenies (*Gly* and ITS) placed the *P. mexicana/P. guzmantlensis* clade either nested within sect. *Populus* or as sister to the rest of the poplars, respectively, with unusually long branch lengths (compared to the rest of the phylogenies in this study). Long branch attraction (LBA) could erroneously group *P. mexicana* and *P. guzmantlensis* together, for example with ML (Rindal and Brower 2011). This was not likely the case here, as these species are almost identical in sequence to each other and all of the phylogenies grouped these two species together with high support in both ML and MP analyses.

4.5.1 Leaf character analysis

The genus *Populus* contains two types of leaves: bifacial and isobilateral. The distribution of this morphology is consistent with the described sections. Across North America, bifacial leaves are seen in *Tacamahaca* and *Leucoides*, while the rest of the sections contain species with isobilateral leaves, typical of the genus (Russin and Evert 1984). Bifacial leaf blades are typically associated with short, rigid, and rounded (in cross section) petioles. Alternatively, isobilateral leaves are typically associated with long, flexible, and mediolaterally flattened petioles, contributing to the "flutter syndrome" characteristic of majority of species within the genus (i.e., *P. tremuloides*) (Cronk 2005). The isobilateral leaf character allows leaves to flutter in the breeze and due to several contributing factors (discussed in Chapter 3), leads to an increase in carbon gain and deterrence of herbivory.

The blade-petiole association was generally conserved within species studied here, with the exception of *P. angustifolia*, *P. fremontii*, and *P. grandidentata*. The petiole of *P.*

angustifolia is flattened, despite being associated with a bifacial leaf, but in the dorsiventral plane. As the petiole is quite short in relation to the blade length, it would not allow the leaf to flutter in the same sense as a mediolaterally flattened petiole, but rather would let the leaf move in the dorsiventral axis, which would likely function more like a radial petiole. *Populus fremontii* and *P. grandidentata*, on the other hand, contain radial petioles that are associated with isobilateral leaves, despite the mediolaterally flattened appearance of the petioles (at the morphological level). The vascular bundle arrangement within the petiole of *P. fremontii* is typical of that observed in other radial petioles (e.g., *P. trichocarpa*), but the radial petiole of *P. grandidentata* is unlike those observed in other species with such petioles. This petiole is long, thin in cross-section, and contains a single horseshoe-shaped vascular bundle. The petioles of both species are long in relation to the leaf blade and thin (in the case of *P. grandidentata*), therefore the morphological characteristic of the petiole length is typical of isobilateral leaves. As the petiole was sampled at mid-length, it is possible that it may become more mediolaterally-flattened along its length, closer to the leaf blade and therefore be more indicative of petioles that are typically associated with isobilateral leaves.

There is clearly a large amount of variability among blade-petiole associations, which need further investigation, but the organization of the vascular bundles and their arrangement is more predictable. Flattened petioles, whether in the mediolateral or dorsiventral plane, contain vascular bundles that are arranged in a row. This is contrary to the bundle arrangement in radial petioles where they are arranged in a ring-like pattern, likely increasing the strength and the rigidity of the petiole. The vascular bundles are arranged in an amphicribral pattern, where the phloem surrounds the xylem, with the exception of the horseshoe-shaped bundle in *P. grandidentata* (where phloem partially surrounds the xylem).

Although there are bundles in species such as *P. deltoides* or *P. tremuloides* which contain collateral bundles, they are arranged in such a way that the two collateral bundles have their xylem oriented toward each other, and so in a sense have formed a larger amphicribral vascular bundle. Therefore, these results point to the overall unifaciality of the poplar petiole whether it is mediolaterally (or dorsiventrally) flattened or radial.

The distribution of leaf blade anatomy was as expected and appears to be the major differentiating factor of leaf type, rather than the petiole. The leaves that morphologically looked bifacial were also bifacial on the anatomical level (e.g., *Tacamahaca* and *Leucoides* species), as were the isobilateral-leaved species (e.g., *Aigeiros* and *Populus* species). Therefore, although *P. mexicana* and *P. guzmantlensis* leaf material was not studied at the anatomical level here due to a lack of available material, it is expected that their leaf blades are isobilateral. A bifacial leaf blade contains palisade mesophyll cells associated with the adaxial surface and spongy mesophyll on the opposite abaxial surface, which contain less chloroplasts and much more air spaces between cells (e.g., *P. trichocarpa*) that reflect more light and give the effect of a lighter underside (compared to the green top surface). On the opposite extreme is the isobilateral leaf blade which contains palisade mesophyll cells on both the top and bottom surfaces (e.g., *P. fremontii* and *P. deltoides* [Russin and Evert 1984]) containing similar amounts of chlorophyll, and therefore the surfaces are virtually indistinguishable in colouration (i.e., abaxial greening). Within isobilateral leaves, there is a gradient in the amount of chlorophyll-containing tissues at the abaxial surface, which depends on a variety of factors including leaf location in the canopy (i.e., shade or sun). For example, if a leaf is higher in the canopy, it is more likely to be exposed to more sunlight and therefore would contain cells at the abaxial surface that are more like those at the adaxial

(i.e., palisade mesophyll), as seen in adult eucalyptus leaves (James and Bell 2001). If a leaf is generally in the shade, then the tree will invest less energy in creating adaxial-like palisade mesophyll cells, and so rather produce an intermediate between spongy and palisade mesophyll. This cell type, which can be termed "green-compact mesophyll", is round (rather than elongate like palisade mesophyll), contains chloroplasts, but almost no air spaces between the cells (compared to spongy mesophyll) and was present in most of the isobilateral leaves observed.

4.5.2 Evolution of the abaxial greening phenotype

According to this study and other North American poplar phylogenies, the majority of the gene trees placed sect. *Abaso*, including *P. guzmantlensis*, as sister to the rest of the poplars. The species with bifacial leaves (*Tacamahaca* and *Leucoides*) are never observed to be as sister to the rest of the poplars, nor are their corresponding sections (i.e., Eckenwalder 1996b, Hamzeh and Dayanandan 2004). It can therefore be hypothesized that the bifacial leaf character is a derived one within the genus *Populus*. Formal ancestral-state reconstructions will require an estimate of the species tree of *Populus*. However, it is intriguing that isobilateral leaves appear to be the ancestral state within the poplars while the most closely related taxa (*Salix* and some other Salicaceae – formerly Flacourtiaceae – genera) (Leskinen and Alstrom-Rapaport 1999, Chase et al. 2002) exclusively contain leaves that are bifacial, as do majority of angiosperms. The genus *Populus* is believed to be tropical in origin (Eckenwalder 1996a), which is consistent with my hypothesis of the isobilateral leaf being the ancestral state of this character. Some of the factors that could have contributed to the

evolution of a bifacial leaf within the poplars could include factors such as environment, change in habitat, and/or physiological features of the leaves.

We can speculate that until the late Eocene (56-34 Mya), species similar to sect. *Abaso* were the solitary North American representatives of the genus until a sect. *Leucoides*-like bifacial-leaved species (similar to *P. heterophylla*) appeared in the fossil record and began to spread to temperate habitats (Eckenwalder 1996b). This event was followed by the radiation (during Miocene [23-5 Mya]) into specific habitats and diversification of the genus, as it is currently known now with the modern sections. At present, sections *Tacamahaca* and *Leucoides*, which in North America exclusively contain bifacial leaves, consist of four species with distribution ranges from eastern to western Canada and United States, as well as into northern Mexico (i.e., *P. angustifolia*). Due to such extensive distribution ranges, which overlap with isobilateral species, it may not be very likely that the differences in environment had a large contribution to the appearance of the bifacial character, although it is currently unknown how or why the *Leucoides*-like bifacial-leaved species evolved.

Despite the wide geographical distribution across North America, poplar species are found in generally either riparian or dryland regions (Dickman 2001, Slavov and Zhelev 2010). Species within sect. *Tacamahaca* are strongly riparian and are generally found at higher elevations and latitudes (Braante et al. 1996, Dickman 2001). *Populus heterophylla* exclusively grows in swamps and a species morphologically similar to this is likely the source of bifacial character in the North American species within *Tacamahaca*, as fossils of this section have been dated back only to Oligocene (34-23 Mya) (Eckenwalder 1996b). The isobilateral-leaved species of *Aigeiros*, better adapted to warmer climates, are also riparian but grow at lower elevations and tend to be more drought-tolerant than *Tacamahaca* species

(Braante et al. 1996). Their close relationship to *Tacamahaca* suggests the recent divergence of these species in occupying similar types of habitat. Species in sect. *Populus*, on the other hand, tend not to be riparian and to grow in drier regions (i.e., *P. tremuloides*) (Dickman 2001), although their leaves are isobilateral (like those of *Aigeiros*). The type of leaf that a poplar has is apparently not obviously correlated with the type of habitat it inhabits.

Not only do poplars show leaf variability between species, but also there is leaf variability within a single tree. These variations include heteroblasty or vegetative phase change (morphological differences between juvenile and adult leaves) and seasonal heterophylly (morphological differences between early and late leaves) (Critchfield 1960, Eckenwalder 1980, Slavov and Zhelev 2010). Juvenile leaves are generally narrower than adult leaves (Woolward 1907) and are bifacial with a radial petiole (Wang et al. 2011). It is likely that all of the poplar species undergo heteroblastic development to some degree (Eckenwalder 1980). Although this has not been specifically documented for all of the poplar species, it is known that *P. mexicana* exemplifies an extreme case of this phenomenon as adult leaf production is delayed to almost ten years of age, compared to other species which produce adult leaves in trees as young as three to five years (Eckenwalder 1980). It is suspected that species with isobilateral leaves would display the heteroblastic character to a more pronounced degree than those with bifacial leaves. Thus, although the bifacial leaf character is derived, the juvenile leaves of isobilateral leaves are bifacial as well. This could suggest a reversion back to the juvenile leaf form or the occurrence of a heterochronic mutation (i.e., in *SPL* gene; see Chapter 3 for a discussion), which did not allow the plant to transition into the adult stage, ultimately developing leaves that are isobilateral, and therefore

contribute to the evolutionary change in the timing of this developmental event (Rudall and Bateman 2004).

The formation and expansion of leaves is essential for photosynthetic efficiency and carbon gain of trees. Apart from morphological variation, the leaf shape is also quite variable in poplars (generally from lanceolate to deltoid in shape) (Eckenwalder 1996b, Van Volkenburgh and Taylor 1996). This shape difference can be attributed to differences in cell proliferation. Leaves that are lanceolate in shape (i.e., *P. trichocarpa*), and therefore possibly predisposed to be generally bifacial, develop a complete cell complement in the adaxial epidermis when the leaves are less than 5% of the final size (Van Volkenburgh and Taylor 1996). The growth to the final leaf shape exclusively occurs through expansion of the developed cells. This contrasts with the development of deltoid leaves (i.e., *P. deltoides*), which are usually isobilateral, where there is continual cell addition and expansion until the leaf is full in size (Van Volkenburgh and Taylor 1996). Division at the base of the blade allows the development of the deltoid shape, which is unnecessary in lanceolate leaves. The functional advantages of bifacial leaves in poplar have not been investigated to the same extent as isobilateral leaves (Roden and Pearcy 1993a, b, c), except for a possible advantage of such large spaces in spongy mesophyll to aid in gas exchange and reflectivity (Givnish 1979, DeLucia et al. 1996). The arrest in cell division could be another advantage to bifacial leaf character, which allows the plant to partition its resources away from leaf development, which would not be possible in isobilateral leaves where cell division continues until the leaf is developed.

4.6 Conclusions

Phylogenetic analyses provide a representation of the relationships (and monophyly) of sections, but morphological characters of the leaf (i.e., bifacial vs. isobilateral) may not be simply explained by phylogenetic position. There are clear advantages to bifacial leaf type, as evidenced by the presence of this leaf type in many angiosperm species. But two questions that remain to be answered are 1) what are some of the factors that may have contributed to the evolution of the bifacial leaf character within poplar species and 2) what may have been the underlying causes of this evolution? Although it is tempting to provide an environmental or ecological explanation for the appearance of the bifacial character, neither are likely caused by to the present-day widespread species distribution and similarity of habitat between bifacial and isobilateral-leaved species. Natural hybridization may have been a major contributing factor to the evolution of extant species (Slavov and Zhelev 2010) and the appearance of *P. heterophylla* allowing the spread of bifacial-leaved character to three other North American species. Hybridization may also complicate future inference of species trees in *Populus.* A simple mutation in the vegetative phase change pathway may have allowed heterochronic retention of the juvenile or bifacial leaf character in an isobilateral-leaved species, typical of the genus.

Table 4.1 ***Populus*** **samples used in phylogenetic analysis.**

Species name (section)	Sample number	Accession number	Origin	Collection location	Collector	Collection date
P. angustifolia (Tacamahaca)	11-2-6	V32005	Saskatchewan	UBC Herbarium	A.J. Breitung	1947 Aug. 20
	11-2-7	4270262	New Mexico	Missouri Botanic Garden Herbarium	M. Merello	1992 Jun. 26
	11-2-8	V110261	Colorado	UBC Herbarium	G.N. Jones	1962 Jul. 16
	203	AH-W2(152)	North America	Alice Holt Forestry Research Station, UK (stool beds)	Q. Cronk	2004 Jun. 10
P. balsamifera (Tacamahaca)	144	UBC-144	Yukon Territory	UBC	Q. Cronk	2004
	11-1-3	V211040	British Columbia	UBC Herbarium	T. Goward	1994 Jun. 13
	11-1-2	V196322	Manitoba	UBC Herbarium	W.J. Cody and W.A. Wojtas	1979 Jul. 04
	11-1-1	V200619	Yukon Territory	UBC Herbarium	G.B. Straley and K.W. Nicholls	1989 Jul. 25
	CHP10	N/A	Cypress Hills, Saskatchewan	Indian Head, Saskatchewan	R. Soolanayakanahally	2010
	WHR10	N/A	Whitehorse, Yukon Territory	Totem Field, UBC	R. Soolanayakanahally	2010
	NWL13	N/A	Norman Wells, Northwest Territories	Indian Head, Saskatchewan	R. Soolanayakanahally	2010
	CAR5	N/A	Carnduff, Saskatchewan	Totem Field, UBC	R. Soolanayakanahally	2010
	GPR13	N/A	Grand Prairie, Alberta	Indian Head, Saskatchewan	R. Soolanayakanahally	2010
P. deltoides (Aigeiros)	125-6	N/A	North America	Puyallup Field Station	J. Nowak	2009 Aug. 19
	125-5	14-66	North America	Puyallup Field Station	J. Nowak	2009 Aug. 19
	125-3	ILL005	Illinois	Puyallup Field Station	J. Nowak	2009 Aug. 19
	185	013/009/032/012 and 185 (294)	Manitoba	Manitoba	J. Saarela	2004
	125-4	ILL028	Illinois	Puyallup Field Station	J. Nowak	2009 Aug. 19
	UGA	1982-0389	North America	University of Guelph Arboretum	C.-A. Lacroix	2009 Oct. 8
	181	UoA-181 (*ssp. occidentales*)	Alberta	Devonian Botanic Garden	J. Saarela	2004
P. fremontii (Aigeiros)	126-1	09-22JN	North America	Puyallup Field Station	J. Nowak	2009 Aug. 19

Species name (section)	Sample number	Accession number	Origin	Collection location	Collector	Collection date
P. fremontii (Aigeiros)	186	013/009/032 /013 and 186 (293)	North America	Manitoba	J. Saarela	2004
	11-2-2	4996383	Alameda Co.	Missouri Botanic Garden Herbarium	B. Ertter and L. Hosley	1993 Apr. 17
	11-2-3	V231501	California	UBC Herbarium	J. Maze et al.	1971 Apr. 13
P. grandidentata (Populus)	UGA	1974-0739	North America	University of Guelph Arboretum	C.-A. Lacroix	2009 Oct. 8
	187	013/009/032 /004 and 187 (286)	North America	Manitoba	J. Saarela	2004
	AUA/ 126-4	N/A	North America	Harriet Irving Botanical Gardens	J. Nowak	2009 May 21
P. guzmantlensis (Populus)	372	R.Luwas y Guzman 2925 21-U-1988	Tecolote, Jalisco	Herbarium material (comm. I. Ojeda)	Guzman	1988
	11-2-11	0024455	Jalisco, Mexico	University of Texas Herbarium (TEX)	R. Cuevas	1988 May 6
P. heterophylla (Leucoides)	206	AH-K2(254)	North America	Alice Holt Forestry Research Station, UK (stool beds)	Q. Cronk	2004 Jun. 10
	11-2-9	V128453	Louisiana	UBC Herbarium	R. Dale Thomas	1969 May 04
	11-2-10	V136500	N. Carolina	UBC Herbarium	M.C. Helms and G.H. Harvey	1969 May 16
P. mexicana (Abaso)	371	Ojeda 11 and 371	Veracruz, Mexico	wild coll.	I. Ojeda	2004 Oct. 9
	370	Ojeda 12 and 370	Veracruz, Mexico	wild coll.	I. Ojeda	2004 Oct. 9
	11-2-12	5549546	Nuevo Ciudad Padilla, Mexico	Missouri Botanic Garden Herbarium	M. Nee	1986 Aug. 16
	376	Ojeda 10	Puete Bado, Km2, Colipa-Yecuatla, Veracruz, Mexico	wild coll.	I. Ojeda	2004 Oct. 9
P. tremuloides (Populus)	AUA	N/A	North America	Harriet Irving Botanical Gardens	J. Nowak	2009 May 21
	UGA	1973-1073	North America	UG Arboretum	C.-A. Lacroix	2009 Oct. 8

Species name (section)	Sample number	Accession number	Origin	Collection location	Collector	Collection date
P. tremuloides (Populus)	197	Cronk s.n.	Little Cottonwood Canyon, Utah	wild coll.	Q. Cronk	2004
	140	012515-0284-1975	British Columbia	UBC Botanic Garden	Q. Cronk	2003 Dec. 1
	195	999/034/011 and 195 (*cv. Erecta*)	Manitoba	Manitoba	J. Saarela	2004
	11-2-5.	N/A	North America	Harriet Irving Botanical Gardens	J. Nowak	2009 May 21
	196	013/009/032 /014 and 196 (291)	Manitoba	Manitoba	J. Saarela	2004
P. trichocarpa (Tacamahaca)	101-1	N/A	British Columbia	UBC, off Chancellor Ave.	N. Temmel	2007
	Ptr2	N/A	North America	Totem Field, UBC	J. Nowak	2008
	11-1-5	V102166	Downie Creek, British Columbia	UBC Herbarium	V.J. Krajna	1953 Jun. 29
	11-1-6	V231500	British Columbia	UBC Herbarium	F. Fodor	1968 Jun. 19
	Ptr33	VNDL27-4	British Columbia	Totem Field, UBC	J. Nowak	2011 May 20
	Ptr34	MCGR15-6	British Columbia	Totem Field, UBC	J. Nowak	2011 May 20
	QCI	N/A	Queen Charlotte Islands, British Columbia	Totem Field, UBC	J. Nowak	2011 May 20
S. arctica	73-1 /Sarc	N/A	McBride, British Columbia	F2 Site I McBride	N. Temmel	2006
S. eleagnos	67-2/ 67-3	013854-0013-1976	Hillier, UK	UBC Botanic Garden	J. Nowak	2011 Aug. 15
S. lapponum	67-5	013859-0013-1976	Hillier, UK	UBC Botanic Garden	J. Nowak	2011 Aug. 15
S. reticulata	75-13	N/A	McBride, British Columbia	M1 Site K McBride	N. Temmel	2006
S. sitchensis	Ssit	002538-0099-1971	British Columbia	UBC Botanic Garden	J. Nowak	2011 Aug. 15

Table 4.2 Primers used in this study to amplify the corresponding genes for phylogenetic analysis. The fragment size produced from both primers amplification is indicated in base pairs (bp).

Gene name	POPTR gene ID	Primer name	Primer sequence	Fragment size
Internal transcribed spacer (ITS)	N/A	ITS1-a	From Hamzeh and Dayanandan (2004)	1000 bp
		ITS2-ITS28kj		
Glycoside hydrolase family 19 protein (Gly)	POPTR_0010s15150	GlyF	GGAAATGAGTCCCAGCAAGA	657 bp
		GlyR	CAAATAGCAGCCTGGAAAGC	
Cinnamyl alcohol dehydrogenase (Cad)	POPTR_0009s09870	CadF	CAAGGAGGCTTTGCTGAATC	515 bp
		CadR	TCCCATCAGGAATTCTCACC	
Phytochelatin synthetase-like protein (Pcs)	POPTR_0015s07110	PcsF	CTGGACACCAGACGGTTATG	767 bp
		PcsR	GTGGGGGTCTTTTTACAGCA	
Major intrinsic protein (Mip)	POPTR_0010s22950	MipF	TGCTGAGTTTATAGCAACAC	735 bp
		MipR2	CAAAGAGACCTTCCTGGCTA	
S-adenosyl-L-homocysteine hydrolase (Sad)	POPTR_0017s08610	SadF	GGTTGAAGAGTGATCCCATG	889 bp
		SadR2	CGGAGACAACATCTTCAAGGG	

Table 4.3 ***Populus*** **samples used for anatomical analysis.**

Species name	Accession number	Origin	Collection location	Collector	Date collected
P. angustifolia (Tacamahaca)	V32005	Saskatchewan	UBC Herbarium	A.J. Breitung	1947 Aug. 20
	V110261	Colorado	UBC Herbarium	G.N. Jones	1962 Jul. 16
	V102483	Utah	UBC Herbarium	V.J. Krajna	1958 Jun. 18
P. balsamifera (Tacamahaca)	N/A	North America	Totem Field, UBC	J. Nowak	2007 Sep. 6
P. deltoides (Aigeiros)	14-66	North America	Puyallup Field Station	J. Nowak	2009 Aug. 21
	ILL-028	North America	Puyallup Field Station	J. Nowak	2009 Aug. 21
P. fremontii (Aigeiros)	Cronk s.n.	California	Rancho Santa Ana Botanic Garden	Q. Cronk	2008 Nov. 10
	N/A	North America	Puyallup	J. Nowak	2009 Aug. 21
P. grandidentata (Populus)	N/A	North America	Harriet Irving Botanical Gardens	J. Nowak	2009 May 21
P. heterophylla (Leucoides)	V136500	North Carolina	UBC Herbarium	M.C. Helms and G.H. Harvey	1969 May 16
P. tremuloides (Populus)	N/A	North America	Harriet Irving Botanical Gardens	J. Nowak	2009 May 21
	N/A	British Columbia	Smithers	Q. Cronk	2011 Jul. 26
	N/A	British Columbia	Smithers	Q. Cronk	2011 Jul. 26
P. trichocarpa (Tacamahaca)	N/A	North America	Totem Field, UBC	J. Nowak	2007 Sep. 6
	NPLN30-4	British Columbia	Totem Field, UBC	J. Nowak	2011 Aug. 16
	VNDL27-3	British Columbia	Totem Field, UBC	J. Nowak	2011 Aug. 16
	LILA26-5	British Columbia	Totem Field, UBC	J. Nowak	2011 Aug. 16
	MTSM27-5	British Columbia	Totem Field, UBC	J. Nowak	2011 Aug. 16

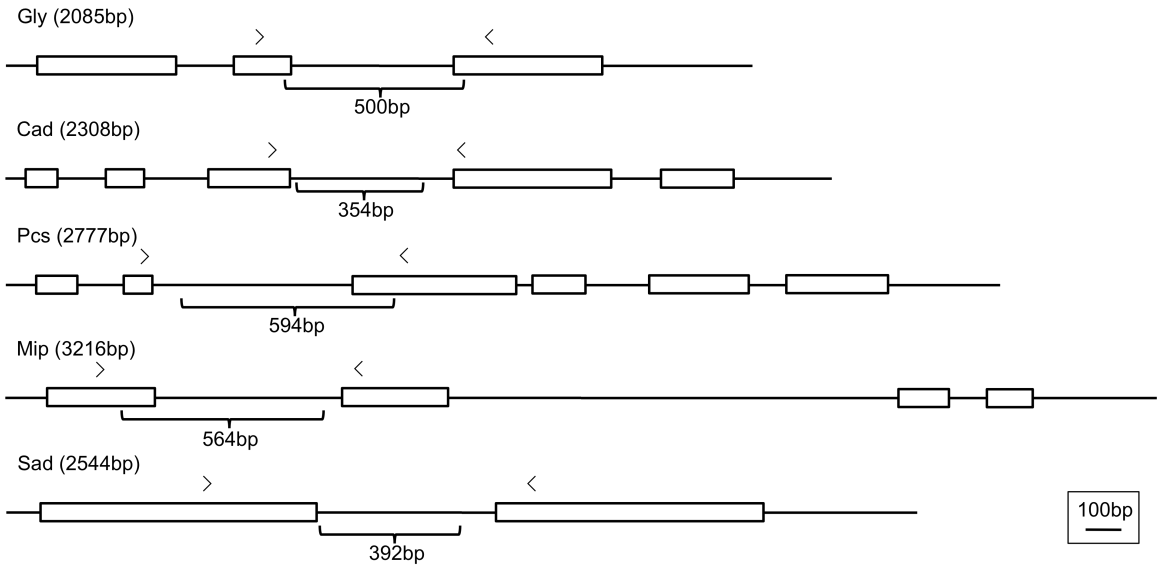

Figure 4.1 Gene models (from *P. trichocarpa* Nisqually-1, Phytozome) of genes used in this study. The length of the whole gene is indicated in brackets next to the gene name (e.g. *Gly* (2085bp)). The regions amplified and used in making phylogenetic trees (in *P. trichocarpa*) are indicated by a bracket, with the size of the fragment in base pairs indicated below. Boxes indicate exons, and lines indicate the intergenic regions. Brackets above each gene model indicate regions flanked by the primers. Scale bar = 100bp.

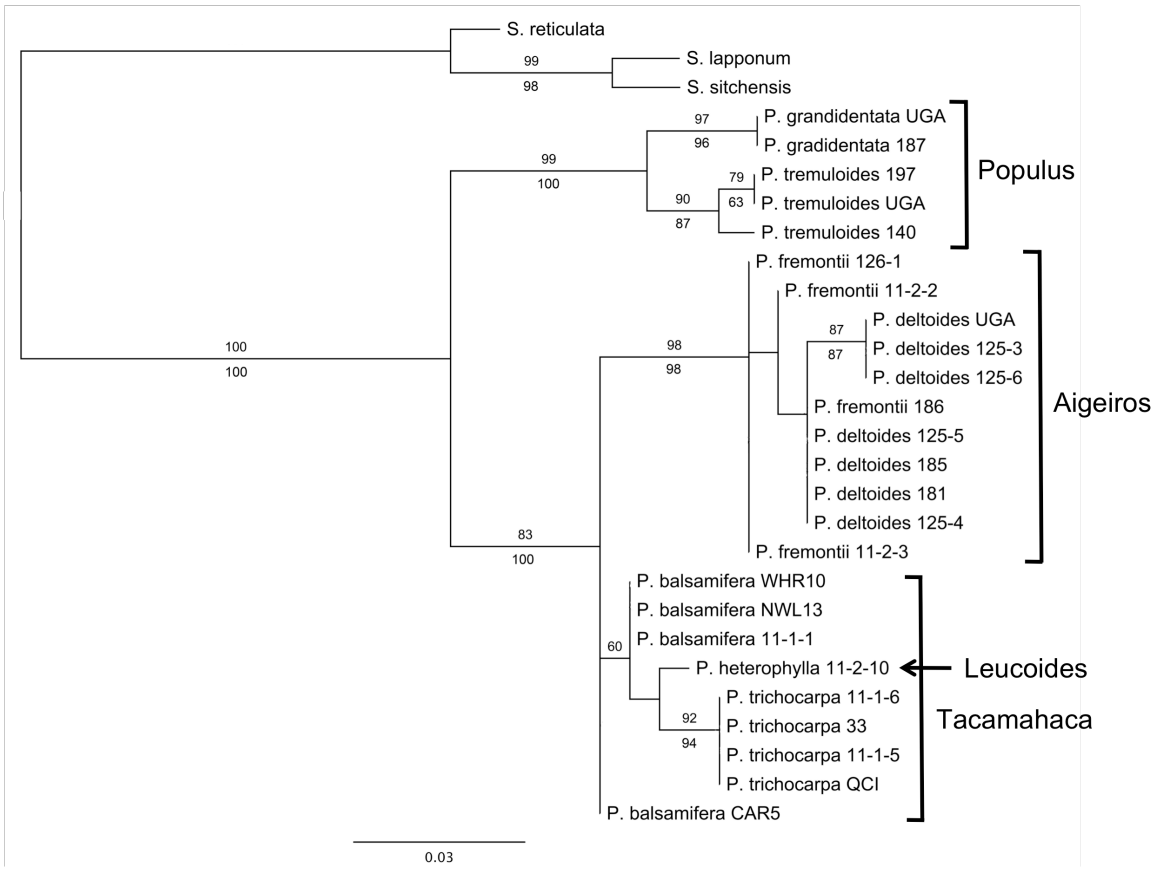

Figure 4.2 ***Cad*** **ML phylogenetic tree of** ***Populus*** **species. ML and MP bootstrap support values are presented on the phylogeny as upper and lower values, respectively. Species that are not monophyletic in this gene tree (of those with multiple accessions) are** ***P. balsamifera, P. deltoides,*** **and** ***P. fremontii.*** **The only section that is not monophyletic in this tree is** ***Tacamahaca*****. Only support values greater than 50% are indicated.**

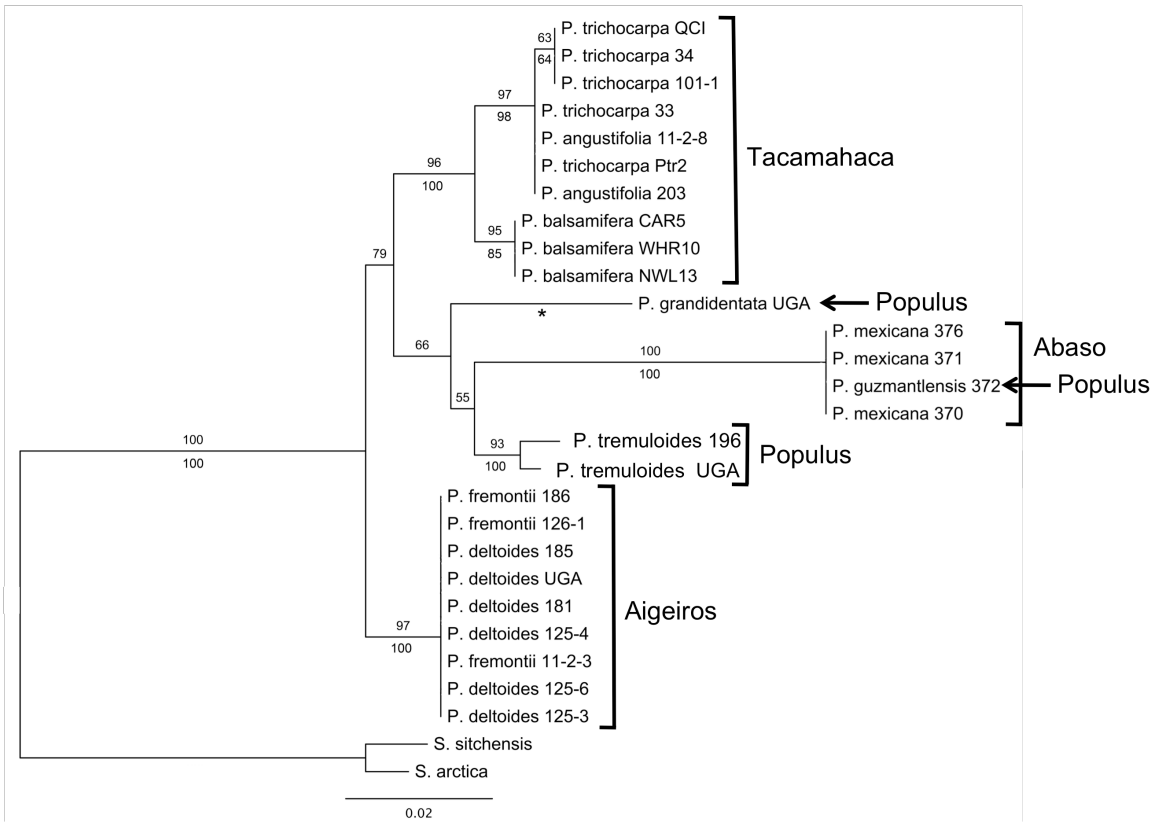

Figure 4.3 ***Gly*** **ML phylogenetic tree of** ***Populus*** **species. ML and MP bootstrap support values are presented on the phylogeny as upper and lower values, respectively. Species that are not monophyletic in this gene tree (of those with multiple accessions) are** ***P. angustifolia, P. deltoides, P. fremontii, P. mexicana,*** **and** ***P. trichocarpa*****. Sections that are not monophyletic in this tree are** ***Abaso*** **and** ***Populus*****. Only support values greater than 50% are indicated. Asterisk indicates where ML and MP topology differ.**

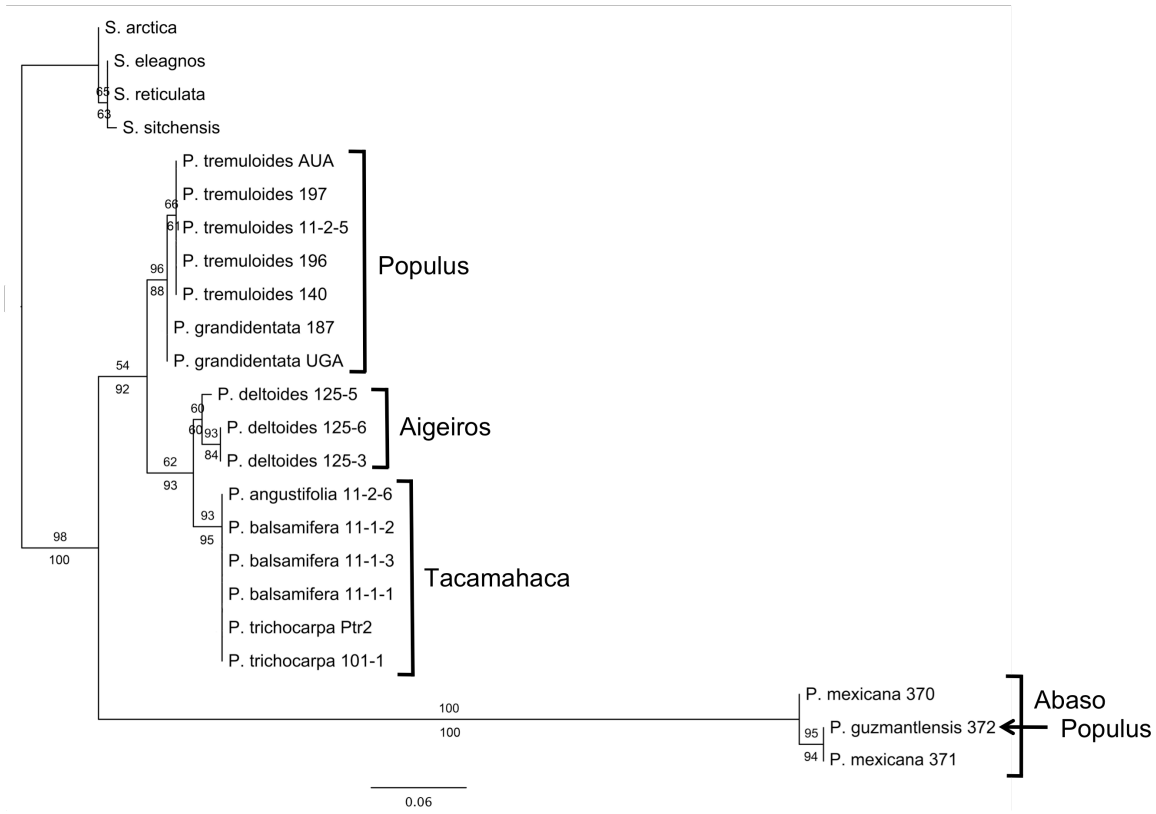

Figure 4.4 ITS ML phylogenetic tree of *Populus* species. ML and MP bootstrap support values are presented on the phylogeny as upper and lower values, respectively. Species that are not monophyletic in this gene tree (of those with multiple accessions) are *P. balsamifera, P. mexicana,* and *P. trichocarpa*. Sections that are not monophyletic in this tree are *Abaso* and *Populus*. Only support values greater than 50% are indicated.

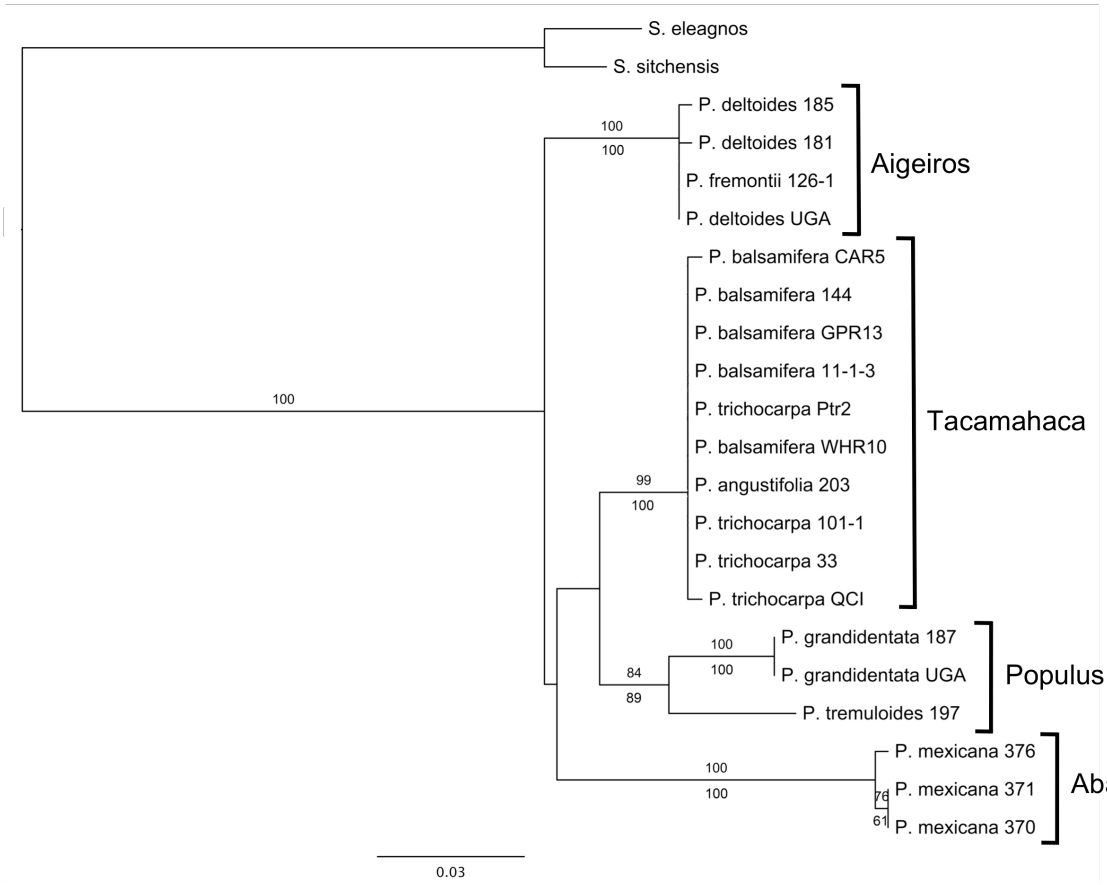

Figure 4.5 ***Mip*** **ML phylogenetic tree of** ***Populus*** **species. ML and MP bootstrap support values are presented on the phylogeny as upper and lower values, respectively. Species that are not monophyletic in this gene tree (of those with multiple accessions) are** ***P. balsamifera, P. deltoides,*** **and** ***P. trichocarpa*****. Only support values greater than 50% are indicated.**

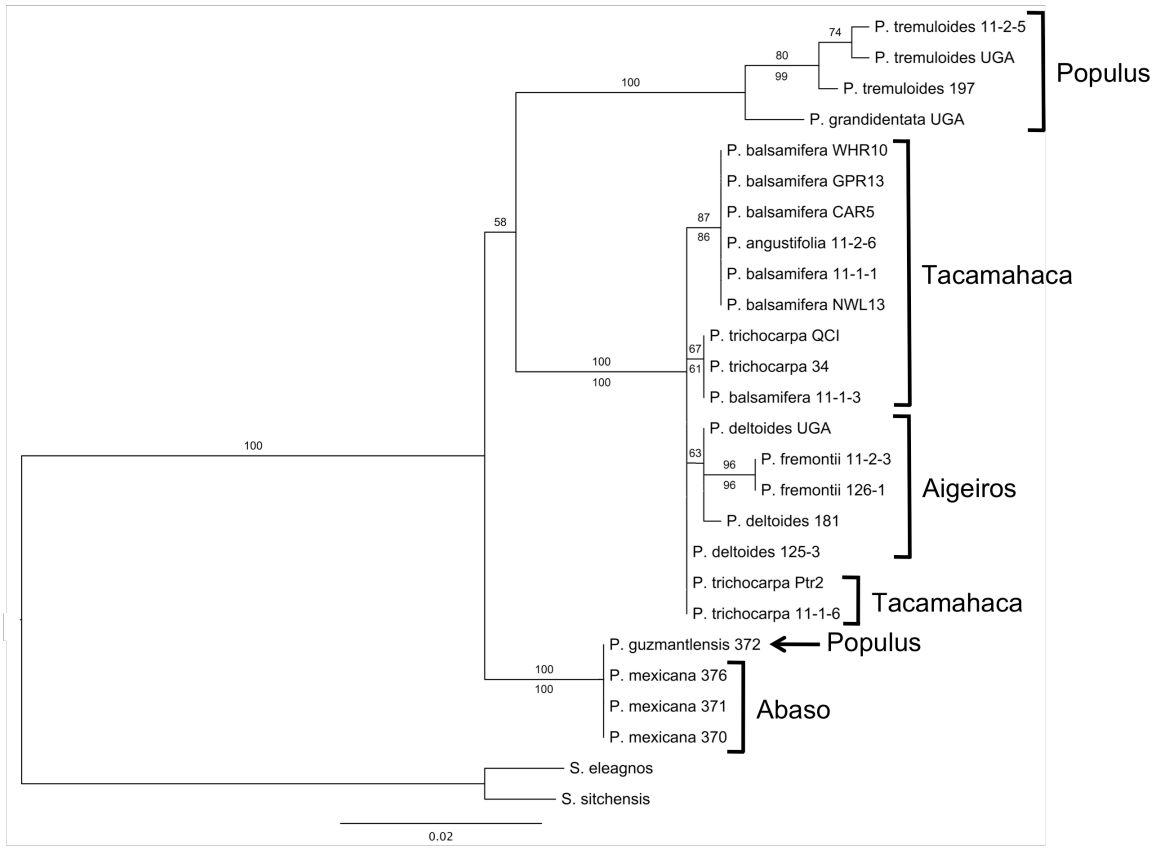

Figure 4.6 ***Pcs*** **ML phylogenetic tree of** ***Populus*** **species. ML and MP bootstrap support values are presented on the phylogeny as upper and lower values, respectively. Species that are not monophyletic in this gene tree (of those with multiple accessions) are** ***P. balsamifera, P. deltoides, P. mexicana,*** **and** ***P. trichocarpa*****. Sections that are not monophyletic in this tree are** ***Abaso, Aigeiros, Populus,*** **and** ***Tacamahaca*****. Only support values greater than 50% are indicated.**

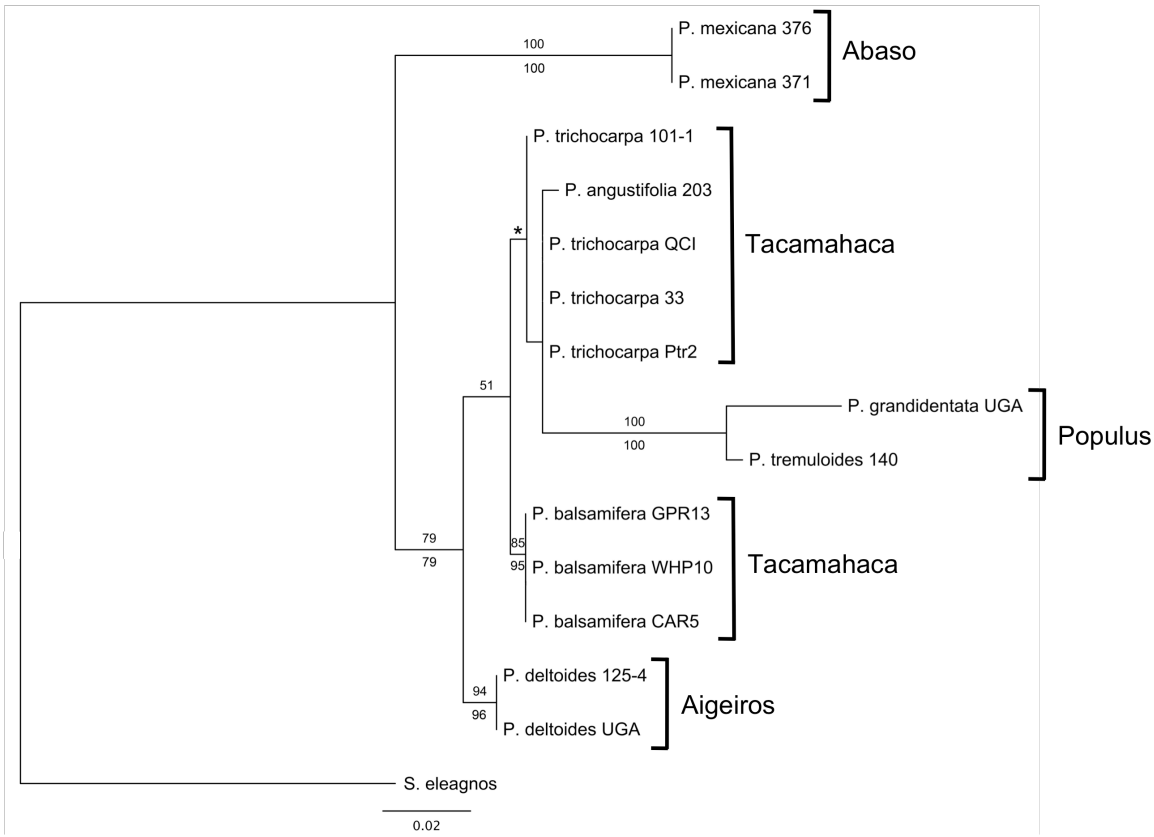

Figure 4.7 ***Sad*** **ML phylogenetic tree of** ***Populus*** **species. ML and MP bootstrap support values are presented on the phylogeny as upper and lower values, respectively. The only species that is not monophyletic in this gene tree (of those with multiple accessions) is** ***P. trichocarpa*****. The only section that is not monophyletic in this tree is** ***Tacamahaca*****. Only support values greater than 50% are indicated. Asterisk indicates where ML and MP topology differ.**

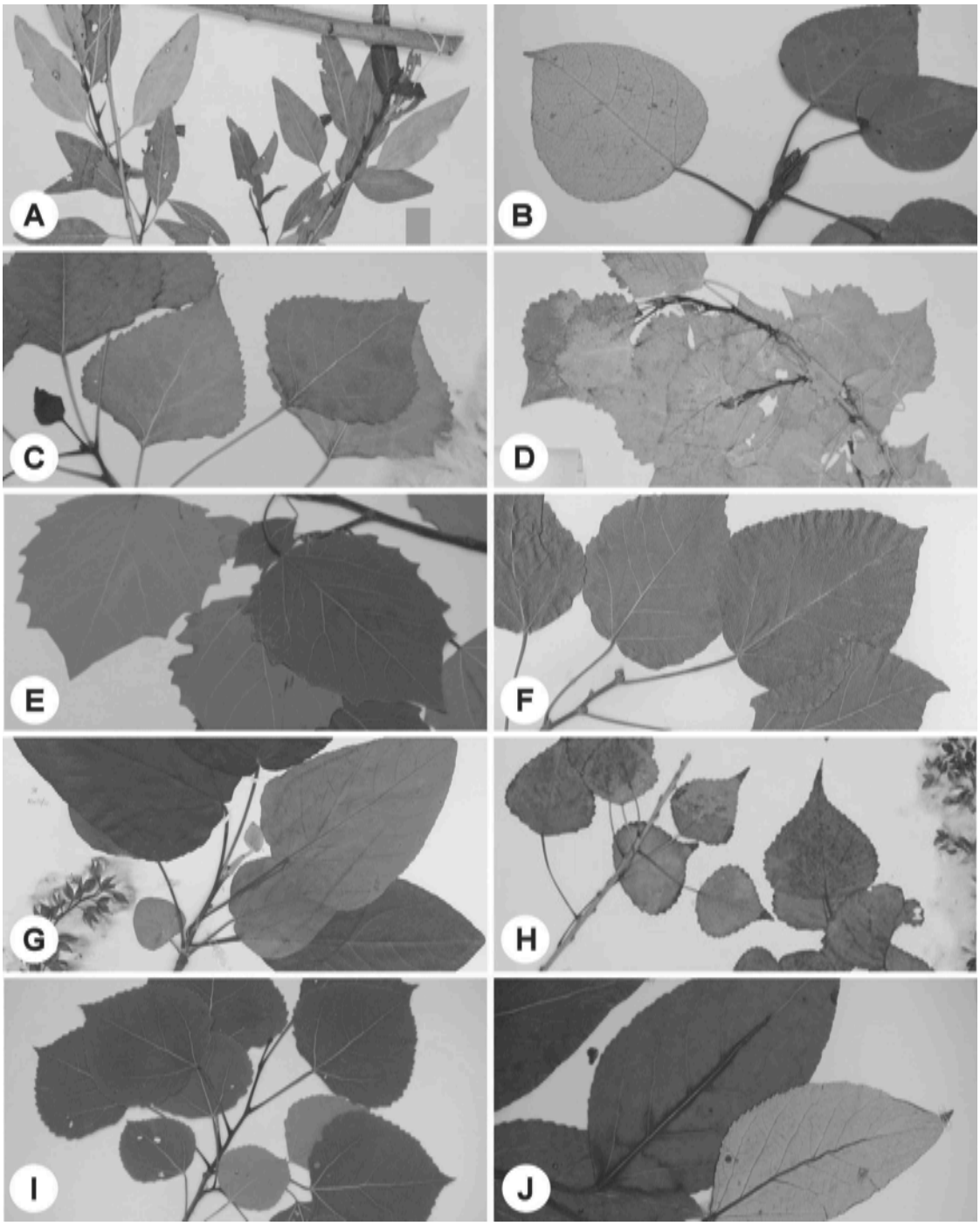

Figure 4.8 Leaf morphology of *Populus* species showing difference between bifacial (A,B, G, J) and isobilateral (C, D, E, F, H, I) leaves: A. *P. angustifolia* (MO 4270262), B. *P. balsamifera* (OAC KK193), C. *P. deltoides* (OAC 7122), D. *P. fremontii* (MO 04996383), E. *P. grandidentata* (OAC No. 366), F. *P. guzmantlensis* (TEX 00244255), G. *P. heterophylla* (UBC V136500), H. *P. mexicana* (MO 5549546), I. *P. tremuloides* (OAC), J. *P. trichocarpa* (OAC 2267).

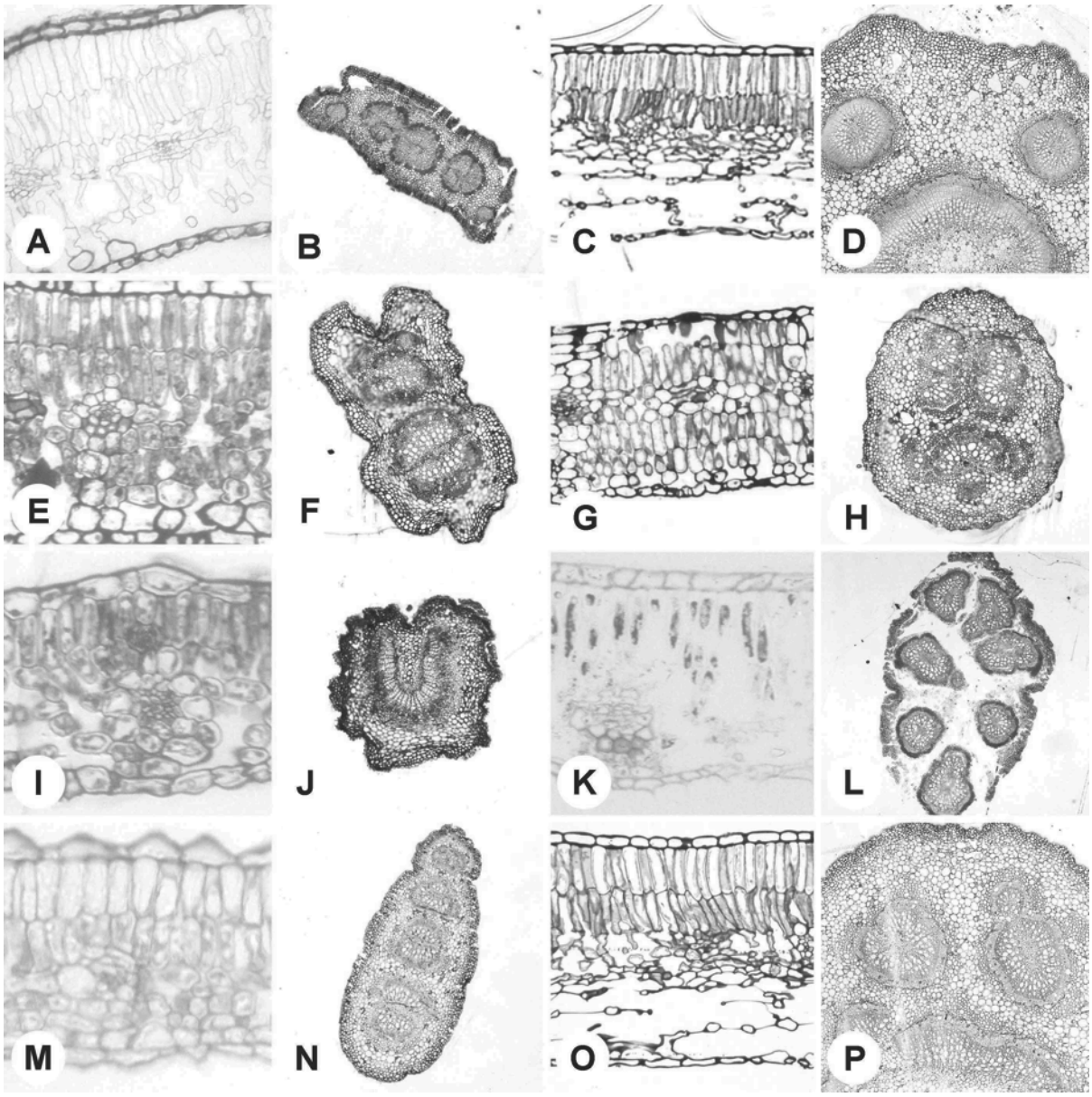

Figure 4.9 Transverse sections of *Populus* species leaf blades (A, C, E, G, I, K, M, O) and petioles (B, D, F, H, J, L, N, P) showing anatomy: A, B. *P. angustifolia* (bifacial leaf and dorsiventrally flattened petiole), C, D. *P. balsamifera* (bifacial leaf and radial petiole), E, F. *P. deltoides* (isobilateral leaf and mediolaterally flattened petiole), G, H. *P. fremontii* (isobilateral leaf and radial petiole), I, J. *P. grandidentata* (isobilateral leaf and radial petiole), K, L. *P. heterophylla* (bifacial leaf and radial petiole), M, N. *P. tremuloides* (isobilateral leaf and mediolaterally flattened petiole), O, P. *P. trichocarpa* (bifacial leaf and radial petiole).

Chapter 5: Abaxial greening and unifacial petiole phenotypes in hybrid aspen

5.1 Synopsis

The genus *Populus* contains species with two types of leaf variants: bifacial and isobilateral. While there is variability in leaf blade structure, the associated petioles also differ. Bifacial leaves are associated with radial petioles while isobilateral leaf blades, exhibiting abaxial greening phenotype, are associated with a unifacial petiole. Due to the difference in abaxial cell types in the blade and dorsiventral polarity differences in the petiole, I analyzed a subset of genes that have been implicated in adaxial-abaxial patterning in *Arabidopsis*. I firstly identified the orthologs in poplar and determined expression levels of these genes in leaves (from mRNA-seq data). A set of criteria allowed me to reduce the initial number of genes to 17. These were amplified in a bifacial- and isobilateral-leaves species (black cottonwood and hybrid aspen, respectively) with quantitative reverse transcriptase polymerase chain reaction (qRT-PCR) in order to determine differences in transcript abundance in the two species in leaf blade and petiole tissues. From these, little variation was observed between the petioles of these two species, but several genes showed a significant difference in expression in hybrid aspen leaf blades, possibly suggesting their contribution to the underlying difference between bifacial and isobilateral leaves in *Populus*.

5.2 Introduction

The genus *Populus* consists of approximately 29 species (Eckenwalder 1996b) containing two types of leaves: bifacial and isobilateral (Van Volkenburgh and Taylor 1996).

Bifacial leaves are usually dark green on the adaxial surface and contain a lightly coloured abaxial surface. These types of leaves are commonly associated with a rigid radial petiole, which allows the adaxial surface of the leaf to be exposed to the sun. The primary photosynthetic tissues, the palisade mesophyll, are associated with the adaxial surface in bifacial leaves, while the abaxial surface consists of spongy mesophyll that scatter light due to air spaces and therefore contribute to the lighter colouration. Isobilateral leaves, on the other hand, are more commonly found within the genus (Van Volkenburgh and Taylor 1996) and have similarly green colouration on both adaxial and abaxial leaf surfaces. The petiole of isobilateral leaves is mediolaterally flattened, allowing the leaves to flutter in the wind (see Chapter 3 for adaptive significance discussion). Both surfaces of isobilateral leaves are able to photosynthesize and palisade mesophyll cells are present on both adaxial and abaxial surfaces.

The radial petiole associated with bifacial leaves is thought to be bifacial as well, in that it contains both adaxial and abaxial surfaces. Mediolaterally flattened petioles, on the other hand, are thought to be unifacial and can be likened to leaves of *Iris* and some species of *Juncus*, which have mediolaterally flattened unifacial leaves (Kaplan 1997, Yamaguchi and Tsukaya 2010, Yamaguchi et al. 2010). Unifacial leaves have only a single type of surface, commonly abaxial, on the outside of the leaf. If a leaf or organ is radialized (or abaxialized), the vasculature is also reoriented but still maintains cell type/surface association, where the xylem is associated with the adaxial surface and phloem with the abaxial (or central and peripheral domains, respectively). For example, unifacial leaves of *Allium* are abaxialized and the bundles within the leaves are oriented such that phloem points

outward (towards the abaxial side) and xylem towards the adaxial domain such as the inside of the leaf (Kaplan 1997; see Chapter 1).

5.2.1 Molecular genetics of leaf variation

The genetic basis of abaxial greening phenotype and the associated unifacial petiole in *Populus* has been investigated (Wu et al. 1997), but the molecular genetic basis has not. The abaxial greening phenotype and the associated unifacial petiole phenotypes were mapped onto two major quantitative trait loci (QTLs) (Wu et al. 1997), but the gene(s) responsible for these phenotypes were not investigated further. A recent study (Wang et al. 2011a), however, discussed the involvement of several genes in vegetative phase change in leaves of *Populus* x *canadensis* (*Populus nigra* x *deltoides*). Vegetative phase change or heteroblasty (see Chapters 3 and 4) involves the transition from juvenile to adult leaf morphology. The differences in morphology are not always evident, but they are when leaves transition from bifacial to isobilateral types (e.g., *P.* x *canadensis*; Wang et al. 2011a). Juvenile leaves of this hybrid, and other isobilateral-leaved poplars (see Chapter 4), are bifacial, while the adult leaves are isobilateral. Wang et al. (2011a) showed that expression levels of *squamosa protein binding-like* (*SPL*) genes and their interacting small RNAs are altered during this phase transition. Gene expression patterns contributing to the differences in leaf morphologies between juvenile bifacial and adult isobilateral leaves have not been investigated.

5.2.2 Objectives

This study was undertaken to determine differences in the patterns of gene expression of bifacial leaves of *Populus trichocarpa* and isobilateral leaves of *Populus tremula* x *tremuloides* (black cottonwood and hybrid aspen, respectively, henceforth). It is not known which genes are responsible for palisade or spongy mesophyll development, but due to the association of the isobilateral blade with a unifacial petiole in hybrid aspen, the immediate candidate genes are those responsible for setting dorsiventral polarity in leaves.

The predicted results can be separated into possible scenarios of gene expression patterns in the leaf blade versus those in the leaf petiole, which may or may not be similar. Because the hybrid aspen blade contains more cell types that are characteristic of the adaxial surface (i.e., palisade mesophyll) in comparison to black cottonwood leaf blade, it is predicted that hybrid aspen blade tissue will exhibit higher expression of some adaxial cell fate determining genes and/or lower expression of abaxial cell fate determining genes. The black cottonwood petiole has both adaxial and abaxial surfaces, and therefore is expected to have normal adaxial-abaxial patterning. Hybrid aspen petioles, on the other hand, are unifacial and lack the adaxial surface. It can therefore be expected that there will be no or little (restricted to the xylem within the petiole) adaxial cell fate gene expression in hybrid aspen petiole and higher expression of some abaxial cell fate genes, in comparison to black cottonwood.

The objective of this study was, therefore, to sample a subset of candidate genes for dorsiventral polarity and determine expression patterns between hybrid aspen and black cottonwood and their blades and petioles, paving the way for a future study that can access expression patterns within the whole genome and elucidate the genetic and developmental

differences leading to the observed phenotypic differences in hybrid aspen and black cottonwood.

5.3 Materials and methods

5.3.1 Leaf analysis

Leaves of *P. trichocarpa* and *P. tremula* x *tremuloides* were collected from a collection at Totem Field (UBC) and imaged using a flatbed scanner. Whole leaves were also photographed using a Nikon stereomicroscope with a DS-Ri1 camera. Leaf blade and petiole lengths were measured from different trees in 129 and 75 replicate leaves of black cottonwood and hybrid aspen, respectively. Leaf blade pieces from the middle of the blade, on either side of the midvein, and petiole pieces (middle) were cut from fresh leaves, fixed in 70% FAA, embedded in LR White, sectioned, and photographed according to the methods described in Chapter 1.

5.3.2 Gene selection

A collection of 42 *Arabidopsis* genes was selected for study (Table 5.1). These genes include those that have been implicated in adaxial-abaxial patterning and vegetative phase change in *Arabidopsis* and poplar. *Arabidopsis thaliana* amino acid sequences were downloaded from TAIR (see Chapter 3) and were BLASTed (tBLASTn) using Phytozome (see Chapter 3; Goodstein et al. 2011) against *Populus trichocarpa* v2.2 genome. The final selection of homologous genes was based on the "Gene Ancestry" output results from Phytozome, which list all of the families (with genomes published on Phytozome, including

P. trichocarpa) that contain the gene of interest. A total of 84 *P. trichocarpa* genes were selected and used in further analyses, described below.

5.3.3 Gene expression data analysis

The transcriptome of various tissues for *P. trichocarpa* was sequenced as part of a larger project (Geraldes et al. 2011). Mean and standard deviation values of transcript expression levels (RPKM) were calculated (see Chapter 3) for each of the 84 genes identified. RPKM data was obtained for *P. trichocarpa* and *P. tremula* (aspen) replicate samples (three and four replicates, respectively) for young expanding leaves and developing stem xylem. The mean values for each of the genes were compared (using a paired t-test, with significant p-value <0.05) between black cottonwood and aspen. The number of genes for further study was narrowed to 71 with the following criteria: 1) genes that showed a significant difference in expression levels between the two species in either leaf and/or xylem samples, 2) genes that had expression levels higher than 5 RPKM, and 3) the remaining putative orthologs of genes that satisfy criteria 1 and 2, even if their RPKM was less than 5. For example, if *Pt-AE3.1* showed RPKM > 5 and a difference in expression levels between black cottonwood and aspen, but *Pt-AE3.2* did not meet either or both of these criteria, both were included in further analyses. Note that xylem data were not further analyzed beyond the summary in Appendix D.1.

5.3.4 Reverse transcriptase PCR

DNA was extracted from black cottonwood and hybrid aspen leaf tissues using a modified CTAB protocol (see Chapter 4). RNA was extracted from each of these species

from leaf blades and petioles using Invitrogen PureLink Plant RNA Reagent (Burlington, Ontario). Both DNA and RNA concentrations were measured with a NanoDrop ND-1000 spectrophotometer (see Chapter 2). RNA was further treated with DNase (TURBO DNA-free, Ambion, Mississauga, Ontario) from which cDNA was synthesized using a RevertAid H Minus First Strand cDNA Synthesis Kit (Fermentas, Burlington, Ontario). cDNA concentration was also measured with a NanoDrop spectrophotometer.

For each of the 71 genes, primers were designed using Primer3 (see Chapter 2) to amplify 200-500bp regions. Polymerase chain reactions (PCR) were run with the GFP3 PCR program (94°C 3min, (94°C 30sec, 56°C 40sec, 72°C 1min) x36, 72°C 1min, 4°C hold). Poplar translation initiation factor 5A (TIF5A), previously used by Ralph et al. (2006), was used as a positive control in all PCR reactions. Each of the 71 primer pairs were run at least three times to determine expression patterns in leaf blade and petiole of black cottonwood and hybrid aspen. DNA of each of the species was amplified using these primers to assess whether the primer specificity was poor instead of the gene not being expressed. Negative controls were also included in each reaction, which excluded DNA or cDNA template. PCR products were run on 1-2% agarose gels (at 120V for 30-60min) to determine fragment sizes and amplification patterns.

In order to quantify the amount of transcript in the two species under investigation, genes that met the following criteria were analyzed further using quantitative RT-PCR (qRT-PCR): 1) hybrid aspen leaf blades showed brighter bands, and therefore higher putative expression, compared to black cottonwood leaf blade samples, or 2) hybrid aspen petiole samples showed no amplified band, and therefore no putative expression, compared to presence of expression in black cottonwood petiole samples. With regard to the second

guideline, genes that did not amplify either in blade or petiole hybrid samples were not included in further analysis as the primers were more likely not specific enough for hybrid aspen, rather than actually not being expressed in both tissue types (these results were not further investigated).

Generally, all of the 84 genes initially obtained from Phytozome were labeled under the following categories, according to the RT-PCR results (Table 5.2): A1) Higher expression in hybrid aspen blade, compared to black cottonwood, A2) Expression not higher in hybrid aspen blade, A3) No expression in black cottonwood blade, compared to expression present in hybrid aspen, B1) No expression in hybrid aspen petiole, B2) Some expression in hybrid aspen petiole, C) No amplification of cDNA or DNA in either or both species, and D) Not tested or no conclusive results.

5.3.5 Relative RT-PCR

Seventeen genes met all of the criteria and were used in qRT-PCR analysis. Five samples, including black cottonwood blade and petiole, hybrid aspen blade and petiole, and negative control, were included in qRT-PCR runs in each of the genes. cDNA samples were all diluted to 1ng/µl to start each qRT-PCR run with the same amount of starting template. The final cDNA concentration was measured using Qubit 2.0 fluorometer (Invitrogen), using the manufacturer's protocol. Reactions were prepared using SsoFast EvaGreen Supermix protocol (Bio-Rad, Mississauga, Ontario) and were run using Bio-Rad iCycler iQ5 Real-Time PCR system with the following program: 95°C 30sec (95°C 5sec, 56°C 5sec) x40, 57°C 5sec, 57°C 5sec x77.

Expression or transcript abundance levels were presented as Cq values or the number of cycles when the template was used up (Bustin et al. 2009). The lower Cq value, the more template cDNA present and therefore more transcript present. Relative transcript abundance for blade and petiole, separately, was calculated using the difference in Cq values or ΔCq (Cq (test) – Cq (control)), which is the gene concentration compared to other control samples (Pfaffl 2004). The "test" sample (as described in the ΔCq formula) was designated as hybrid aspen as it was compared to the "control" or black cottonwood samples. The final results are graphed and presented as relative expression ratio: 2^ΔCq (Pfaffl 2004).

5.4 Results

5.4.1 Leaf analysis

Black cottonwood trees have leaves that are bifacial and contain palisade mesophyll tissues associated with the dark green adaxial side and spongy mesophyll associated with the lighter coloured abaxial surface (Figures 5.1A, 5.1C). These trees have leaves with petioles that are typically shorter than those of hybrid aspen, in relation to whole leaf length. The petiole to total length ratio is consequently smaller in black cottonwood leaves (0.17±0.05) compared to hybrid aspen leaves (0.40±0.06). Unlike black cottonwood, hybrid aspen leaves are isobilateral and contain palisade mesophyll cells in association with both adaxial and abaxial sides (Figures 5.1B, 5.1D).

Bifacial leaves are usually associated with radial petioles and isobilateral with mediolaterally flattened petioles. This is evident in both of these species where black cottonwood leaves have radial petioles with a small region of adaxial surface that extends down the petiole (Figure 5.1E, 5.1G). Hybrid aspen leaves are associated with mediolaterally

flattened petioles, which consist of entirely abaxial surface as the adaxial surface does not extend down the petiole as in black cottonwood leaves as glands are present at the petiole/blade junction in hybrid aspen leaves (Figures 5.1F, 5.1H). Both species contain several amphicribral bundles (phloem surrounding xylem) within the petioles (Figures 5.1G, 5.1H), indicative of abaxialization.

5.4.2 Transcriptome data analysis

Mean RPKM values for 84 selected genes were calculated and expression levels of black cottonwood and aspen (*P. tremula*) were compared. A large number of genes (28) showed a significant difference in expression in leaves between the two species with p-values less than 0.05 (underlined in Table 5.2; see Chapter 3). Of these, 11 showed higher expression in aspen leaf tissues, which may indicate candidate genes for investigating differences in leaf blade types between the two species. Using the 28 genes as a guideline, other putative orthologues were included and used for further RT-PCR analysis (71 genes in total). Genes that were not included in further analysis were *Pt-CRC.1, Pt-CRC.2, Pt-INO.1, Pt-INO.2, Pt-SGS3.3, Pt-SGS3.4, Pt-SGS3.5, Pt-SGS3.6, Pt-SGS3.7, Pt-YUC.1, Pt-YUC.2, Pt-YUC2.1,* and *Pt-YUC2.2* due to low expression levels (RPKM < 5).

5.4.3 Leaf blade gene expression patterns

According to the RT-PCR results, the following genes had higher expression in hybrid aspen blade tissues compared to black cottonwood (category A1): *Pt-AGO1.2, Pt-AGO7.4, Pt-AGO10.1, Pt-AS2.2, Pt-ATS.2, Pt-KAN.3, Pt-KAN2/3.1, Pt-SPL4.1* (the latter also had higher expression in hybrid aspen petiole), *Pt-YAB3.2*, and *Pt-ZPR3.2* (Table 5.2).

Pt-PGY3.1 consistently showed no expression in hybrid aspen leaf blades (category A3), while still being expressed in hybrid aspen petioles. Several genes were selected for further analysis with qRT-PCR based on these results as well as results from petiole samples. qRT-PCR results showed that several genes showed a significantly higher expression in the hybrid aspen blade tissues compared to the blades of black cottonwood, including: *Pt-AE7.2* (p=0.0018), *Pt-AGO1.2* (p=0.0065), *Pt-AS2.1* (p=0.0470), *Pt-AS2.2* (p=0.0028), *Pt-ATS.2* (p=0.0109), *Pt-RDR6.1* (p=0.0169), *Pt-RDR6.2* (p=0.0009), *Pt-YAB3.2* ($p=1.00x10^{-5}$), and *Pt-ZPR3.1* (p=0.0086) (Figure 5.2). *Pt-ZPR3.2* (p=0.0038), on the other hand, showed higher expression in black cottonwood blades compared to hybrid aspen. The remaining genes analyzed did not show a significant difference in transcript abundance between the leaf blades of the two species.

5.4.4 Leaf petiole gene expression patterns

According to the RT-PCR results, the following genes showed no expression in hybrid aspen petiole tissues when compared to black cottonwood petioles (category B1): *Pt-AE7.2, Pt-AGO1.2, Pt-AGO7.4, Pt-AGO10.1, Pt-AS1.1, Pt-AS1.2, Pt-AS2.1, Pt-AS2.2, Pt-ATS.2, Pt-ETT.1, Pt-ETT.2, Pt-HYL1.1, Pt-HYL1.2, Pt-KAN2/3.1, Pt-RDR6.1, Pt-RDR6.2, Pt-SPL43.2*, and *Pt-ZPR3.1* (Table 5.2). Gene selection for further qRT-PCR analysis was based on these results as well as those from leaf blade samples.

qRT-PCR results showed that two genes had significantly higher expression when the petiole tissue was compared between the two species, but none of the 17 genes tested using qRT-PCR showed a lack of expression in petioles of hybrid aspen or black cottonwood. *Pt-AE7.2* (p=0.0006) was significantly more highly expressed in hybrid aspen petiole compared

to black cottonwood, and *Pt-ZPR3.2* (p=0.0039) showed significantly higher expression in black cottonwood petiole compared to hybrid aspen (Figure 5.3). The remaining 15 genes tested did not show a significant difference in transcript abundance between the petioles of the two species.

5.5 Discussion

The black cottonwood and hybrid aspen represent two major leaf variants in the genus *Populus*. Leaves of black cottonwood are bifacial and are associated with a short radial petiole, which contain both adaxial and abaxial surfaces. Hybrid aspen leaves, on the other hand, are isobilateral and are associated with a long mediolaterally flattened petiole. The latter type of leaves, therefore, exhibits abaxialized greening and unifacial petiole phenotypes. In comparison to black cottonwood, hybrid aspen blade tissue may be expected to have higher expression of genes that are responsible for setting adaxial surface polarity and/or the absence of expression of genes responsible for adaxial surface identity in the petiole tissues. The expected appropriate differential expression of abaxial and adaxial polarity genes, between petiole and blade and between the two species, forms a scenario that can be tested against the results reported here.

A large number of candidate genes (84 in total) were initially selected for this study. Using various selection criteria, this number was narrowed to 17 genes that were tested using qRT-PCR. The results produced were not as expected, possibly due to difference in gene function in poplar compared to *Arabidopsis* (from which the function is known), as ten genes showed a significantly higher transcript abundance in the blade tissue of hybrid aspen in comparison to black cottonwood including *AS1/2 ENHANCER7* (*Pt-AE7.2*), *ARGONAUTE1*

(*Pt-AGO1.2*), *ASYMMERTIC LEAF2* (*Pt-AS2.1* and *Pt-AS2.2*), *ABERRANT TESTA SHAPE* (*Pt-ATS.2*), *RNA-DEPENDENT RNA POLYMERASE6* (*Pt-RDR6.1* and *Pt-RDR6.2*), *YABBY3* (*Pt-YAB3.2*), and *LITTLE ZIPPER3* (*Pt-ZPR3.1*). *Pt-ZPR3.2*, on the other hand, showed a significantly higher expression in black cottonwood blade tissues, but significantly higher expression in hybrid aspen petioles. Similar to results in blade tissues, *Pt-AE7.2* also had higher transcript abundance in hybrid aspen petioles. Surprisingly, none of the genes tested using qRT-PCR showed a lack of expression in the unifacial hybrid aspen petiole tissues, as predicted from the results of non-quantitative RT-PCR and hypotheses presented due to similarities in vascular patterning in black cottonwood and hybrid aspen and, therefore, likely the lack of a significant difference in morphology.

5.5.1 Adaxial determinants in hybrid aspen blade

Hybrid aspen leaf blades exhibit abaxial greening phenotype where the abaxial surface is virtually indistinguishable from the adaxial surface, in comparison to black cottonwood, which contains bifacial leaves and highly different adaxial and abaxial surfaces. As both leaf blades are flat and do not exhibit severe dorsiventral polarity defects, such as radialization of leaf blades, one would not anticipate extreme gene expression patterns between the two species since the abaxial surface in hybrid aspen contains a cell type that is normally adaxial (i.e., palisade mesophyll). It can be expected that only some genes may exhibit differences in transcript abundance in relation to the difference in leaf phenotype. The genes that are responsible for adaxial polarity specification are predicted to be upregulated in hybrid aspen blade tissue, such as *AS2*, *AE7*, and *RDR6*.

The *AS2* gene is expressed throughout leaf primordia and associates with *AS1* by promoting cell determinacy and repressing *KNOX*, *ETT/ARF3*, *KAN2*, and *YAB5* genes (Byrne et al. 2000, Lin et al. 2003, Kidner and Timmermans 2010, Kojima et al. 2011). In *Arabidopsis*, loss–of-function (LOF) *as2* mutants do not exhibit strong dorsiventral polarity defects, but rather develop downwardly curled asymmetric leaves without obvious loss of adaxial identity, while dominant *AS2* mutations cause adaxialization (Iwakawa et al. 2002, Lin et al. 2003, Kidner and Timmermans 2010). Due to the presence of significantly more transcript of both *Pt-AS2.1* and *Pt-AS2.2* in hybrid aspen, the expected phenotype of hybrid aspen petiole would resemble that of gain-of-function (GOF) mutants.

While little is known about *AE7* in *Arabidopsis*, a recent study (Yuan et al. 2010) showed that it interacts with *AS1/2* and promotes adaxial identity. It is therefore not unexpected for this gene (*Pt-AE7.2*) to also be upregulated along with *Pt-AS2* genes. The qRT-PCR results were consistent with RT-PCR results in regard to these three genes, but transcriptome data showed the converse. *Pt-AS2.1*, *Pt-AS2.2*, and *Pt-AE7.2* all showed higher expression in young leaves of black cottonwood in comparison to aspen leaves. The discrepancy of these results might be attributed to the difference in tissue type (leaf blade vs. whole leaf tissues) and developmental stage of leaves, where tissue used for transcriptome sequencing was likely at an earlier developmental stage compared to the maturing leaf blades used in this study.

Along with *SGS3*, *DCL4*, and *AGO7*, *RDR6* is involved in the biogenesis of trans-acting small interfering RNAs (ta-siRNAs), which repress and restrict *ETT/ARF3* expression from the adaxial domain (Peragine et al. 2004, Allen et al. 2005, Adenot et al. 2006). Double mutants with *AGO1* or *AS2* (*ago1 rdr6* or *as2 rdr6*) in *Arabidopsis*, on the other hand, exhibit

strong polarity defects, producing abaxialized leaves (Xu et al. 2006). This suggests that the interaction between *RDR6* and *AS2* is similar to the interaction between *AE7* and *AS2*. The upregulation of these genes (*Pt-AE7.2*, *Pt-AS2.1*, *Pt-AS2.2*, *Pt-RDR6.1*, and *Pt-RDR6.2*) in hybrid aspen blade, therefore points to a similar interaction being present among these genes in poplar too. Higher expression of *RDR6* genes in hybrid aspen blade is consistent with transcriptome data, which shows higher expression in aspen leaves when compared to black cottonwood.

RDR6 maintains juvenile leaf fate, as *rdr6* mutants exhibit accelerated vegetative phase change (Peragine et al. 2004). GOF mutants would therefore be expected to produce plants with juvenile leaf characteristics. Although both species studied here are from fully adult trees containing leaves with adult morphological characteristics, it is reasonable to assume that isobilateral leaves in hybrid aspen would exhibit lower expression of *RDR6* genes. This is in comparison to black cottonwood, which contains bifacial leaves that are representative of juvenile leaf morphology. The presence of higher transcript abundance of *RDR6* genes in leaf blades can be expected in relation to the role of adaxial cell fate specification, but not to the delay of vegetative phase change. This may suggest that, in this system, *RDR6* genes have a greater effect on dorsiventral patterning than vegetative phase change, in which *SPL* genes have important contributing functions (Wang et al. 2011a).

5.5.2 Abaxial determinants in hybrid aspen blade

According to the hypotheses presented here, some of the genes responsible for abaxial cell fate specification were expected to be downregulated in leaf blades of hybrid aspen or to maintain similar levels of expression in both species. *ATS.2*, *YAB3.2*, and *ZPR3.1*

produced contrasting results and were expressed at significantly higher levels in hybrid aspen blades, compared to black cottonwood. *ZPR3.2*, on the other hand, had lower expression in hybrid aspen blade tissue, in accordance with a simple polarity scenario.

ATS and *YAB3* are determinants of abaxial cell fate. *ATS* belongs to the *KANADI* gene family and has not been reported to have a function in dorsiventral leaf polarity in *Arabidopsis*, but rather is known to determine polarity in ovule integuments (McAbee et al. 2006, Kelley et al. 2009) and to regulate flavonoid biosynthesis in developing seeds (Gao et al. 2010). It is therefore unexpected to detect such high levels of expression in hybrid aspen compared to black cottonwood blade tissues. This is consistent with what was found in transcriptome data, where aspen had significantly higher expression in young leaves compared to black cottonwood. These results may be suggestive of a different function of *Pt-ATS.2* in poplar, one that is not present in *Arabidopsis*. *Pt-ATS.1* did not amplify in RT-PCR analysis, but transcriptome data suggests the absence of differential expression in the two species.

YABBY gene expression is restricted to the abaxial domain and these genes are responsible for abaxial identify specification (Siegfried et al. 1999, Bowman 2000). Four of the *YABBY* family members are expressed in *Arabidopsis* leaves (*AFO/FIL*, *YAB2*, *YAB3*, and *YAB5*) with *AFO/FIL* and *YAB3* acting in a partially redundant manner and having their highest expression in leaves (Siegfried et al. 1999; see Chapter 3). In *Arabidopsis*, *fil yab3* double mutants cause adaxialization of leaves, while GOF mutations cause the inverse, abaxialization of leaves (Sawa et al. 1999, Siegfried et al. 1999, Eshed et al. 2004). Single LOF mutations do not show leaf polarity defects, but *fil* mutants produce radial floral organs (Szakonyi et al. 2010). The predicted downregulation of these genes would be similar to LOF

mutations, possibly causing slight effects on leaf polarity, if any. But the observed upregulation in hybrid aspen blade tissues of *Pt-YAB3.2* may be more suggestive of GOF mutations in *Arabidopsis*. As abaxialized leaf blades are not observed in hybrid aspen, the action of *Pt-YAB3.2* may be counteracted with its putative paralog, *Pt-YAB3.1*, which does not show significant expression differences between the two species in either qRT-PCR or transcriptome analysis. Higher expression of *Pt-YAB3.2* hybrid aspen blades was also observed with transcriptome data analysis and RT-PCR.

Genes responsible for abaxial cell fate specification were predicted to be downregulated in hybrid aspen blades, but still expressed to some degree due to the presence of an abaxial surface, despite containing adaxial cell types. This pattern was not generally observed in the genes tested with qRT-PCR (except *Pt-ZPR3.2*), but transcriptome data showed that *Pt-YAB2.1* and *Pt-YAB5.2* had virtually undetectable levels of expression in aspen leaves, in comparison to black cottonwood. This pattern was not observed in RT-PCR or qRT-PCR analysis with *Pt-YAB2.1*, and *Pt-YAB5.2* transcripts were not amplified successfully (due to absence of transcript or technical failure), possibly due to the differences in type of leaf sample used in the different experiments, as previously described. The absence or reduced level of *Pt-YAB5.2* expression is consistent with the role that *AS2* plays in the repression of *YAB5* in *Arabidopsis* (Iwakawa et al. 2007).

ZPR genes restrict *HD-ZIPIII* gene expression and the expression of *ZPR3*, detected late in leaf development, is found in patches throughout the adaxial epidermis (Wenkel et al. 2007). Leaves are abaxialized in *ZPR3* mutants, a phenotype similar to LOF mutations in *HD-ZIPIII* genes (Emery et al. 2003, Kim et al. 2008). The two tested *ZPR3* genes showed different patterns of transcript abundance between the two species: *Pt-ZPR3.1* was more

highly expressed in hybrid aspen blades and *Pt-ZPR3.2* showed greater transcript abundance in black cottonwood blades. Although *ZPR* genes interact with *HD-ZIPIII* genes via a negative feedback loop (Wenkel et al. 2007, Kim et al. 2008), none of the *HD-ZIPIII* genes tested showed a significant difference in expression using RT-PCR and so were not tested with qRT-PCR.

The *HD-ZIPIII* genes important to leaf polarity in *Arabidopsis* include *PHABULOSA* (*PHB*), *PHAVOLUTA* (*PHV*), and *REVOLUTA* (*REV*) (McConnell et al. 2001, Emery et al. 2003). Transcriptome data reveals that poplar orthologs of these genes (as determined in Chapter 3) have a similar pattern of expression, as do *Pt-ZPR3* genes. While *Pt-PHB.1* (*PHB/PHV* ortholog) was more highly expressed in hybrid aspen leaves, *Pt-PHB.2* had higher expression in black cottonwood leaves. Similarly, *Pt-HB1.6* (*REV* ortholog) showed higher expression in black cottonwood, while *Pt-HB1.7* was more highly expressed in hybrid aspen leaves. These patterns of expression suggest the presence of an interaction between *HD-ZIPIII* and *ZPR3* genes in poplar, as seen in *Arabidopsis* (Wenkel et al. 2007, Kim et al. 2008). The differences between the PCR and transcriptome results could be due to differences in developmental stage of the tissue. This variability could easily be determined by repeating these experiments on a developmental series (from developing leaf primordia to mature leaves) of black cottonwood and hybrid aspen blade and petiole tissues.

5.5.3 *ARGONAUTE1* in hybrid aspen blade

AGO1 is expressed throughout leaf primordia (Lynn et al. 1999) and interacts with *AS1/2*. It is also required for *KNOX* repression and juvenile leaf fate maintenance, by delaying vegetative phase change (Yang et al. 2006). LOF *ago1* mutations can have a variety

of effects, including abaxialized organs and defects in the meristem (Bohmert et al. 1998, Baumberger and Baulcombe 2005). Most genes within the dorsiventral leaf polarity network are involved in setting either the adaxial or abaxial surface polarity in *Arabidopsis*. *AGO1*, on the other hand, appears to be responsible for both abaxial and adaxial cell fate determination in lateral organs (Xu et al. 2006), although previous studies reported its role in abaxial cell fate specification in leaves (Kidner and Martienssen 2004) and adaxial cell fate specification in petals (Lynn et al. 1999). Due to this variability in cell fate specification, it is reasonable to assume that in poplar, *Pt-AGO1* genes may be expressed in either the abaxial or adaxial domain in leaves or both. Functional studies would be required to determine the precise expression domains of these genes in poplar in order to predict its effect in the abaxial greening phenotype.

Pt-AGO1.2 was expressed at a higher level in hybrid aspen blade in comparison to black cottonwood. These qRT-PCR results were consistent with the non-quantitative analysis. The transcriptome data, on the other hand, did not show a significant difference between expression levels in leaves of aspen and black cottonwood. This inconsistency between my and transcriptome results is likely due to the difference in developmental stages investigated, previously discussed.

5.5.4 Hybrid aspen unifacial petiole

The RT-PCR results showed a group of genes that lacked expression in hybrid aspen petiole tissues. qRT-PCR, on the other hand, contradicted these results by showing that all of the genes tested had some level of detectable transcript expression, with none significantly lower than the black cottonwood petiole samples, likely reflecting the higher sensitivity of

qRT-PCR in comparison to the non-quantitative RT-PCR method. Two genes showing a significant difference in petiole expression were adaxial and abaxial cell fate specifying genes, *Pt-AE7.2* and *Pt-ZPR3.2*, respectively. While the former showed higher expression in hybrid aspen petioles, the latter showed higher transcript abundance in black cottonwood petioles. This was the same pattern of expression between the two species as that observed for blade samples. These results suggest that these two genes may have higher expression in hybrid aspen and black cottonwood regardless of tissue type.

Although *Pt-AE7.2* expression was detected with RT-PCR, *Pt-ZPR3.2* was not. This is likely due to the very low expression of *Pt-ZPR3.2* in leaves of both species (from transcriptome data). The difference in expression of *Pt-ZPR3.2* is consistent with transcriptome data that shows low, but nonetheless higher (compared to black cottonwood) expression in aspen leaves. These petiole results cannot be compared to transcriptome data since RNA was extracted from young leaf samples that may or may not have included the petiole, but that were primarily blade tissues.

The absence of genes having no expression in the petiole tissues of hybrid aspen is unexpected since the scenario tested here suggests that the morphological difference of the petiole between the two species would be the result of a difference in gene expression. However, these results may not be completely surprising. Although the black cottonwood radial petiole contains adaxial surface along with the abaxial, while hybrid aspen petiole consists only of the abaxial surface, the vascular arrangement is very similar in these species. All of the vascular bundles in both black cottonwood and hybrid aspen are amphicribral. This suggests that not only is the mediolaterally flattened petiole of hybrid aspen abaxialized, but also that the radial black cottonwood petiole may be considered more abaxialized than

bifacial, since surface identity is determined by the vascular arrangement (see Chapter 1). The presence of the adaxial surface in black cottonwood petiole could be so insignificant that a difference, if any, between the two species may not be detected by sampling whole petiole tissues.

5.5.5 Hybrid aspen leaf phenotypes

Isobilateral leaves exhibit abaxial greening, where the abaxial surface consists of adaxial-like palisade mesophyll cells, and therefore, it would follow that more adaxial genes may be expressed in the leaf blade of hybrid aspen, while there would be a reduction in "normal" abaxial gene expression. A collection of genes was differentially expressed in hybrid aspen leaf blades in comparison to black cottonwood. These included genes responsible for setting both the adaxial (*Pt-AE7.2, Pt-AS2.1, Pt-AS2.2, Pt-RDR6.1, Pt-RDR6.2, Pt-AGO1.2*) and abaxial (*Pt-ATS.2, Pt-YAB3.2, Pt-ZPR3.1, Pt-ZPR3.2, Pt-AGO1.2*) surface identities in *Arabidopsis*. Although the upregulation or significantly higher transcript abundance of adaxial cell fate determinants is not surprising, as it accords with the polarity scenario tested here, the upregulation of abaxial cell fate determinants was not predicted in this scenario.

Although the abaxial surface of the hybrid aspen blade contains cells that are characteristic of the adaxial domain in other species, the leaf blade maintains its dorsiventral polarity. The presence of both surfaces indicates functionality of both domains and therefore the absence of blade radialization that would occur in the presence of genes responsible for setting adaxial surface identity. The observed upregulation of the opposing abaxial surface identity determinants may be responsible for maintaining the dorsiventrally flattened leaf

blades in hybrid aspen, while still allowing for the development of adaxial cell types in the abaxial side of the leaf.

Table 5.1 ***Arabidopsis*** **genes names and identified putative** ***P. trichocarpa*** **orthologs, including poplar gene id and gene name. Gene function in** ***Arabidopsis*****, from various references (cited within text or TAIR), is also presented.**

Arabidopsis **gene name**	***Arabidopsis*** **accession number**	**Gene function in** ***Arabidopsis***	**POPTR gene id (v2.2)**	**Poplar gene name**
AE3 (AS1/2 enhancer 3)	AT5G05780	Adaxial leaf identity specification	POPTR_0008s06540	*Pt-AE3.1*
			POPTR_0008s06550	*Pt-AE3.2*
AE7 (AS1/2 enhancer 7)	AT1G68310	Adaxial polarity formation	POPTR_0001s01820	*Pt-AE7.1*
			POPTR_0003s09670	*Pt-AE7.2*
AFO (abnormal flower organ)	AT2G45190	Abaxial cell fate specification	POPTR_0014s06210	*Pt-AFO.1*
			POPTR_0002s14600	*Pt-AFO.2*
AGO1 (argonaute 1)	AT1G48410	Adaxial/abaxial cell fate specification; vegetative phase change	POPTR_0012s03410	*Pt-AGO1.1*
			POPTR_0015s05550	*Pt-AGO1.2*
AGO7 (argonaute 7)	AT1G69440	Regulation of vegetative phase change	POPTR_0009s00660	*Pt-AGO7.1*
			POPTR_0010s17100	*Pt-AGO7.4*
AGO10 (argonaute 10)	AT5G43810	Primary SAM specification; miRNA binding	POPTR_0008s15860	*Pt-AGO10.1*
			POPTR_0010s09150	*Pt-AGO10.2*
AN3 (angustifolia 3)	AT5G28640	Leaf development	POPTR_0013s04090	*Pt-AN3.1*
			POPTR_0019s02320	*Pt-AN3.2*
ARF4 (auxin response factor 4)	AT5G60450	Abaxial cell fate specification	POPTR_0009s01700	*Pt-ARF4.1*
AS1 (asymmetric leaves 1)	AT2G37630	Adaxial axis specification	POPTR_0006s08610	*Pt-AS1.1*
			POPTR_0004s10250	*Pt-AS1.2*
			POPTR_0017s13950	*Pt-AS1.3*
AS2 (asymmetric leaves 2)	AT1G65620	Adaxial axis specification	POPTR_0010s18460	*Pt-AS2.1*
			POPTR_0008s07930	*Pt-AS2.2*
CNA (corona)	AT1G52150	Adaxial identity determination; vascular histogenesis	POPTR_0003s04860	*Pt-ATHB.11*
			POPTR_0001s18930	*Pt-ATHB.12*
ATS (aberrant test shape)	AT5G42630	Integument development; abaxial cell fate	POPTR_0002s13170	*Pt-ATS.1*
			POPTR_0014s03650	*Pt-ATS.2*
CRC (crabs claw)	AT1G69180	Abaxial axis specification; floral meristem determinacy	POPTR_0008s09740	*Pt-CRC.1*
			POPTR_0010s16410	*Pt-CRC.2*
DCL4 (dicer-like 4)	AT5G20320	Vegetative phase change	POPTR_0006s20310	*Pt-DCL4.1*

***Arabidopsis* gene name**	***Arabidopsis* accession number**	**Gene function in *Arabidopsis***	**POPTR gene id (v2.2)**	**Poplar gene name**
DUF59 (domain of unknown function 59)	AT3G50845	Adaxial polarity formation (AE7-like)	POPTR_0005s12480	*Pt-DUF59.1*
ETT (ettin)	AT2G33860	Abaxial cell fate specification	POPTR_0004s04970	*Pt-ETT.1*
			POPTR_0011s05830	*Pt-ETT.2*
ATHB8 (Arabidopsis thaliana homeobox 8)	AT4G32880	Xylem development	POPTR_0018s08110	*Pt-HB1.5*
			POPTR_0006s25390	*Pt-HB1.6*
REV (revoluta)	AT5G60690	Adaxial axis specification; vascular pattern formation	POPTR_0004s22090	*Pt-HB1.7*
			POPTR_0009s01990	*Pt-HB1.8*
HYL (hyponastic leaves 1)	AT1G09700	Vegetative phase control (Li et al. 2012)	POPTR_0005s19650	*Pt-HYL1.1*
			POPTR_0002s11200	*Pt-HYL1.2*
INO (inner-no-outer)	AT1G23420	Abaxial cell fate specification; ovule development	POPTR_0008s19330	*Pt-INO.1*
			POPTR_0010s05220	*Pt-INO.2*
KAN (KANADI 1)	AT5G16560	Abaxial identity specification	POPTR_0017s02220	*Pt-KAN.1*
			POPTR_0004s08070	*Pt-KAN.2*
			POPTR_0015s05340	*Pt-KAN.3*
			POPTR_0012s03900	*Pt-KAN.4*
KAN2, KAN3 (KANADI 2, KANADI3)	AT1G32240 AT4G17695	Abaxial cell fate specification; ovule development	POPTR_0003s09490	*Pt-KAN2/3.1*
			POPTR_0001s02010	*Pt-KAN2/3.2*
PHB (phabulosa) PHV (phavoluta)	AT2G34710 AT1G30490	Adaxial cell fate specification	POPTR_0011s10070	*Pt-PHB.1*
			POPTR_0001s38120	*Pt-PHB.2*
PGY1 (piggyback 1)	AT2G27530	Adaxial pattern specification; AS1 enhancer	POPTR_0007s11880	*Pt-PGY1.1*
PGY2 (piggyback 2)	AT1G33140	Adaxial pattern specification; AS1 enhancer	POPTR_0001s45810	*Pt-PGY2.1*
			POPTR_0011s15170	*Pt-PGY2.2*
PGY3 (piggyback 3)	AT3G25520	Adaxial pattern specification	POPTR_0013s13220	*Pt-PGY3.1*
RDR6 (RNA-dependent RNA polymerase 6)	AT3G49500	Leaf development	POPTR_0006s26980	*Pt-RDR6.1*
			POPTR_0018s01670	*Pt-RDR6.2*
SE (serrate)	AT2G27100	Adaxial/abaxial pattern regulation	POPTR_0004s20730	*Pt-SE.1*
			POPTR_0009s16020	*Pt-SE.2*
SGS3 (suppressor of gene silencing 3)	AT5G23570	Vegetative phase change	POPTR_0019s00300	*Pt-SGS3.1*
			POPTR_0001s07410	*Pt-SGS3.2*
			POPTR_0001s07420	*Pt-SGS3.3*
			POPTR_0003s18660	*Pt-SGS3.4*
			POPTR_0003s18670	*Pt-SGS3.5*
			POPTR_0003s18680	*Pt-SGS3.6*
			POPTR_0003s18690	*Pt-SGS3.7*
			POPTR_0003s01530	*Pt-SGS3.8*
SPL4 (squamosa promoter binding-like 4)	AT1G53160	Vegetative phase change	POPTR_0001s40870	*Pt-SPL4.1*
			POPTR_0011s11770	*Pt-SPL4.2*

***Arabidopsis* gene name**	***Arabidopsis* accession number**	**Gene function in *Arabidopsis***	**POPTR gene id (v2.2)**	**Poplar gene name**
SPL4, SPL3 (squamosa promoter binding-like 3)	AT2G33810 (SPL3)	Vegetative phase change regulation	POPTR_0004s04630	*Pt-SPL43.1*
			POPTR_0011s05480	*Pt-SPL43.2*
SPL9 (squamosa promoter binding-like 9)	AT2G42200	Vegetative to reproductive phase change transition	POPTR_0016s04890	*Pt-SPL9.1*
YAB2 (YABBY 2)	AT1G08465	Abaxial cell fate specification	POPTR_0001s22180	*Pt-YAB2.1*
			POPTR_0127s00201	*Pt-YAB2.2*
			POPTR_0016s06760	*Pt-YAB2.3*
YAB3 (YABBY 3)	AT4G00180	Abaxial cell fate specification	POPTR_0003s11230	*Pt-YAB3.1*
			POPTR_0001s00240	*Pt-YAB3.2*
YAB5 (YABBY 5)	AT2G26580	Abaxial cell fate specification	POPTR_0006s06700	*Pt-YAB5.1*
		Abaxial cell fate specification	POPTR_0018s12990	*Pt-YAB5.2*
YUC (yucca)	AT4G32540	Auxin biosynthesis; regulation of leaf development	POPTR_0006s26430	*Pt-YUC.2*
			POPTR_0018s01210	*Pt-YUC.1*
YUC2 (yucca 2)	AT4G13260	Auxin biosynthesis	POPTR_0006s26000	*Pt-YUC2.1*
			POPTR_0018s00840	*Pt-YUC2.2*
ZPR1 (little zipper 1)	AT2G45450	Adaxial cell fate specification; interacts with REV	POPTR_0003s11710	*Pt-ZPR1.1*
			POPTR_0001s08220	*Pt-ZPR1.2*
ZPR2 (little zipper 2)	AT3G60890	Adaxial cell fate specification	POPTR_0002s15060	*Pt-ZPR2.1*
			POPTR_0014s06690	*Pt-ZPR2.2*
ZPR3 (little zipper 3)	AT3G52770	Adaxial cell fate specification	POPTR_0006s08320	*Pt-ZPR3.1*
			POPTR_0010s24410	*Pt-ZPR3.2*

Table 5.2 Transcriptome data for leaf tissues comparing black cottonwood (Ptr) and hybrid aspen (Ptmx) expression levels (RPKM) analyzed using RT-PCR. Grey shading denotes genes that have higher expression (RPKM) in hybrid aspen, compared to black cottonwood. A significant difference in expression levels between two species is determined with p-value < 0.05 (underlined). RT-PCR results are categorized for each gene in the last column: A1) Higher expression in hybrid aspen blade, A2) Expression not higher in hybrid aspen blade, A3) No expression in black cottonwood blade (*Pt-PGY3.1* only), B1) No expression in hybrid aspen petiole, B2) Some expression in hybrid aspen petiole, C) No amplification of cDNA or DNA in either or both species, and D) Not tested or no conclusive results.

Bolded genes indicate RPKM > 5 in either species. Asterisks indicate genes that were analyzed further with qRT-PCR.

Gene id	Gene name	Ptr mean RPKM	Ptmx mean RPKM	p-value	RT-PCR result category
POPTR_0008s06540	***Pt-AE3.1***	**57.44±8.16**	**40.04±6.03**	**0.0221**	**C**
POPTR_0008s06550	***Pt-AE3.2***	**130.53±7.99**	**95.61±12.10**	**0.0077**	**C**
POPTR_0001s01820	***Pt-AE7.1***	**14.13±4.50**	**11.69±0.74**	**0.3228**	**C**
POPTR_0003s09670	***Pt-AE7.2****	**26.16±6.35**	**16.34±1.34**	**0.0268**	**A2, B1**
POPTR_0014s06210	***Pt-AFO.1***	**98.67±16.85**	**52.38±25.72**	**0.0437**	**A2, B2**
POPTR_0002s14600	***Pt-AFO.2***	**115.90±22.05**	**58.60±24.51**	**0.0244**	**A2**
POPTR_0012s03410	***Pt-AGO1.1***	**68.79±21.07**	**80.39±13.30**	**0.4085**	**C**
POPTR_0015s05550	***Pt-AGO1.2****	**32.07±11.43**	**30.67±6.36**	**0.8422**	**A1, B1**
POPTR_0009s00660	***Pt-AGO7.1***	**7.09±2.27**	**7.05±0.88**	**0.9738**	**C**
POPTR_0010s17100	***Pt-AGO7.4****	**29.99±5.89**	**24.16±14.50**	**0.5471**	**A1, B1**
POPTR_0008s15860	***Pt-AGO10.1****	**12.84±5.27**	**21.34±6.48**	**0.1241**	**A1, B1**
POPTR_0010s09150	***Pt-AGO10.2***	**30.49±10.63**	**17.88±8.20**	**0.1343**	**C**
POPTR_0013s04090	***Pt-AN3.1***	**44.23±11.87**	**33.86±14.80**	**0.3674**	**C**
POPTR_0019s02320	***Pt-AN3.2***	**94.75±41.53**	**76.91±43.04**	**0.6057**	**B1**
POPTR_0009s01700	***Pt-ARF4.1***	**25.40±9.95**	**24.31±4.08**	**0.8477**	**C**
POPTR_0006s08610	***Pt-AS1.1****	**52.68±7.63**	**82.05±41.07**	**0.2857**	**A2, B1**
POPTR_0004s10250	***Pt-AS1.2****	**25.90±13.53**	**7.36±5.93**	**0.0544**	**B1**
POPTR_0017s13950	***Pt-AS1.3***	**51.14±9.22**	**40.39±11.10**	**0.2334**	**C**
POPTR_0010s18460	***Pt-AS2.1****	**23.81±5.22**	**9.81±6.46**	**0.0282**	**A2, B1**
POPTR_0008s07930	*Pt-AS2.2**	4.85±0.24	1.07±0.75	0.0004	**A2, B1**
POPTR_0003s04860	***Pt-ATHB.11***	**13.90±4.42**	**16.57±6.17**	**0.5555**	**C**
POPTR_0001s18930	***Pt-ATHB.12***	**14.90±4.21**	**36.77±12.95**	**0.0399**	**C**
POPTR_0002s13170	***Pt-ATS.1***	**5.59±0.60**	**4.54±2.29**	**0.4815**	**C**
POPTR_0014s03650	***Pt-ATS.2****	**13.96±3.14**	**35.83±7.50**	**0.0055**	**A1, B1**
POPTR_0008s09740	*Pt-CRC.1*	0.00	0.02±0.03	0.2751	D
POPTR_0010s16410	*Pt-CRC.2*	0.00	0.00	n/a	D
POPTR_0006s20310	*Pt-DCL4.1*	2.54±1.04	4.97±1.47	0.0592	C
POPTR_0005s12480	***Pt-DUF59.1***	**23.32±9.89**	**21.87±3.62**	**0.7928**	**C**
POPTR_0004s04970	***Pt-ETT.1***	**17.98±5.65**	**20.09±2.29**	**0.5199**	**B2**
POPTR_0011s05830	***Pt-ETT.2***	**6.33±1.56**	**8.77±2.76**	**0.2322**	**A2, B1**
POPTR_0018s08110	***Pt-HB1.5 (ATHB8)***	**6.76±2.39**	**19.63±6.46**	**0.0234**	**C**
POPTR_0006s25390	***Pt-HB1.6 (ATHB8)***	**32.29±7.56**	**23.22±3.89**	**0.0897**	**C**
POPTR_0004s22090	***Pt-HB1.7 (REV)***	**6.04±2.20**	**10.26±3.55**	**0.1330**	**C**
POPTR_0009s01990	***Pt-HB1.8 (REV)***	**25.92±8.83**	**9.02±1.62**	**0.0118**	**C**
POPTR_0005s19650	***Pt-HYL1.1***	**16.41±5.81**	**19.42±2.47**	**0.3851**	**B1**
POPTR_0002s11200	***Pt-HYL1.2***	**5.71±1.29**	**8.58±0.69**	**0.0121**	**B1**
POPTR_0008s19330	*Pt-INO.1*	0.01±0.01	0.00	0.2856	D
POPTR_0010s05220	*Pt-INO.2*	0.01±0.02	0.00	0.2856	D
POPTR_0017s02220	***Pt-KAN.1***	**4.80±0.39**	**7.01±5.89**	**0.5545**	**C**

Gene id	Gene name	Ptr mean RPKM	Ptmx mean RPKM	p-value	RT-PCR result category
POPTR_0004s08070	***Pt-KAN.2***	**15.22±1.36**	**9.80±0.67**	**0.0009**	**A2, B2**
POPTR_0015s05340	***Pt-KAN.3***	**2.61±1.64**	**6.26±1.94**	**0.0471**	**A1, B2**
POPTR_0012s03900	*Pt-KAN.4*	3.27±2.60	2.48±0.85	0.5828	B2
POPTR_0003s09490	***Pt-KAN2/3.1***	**8.34±0.93**	**1.08±0.29**	**$2.281x10^{-05}$**	**A1, B1**
POPTR_0001s02010	***Pt-KAN2/3.2***	**5.48±1.11**	**7.81±2.46**	**0.1925**	**C**
POPTR_0011s10070	***Pt-PHB.1***	**27.16±5.37**	**45.01±8.31**	**0.0238**	**A2, B2**
POPTR_0001s38120	***Pt-PHB.2***	**25.69±9.86**	**8.84±1.02**	**0.0171**	**A2, B2**
POPTR_0007s11880	***Pt-PGY1.1***	**197.62±39.30**	**99.77±34.79**	**0.0174**	**A2, B2**
POPTR_0001s45810	***Pt-PGY2.1***	**61.44±25.32**	**41.11±19.57**	**0.2812**	**A2, B2**
POPTR_0011s15170	***Pt-PGY2.2***	**129.11±57.05**	**63.09±17.23**	**0.0746**	**A2, B2**
POPTR_0013s13220	***Pt-PGY3.1****	**406.38±60.21**	**428.42±107.56**	**0.7654**	**A3, B2**
POPTR_0006s26980	***Pt-RDR6.1****	**5.83±2.12**	**15.81±1.06**	**0.0004**	**A2, B1**
POPTR_0018s01670	***Pt-RDR6.2****	**1.13±0.39**	**8.05±2.57**	**0.0063**	**A2, B1**
POPTR_0004s20730	***Pt-SE.1***	**19.68±2.93**	**24.42±3.09**	**0.0956**	**B2**
POPTR_0009s16020	***Pt-SE.2***	**25.06±2.54**	**26.09±5.93**	**0.7938**	**A2, B2**
POPTR_0019s00300	***Pt-SGS3.1***	**49.70±3.60**	**44.12±10.69**	**0.4333**	**A2, B2**
POPTR_0001s07410	***Pt-SGS3.2***	**20.06±9.14**	**15.20±15.20**	**0.3650**	**C**
POPTR_0001s07420	*Pt-SGS3.3*	0.27±0.22	0.39±0.07	0.3351	D
POPTR_0003s18660	*Pt-SGS3.4*	2.06±0.65	1.84±0.54	0.6411	D
POPTR_0003s18670	*Pt-SGS3.5*	0.30±0.07	0.10±0.04	0.0061	D
POPTR_0003s18680	*Pt-SGS3.6*	3.56±0.07	2.99±0.89	0.4061	D
POPTR_0003s18690	*Pt-SGS3.7*	0.41±0.14	0.15±0.06	0.0188	D
POPTR_0003s01530	***Pt-SGS3.8***	**2.22±1.37**	**9.80±6.01**	**0.0898**	**C**
POPTR_0001s40870	***Pt-SPL4.1****	**28.12±3.72**	**60.65±8.68**	**0.0019**	**A1, B2**
POPTR_0011s11770	***Pt-SPL4.2***	**9.61±0.10**	**11.10±7.10**	**0.7370**	**B2**
POPTR_0004s04630	***Pt-SPL43.1***	**2.70±0.96**	**9.59±9.15**	**0.2605**	**C**
POPTR_0011s05480	***Pt-SPL43.2****	**51.31±15.58**	**65.37±24.85**	**0.4335**	**A2, B1**
POPTR_0016s04890	***Pt-SPL9.1***	**4.74±1.95**	**9.24±4.78**	**0.1914**	**C**
POPTR_0001s22180	***Pt-YAB2.1***	**102.90±13.76**	**1.97±1.53**	**$2.352x10^{-05}$**	**A1, B2**
POPTR_0127s00201	***Pt-YAB2.2***	**16.82±5.87**	**58.12±30.25**	**0.0717**	**A2, B2**
POPTR_0016s06760	***Pt-YAB2.3***	**75.42±16.33**	**64.62±29.43**	**0.5962**	**C**
POPTR_0003s11230	***Pt-YAB3.1***	**61.42±10.31**	**114.00±51.14**	**0.1470**	**A2, B2**
POPTR_0001s00240	***Pt-YAB3.2****	**14.74±2.50**	**66.94±10.40**	**0.0004**	**A1, B2**
POPTR_0006s06700	***Pt-YAB5.1***	**47.58±19.28**	**60.05±2.61**	**0.2434**	**C**
POPTR_0018s12990	***Pt-YAB5.2***	**220.13±18.32**	**0.01±0.01**	**$1.959x10^{-06}$**	**A2, B2**
POPTR_0006s26430	*Pt-YUC.2*	1.35±0.63	1.08±0.77	0.6348	D
POPTR_0018s01210	*Pt-YUC.1*	3.45±1.59	1.27±0.88	0.0652	D
POPTR_0006s26000	*Pt-YUC2.1*	2.91±0.39	4.94±1.81	0.1211	D
POPTR_0018s00840	*Pt-YUC2.2*	1.01±0.67	0.76±0.45	0.5844	D
POPTR_0003s11710	*Pt-ZPR1.1*	2.81±1.35	2.76±0.68	0.9491	C
POPTR_0001s08220	*Pt-ZPR1.2*	3.20±1.47	1.47±0.65	0.0845	C
POPTR_0002s15060	*Pt-ZPR2.1*	4.29±3.00	3.35±1.11	0.5780	C
POPTR_0014s06690	***Pt-ZPR2.2***	**17.75±13.61**	**2.07±1.45**	**0.0643**	**C**
POPTR_0006s08320	***Pt-ZPR3.1****	**18.88±10.63**	**5.15±1.65**	**0.0467**	**A2, B1**
POPTR_0010s24410	*Pt-ZPR3.2**	0.47±0.19	2.62±0.80	0.0066	A1, B2

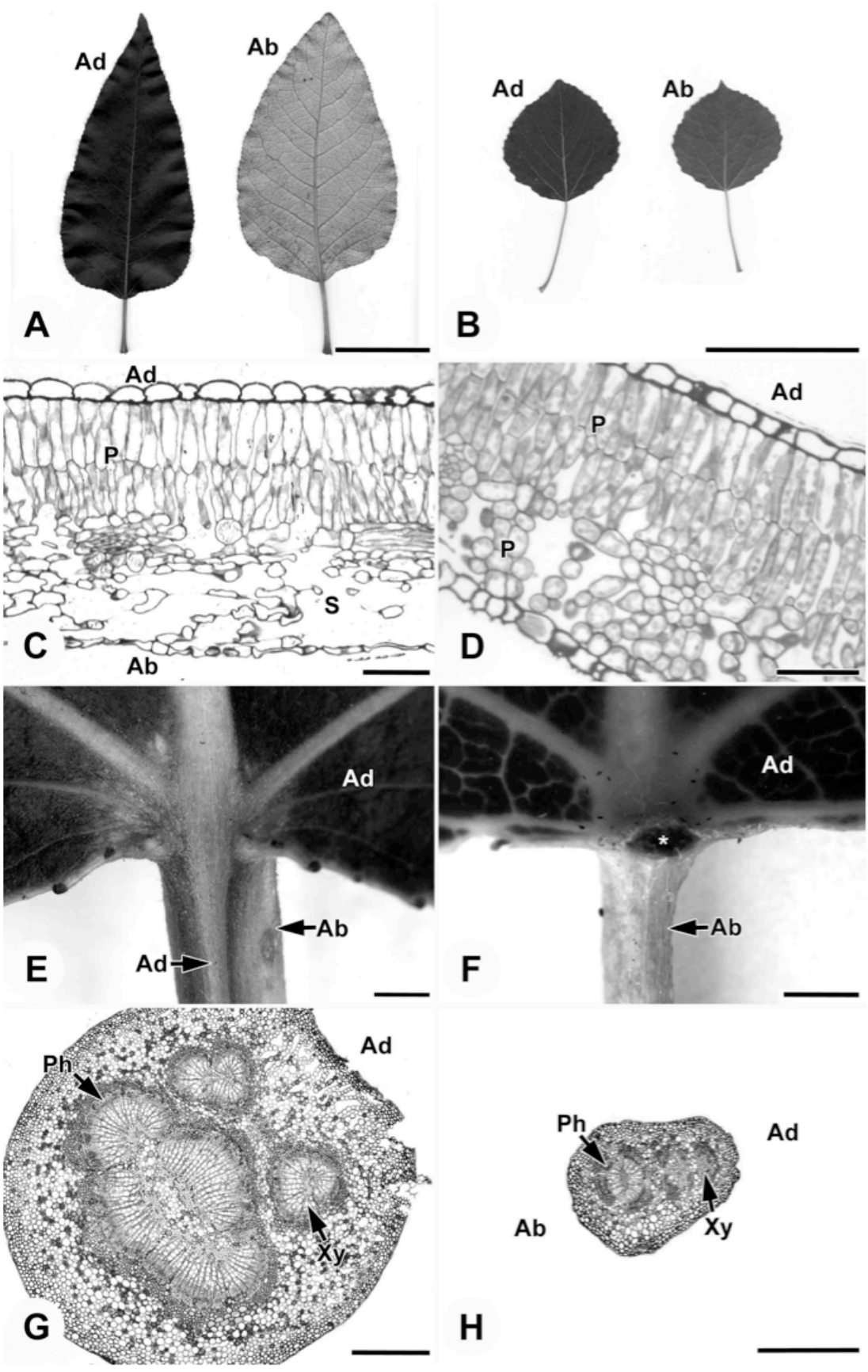
Ad
Ab
A
Ad
Ab
B
Ad
P
S
Ab
C
Ad
P
P
D
Ad
Ab
E
Ad
Ad
*
Ab
F
Ph
Ad
Xy
G
Ph
Ad
Ab
Xy
H

Figure 5.1 ***Populus trichocarpa*** **(black cottonwood) and** ***P. tremula*** **x** ***tremuloides*** **(hybrid aspen) leaf morphology and anatomy.** A. **Black cottonwood leaves showing dark green adaxial surface and lighter abaxial surface.** B. **Hybrid aspen leaves showing similarity in colouration of both adaxial and abaxial surfaces.** C. **Transverse section of black cottonwood leaf blade showing palisade mesophyll at the adaxial surface and spongy mesophyll at the abaxial.** D. **Transverse section of hybrid aspen leaf blade showing palisade mesophyll at both adaxial and abaxial surfaces.** E. **Higher magnification of the adaxial side of the petiole/blade junction in black cottonwood leaf. The adaxial surface from the leaf blade is continued in the narrow region down the petiole, while the back and majority of the petiole consists of the abaxial surface.** F. **Higher magnification of the adaxial side of the petiole/blade junction in hybrid aspen leaf. The adaxial surface of the leaf blade does not extend down the petiole, but is instead interrupted by the gland (asterisk) located at the petiole/blade junction. The petiole, therefore, consists mostly of the abaxial surface.** G. **Transverse section of black cottonwood petiole with the adaxial surface labeled. The petiole contains three amphicribral vascular bundles.** H. **Transverse section of hybrid aspen petiole with the adaxial and abaxial sides, labeled in relation to the shoot. There are two amphicribral vascular bundles within the petiole. Ad – adaxial side/surface, Ab – abaxial side/surface, P – palisade mesophyll, S – spongy mesophyll, Ph – phloem, Xy – xylem. Scale bars = 1cm (A, B), 50µm (C, D), 1mm (E, F), 500µm (G, H).**

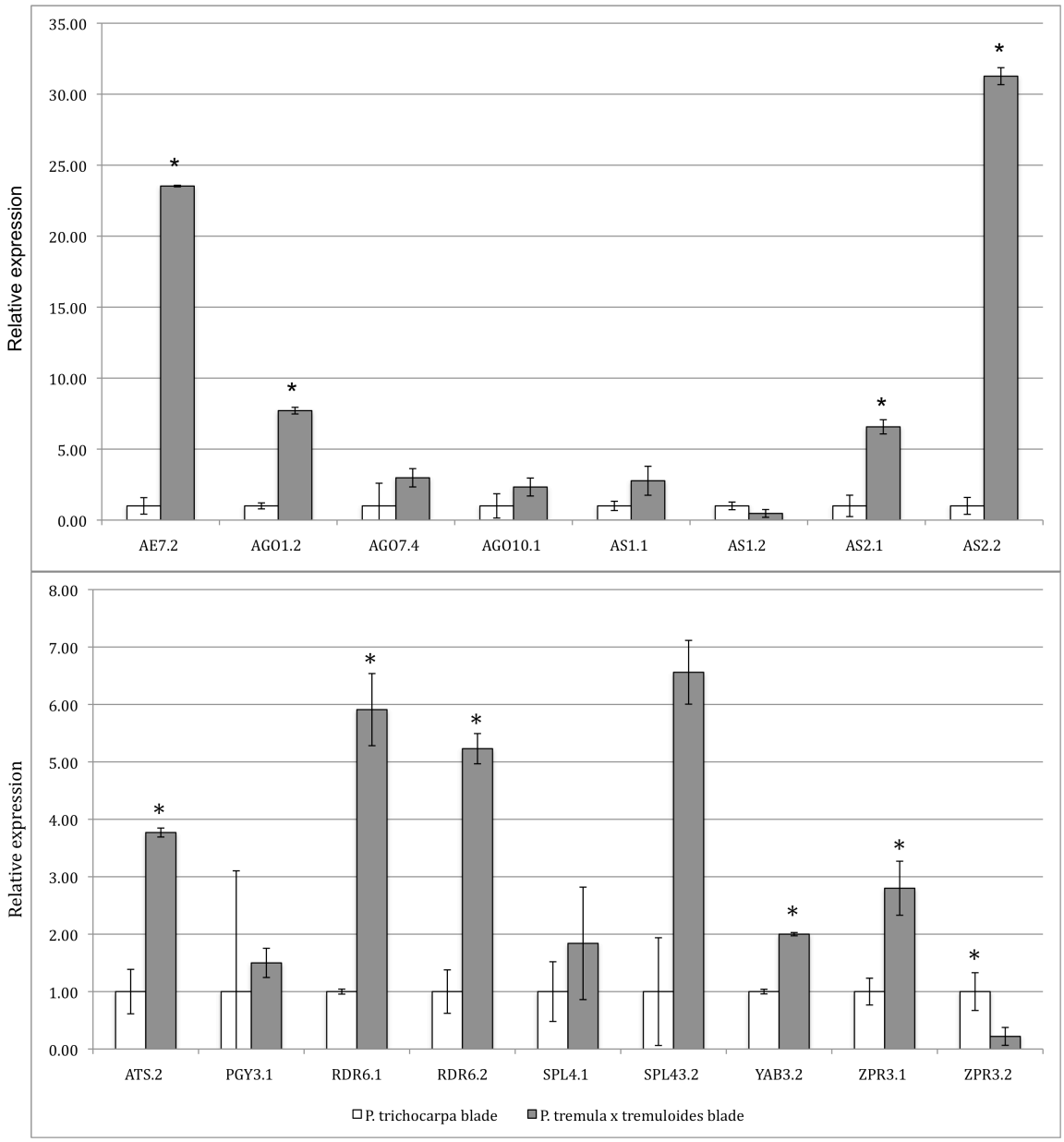

Figure 5.2 qRT-PCR results of the blade tissues comparing *P. trichocarpa* and *P. tremula* x *tremuloides*. Asterisks indicate the genes that show a significant difference in expression between the two species, with the asterisk above the species that has significantly higher expression. White bars indicate relative expression in *P. trichocarpa* blades, while grey bars show relative expression in *P. tremula* x *tremuloides* blades.

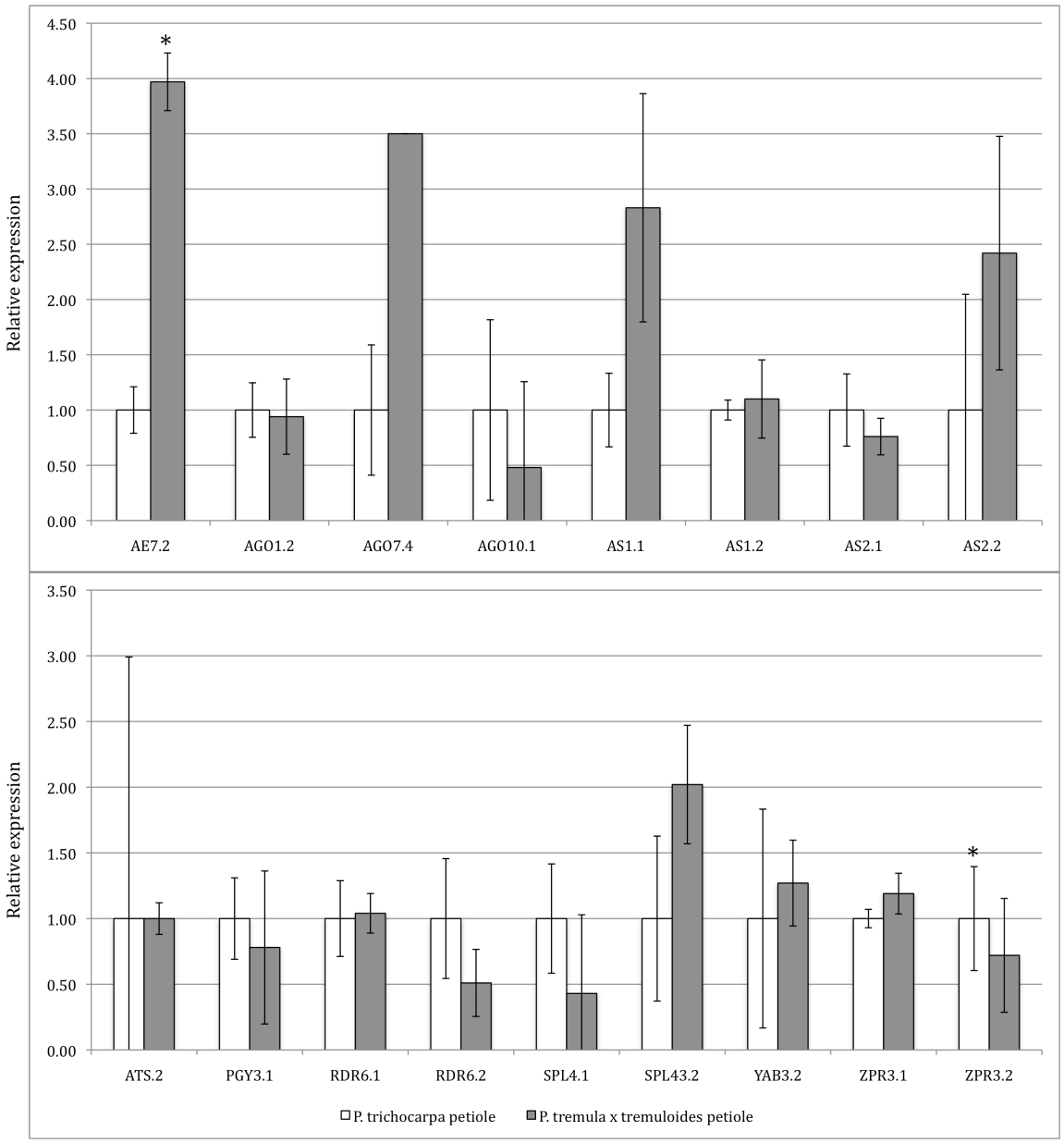

Figure 5.3 qRT-PCR results of the petiole tissues comparing *P. trichocarpa* and *P. tremula* x *tremuloides*. Asterisks indicate the genes that show a significant difference in expression between the two species, with the asterisk above the species that has significantly higher expression. White bars indicate relative expression in *P. trichocarpa* petioles, while grey bars show relative expression in *P. tremula* x *tremuloides* petioles.

Chapter 6: Conclusion

The unifying theme of this thesis is the determination of the adaxial-abaxial or dorsiventral polarity in leaves. Although this topic has been extensively investigated over the last 20 years (e.g., Waites and Hudson 1995, Townsley and Sinha 2012), the majority of these studies focus on the genetic mechanisms underlying a mutant phenotype. Model systems such as *Arabidopsis*, *Antirrhinum*, maize, rice, and non-model systems such as *Juncus* have been relatively well investigated and these results form the basis of our current knowledge in the field. In this thesis, I aimed to investigate the morphological and anatomical bases of leaves exhibiting dorsiventral polarity defects in non-model species, including those found in nature with such "variation". The majority of the thesis focuses on poplar, which is an emerging model system for tree biology and wood formation rather than leaf development. One chapter discusses a mutant of canola, which is another system that has not been used as a model for leaf development (although it is closely related to *Arabidopsis*).

This thesis consists of five preceding chapters, which all relate to one another under this theme of dorsiventral polarity:

1) Adaxial-abaxial polarity in leaves: integration of genetics and morphology

2) *Lamina epiphylla*: a novel adaxialized leaf mutant of canola

3) Phylogenomics and expression of dorsiventral polarity genes in leaves of forest trees

4) North American *Populus* phylogeny and leaf analysis

5) Abaxial greening and unifacial petiole phenotypes in hybrid aspen.

6.1 Chapter 1

In Chapter 1, I introduced the topic of adaxial-abaxial polarity. Here, my aim was to cover our current knowledge of the genetic basis of dorsiventral polarity, primarily in *Arabidopsis*, but also in other species such as *Antirrhinum* and maize that show functional differences from *Arabidopsis* in their adaxial-abaxial polarity gene network patterning. Further, morphology and anatomy of plants with naturally radialized leaves was described. The primary objective of this chapter was to determine whether the conceptual models about adaxial-abaxial polarity mutants could be correlated to the types of leaves that are observed in nature.

The primary indicator of the type of radialization in a leaf is its vasculature. The collateral arrangement of the vascular bundles is conserved where xylem is located towards the adaxial surface and phloem towards the abaxial. Radialized leaf mutants in *Arabidopsis* generally contain a single vascular bundle that is also radialized. This is an example where the information that we learn from *Arabidopsis* mutants cannot be transferred to natural variation in non-model systems. In these, there are usually several bundles that are reoriented in relation to the type of domain on the periphery (adaxial or abaxial), while their collateral arrangement is maintained. This, therefore, is an important indicator of the difference in the basic morphology of naturally radialized leaves in comparison to mutants in the model system from which the majority of our plant genetic and developmental knowledge is based.

It can be predicted that adaxialized leaves would have an upregulation of adaxial surface identity determinants or a downregulation of abaxial determinants. The inverse would be expected for abaxialized leaves. Due to functional variation of some genes (e.g., *AS1/2*, *YABBY*) in other studied model species, one should exercise caution in transferring molecular

genetic insights about dorsiventral polarity to non-model systems, and variation in gene function is to be expected.

6.2 Chapter 2

A novel *Brassica napus* (canola) mutant with an extreme leaf phenotype displaying altered adaxial-abaxial polarity, identified from a mutagenesis screen, was investigated in Chapter 2. The leaves of this mutant, named *lamina epiphylla* (*lip*), are adaxialized, where the top surface identity surrounds the outside of the most commonly observed trumpet-shaped or filamentous leaf, and the abaxial surface either makes up the surface located on the inside of the trumpet or is altogether absent as in filamentous leaves. *Brassica napus* plants exhibiting a moderate *lip* phenotype contain leaves that are similar to bifacial leaves in wild type canola plants, except for epilaminar outgrowths present on the abaxial surface of the leaves.

In this chapter, this *lip* mutant phenotype was characterized using morphological and anatomical analyses. Due to morphological and anatomical similarities to previously described *Arabidopsis* mutants, genes in the *HD-ZIPIII* family were used as candidates to determine the molecular nature of the *LIP* mutation. This study identified eight of the putative 20 *B. napus* orthologs of the five *Arabidopsis HD-ZIPIII* genes, all of which were identical in sequence both in *lip* and wild type plants. Since the release of the *B. rapa* and *B. oleracea* genomes, I have identified the orthologous genes in these species, corresponding to the eight *B. napus* genes sequenced here, which will facilitate further investigations into the basis for the *LIP* mutation.

6.3 Chapter 3

In Chapter 3, the genera *Populus* and *Eucalyptus*, important as pulp and paper crops (and in the future potentially important as bioenergy crops), were investigated. These are also genera that show leaf heteromorphism between species in the genus and within a single individual. This heteromorphism corresponds to differences in leaf morphology that are likely due to differences in gene expression of dorsiventral polarity genes. Candidate genes for these differences therefore include those belonging to the *YABBY* and *KANADI* gene families, which in *Arabidopsis* determine the abaxial domain, and the *HD-ZIPIII* gene family, which sets the complementary adaxial domain. I determined the orthologous genes from these gene families in poplar and eucalyptus. The general trend observed was a 2:1 ratio of poplar to *Arabidopsis* orthologs and a 1:1 ratio of eucalyptus genes compared to *Arabidopsis*. These results are consistent with a previously described whole genome duplication event in poplar.

mRNA-seq transcriptome data was analyzed for poplar and eucalyptus to identify gene(s) of each of the determined orthologs that may be important to leaf function. My results showed that one paralog of each of the *ATS* and *YAB2* orthologs had expression that differed from previous *Arabidopsis* results. This difference may possibly suggest a different function in both poplar and eucalyptus leaves that may not be present in *Arabidopsis* leaves.

6.4 Chapter 4

In Chapter 4, in order to investigate the evolution of leaf traits in poplar, I investigated the phylogenetic relationships among the North American *Populus* species. Maximum likelihood phylogenies were reconstructed based on six nuclear genes sequenced

from each of the ten species studied. Although the initial intent was to include three representatives of each species within each gene tree, this was not possible due to poor sequence quality following preliminary sequence analysis. This study was, therefore, largely preliminary and allowed the identification of similarities and differences in species placement in relation to the published literature. The major discrepancy observed was the placement of *Populus guzmantlensis* within section *Abaso* as the sister group of *P. mexicana*. This was unexpected, as *P. guzmantlensis* has been reported to belong to section *Populus*.

The genus has leaves with two basic types of morphology: bifacial and isobilateral. This study further investigated the morphological and anatomical characteristics of the North American poplars (with the exception of the Mexican species: *P. mexicana* and *P. guzmantlensis*). According to the results, the grouping of species within its section was consistent with the type of leaf that the species contained. In other words, each section consisted of species that had either bifacial or isobilateral leaves, but not both.

Leaf type was then accessed for the resulting six phylogenies in order to draw inference as to which leaf character (bifacial or isobilateral) can be considered as ancestral. Section *Tacamahaca* is the only one investigated that contains bifacial leaves. None of the phylogenetic trees produced showed the placement of this section as sister to the rest of the poplars. It is more parsimonious to assume that the bifacial leaf is more derived, in comparison to isobilateral leaves.

6.5 Chapter 5

The final data-based chapter of this thesis examined the molecular genetic basis of the abaxial greening and unifacial petiole phenotypes of isobilateral leaves in poplar. Isobilateral

leaves of *Populus tremula* x *tremuloides* (hybrid aspen) were compared to the bifacial-leaved *P. trichocarpa* (black cottonwood) on the basis of morphology, anatomy, and gene expression levels of genes of interest.

Genes responsible for setting dorsiventral polarity in *Arabidopsis* were identified in poplar and were used here as candidates to test for differences in gene expression between the two poplar species. Experiments were performed to narrow down the initially chosen 84 candidate genes. These included transcriptome data analysis and RT-PCR. Final qRT-PCR experiments were also performed on 17 genes. These genes were chosen based on differential expression from transcriptome data and either significantly higher expression level in hybrid aspen blade tissues or the lack of detectable expression in hybrid aspen petioles.

It was predicted that hybrid aspen would have an upregulation of some adaxial genes, in comparison to black cottonwood, due to the presence of adaxial palisade mesophyll in the abaxial surface of the leaf blade. Some adaxial identity genes had significantly higher transcript abundance in hybrid aspen blades, including *Pt-AE7.2, Pt-AS2.1, Pt-AS2.2, Pt-RDR6.1, Pt-RDR6.2,* and *Pt-AGO1.2*. Contrary to what was expected, some abaxial identity genes were also upregulated, including *Pt-ATS.2, Pt-YAB3.2, Pt-ZPR3.1, Pt-ZPR3.2,* and *Pt-AGO1.2*.

Finally, it was predicted that there would be effectively no expression of adaxial surface identity genes in hybrid aspen petioles due to the absence of this surface. This was not observed in any of the genes tested with qRT-PCR. It is possible that the lack of detectable differential expression in the petiole is due to anatomical similarities between hybrid aspen and black cottonwood, which as not obvious at the morphological level.

6.6 Future directions

As with the majority of research, one can never "finish" a project, as there are always new questions that can be asked on the basis of the current findings and the new techniques that become available. Adaxial-abaxial leaf polarity determination is important to learning the molecular genetic basis of leaf development. Most of our knowledge is based on *Arabidopsis*, it is therefore extremely important to study other non-model systems that exhibit natural dorsiventral polarity variation. Studying the morphology and anatomy of such species is an important step and should not be omitted, as this elucidates the differences between these and model systems. Hypotheses about genetic mechanisms for such leaf morphologies can then be made.

As next-generation sequencing becomes more accessible and cheaper (Harrison and Kidner 2011), it will become easier to sequence the genome or transcriptome of any of the species exhibiting dorsiventral polarity variation. This will allow the determination of the *LIP* mutation through a comparison of mutant and wild type plant transcriptomes. We can anticipate that all of the *HD-ZIPIII* genes in *B. napus* will be sequenced and characterized in such studies and that it will be much easier to identify whether a particular gene contains the mutation causing adaxialization of leaves in *LIP* mutants.

Whole-genome sequencing can also be used for inferring poplar species phylogeny. Although a phylogeny based on such a large amount of data has never been attempted, at least in poplar, it would eliminate biases seen from single gene trees. Rather than comparing species based on histories of genes sequenced, one would be comparing species relationships as a whole.

Expression levels can also be obtained from transcriptome sequencing. This will be

useful when determining genes that have contributing factors to or indicative of a specific tissues type (e.g., leaves). Transcriptome sequencing could also be crucial to determining phenotypic variation seen between species, such as abaxial greening and unifacial petiole phenotypes in isobilateral leaves (e.g., hybrid aspen). Rather than using the candidate gene approach, as done here, the genes expressed within a specific tissue type would be detected and characterized. This would allow the comparison of leaf blades between bifacial and isobilateral species, and the comparison between radial and mediolaterally flattened petioles. Transcriptome analysis of a developmental series in these species would also be important for determining the patterns of genes underlying these phenotypes of interest in poplar. Any slight differences would be detected in genes involved in dorsiventral polarity, or in genes that have completely different known or unknown function(s) that could have not been chosen if using a candidate gene approach.

6.7 Concluding remarks

The work presented in this thesis is novel and provides a significant contribution to the field of abaxial-adaxial patterning and to biology of *Populus*. With the exception of *Juncus*, there has not been a published link between molecular studies of dorsiventral polarity mutants of *Arabidopsis* and species with similar leaf phenotypes found in nature. Although functional studies are necessary, it is important to first realize that this link can be made. The study of a novel dorsiventral polarity mutant in canola provides and example of how this link can be applied to either newly discovered mutants in non-model systems or to such phenotypes in naturally occurring systems. The phylogeny of the genus *Populus* is difficult to resolve. There has not been a previously published molecular phylogeny that has included *P.*

guzmantlensis and I showed that it may not belong to the section that it has been previously assigned. Leaf heteromorphism in *Populus* has not been extensively investigated, nor the ancestral leaf character state. I showed that bifacial leaves are probably derived within the genus, which may be unexpected as the sister group to the genus (*Salix*) contains exclusively bifacial leaves. I determined orthologs and transcript levels (in leaf and xylem tissues) of three major gene families and other genes involved in dorsiventral leaf polarity and vegetative phase change in order to try to elucidate gene(s) responsible for the underlying phenotypes of abaxial greening and unifacial petiole in isobilateral leaves. I showed a subset of genes that showed a significantly higher expression in hybrid aspen (isobilateral-leaves species) in comparison to bifacial-leaves black cottonwood. These results provide a framework for future research, which should include functional studies, into the underlying genetic mechanisms of the abaxial greening and unifacial phenotypes in isobilateral leaves.

The aim of this thesis was to investigate adaxial-abaxial patterns in leaves. Although the molecular genetic basis of species with dorsiventral polarity requires further investigation, morphological and anatomical studies should not be forgotten and should be done prior to or in parallel with determining the genetics of these adaxial-abaxial variations. Slight morphological or anatomical differences from model systems can give us clues as to which genes may have variability in expression between species. Further, the molecular genetic basis of dorsiventral polarity needs to be investigated in non-model species, as developmental genetic mechanisms may not be conserved compared to model systems. These investigations can allow us to gain further knowledge about leaf development and ultimately even the genes that have contributed to the evolution of these organs.

References

Abascal, F., R. Zardoya, D. Posada. 2005. ProtTest: Selection of best-fit models of protein evolution. Bioinformatics 21(9): 2104-2105.

Adenot, X., T. Elmayan, D. Lauressergues, S. Boutet, N. Bouche, V. Gasciolli, H. Vaucheret. 2006. DRB4-dependent TAS3 trans-acting siRNAs control leaf morphology through AGO7. Curr Biol 16: 927-932.

Allen, E., Z. Xie, A.M. Gustafson, J.C. Carrington. 2005. microRNAdirected phasing during trans-acting siRNA biogenesis in plants. Cell 121: 207-221.

Alvarez, J., D.R. Smyth. 1999. CRABS CLAW and SPATULA, two Arabidopsis genes that control carpel development in parallel with AGAMOUS. Development 126: 2377-2386.

Arber, A. 1918. The phyllode theory of the monocotyledonous leaf, with species reference to anatomical evidence. Ann Bot 32(4): 465-501.

Arber, A. 1941. On the morphology of the pitcher-leaves in *Heliamphora, Sarracenia, Darlingtonia, Cephalotus*, and *Nepenthes*. Ann Bot 5: 563-578.

Ariel, F.D., P.A. Manavella, C..A. Dezar, R.L. Chan. 2007. The true story of HD-Zip family. Trends in Plant Sci 12(9): 419-426.

Azuma, T., T. Kajita, J. Yokoyama, H. Ohashi. 2000. Phylogenetic relationships of *Salix* (Salicaceae) based on *rbcL* sequence data. Am J Bot 87(1): 67-75.

Bailey, I.W. 1967. Comparative anatomy of the leaf-bearing Cactaceae, XVII. Preliminary observations on the problem of transitions from broad to terete leaves. J Arnold Arboretum 49: 370-376.

Baima, S., F. Nobili, G. Sessa, S. Lucchetti, I. Ruberti, G. Morelli. 1995. The expression of the Athb-8 gene is restricted to provascular cells in Arabidopsis thaliana. Development 121: 4171-4182.

Barnes, B.V. 1975. Phenotypic variation of trembling aspen of western North America. Forest Sci 21: 319-328.

Baum, S.F., Y. Eshed, J.L. Bowman. 2001. The *Arabidopsis* nectary is an ABC-independent floral structure. Development 128: 4657-4667.

Baumberger, N., D.C. Baulcombe. 2005. Arabidopsis ARGONAUTE1 is an RNA Slicer that selectively recruits microRNAs and short interfering RNAs. Proc Natl Acad Sci USA 102: 11928-11933.

Bell, C.D., D. E. Soltis, P. S. Soltis. 2010. The age and diversification of the angiosperms re-revisited. Am J Bot 97(8): 1296-1303.

Biswas, B., C. Pick Kuen, P.M. Gresshoff. 2009. A novel ABA insensitive mutant of *Lotus japonicus* with a wilty phenotype displays unaltered nodulation regulation. Mol Plant 2: 487-399.

Biswas, K. 1932. Bud mutation in *Ficus.* Nature 130: 780.

Biswas, K. 1935. Observations on the systematic position of *Ficus krishnae* growing at the Royal Botanic Garden, Calcutta. Curr Sci 9:424-425.

Bohmert, K., I. Camus, C. Bellini, D. Bouchez, M. Caboche, C. Benning. 1998. AGO1 defines a novel locus of Arabidopsis controlling leaf development. EMBO J 17: 170-180.

Bowman, J.L. 2000. The *YABBY* gene family and abaxial cell fate. Curr Op Plant Biol 3: 17-22.

Bowman, J.L., D.R. Smyth. 1999. CRABS CLAW, a gene that regulates carpel and nectary development in Arabidopsis, encodes a novel protein with zinc finger and helix-loop-helix domains. Development 126: 2387-2396.

Braante, J.H., R.B. Rood, P.E. Heilman. 1996. Life history, ecology, and conservation of riparian cottonwoods in North America. *In* Biology of *Populus* and its implications for management and conservation. Part I, Chapter 3. *Edited by* R.F. Stettler, H.D. Bradshaw, Jr., P.E. Heilman, and T.M. Hinckley. NRC Research Press, National Research Council of Canada, Ottawa, Canada. pp. 57-85.

Bustin, S.A., V. Benes, J.A. Garson, J. Hellemans, J. Huggett, M. Kubista, R. Mueller, T. Nolan, M.W. Pfaffl, G.L. Shipley, J. Vandesompele, C.T. Wittwer. 2009. The MIQE guidelines: minimum information for publication of quantitative real-time PCR experiments. Clinical Chem 55(4): 611-622.

Byrne, M. E., R. Barley, M. Curtis, J.M. Arroyo, M. Dunham, A. Hudson, R.A. Martienssen. 2000. ASYMMETRIC LEAVES1 mediates leaf patterning and stem cell function in Arabidopsis. Nature 408: 967-971.

Byrne, M.E. 2005. Networks in leaf development. Curr Op Plant Biol 8: 59-66.

Carlier, J.D., C.S. Alabaça, N.H. Sousa, P.S. Coelho, A. A. Monteiro, A.H. Paterson, J.M. Leitao. 2011. Physical mapping in a triplicated genome mapping the downy mildew resistance locus Pp523 in *Brassica oleracea* L. Genes, Genomes, and Genetics 1: 593-601.

Cervera, M.T., V. Storme, A. Soto, B. Ivens, M.V. Montagu, O.P. Rajora, W. Boerjan. 2005. Intraspecific and interspecific genetic and phylogenetic relationships in the genus *Populus* based on AFLP markers. TAG Theoretical App Genet 111(7): 1440-1456.

Chase, M., W.S. Zmarzty, M.D. Lledó, K.J. Wurdack, S.M. Swensen, M.F. Fay. 2002. When in doubt, put it in Flacourtiaceae: a molecular phylogenetic analysis based on plastid rbcL DNA sequences. Kew Bulletin 57: 141-181.

Chitwood, D.H., M. Gue, F.T.S. Nogueira, M.C.P. Timmermans. 2007. Establishing leaf polarity: the role of small RNAs and positional signals in the shoot apex. Development 134: 813-823.

Coté, C.L., F. Boileau, V. Roy, M. Ouellet, C. Levasseur, M.-J. Morency, J. E.K. Cooke, A. Séguin, J.J. MacKay. 2010. Gene family structure, expression and functional analysis of HD-Zip III genes in angiosperm and gymnosperm forest trees. BMC Plant Biol 10: 273.

Critchfield, W.B. 1960. Leaf dimorphism in Populus trichocarpa. Am J Bot 47: 699-711.

Cronk, Q.C.B. 2001. Plant evolution and development in a post-genomic context. Nature Rev Genetics 2: 607-619.

Cronk, Q.C.B. 2005. Plant eco-devo: the potential of poplar as a model organism. New Phytol 166 (1): 39-48.

Cronk, Q.C.B. 2009. The molecular organography of plants. Oxford University Press, Oxford.

De Candolle, C. 1897. Sur les phyllomes hypopeltés. Bulletin des Travaux de la Société Botanique de Genève 8: 59-69.

De Candolle, C. 1901. Sur un *Ficus* à hypoascidies. Archives des Sciences Physiques et Naturelles 106: 623-631.

De Candolle, C. 1902. Nouvelles etudes des hypoascidies de *Ficus.* Bulletin de l'Herbier Boissier 2ème série 9: 753-762.

Degenhardt, R.F., P.C. Bonham-Smith. 2008. Arabidopsis ribosomal proteins RPL23aA and RPL23aB are differentially targeted to the nucleolus and are disparately required for normal development. Plant Physiol 147: 128-142.

Degnan, J.H., N.A. Rosengerg. 2009. Gene tree discordance, phylogenetic inference and the multispecies coalescent. Trends Eco Evol 24(6): 332-340.

DeLucia, E.H., K. Nelson, T.C. Vogelmann, W.K. Smith. 1996. Contribution of intercellular reflectance to photosynthesis in shade leaves. Plant Cell Environ 19: 159-170.

Dengler, N., J. Kang. 2001. Vascular patterning and leaf shape. Curr Op Plant Biol 4: 50-56.

Dickinson, T.A. 1978. Epiphylly in angiosperms. Bot Rev 44(2): 181-232.

Dickmann, D.I. 2001. An overview of the genus *Populus*. *In* Poplar Culture in North America. Part A, Chapter 1. *Edited by* D.I. Dickmann, J.G. Isebrands, J.E. Eckenwalder, and J. Richardson. NRC Research Press, National Research Council of Canada, Ottawa, Canada. pp. 1-42.

Doyle, J.J., Doyle, J.L. 1987. A rapid DNA isolation procedure for small quantities of fresh leaf tissue. Phytochemical Bulletin 19: 11-15.

Du, J., E. Miura, M. Robischon, C. Martinez, A. Groover. 2011. The *Populus* class III HD ZIP transcription factor *POPCORONA* affects cell differentiation during secondary growth of woody stems. PLoS ONE 6(2): e17458.

Dupuy, P., M. Guédès. 1979. Hypoascidiate bracts in *Pelargonium.* Bot J Linn Soc 78: 117-121.

Eckardt, N.A. 2007. Positive and negative feedback coordinate regulation of disease resistance gene expression. Plant Cell 19: 2700-2702.

Eckenwalder, J.E. 1977a. North American cottonwoods (*Populus*, Salicaceae) of sections *Abaso* and *Aigeiros*. J Arnold Arbor Harv Univ 58: 193-208.

Eckenwalder, J.E. 1977b. Systematics of *Populus* L. (Salicaceae) in southwestern North America with special reference to sect. *Aigeiros* Duby. Ph.D. Thesis, University of California, Berkeley, CA.

Eckenwalder, J.E. 1980. Foliar heteromorphism in *Populus* (Salicaceae), a source of confusion in the taxonomy of Tertiary leaf remains. Syst Bot 5: 366-383.

Eckenwalder, J.E. 1996a. Taxonomic signal and noise in multivariate interpopulational relationships in *Populus mexicana* (Salicaceae). Syst Bot 21: 261-271.

Eckenwalder, J.E. 1996b. Systematics and evolution of *Populus*. *In* Biology of *Populus* and its implications for management and conservation. Part I, Chapter 1. *Edited by* R.F. Stettler, H.D. Bradshaw, Jr., P.E. Heilman, and T.M. Hinckley. NRC Research Press, National Research Council of Canada, Ottawa, Canada. pp. 7-32.

Edgar, R.C. 2004. MUSCLE: multiple sequence alignment with high accuracy and high throughput. Nucleic Acids Res. 32(5): 1792-1797.

Emery, J.F., S.K. Floyd, J. Alvarez, Y. Eshed, N.P. Hawker, A. Izhaki, S.F. Baum, J.L. Bowman. 2003. Radial patterning of *Arabidopsis* shoots by class III HD-ZIP and *KANADI* genes. Curr Biol 13: 1768-1774.

Eshed, Y., S.F. Baum, J.V. Perea, J.L. Bowman. 2001. Establishment of polarity in lateral organs of plants. Curr Biol 11: 1251–1260.

Eshed, Y., A. Izhaki, S.F. Baum, S.K. Floyd, J.L. Bowman. 2004. Asymmetric leaf development and blade expansion in Arabidopsis are mediated by *KANADI* and *YABBY* activities. Development 131: 2997–3006.

Fahlgren, N., T.A. Montgomery, M.D. Howell, E. Allen, S.K. Dvorak, A.L. Alexander, J.C. Carrington. 2006. Regulation of AUXIN RESPONSE FACTOR3 by TAS3 ta-siRNA affects developmental timing and patterning in Arabidopsis. Curr Biol 16: 939-944.

Felsenstein, J. 1989. PHYLIP - Phylogeny Inference Package (Version 3.2). Cladistics 5: 164-166.

Felsenstein, J. 2005. PHYLIP (Phylogeny Inference Package) version 3.6. Distributed by the author. Department of Genome Sciences, University of Washington, Seattle.

Flagel, L.E., J.F. Wendel. 2009. Gene duplication and evolutionary novelty in plants. New Phytol 183: 557-564.

Floyd, S.K., J.L. Bowman. 2007. The ancestral developmental tool kit of land plants. Int J Plant Sci 168: 1-35.

Floyd, S.K., J.L. Bowman. 2010. Gene expression patterns in seed plant shoot meristems and leaves: homoplasy or homology? J Plant Res 123(1): 43-55.

Franck, D.H. 1976. The morphological interpretation of epiascidiate leaves: an historical perspective. Bot Rev 42(3): 345-387.

Fuchs, C. 1963. Fuchsin staining with NaOH clearing for lignified elements of whole plants or plant organs. Stain Technology 38: 141-144.

Gao, P., X. Li, D. Cui, L. Wu, I. Parkin, M.Y. Gruber. 2010. A new dominant Arabidopsis transparent testa mutant, *sk21-D*, and modulation of seed flavonoid biosynthesis by *KAN4*. Plant Biotechnol J 8(9): 979-993.

Geraldes, A., J. Pang, N. Thiessen, T. Cezard, R. Moore, Y. Zhao, A. Tam, S. Wang, M. Friedmann, I. Birol, S.J.M. Jones, Q.C.B. Cronk, C.J. Douglas. 2011. SNP discovery in black cottonwood (*Populus trichocarpa*) by population transcriptome resequencing. Mol Ecol Res 11: 81-92.

Givnish, T.J. 1979. On the adaptive significance of leaf form. *In* Topics in Plant Population Biology. *Edited by* O.T. Solbrig, S. Jain, G.B. Johnson, P.H. Raven. Columbia University Press, New York, NY.

Gleissberg, S., E.P. Groot, M. Schmalz, M. Eichert, A. Kolsch, S. Hutter. 2005. Developmental events leading to peltate leaf structure in *Tropaeolum majus* (Tropaeolaceae) are associated with expression domain changes of a *YABBY* gene. Dev Genes Evol 215: 313-319.

Gómez-Campo, C., S. Prakash. 1999. Origin and domestication. In *Biology of Brassica Coenospecies*. Edited by Gomez-Campo C. Elsevier, Amsterdam.

Goodstein, D.M., S. Shu, R. Howson, R. Neupane, R.D. Hayes, J. Fazo, T. Mitros, W. Dirks, U. Hellsten, N. Putnam, D.S. Rokhsar. 2011. Phytozome: a comparative platform for green plant genomics. Nucleic Acids Res 40: D1178-D1186.

Green, K.A., M.J. Prigge, R.B. Katzman, S.E. Clark. 2005. CORONA, a member of the class III homeodomain leucine zipper gene family in Arabidopsis, regulates stem cell specification and organogenesis. Plant Cell 17(3): 691-704.

Greene, E.A., C.A. Codomo, N.E. Taylor, J.G. Henikoff, B.J. Till, S.H. Reynolds, L.C. Enns, C. Burtner, J.E. Johnson, A.R. Odden, L. Comai, S. Henikoff. 2003. Spectrum of chemically induced mutations from a large-scale reverse-genetic screen in Arabidopsis. Genetics 164: 731-740.

Guindon, S., O. Gascuel. 2003. A simple, fast, and accurate algorithm to estimate large phylogenies by maximum likelihood. Syst Biol 52: 696-704.

Golz, J.F., M. Roccaro, R. Kuzoff, A. Hudson. 2004. GRAMINIFOLIA promotes growth and polarity of Antirrhinum leaves. Development 131: 3661–3670.

Hagemann, W. 1984. Morphological aspects of leaf development in ferns and angiosperms. *In* Contemporary problems in plant anatomy. *Edited by*. R. A. White and W. C. Dickison. Academic Press, Orlando, USA. pp. 301-349.

Hake, S., N. Ori. 2002. Plant morphogenesis and *KNOX* genes. Nat Genet 31: 121-122.

Hake, S., H.M.S. Smith, H. Holtan, E. Magnani, G. Mele, J. Ramirez. 2004. The role of *KNOX* genes in plant development. Annu Rev Cell Dev Biol 20: 125-151.

Hamzeh, M., S. Dayanandan 2004. Phylogeny of *Populus* (Salicaceae) based on nucleotide sequences of chloroplast *trnT– trnF* region and nuclear rDNA. Am J Bot 91(9): 1398-1408.

Hamzeh, M., P. Perinet, S. Dayanandan. 2006. Genetic relationships among species of *Populus* (Salicaceae) based on nuclear genomic data. J Torr Bot Soc 133(4): 519-527.

Harrison, N., C.A. Kidner. 2011. Next-generation sequencing and systematics: What can a billion base pairs of DNA sequence data do for you? Taxon 60(6): 1552-1566.

Hay, A., M. Tsiantis. 2010. KNOX genes: versatile regulators of plant development and diversity. Development 137: 3153-3165.

Hinchee, M., W. Rottmann, L. Mullinax, C. Zhang, S. Chang, M. Cunningham, L. Pearson, N. Nehra. 2009. Short-rotation woody crops for bioenergy and biofuels applications. In Vitro Cell Dev Biol - Plant 45: 619-629.

Hong, C.P., S.-J. Kwon, J.S. Kim, T.-J. Yang, B.-S. Park, Y.P. Lim. 2008. Progress in understanding and sequencing the genome of *Brassica rapa*. International Journal of Plant Genomics Volume 2008, Article ID 582837, 9 pages.

Hsu, C.-Y., J.P. Adams, H. Kim, et al. 2011. *FLOWERING LOCUS T* duplication coordinates reproductive and vegetative growth in perennial poplar. PNAS 108(26): 10756-10761.

Hunter, C., H. Sun, R.S. Poethig. 2003. The Arabidopsis heterochronic gene ZIPPY is an ARGONAUTE family member. Curr Biol 13: 1734 -1739.

Hunter, C., M.R. Willmann, G. Wu, M. Yoshikawa, M. de la Luz Gutierrez-Nava, S.R. Poethig. 2006. Trans-acting siRNA-mediated repression of ETTIN and ARF4 regulates heteroblasty in Arabidopsis. Development 133: 2973-2981.

Husbands, A.Y., D.H. Chitwood, Y. Plavskin, M.C.P. Timmermans. 2009. Signals and prepatterns: new insights into organ polarity in plants. Genes and Development 23: 1986-1997.

Ishikawa, M. , Y. Ohmori, W. Tanaka, C. Hirabatashi, K. Murai, Y. Ogihara, T. Yamaguchi, H.-Y. Hirano. 2009. The expression patterns of *DROOPING LEAF* orthologs suggest a conserved function in grasses. Genes Genetic Systems 84: 137-146.

Iwakawa, H., Y. Ueno, E. Semiarti, H. Onouchi, S. Kojima, H. Tsukaya, M. Hasebe, T. Soma, M. Ikezaki, C. Machida, et al. 2002. The ASYMMETRIC LEAVES 2 gene of Arabidopsis thaliana, required for formation of a symmetric flat leaf lamina, encodes a member of a novel family of proteins characterized by cysteine repeats and a leucine zipper. Plant Cell Physiol 43: 467-478.

Iwakawa, H., M. Iwasaki, S. Kojima, Y. Ueno, T. Soma, H. Tanaka, E. Smiarti, Y. Machida, C. Machida. 2007. Expression of the *ASYMMETRIC LEAVES2* gene in the adaxial domain of Arabidopsis leaves represses cell proliferation in this domain and is critical for the development of properly expanded leaves. Plant J 51(2): 173-184.

Izhaki, A., J.L. Bowman. 2007. *KANADI* and class III HD-Zip gene families regulate embryo patterning and modulate auxin flow during embryogenesis in *Arabidopsis*. Plant Cell 19(2): 495-508.

James, S.A., D.T. Bell. 2001. Leaf morphological and anatomical characteristics of heteroblastic *Eucalyptus globulus* ssp. *globulus* (Myrtaceae). Aust J Bot 49: 259-269.

Jaillon, O., J.-M. Aury, B. Noel, et al. 2007. The grapevine genome sequence suggests ancestral hexaploidization in major angiosperm phyla. Nature 449: 463-467.

Jansson, S., C.J. Douglas. 2007. *Populus*: a model system for plant biology. Ann Rev Plant Biol 58: 435-458.

Juarez, M.T., R.W. Twigg, M.C.P. Timmermans. 2004. Specification of adaxial cell fate during maize development. *Development* 131: 4533-4544.

Jung, J.-H., C.-M. Park. 2007. *MIR166/165* genes exhibit dynamic expression patterns in regulating shoot apical meristem and floral development in *Arabidopsis*. Planta 225: 1327-1338.

Kang, J., J. Tang, P. Donnelly, N. Dengler. 2003. Primary vascular pattern and expression of *ATHB8* in shoots of *Arabidopsis*. New Phytologist 158: 443-454.

Kaplan, D.R. 1997. Principles of Plant Morphology. Vol 3. Odin Readers, Berkeley, California.

Kelley, D.R., D.J. Skinner, C.S. Gasser. 2009. Roles of polarity determinants in ovule development. Plant J 57: 1054-1064.

Kerstetter, R.A., K. Bollman, R.A. Taylor, K. Bomblies, R.S. Poethig. 2001. *KANADI* regulates organ polarity in Arabidopsis. Nature 411: 706–709.

Kidner, C. A., R.A. Martienssen. 2004. Spatially restricted microRNA directs leaf polarity through ARGONAUTE1. Nature 428: 81-84.

Kidner, C.A., M.C.P. Timmermans. 2007. Mixing and matching pathways in leaf polarity. Curr Op Plant Biol 10: 13-20.

Kidner, C.A., M.C. Timmermans. 2010. Signaling sides: adaxial-abaxial patterning in leaves. Curr Topics Dev Biol 91:141-168.

Kim, M., S. McCormick, M. Timmermans, N. Sinha. 2003. The expression domain of PHANTASTICA determines leaflet placement in compound leaves. Nature 424: 438-443.

Kim, Y.S., S.G. Kim, M. Lee, et al. 2008. HD-ZIP III activity is modulated by competitive inhibitors via a feedback loop in Arabidopsis shoot apical meristem development. Plant Cell 20: 920-933.

King, D.A. 1997. The functional significance of leaf angle in *Eucalyptus*. Australian J Bot 45(4): 619-639.

Ko, J.H., C. Prassinos, K.H. Han. Developmental and seasonal expression of PtaHB1, a Populus gene encoding a class III HD-Zip protein, is closely associated with secondary growth and inversely correlated with the level of microRNA (miR166). New Phytol 169: 469-478.

Kojima, S., M. Iwasaki, H. Takahashi, T. Imai, Y. Matsumura, D. Fleury, M.V. Lijsebettens, Y. Machida, C. Machida. 2011. ASYMMERTIC LEAVES2 and elongator, a histone acetyltransferase complex, mediate the extablishment ofpolarity in leaves of *Arabidopsis thaliana.* Plant Cell Physiol 52(8): 1259-1273.

Lagercrantz, U. 1998. Comparative mapping between *Arabidopsis thaliana* and *Brassica nigra* indicates that *Brassica* genomes have evolved through extensive genome replication accompanied by chromosome fusions and frequent rearrangements. Genetics 150: 1217-1228.

Leskinen, E., C. Alstrom-Rapaport. 1999. Molecular phylogeny of Salicaceae and closely related Flacourtiaceae: evidence from *5.8S, ITS1* and *ITS2* of the rDNA. Plant Syst Evol 215: 209-227.

Levsen, N.D., P. Tiffin, M.S. Olson. 2012. Pleistocene speciation in the genus *Populus* (Salicaceae). Syst Biol 61(3): 401-412.

Lev-Yadun, S. 2010. Plant fibers: initiation, growth, model plants, and open questions. Russian J Plant Physiol 57(3): 305-315.

Li, S., X. Yang, F. Wu, Y. He. 2012. HYL1 controls the miR156-mediated juvenile phase of vegetative growth. J Exp Bot 63(7): 2787-2798.

Lin, W.C., B. Shuai, P.S. Springer. 2003. The Arabidopsis LATERAL ORGAN BOUNDARIES-domain gene ASYMMETRIC LEAVES2 functions in the repression of KNOX gene expression and in adaxial-abaxial patterning. Plant Cell 15: 2241-2252.

Liu, Q., X. Yao, L. Pi, H. Wang, X. Cui, H. Huang. 2008. The ARGONAUTE10 gene modulates shoot apical meristem maintenance and leaf polarity establishment by repressing miR165/166 in *Arabidopsis*. Plant J 58: 27–40.

Liu, K., S. Raghavan, S. Nelesen, C. R. Linder, T. Warnow. 2009. Rapid and accurate large scale coestimation of sequence alignments and phylogenetic trees. Science 324(5934): 1561-1564.

Long, J., E. Moan, J. Medford, M. Barton. 1996. A member of the KNOTTED class of homeodomain proteins encoded by the *STM* gene of *Arabidopsis*. Nature 379: 66-69.

Lukens, L.N., P.A. Quijada, J. Udall, J.C. Pires, M.E. Schranz, T.C. Osborn. 2004. Genome redundancy and plasticity within ancient and recent *Brassica* crop species. Biol J of the Linn Soc 82: 665-674.

Lynn, K., A. Fernandez, M. Aida, J. Sedbrook, M. Tasaka, P. Masson, M.K. Barton. 1999. The PINHEAD/ZWILLE gene acts pleiotropically in *Arabidopsis* development and has overlapping functions with the ARGONAUTE1 gene. Development 126: 469–481.

Lysak, M.A., M.A. Koch, A. Pecinka, I. Schubert. 2005. Chromosome triplication found across the tribe Brassicaceae. Genome Res 15: 516-525.

Lysak, M.A., K. Cheung, M. Kitschke, P. Bures, 2007. Ancestral chromosomal blocks are triplicated in Brassicaceae species with varying chromosome number and genome size. Plant Physiol 145: 402-410.

Manchester, S.R., D.L. Dilcher, W.D. Tidwell. 1986. Interconnected reproductive and vegetative remains of *Populus* (Salicaceae) from the middle Eocene Green river formation, Northeastern Utah. Am J Bot 73(1): 156-160.

Mallory, A.C., A. Hinze, M.R. Tucker, N. Bouché, V. Gasciolli, T. Elmayan, D. Lauressergues, V. Jauvion, H. Vaucheret, T. Laux. 2009. Redundant and Specific Roles of the ARGONAUTE Proteins AGO1 and ZLL in Development and Small RNA-Directed Gene Silencing. PLoS Genet 5(9): e1000646.

Mano, E., G. Horiguchi, H. Tsukaya. 2006. Gravitropism in leaves of *Arabidopsis thaliana* (L.) Heynh. Plant Cell Physiol 47(2): 217-223.

Mauseth, J.D. 2007. Tiny but complex foliage leaves occur in many “leafless” cacti (Cactaceae). Int J Plant Sci 168(6): 845-853.

McAbee, J.M., T.A. Hill, D.J. Skinner, A. Izhaki, B.A. Hauser, R.J. Meister, G.V. Reddy, E.K. Meyerowitz, J.L. Bowman, C.S. Gasser. 2006. *ABERRANT TESTA SHAPE* encodes a *KANADI* family member, linking polarity determination to separation and growth of Arabidopsis ovule integuments. Plant J 46: 522-531.

McConnell, J.R., M.K. Barton. 1998. Leaf polarity and meristem formation in *Arabidopsis*. Development 125: 2935-2942.

McConnell, J.R., J. Emery, Y. Eshed, N. Bao, J. Bowman, M.K. Barton. 2001. Role of *PHABULOSA* and *PHAVOLUTA* in determining radial patterning in shoots. Nature 411: 709-713.

Mizrachi, E., C.A. Hefer, M. Ranik, F. Joubert, A.A. Myburg. 2010. *De novo* assembled expressed gene catalog of a fast-growing *Eucalyptus* tree produced by Illumina mRNA-Seq. BMC Genomics 11: 681.

Moon, J., S. Hake. 2011. How a leaf gets its shape. Curr Op Plant Biol 14:24-30.

Moore, M. J., P. S. Soltis, C. D. Bell, J. G. Burleigh, D. E. Soltis. 2010. Phylogenetic analysis of 83 plastid genes further resolves the early diversification of eudicots. PNAS 107(10): 4623-4628.

Moore, R.C., M.D. Purugganan. 2005. The evolutionary dynamics of plant duplicate genes. Curr Op Plant Biol 8: 122-128.

Mortazavi, A., B.A. Williams, K. McCue, L. Schaeffer, B. Wold. 2008. Mapping and quantifying mammalian transcriptomes by RNA-Seq. Nat Methods 5: 621-681.

Moussian, B., H. Schoof, A. Haecker, G. Jurgens, T. Laux. 1998. Role of the ZWILLE gene in the regulation of central shoot meristem cell fate during *Arabidopsis* embryogenesis. EMBO J 17: 1799–1809.

Mun, J.-H., S.-J. Kwon, T.-J. Yang, Y.-J. Seol, M. Jin, J.-A Kim, M.-H. Lim, J.S. Kim, S. Baek, B.-S. Choi, H.-J. Yu, D.-S. Kim, N. Kim, K.-B. Lim, S.-I. Lee, J.-H. Hahn, Y.P. Lim, I. Bancroft, B.-S. Park. 2009. Genome-wide comparative analysis of the *Brassica rapa* gene space reveals genome shrinkage and differential loss of duplicated genes after whole genome triplication. Genome Biology 10(10): R111.

Myburg, A.A., D. Grattapaglia, G.A. Tuskan, J. Schmutz, K. Barry, J. Bristow. 2008. The Eucalyptus genome network: Sequencing the *Eucalyptus* genome: Genomic resources for renewable energy and fiber production. Plant and Animal Genome XVI Conference: January 12-16, 2008, San Diego, CA.

Myburg, A., D. Grattapaglia, G.A. Tuskan. 2012. Sequencing and analysis of the *Eucalyptus grandis* genome. Plant and Animal Genome XX Conference: January 14-18, 2012, San Diego, CA.

Nowak, J., N.G. Dengler, and U. Posluszny. 2007. The role of abscission during leaflet separation in *Chamaedorea elegans* (Arecaceae). Int J Plant Sci 168(5): 533-545.

Ochando, I., S. Jover-Gil, J.J. Ripoll, H. Candela, A. Vera, M.R. Ponce, A. Martinez-Laborda, J.L. Micol. 2006. Mutations in the microRNA complementarity site of the INCURVATA4 gene perturb meristem function and adaxialize lateral organs in Arabidopsis. Plant Physiol 141: 607–619.

Ogburn, R.M., E.J. Edwards. 2009. Anatomical variation in Cactaceae and relatives: trait lability and evolutionary innovation. Am J Bot 96(2): 391-408.

Ori, N., Y. Eshed, G. Chuck, J.L. Bowman, S. Hake. 2000. Mechanisms that control knox gene expression in the Arabidopsis shoot. Development 127: 5523-5532.

Otsuga, D., B. DeGuzman, M.J. Prigge, G.N. Drews, S.E. Clark. 2001. *REVOLUTA* regulates meristem initiation at lateral positions. Plant J 25(2): 223-236.

Parkin, I.A.P., A.G. Sharpe, D.J. Lydiate. 2003. Patterns of genome duplication within the *Brassica napus* genome. Genome 46: 291–303.

Pekker, I., J.P. Alvarez, Y. Eshed. 2005. Auxin response factors mediate Arabidopsis organ asymmetry via modulation of *KANADI* activity. Plant Cell 17: 2899-2910.

Peragine, A., M. Yoshikawa, G. Wu, H.L. Albrecht, R.S. Poethig. 2004. SGS3 and SGS2/SDE1/RDR6 are required for juvenile development and the production of trans-acting siRNAs in Arabidopsis. Genes Dev 18: 2368-2379.

Pfaffl, M.W. 2004. Relative quantification. *In* Real-time PCR. *Edited by* T. Dorak. International University Line. pp. 63-82.

Poethig, R.S. 2010. The past, present, and future of vegetative phase change. Plant Physiol 154(2): 541-544.

Posada, D. 2008. jModelTest: phylogenetic model averaging. Mol Biol Evol 25:1253-1256.

Prain, D. 1906. *Ficus Krishnae.* Curtis's Bot. Mag. 4th Series 132: tab. 8092.

Prigge, M.J., D. Otsuga, J.M. Alonso, J.R. Ecker, G.N. Drews, S.E. Clark. 2005. Class III homeodomain-leucine zipper gene family members have overlapping, antagonistic, and distinct roles in Arabidopsis development. Plant Cell 17: 61-76.

Puri, G.S. 1946. Further observations on the systematic position of *Ficus Krishnae* C. de Candolle. J Royal Asiatic Soc Bengal 12: 7-12.

Ralph, S., C. Oddy, D. Cooper, H. Yueh, S. Jancsik, N. Kolosova, R.N. Philippe, D. Aeschliman, R. White, D. Huber, et al. 2006. Genomics of hybrid poplar (*Populus trichocarpa* x *deltoides*) interacting with forest tent caterpillars (*Malacosoma disstria*): normalized and full-length cDNA libraries, expressed sequence tags, and a cDNA microarray for the study of insect-induced defences in poplar. Mol Ecol 15: 1275–1297.

Reinhardt, D., M. Frenz, T. Mandel, C. Kuhlemeier. 2005. Microsurgical and laser ablation analysis of leaf positioning and dorsoventral patterning in tomato. Development 132: 15-26.

Rhoades, M.W., B.J. Reinhart, L.P. Lim, C.B. Burge, B. Bartel, D.P. Bartel. 2002. Prediction of plant microRNA targets. Cell 110(4): 513-520.

Rindal, E., A.V.Z. Brower. 2011. Do model-based phylogenetic analyses perform better than parsimony? A test with empirical data. Cladistics 27(3): 331-334.

Robischon, M., J. Du, E. Miura, A. Groover. 2011. The *Populus* class III HD ZIP, *popREVOLUTA*, influences cambium initiation and patterning of woody stems. Plant Physiol 155: 1214-1225.

Roden, J.S., R.W. Pearcy. 1993a. Effect of leaf flutter on the light environment in poplars. Oecologia 93(2): 201-207.

Roden, J.S., R.W. Pearcy. 1993b. The effect of leaf flutter on the flux of CO_2 in poplar leaves. Functional Ecol 7(6): 669-675.

Roden, J.S., R.W. Pearcy. 1993c. Photosynthetic gas exchange response of poplars to steady-state and dynamic light environments. Oecologia 93(2): 208-214.

Rodgers-Melnick, E., S.P. Mane, P. Dharmawardhana, G.T. Slavov, O.R. Crasta, S.H. Strauss, A.M. Brunner, S.P. DiFazio. 2012. Contrasting patterns of evolution following whole genome versus tandem duplication events in *Populus*. Genome Res 22: 95-105.

Rozen, S., H.J. Skaletsky. 2000. Primer3 on the WWW for general users and for biologist programmers. *In:* Bioinformatics Methods and Protocols: Methods in Molecular Biology. *Edited by:* S. Krawetz and S. Misener. Humana Press, Totowa, NJ, pp 365-386.

Rudall, P. 1990. Comparative leaf morphogenesis in Iridaceae. Bot Jahrb Syst 112(2): 241-260.

Rudall, P.J., R.M. Bateman. 2004. Evolution of zygomorphy in monocot flowers: iterative patterns and developmental constraints. New Phytol 162(1): 25-44.

Rudall, P.J., and M. Buzgo. 2002. Evolutionary history of the monocot leaf. *In* Developmental Genetics and Plant Evolution. *Edited by:* Q.C.B. Cronk, R.M. Bateman, and J.A. Hawkins. Taylor & Francis, London, pp. 431-458.

Russin, W.A., R.F. Evert. 1984. Studies on the leaf of *Populus deltoides* (Salicaceae): morphology and anatomy. Am J Bot 71(10): 1398-1415.

Sarojam, R., P.G. Sappi, A. Goldshmidt, I. Efroni, S.K. Floyd, Y. Eshed, J.L. Bowman. 2010. Differntiating Arabidopsis shoots from leaves by combined *YABBY* activities. Plant Cell 22: 2113-2130.

Sawa, S., K. Watanabe, K. Goto, Y.G. Liu, D. Shibata, E. Kanaya, E.H. Morita, K. Okada. 1999. FILAMENTOUS FLOWER, a meristem and organ identity gene of Arabidopsis, encodes a protein with a zinc finger and HMG related domains. Genes Dev 13: 1079-1088.

Schmid, M., T.S. Davison, S.R. Henz, U.J. Pape, M. Demar, M. Vingron, B. Scholkopf, D. Weigel, J.U. Lohmann. 2005. A gene expression map of *Arabidopsis thaliana* development. Nat Genet 37: 501-506

Schoof, H., M. Lenhard, A. Haecker, K.F.X. Mayer, G. Jürgens, T. Laux. 2000. The stem cell population of Arabidopsis shoot meristems is maintained by a regulatory loop between the CLAVATA and WUSCHEL genes. Cell 100(6): 635-644.

Siegfried, K.R., Y. Eshed, S.F. Baum, D. Otsuga, D.N. Drews, J.L. Bowman. 1999. Members of the *YABBY* gene family specify abaxial cell fate in Arabidopsis. Development 128: 4117–4128.

Shulaev, V., D.J. Sargent, R.N. Crowhurst, et al. 2011. The genome of woodland strawberry (*Fragaria vesca*). Nature Genet 43: 109-116.

Sinha, N. 1999. Leaf development in angiosperms. Annu Rev Plant Physiol Plant Mol Biol 50:419-446.

Slavov, G. T., P. Zhelev. 2010. Salient biological features, systematics, and genetic variation of Populus, *In* Genetics and Genomics of Populus, *Edited by* S. Jansson, R. Bhalerao and A. T. Groover, Springer, NY. pp. 15–38.

Smith, R.L. 1988. Phylogenetics of *Populus* L. (Salicaceae) based on restriction site fragment analysis of cpDNA. M.Sc. Thesis, University of Wisconsin, Maddison, WI.

Smith, R.L., K.J. Sytsma. 1990. Evolution of *Populus nigra* (sect. *Aigeiros*): introgressive hybridization and the chloroplast contribution of *Populus alba* (sect. *Populus*). Am J Bot 77: 1176-1187.

Soltis, D. E., M. J. Moore, J. G. Burleigh, C. D. Bell, P. S. Soltis. 2010. Assembling the angiosperm tree of life: progress and future prospects. Ann Miss Bot Garden 97(4): 514-526.

Stamatakis, A., M. Ott, T. Ludwig. 2005. RAxML-OMP: An Efficient Program for Phylogenetic Inference on SMPs. *In* Proceedings of 8th International Conference on Parallel Computing Technologies (PaCT2005), Volume 3606 of Lecture Notes in Computer Science, Springer Verlag. pp. 288-302.

Sterck, L., S. Rombauts, S. Jansson, F. Sterky, P. Rouze, Y.V. de Peer. 2005. EST data suggest that poplar is an ancient polyploid. New Phytol 167: 165-170.

Stevens, P.F. 2010. Angiosperm phylogeny Website. Version 10, July 2009. http://www.mobot.org/MOBOT/research/APweb/. [APG]

Street, N.R., A. Sjodin, M. Bylesjo, P. Gustafsson, J. Trygg, S. Jansson. 2008. A cross-species transcriptomics approach to identify genes involved in leaf development. BMC Genomics 9: 589.

Sussex, I. 1951. Experiments on the cause of dorsiventrality in leaves. Nature 167: 651-652.

Sussex, I. 1954. Morphogenesis in *Solanum tuberosum* L.: experimental investigation of leaf dorsiventrality and orientation in the juvenile shoot. Phytomorphology 5: 286-300.

Szakonyi, D., A. Moschopoulos, M.E. Byrne. 2010. Perspectives on leaf dorsoventral polarity. J Plant Res 123: 281-290.

Talbert, P.B., H.T. Adler, D.W. Parks, L. Comai. 1995. The *REVOLUTA* gene is necessary for apical meristem development and for limiting divisions in the leaves and stems of *Arabidopsis thaliana*. Development 121: 2723-2735.

Timmermans, M.C.P., N.P. Schultes, J.P. Jankovsky, T. Nelson. 1998. Leafbladeless1 is required for dorsoventrality of lateral organs in maize. Development 125: 2813-2823.

Tomescu, A.M.F. 2009. Megaphylls, microphylls and the evolution of leaf development. Trends Plant Sci 14: 5-12.

Town, C.D., F. Cheung, R. Maiti, J. Crabtree, B.J. Haas, J.R. Wortman, E.E. Hine, R. Althoff, T.S. Arbogast, L.J. Tallon, M. Vigouroux, M. Trick, I. Bancroft. 2006. Comparative genomics of *Brassica oleracea* and *Arabidopsis thaliana* reveal gene loss, fragmentation, and dispersal after polyploidy. Plant Cell 18: 1348-1359.

Townsley, B.T., N.R. Sinha. 2012. A new development: evolving concepts in leaf ontogeny. Annu Rev Plant Biol 63: 535-562.

Trapnell, C., S.L. Salzberg. 2009. How to map billions of short reads onto genomes. Nature Biotechnol 27: 455-457.

Trapnell, C., B.A. Williams, G. Pertea, A. Mortazavi, G. Kwan, M.J. van Baren, S.L. Salzberg, B.J. Wold, L. Pachter. 2010. Transcript assembly and quantification by RNA-Seq reveals unannotated transcripts and isoform switching during cell differentiation. Nat Biotechnol 28(5): 511-515.

Traub, H.P. 1968. Orientation of vascular bundles in *Allium* leaves. Plant Life 24: 143-146.

Troll, W. 1939. Vergleichende Morphologie der horheren Pflanzen. Band 1: Vegetationsorgane, 1. Teil. Berlin: Borntrager.

Tuskan, G.A., S. DiFazio, S. Jansson, et al. 2006. The genome of black cottonwood, *Populus trichocarpa* (Torr. & Gray). Science 313: 1596-1604.

U, N. 1935. Genome analysis in Brassica with special reference to the experimental formation of *B. napus* and peculiar mode of fertilization. Jpn J Bot 7: 389–452.

Van Volkenburgh, E., G. Tayor. 1996. Leaf growth physiology. *In* Biology of *Populus* and its implications for management and conservation. Part II, Chapter 12. *Edited by* R.F. Stettler, H.D. Bradshaw, Jr., P.E. Heilman, and T.M. Hinckley. NRC Research Press, National Research Council of Canada, Ottawa, Canada. pp 283-299.

Waites, R., A. Hudson. 1995. *phantastica*: a gene required for dorsoventrality of leaves in *Antiffhinum majus*. Development 121: 2143-2154.

Waites, R., H.R.N. Selvadurai, I.R. Oliver, A. Hudson. 1998. The *PHANTASTICA* gene encodes a MYB transcription factor involved in growth and dorsoventrality of lateral organs in *Antirrhinum*. Cell 93: 779-789.

Wang, W., J.J. Esch, S.-H. Shiu, H. Agula, B.M. Binder, C. Chang, S.E. Patterson, A.B. Bleecker. 2006. Identification of important regions for ethylene binding and signaling in the transmembrane domain of the ETR1 ethylene receptor of Arabidopsis. Plant Cell 18: 3429-3442.

Wang, J.W., M.Y. Park, L.-J. Wang, Y. Koo, X.-Y. Chen, D. Weigel, R.S. Poethig. 2011a. MiRNA control of vegetative phase change in trees. PLoS Genet 7(2): e1002012.

Wang, X., H. Wang, J. Wang, et al. (The *Brassica rapa* Genome Sequencing Project Consortium). 2011b. The genome of the mesopolyploid crop species *Brassica rapa*. Nature Genet 43(10):1035-1040.

Welsh, M. 2009. Evolution and systematic significance of reproductive structures in the genus *Cuscata* (dodders, Convolvulaceae): pollen and gynoecium. Thesis, Master of Science in Integrative Biology, Wilfrid Laurier University, Waterloo, Ontario, Canada.

Wenkel, S., J. Emery, B.H. Hou, M.M. Evans, M.K. Barton. 2007. A feedback regulatory module formed by LITTLE ZIPPER and *HD-ZIPIII* genes. Plant Cell 19: 3379–3390.

Wilkie, A.O. 1994. The molecular basis of genetic dominance. J Med Genet 31: 89-98.

Wilkins O., H. Nahal, J. Foong, N.J. Provart, M.M. Campbell. 2008. Expansion and diversification of the *Populus* R2R3-MYB family of transcription factors. Plant Physiol 149(2): 981-993.

Winter, D., B. Vinegar, H. Nadal, R. Ammar, G.V. Wilson, N.J. Provart. 2007. An "Electronic Florescent Pictograph" Browser for exploring and analyzing large-scale biological data sets. PLoS One 2(8): e718.

Woolward, F.H. 1907. The germination of poplars. J Bot 45: 417-419.

Worden, A.Z., J.-H. Lee, T. Mok, et al. 2009. Green evolution and dynamic adaptations revealed by genomes of marine picoeukaryotes *Micromonas*. Nature 324: 268-272.

Wu, R., H.D. Bradshaw, Jr., R.F. Stettler. 1997. Molecular genetics of growth and development in *Populus* (Salicaceae). V. Mapping quantitative trait loci affecting leaf variation. Am J Bot (84(2): 143-153.

Xu, L., L. Yang, L. Pi, Q. Liu, Q. Ling, H. Wang, R.S. Poethig, H. Huang. 2006. Genetic interaction between the AS1-AS2 and RDR6-SGS3-AGO7 pathways for leaf morphogenesis. Plant Cell Physiol 47: 853-863.

Yamaguchi, T., H. Tsukaya. 2010. Evolutionary and developmental studies of unifacial leaves in monocots: Juncus as a model system. J Plant Res 123: 35-41.

Yamaguchi, T., S. Yano, H. Tsukaya. 2010. Genetic framework for flattened leaf blade formation in unifacial leaves of *Juncus prismaticarpus*. Plant Cell 22(7): 2141-2155.

Yamazaki, K. 2011. Gone with the wind: trembling leaves may deter herbivory. Biol J Linn Soc 104: 738-747.

Yang, L., Z. Liu, F. Lu, A. Dong, H. Huang. 2006. SERRATE is a novel nuclear regulator in primary microRNA processing in Arabidopsis. Plant J 47: 841-850.

Yoshikawa, M., A. Peragine, M.Y. Park, R.S. Poethig. 2005. A pathway for the biogenesis of trans-acting siRNAs in Arabidopsis. Genes Dev 19: 2164-2175.

Yu, J., M.T. Holder, J. Sukumaran, S. Mirarab. SATé version 1.3.1. Downloaded from http://phylo.bio.ku.edu/software/sate/sate.html 13 April 2011.

Zhong, R., Z.-H. Ye. 1999. *IFL1*, a gene regulating interfascicular fiber differentiation in Arabidopsis, encodes a homeodomain-leucine zipper protein. Plant Cell 11: 2139-2152.

Zhong, R., Z.-H.Ye. 2004. *Amphivasal vascular bundle 1*, a gain-of-function mutation of the *IFL1/REV* gene, is associated with alternations in the polarity of leaves, stems and carpels. Plant Cell Physiol 45(4): 369-385.

Zhong R, J.J. Taylor, Z-H. Ye. 1999. Transformation of the collateral vascular bundles into amphivasal vascular bundles in an *Arabidopsis* mutant. Plant Physiol 120: 53-64.

Zhu, X.Y., M.W. Chase, Y.L. Qiu, H.Z. Kong, D.L. Dilcher, J.H. Li, Z.D. Chen. 2007. Mitochondrial matR sequences help resolve deep phylogenetic relationships in rosids. BMC Evol Biol 7: 217.

Zoulias, N., D. Koenig, A. Hamidi, S. McCornick, M. Kim. 2012. A role for *PHANTASTICA* in medio-lateral regulation of adaxial domain development in tomato and tobacco leaves. Ann Bot 109(2): 407-418.

Appendices

Appendix A : Supplementary data from Chapter 2.

A.1 Primers used in this study to amplify the corresponding genes.

Arabidopsis gene name	Primer name	Primer sequence	Direction
CORONA (CNA)	bnATHB15-1f	CTCTGTCTCGTTCACTAAGTTGTGGGG	forward
	bnATHB15-1r	CATAACATCAACAGCTCGGCATTCGCG	reverse
	bnATHB15-2f	GTCCTGCAGGGTTAGTGCTTTAGTGAG	forward
	bnATHB15-2r	ACCATCACAAGGCCGTATCAAGTACCC	reverse
	bnATHB151f	CTTTGGTATTAAGGAGTAATGGCAATGTCTTGC	forward
	bnATHB151r	CATAACATCAACAGCTCGGCATTCGC	reverse
	bnATHB152f	AGTGGTCAGCACCAATTAGCATCACAG	forward
	bnATHB152fb	CCTGCAGGGTTAGTGCTTTAGTGAGAG	forward
	bnATHB152r	CCACTGGGAAGCATCTCTGCTCTAAC	reverse
	bnATHB153f	ACTTCTGGCTGCTGCGTTATACATCTG	forward
	bnATHB153r	GACCGACTTGTGAACTGATGTGAGAAGG	reverse
	bnATHB154f	GACAGCATGGATGATGTCACAATCACTG	forward
	bnATHB154r	GAACACAAAGCAGATACAATGAGCGTTCTC	reverse
ARABIDOPSIS THALIANA HOMEOBOX8 (ATHB8)	bnATHB8-1f	TTCATTTCTAAGGCCACTGGAACCGCC	forward
	bnATHB8-1r	GAGATCTACAATCACGCAACCAAGAAGGC	reverse
	bnATHB8-2f	CAGGTGTAGAGAGAAGCAACGTAAAGAGG	forward
	bnATHB8-2r	CGACAATGTGAAGAATGGAACCACCTCC	reverse
	bnATHB8-3f	CCATTGAAAGCCTCCATCTCTGGTAACC	forward
PHABULOSA (PHB)	bnPHAB1f	ATATGTTGTCACTGTTCATCCACTACT	forward
	bnPHAB1fb	GAGCAAGTGGAAGCTCTTGAGAGAG	forward
	bnPHAB1r	CTCGATAGTTCCACCGTTTCCAGC	reverse
	bnPHAB2f	AGTCTGTGGTCGTAAGTGGTCAGC	forward
	bnPHAB2r	TTCTTAAAACAGCAGGTTGCCGCC	reverse
	bnPHAB3f	GGTGGTGGTTCCATTCTCCACATTG	forward
	bnPHAB3r	TCAATAGGAGCAAAGACAAGCTGTGC	reverse
	bnPHAB4f	GCTAGTCCTTTTGCTGTTCCTTGCG	forward
	bnPHAB4r	GGAAGATGAGCATAGCCCTGTTGC	reverse
	bnPHAB4rb	CAAAATACTTGAGCATAGAAGCCCTAAC	reverse
	bnPHAB5f	AGTTTTGGTACGTTTCTTTGGAGTGTAGGC	forward
	bnPHAB5r	CAACAAGAACTGAGATGGACCTGCGTG	reverse
	bnPHAB6f	AAGCTGCTCGTCTCCAGACAGTGAAC	forward
	bnPHAB6r	TTGAAACTATTTGGCTCGTTGCTTACATCC	reverse
	bnPHAB7f	GCAGAGTTCCTTTCCAAGGCTACAGG	forward
	bnPHAB8f	CAGCAAAACCCGACACATCAGCATCCT	forward
	bnPHAB8r	CACTTCGACAGTCACGGAACCAAGATG	reverse
	bnPHAB9f	CAACGGCTGTGAATCTGTGGTCGCG	forward
	bnPHAB9r	AGCTCGATAGTACCGCCATTTCCAGTG	reverse
PHAVOLUTA (PHV)	bnPHV1f	GAGGGCTTACCCGTTTGAATCAATCC	forward
	bnPHV1fb	GGACGATAGAGACTCTCCTGTCAAAGG	forward
	bnPHV1r	TCGACAGCAGTTCCTGTAGCCTTG	reverse
	bnPHV2f	GAATCTGCTCGGCTTCAGACAGTG	forward
	bnPHV2r	GCCTCAGGACTTCAGGAACACTTG	reverse

Arabidopsis gene name	Primer name	Primer sequence	Direction
PHAVOLUTA (PHV)	bnPHV3f	AGCTCGTGACTTTTGGACCCTGAG	forward
	bnPHV3r	CCACATTCTCATCAACACCGCTGC	reverse
	bnPHV4f	GTGCCACCTCTTGTACTGATTCGG	forward
	bnPHV4r	ACGACCAGAGTCATCTAGAGTCTTGTCC	reverse
	bnPHV5f	TTTGCTGACGATGCACCTTTGCTTC	forward
	bnPHV5r	CATCTTCTTCACACGAAGGACCAGTTC	reverse
	bnPHV6f	GCATGTTTCTTTGCTCTGTCTTCTGTTC	forward
	bnPHV6r	GGGTGGTTTTTAAGACTCACCACATAGC	reverse
	bnPHV7f	TCTCATAGGCAACTGGGACGACCAC	forward
	bnPHV7r	GAAACAGACCTGAGTGTTGATGAGCTCG	reverse
REVOLUTA (REV)	bnREV1f	GAAGAAAGTTTGGAGAAAGAAGATGG	forward
	bnREV1r	GCATTTCTGCTCTTACAAACTGAG	reverse
	bnREV2f	GTTTCTTAGGCTGCTCTCGATCGCAG	forward
	bnREV2r	GAATGGCTCTTTCTTACCTTGACAGGCTC	reverse
	bnREV3f	CGGTTTAGGTGTCGAGATAAGCAGAGG	forward
	bnREV3r	ATCGGGAACACTCCAAGCCTACAATGC	reverse
	bnREV4f	GAACGATGTAAGCTGTGACTCTGTGGTC	forward
	bnREV4r	GGATGACTCATAAAGGGGTCTAAGCACATCAGG	reverse
	bnREV5f	CTCTGTGGTCACAACTCCTAAGCATTCTA	forward
	bnREV5r	CCTGCTGGGAACATGGTGAAAACTTCG	reverse

A.2 *B. napus* sequences (and NCBI GenBank accession numbers).

Gene name	Accession number	Partial gene sequence (miRNA166/165 binding site underlined, split in two by the intron)
BnPHB.1	JN975041	TTTTTTTTTTTTTTGGTTTTAGTCTCCTTTCGATAGCAGAGGAGGCCCTC GCAGAGTTCCTTTCCAAGGCTACAGGAACTGCTGTTGACTGGGTTCAGAT GATTGGTATGAAGGTAATAATCTCTTCAAGTTGTATTAATCTCATTTCTG TTTCTTTTATTATTATGTGACAACATAAAATTAATATTGTTTTGATGAAC CTTTCTTTTATTTGGTTGTAGCCTGGTCCGGATTCTATTGGCATCGTCTC TATTTCGCGCAACTGCAGCGGAATTGCAGCACGTGCCTGCGGCCTCGTGA GTTTAGAACCCATGAAGGTAAGTGTGACATTGTTTCATTTGCTTGTATCT GCAAGTAAGAGAAAAAAATAGAGTTCTAGTCAAATCTTGATTTGAACAAA AAACTGTAGGTTGCTGAAATCCTCAAAGATCGTCAATCTTGGCTCCGTGA TTGTCGATGTGTGGATACTCTGAGTGTGATTCCTGCTGGAAACGGTGGAA CTATCGAGCTTATATACACGCAGGTCCATCTCAGTTCTTGTTG
BnPHV.1	JN975040	TTATCATACTACTGCTGTTTTGTCTTTAGCTGTTTCTTTTTGAAGTTTAT TCTTTTTTATTGGTTGTTTTGAAATTGTTAGATGTCGAGAGAAGCAGAGG AAAGAATCTGCTCGGCTTCAGACAGTGAACAGAAAGCTGAGTGCTATGAA CAAGCTTTTGATGGAGGAGAATGACCGTTTGCAGAAGCAAGTCTCCCACT TGGTTTACGAGAATGGGTTCATGAAACACCGAATCAACACTGTAAGTATT TGAATTCAATGCAATGCAATGCAATGCAATGCAATGAAGAAGTTAAATTT GTTTAAAGAGTGAATTATTCTGTAGTTAGAAAATGACTGGTCTAGCTCTT CTGTGTATGGTCTCATAGGCAACTGGGACGACCACAGACAACGGCTGTGA ATCTGTGGTCGCGAGTGGTCAGCAACGTCAGCAGCAAAACCCGACACATC AGCATCCTCAACGTGATGCTAACAACCCAGCTGGGTAATGAAGGCTCTTC TGTTATTTATGTTGACTTTCTTTCTCAATGTTAGACTAAAATGGTTTTGT TTGAACATTTTTTAATGTAGTCTTCTCTCGATTGCGGAGGAGACCTTGGC GGAGTTCCTTTGCAAGGCTACAGGAACTGCTGTTGACTGGGTTCAGATGA

Gene name	Accession number	Partial gene sequence (miRNA166/165 binding site underlined, split in two by the intron)
		TTGGGATGAAGGTATATTAAGGGTTTCATGTGTACTAATGAAGTAATCTT TCTGAGGGTTTTACTAATATGTATTTTCTCTGGTAATGTATAAATAGCCT GGTCCGGATTCGATTGGCATCGTCGCTGTTTCACGCAACTGCAGTGGAAT AGCAGCACGTGCCTGTGGCCTCGTGAGTTTAGAACCCATGAAGGTAATAA TTGCATATTTTGTTTTATCTCTATATACATTTTGTTTTTTTGTAAGAAGG CACTCTAAACTTCAAGTACTGTGGTTTAGGTTGCTGAAATCCTCAAAGAT CGTCCATCTTGGTTCCGTGACTGTCGAAGTGTGGAGACTCTGAGTGTTAT ACCCACTGGAAATGGCGGTACTATCGAGCTCATCAACACTCAGGTCTGTT TCATCAATCTTATCATTCTCCTGTTTATTTCCTTGTAGAATGTTTCTGAC TGCGTGTTGTCAGATTTATGCTCCCACAACACTAGC
BnPHV.2	JN975039	TTATCATACTACTGCTGTTTTGTCTTTAGCTGTTTCTTTTTGAAGTTTAT TCTTTTTTATTGGTTGTTTTGAAATTGTTAGATGTCGAGAGAAGCAGAGG AAAGAATCTGCTCGGCTTCAGACAGTGAACAGAAAGCTGAGTGCTATGAA CAAGCTTTTGATGGAGGAGAATGACCGTTTGCAGAAGCAAGTCTCCCACT TGGTTTACGAGAATGGGTTCATGAAACACCGAATCAACACTGTAAGTATT TGAATTCAATGCAATGCAATGCAATGCAATGCAATGAAGAAGTTAAATTT GTTTAAAGAGTGAATTATTCTGTAGTTAGAAAATGACTGGTCTAGCTCTT CTGTGTATGGTCTCATAGGCAACTGGGACGACCACAGACAACGGCTGTGA ATCTGTGGTCGTGAGTGGTCAGCAACGTCAGCAGCAAAACCCAACACATC AGCATCCTCAACGTGATGCTAACAACCCAGCTGGGTAAGGAAGCCTCTTG TTTATTTATTTAGAGTTTCTTTCTCACTGTTAGACTAAAATGGTTTTGTT TGAACATTATTAATGCACAGTCTTCTCTCGATTGCGGAGGAGACCTTGGC GGAGTTCCTTTGCAAGGCTACAGGAACTGCTGTCGACTGGGTTCAGATGA TTGGGATGAAGGTATTATATAAAGGGTTTCATTTGTTCTAATGAAGTAAT CTTTTTTGAGGGTTTTGCTAATATGTATTTTCTCTGGTAATGTATAAATA GCCTGGTCCGGATTCGATTGGCATCGTCGCTGTTTCACGCAACTGCAGTG GAATAGCAGCACGTGCCTGTGGCCTCGTGAGTTTAGAACCCATGAAGGTA ATTGCATATTTTGTTTTATCTCTCTATATACATTTTTTTTTGTAAGAAGG CAGTCTAAAGTTTGAAGTACTGTGGTTTAGGTTGCTGAAATCCTCAAAGA TCGTCCATCTTGGTTCCGTGACTGTCGAAGTGTTGAGACTCTGAGTGTTA TACCCACTGGAAATGGTGGTACTATCGAGCTCATCAACACTCAGGTCTGT TTCATAAATCTTATCATTCTCCTCTGTTTATTTCCTTCTAGAATCTTTCT GACTGCTGTTCTTTTGGCGCGTTGTCAGATTTATGCTCCCACAACACTAG CAGCAGCTCGTGACTTTTGGACCCTGAGATACAGTACTAGTCTAGAAGAT GGAAGCTATGTGGTGAGTCTTAAAA
BnREV.1	JN975038	GCTCTCGATCGCAGAGGAGACATTGGCAGAGTTCCTATCCAAGGCTACAG GAACTGCTGTTGATTGGGTTCAGATGCCTGGGATGAAGGTTTTACACTCC TCTCCTCTCCTCTCATTACTTTTGTGTAATATTGAGATCTGATGTTTGGT TGTGTGTGTTTAAGCCTGGTCCGGATTCGGTTGGGATCTTTGCTATATCG CAAAGATGCAGTGGGGTGGCAGCTCGAGCCTGTGGTCTTGTTAGTTTAGA GCCTGTCAAGGTAAGAAAGAGCCATTCAAGACTTATTACTGTCAAACATG TTACATTGTTAAACCAGTTTGGTGTTATTATCTTTCTTTTTTGCAGATTG CAGAGATACTCAAAGATAGGCCATCTTGGTTCCGTGACTGTAGGAGCCTT GAAGTCTTCACTATGTTCCCGGCTGGTAATGGCGGCACCATTGAGCTCGT CTATATGCAGACATATGCACCAACGACTCTGGCTCCTGCCCGCGATTTCT GGACCCTGAGATACACAACGAGCCTAGACAATGGCAGTTTTGTGGTATGC AACTCCTCATAGTGTTATGTTTGTGTATGTCTATCTCTCTGGTTATTGAC TTTTTTTCTTTAATAAGGTTTGTGAGAGGTCACTCTCTGGTTCTGGTGCT GGTCCTAACGCTGCATCAGCTTCTCAGTTTGTAAGAGCAGAAATGCTTTC TAGTGGGTATCTAATAAGGCCTTGTGATGGTGGCGGTTCCATTATTCACA TTGTCGATCACCTTAATCTTGAGGTAAGTAGAATCTTCTTATTGTACATT TTCTGTTTGCTTCCT
BnATHB8.12	JN975044	GTAAACCGGAAGCTAACGGCGATGAACAAGCTTTTAATGGAAGAGAATGA CCGGTTGCAAAAGCAAGTGTCTCACTTGGTTTATGAGAACAGCTATTTTC

Gene name	Accession number	Partial gene sequence (miRNA166/165 binding site underlined, split in two by the intron)
		GCCAACACCCTCAAAACGTATACATATTAATTCATCTTTTGATTATTTCA CGTGTAACTTGACGCATAAGCTATGTAATTGATAGTCTCTATGGTTTCTT GTGATTTGTCAATAGCAAGGGAACTTGGCGACTACGGATACGAGCTGTGA GTCGGTTGTGACAAGTGGTCAGCACCACTTGACCCCTCAACATCAGCCTC GTGATGCTAGCCCTGCTGGGTAAGCTAAAAGTCATGTTAGACCGCAAAAA ATTTGATTGAAAATCATGAAACAAAATTTGTTGGGAACATAATAGAAATG CAAAAAA ***Note: this region is upstream of the miRNA binding site**
BnATHB8.11	JN975045	TCTTTTTTTCAGATTATTGTCCATTGCGGATGAAACTTTAACAGAGTTCA TTTCTAAGGCCACTGGAACCGCCGTCGAGTGGGTCCAAATGCCTGGGATG AAGGTACTTTCCATAAGTCTCTAGCTTGTCTCTTTGTCTACGTCTTCATT GTTATACTGACTAATGAATTTTCAGCCTGGTCCGGATTCCATTGGAATCG TTGCTATTTCTCATGGATGCACGGGAATCGCAGCTCGTGCTTGCGGCCTC GTGGGTCTTGACCCCACAAGAGTTGCAGAGATCCTTAAAGATAAGCCTTC TTGGTTGCGTGATTGTAGATCTCTTGATATCGTTAACGTCCTCTCCACTG CAAATGGTGGAACTCTAGAACTAATCTACATGCAGGTATTAATGAATGAT GATTGAGAACCATCAAGAATCATATCCAAACGAATGAACCAAAACAAAAC TAAAACTTCCTCTTGTTTATGTTCTTTCTTATGAAAAAAGCTTTATGCAC CGACAACACTGGCACCAGCACGTGATTTCTGGATGCTACGTTACACATCT GTAATGGAAGATGGGAGTCTTGTGGTATAATACTTAGCAAATAATCCTTA ATTATTCTGTTAATATATATACATCAGTCGCAGATACTGAATTTTGATTG ATACAGATATGCGAACGGTCACTGAACAATACACAAAACGGGCCAAGTAT GCCACCATCTCCTCATTTCGTTAGAGCAGAGATTTTACCAAGTGGATACC TCATTAGACCCTGTGAAGGAGGTGGTTCC
BnCNA.1	JN975043	ACTTTGGTATTAAGGAGTAATGGCAATGTCTTGCAAAGATGGGAAGATGG GATGCTTAGACAACGGGAAGTATGTGAGGTACACACCTGAGCAAGTTGAA GCACTTGAGAGGCTTTATCATGACTGTCCTAAACCCAGTTCCATCCGCCG TCAGCAGTTGATCAGAGAGTGTCCTATTCTCTCTAACATTGAGCCTAAAC AGATCAAAGTATGGTTTCAGAACCGAAGGTAATGATACTAACACTCCTTA ATGCAGTTTTGGGGACTGTAATAAATGGAAGTTTCTTTGATCTAATCTTT TATGAACTTCAGATGCAGAGAGAAACAGAGGAAAGAGGCTTCACGGCTTC AAGCTGTGAACAGGAAGTTGACGGCGATGAACAAGCTGTTGATGGAGGAG AATGATAGGTTGCAGAAGCAAGTGTCACAGCTGGTTCATGAAAACAGCTA CTTCCGTCAACACACTCCCAATGTGAGACTCTTTAATGCTTCCTTACAAT AAAAGAGTTTCATTTTGATTTTTTTTTTATCTTTTTTTTTCCAGCCTACC CTTCCAGCTAAAGACACAAGCTGTGAATCGGTTGTGACGAGTGGTCAGCA CCAATTAGCATCACAGAATCCTCCAAGAGATGCTAGTCCTGCAGGGTTAG TGCTTTAGTGAGAACATGTTACTCTCTTAGTTACACAATTATATTATAGT TCTGAATTAAATTTTGTGTGTTTGCAGACTTTTGTCCATTGCAGAAGAAA CTTTAGCAGAGTTTCTTTCAAAGGCAACTGGAACCGCTGTTGAGTGGGTT CAGATGCCTGGAATGAAGGTATGCCCCTTGATCCACTTCCTCTAGTTTTC TTTCTGATTATTGCATATTGTAACAATCAAAAAAATAAATAATCAAAGAG TTATTAAACTTCTCTGTAACGGTTTGTTTTGTACATATATGTAACAGCCT GGTCCGGATTCCATTGGAATCATTGCTATTTCTCACGGTTGCGCTGGTGT GGCAGCACGCGCCTGTGGCCTAGTTGGTCTCGAGCCTACAAGGGTACGTG TAGAGATAGAACCATTCCCTATGCATTCTTCTACTACTCTACCTTTACAT TTGCAGCAAGATTGATCTGCTTTCTCTTTATTTACAGGTCGCAGAGATCG TCAAGGATCGGCCTTCGTGGTTCCGCGAATGCCGAGCTGTTGATGTTATG AACGTGTTGCCAACAGCCAATGGTGGAACCATTGAGCTGCTTTATATGCA GCTCTATGCACCAACTACGTTGGCCCCACCGCGCGACTTCTGGCTGCTGC GTTATACATCTGTTTTAGAAGATGGCAGCCTTGTGGTGTGCGAGAGGTCT CT

Gene name	Accession number	Partial gene sequence (miRNA166/165 binding site underlined, split in two by the intron)
BnCNA.2	JN975042	ACTTTGGTATTAAGGAGTAATGGCAATGTCTTGCAAAGATGGGAAGATGG GATGCTTAGACAACGGGAAGTATGTGAGGTACACACCTGAGCAAGTTGAA GCACTTGAGAGGCTTTATCATGACTGTCCTAAACCCAGTTCCATCCGCCG TCAGCAGTTGATCAGAGAGTGTCCTATTCTCTCTAACATTGAGCCTAAAC AGATCAAAGTATGGTTTCAGAACCGAAGGTAATGATACTAACACTCCTTA ATGCAGTTTTGGGGACTGTAATAAATGGAAGTTTCTTTGATCTAATCTTT TATGAACTTCAGATGCAGAGAGAAACAGAGGAAAGAGGCTTCACGGCTTC AAGCTGTGAACAGGAAGTTGACGGCGATGAACAAGCTGTTGATGGAGGAG AATGATAGGTTGCAGAAGCAAGTGTCACAGCTGGTTCATGAAAACAGCTA CTTCCGTCAACACACTCCCAATGTGAGACTCTTTAATGCTTCCTTACAAT AAAAGAGTTTCATTTTGATTTTTTTTTTATCTTTTTTTTTCCAGCCTACC CTTCCAGCTAAAGACACAAGCTGTGAATCGGTTGTGACGAGTGGTCAGCA CCAATTAGCATCACAGAATCCTCCAAGAGATGCTAGTCCTGCAGGGTTAG TGCTTTAGTGAGAGAACATGTTACTCTCTTAGTTGCACAATTACGTTATA TTTCTGAATTAAATTTTGTGTGTTTGCAGACTTTTGTCCATTGCAGAAGA AACTTTAGCAGAGTTTCTTTCAAAGGCAACTGGAACCGCTGTTGAGTGGG TACAGATGCCTGGAATGAAGGTATGCCCCTTGGTCCACTTTCTCTAATTG TGTGAATCATTCTTCTTCTCTGTAACGGTTTGCCTTTGTGTTTTTTGTAA CAGCCTGGTCCGGATTCCATTGGAATCATTTCTATTTCTCACGGTTGCGC AGGTGTGGCAGCACGCGCCTGTGGCCTAGTGGGTCTCGAGCCTACAAGGG TACGTGTAGAGATAGAACCATTCCTTATGCAATCTTCTACTACTCTACCT TAGATTGATCTGCTCTCTCTTTATTTACAGGTCGCAGAGATCGTCAAGGA TCGGCCTTCGTGGTTCCGCGAATGCCGAGCTGTTGATGTTATGAACGTGT TGCCAACCGCCAACGGTGGAACCATTGAGCTGCTTTATATGCAGCTCTAC GCACCAACTACGTTGGCTCCACCACGCGACTTCTGGCTGCTGCGTTATA

A.3 Gene names and corresponding accession numbers for *A. thaliana*, *B. rapa*, and *B. oleracea HD-ZIPIII* genes.

A. thaliana		*B. rapa*		*B. oleracea*	
PHB	AT2G34710	BrPHB.1 BrPHB.2	Bra005398 Bra021926	BoPHB.1 BoPHB.2	ctg7180014773726 ctg7180014758096
PHV	AT1G30490	BrPHV.1	Bra032394	BoPHV.1	ctg7180014745595
REV	AT5G60690	BrREV.1 BrREV.2 BrREV.3	Bra002457 Bra020235 Bra038295	BoREV.1 BoREV.2	ctg7180014731467 ctg7180014766592
ATHB8	AT4G32880	BrATHB8.1 BrATHB8.2	Bra034539 Bra011392	BoATHB8.1	ctg7180014734369
CNA	AT1G52150	BrCNA.1 BrCNA.2	Bra014315 Bra018948	BoCNA.1 BoCNA.2	ctg7180014731497 ctg7180014737316

A.4 Alignment of *A. thaliana, B. rapa, B. oleracea,* and *B. napus HD-ZIPIII* genes.

Available as supplementary data.

A.5 Segregation ratios of phenotypic classes in progeny tests.

Accession	M_3 phenotype	M_4 and M_5 phenotypic ratios			
		Wild type	Moderate *lip*	Severe *lip*	Died
CT229-2-8	moderate lip	0	15	8	22
CT229-2-14	moderate lip	5	4	2	9
CT229-2-22	moderate lip	9	2	7	2
CT229-2-23	moderate lip	2	5	9	11
CT229-2-23-3	moderate lip	3	4	4	4
CT229-2-23-9	moderate lip	3	4	2	6
CT229-2-23-12	moderate lip	3	8	4	0
CT229-2-29	moderate lip	4	1	1	24
CT229-2-31	moderate lip	0	0	0	20
CT229-2-37	moderate lip	7	4	3	1
CT229-2-40	moderate lip	6	4	5	0
CT229-2-65	moderate lip	4	6	5	0
CT229-2-11	wild type	18	0	0	3
CT229-2-12	wild type	7	0	0	3
CT229-2-20	wild type	9	0	0	1
CT229-2-24	wild type	10	0	0	0

A.6 Stem and root anatomy of wild type and severe *lip* phenotype mutants. (A-D) Stem anatomy: A. **Transverse section of wild type stem.** B. **Transverse section of severe *lip* phenotype stem. Amphivasal leaf traces are indicated by arrowheads The sections were made at the mid-point of the stem but sectioning through leaf bases in *lip* plants was not avoidable due to the lack of stem elongation.** C. **High magnification of a collateral vascular bundle (from A) in wild type stem.** D. **Higher magnification of B of an amphivasal leaf trace (arrowhead) in *lip* mutant stem. Note the similarity of overall vascular arrangement compared to wild type. (E, F) Root anatomy:** E. **Transverse section of a wild type root.** F. **Transverse section of a severe *lip* mutant root.**

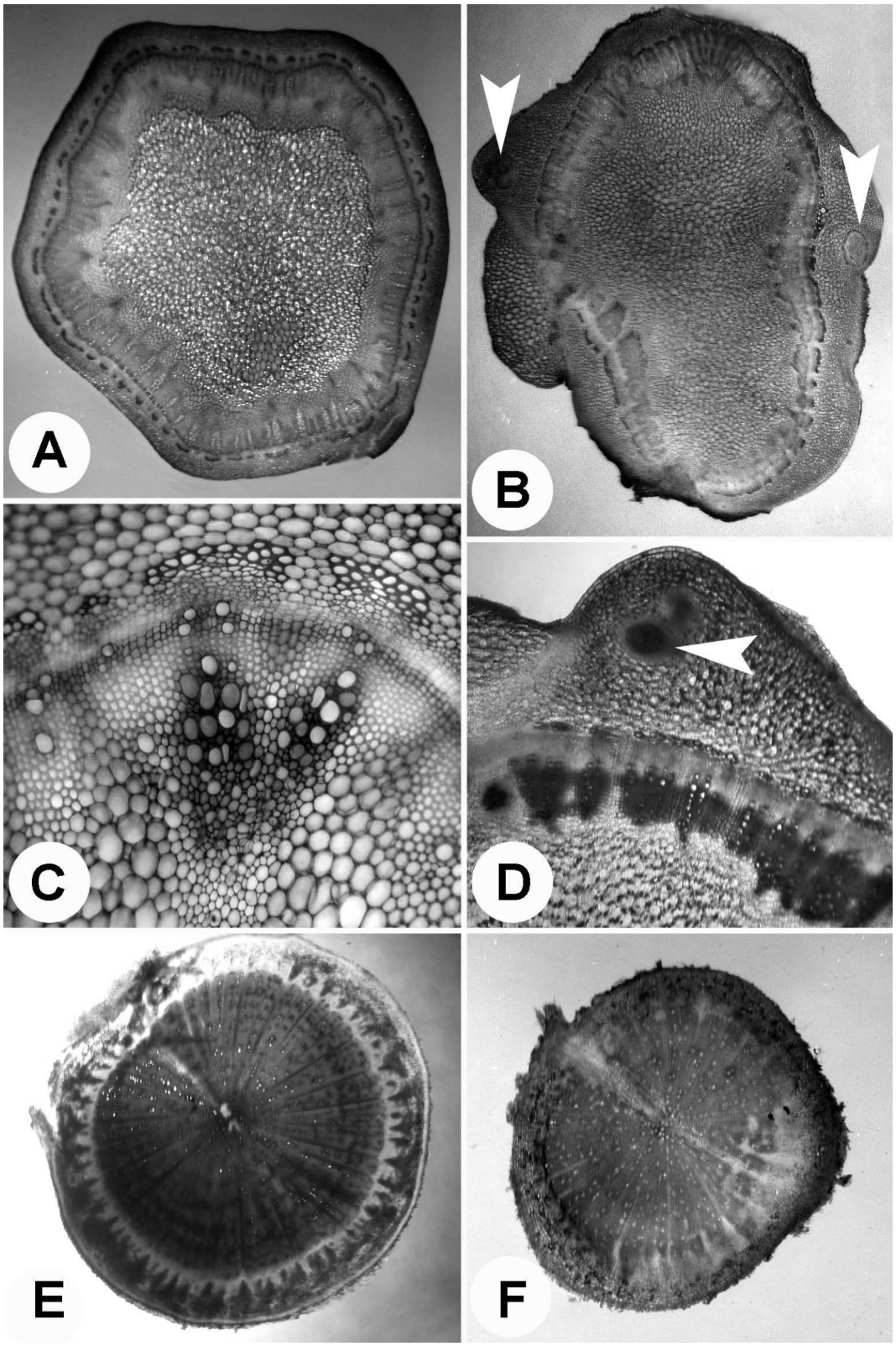
A
B
C
D
E
F

A.7 Flower morphology of wild type and moderate *lip* mutant. A. **Wild type flower consisting of 4 oblong sepals, 4 obovate petals, 6 stamens arranged in two whorls, and a central carpel. Floral diagram on the lower left shows organ arrangement.** B. **Flower typically observed in moderate *lip* phenotype plants consisting of 4 trumpet-shaped petals, 10-14 filamentous sepals (occasionally somewhat flattened and similar to wild type), 6 stamens arranged in two whorls, and a central carpel. Floral diagram on the lower right shows flower organ arrangement.**

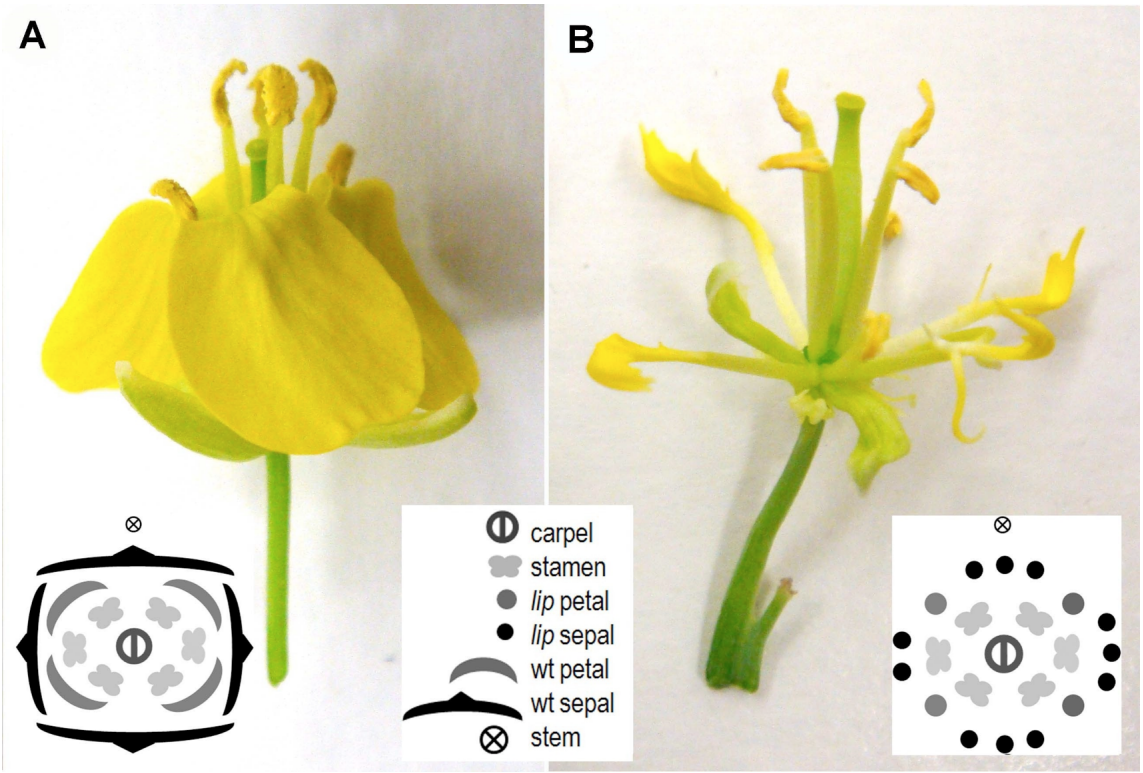

Appendix B : Supplementary data from Chapter 3.

B.1 *YABBY* alignment file. Available as supplementary data.

B.2 *KANADI* alignment file. Available as supplementary data.

B.3 *HD-ZIPIII* alignment file. Available as supplementary data.

B.4 RPKM expression values of *YABBY*, *KANADI*, and *HD-ZIPIII* gene families for each sample of *P. trichocarpa* (mean values are graphed in Fig. 3.2).

Gene	Leaf RPKM expression				Xylem RPKM expression			
YABBY	PT0033	PT0034	PT0035	**Mean leaf**	PT0005	PT0006	PT0010	**Mean xylem**
Pt-AFO.1	87.02	118.00	91.00	**98.67±16.85**	0.04	0.04	0.03	**0.04±0.01**
Pt-AFO.2	99.43	140.96	107.32	**115.90±22.05**	0	0.04	0	**0.01±0.02**
Pt-YAB2.1	104.01	88.61	116.07	**102.90±13.76**	2.19	0.37	1.22	**1.26±0.91**
Pt-YAB2.2	16.49	22.86	11.13	**16.82±5.87**	0	0	0	**0**
Pt-YAB2.3	60.52	92.88	72.87	**75.42±16.33**	0.11	1.12	0.17	**0.47±0.56**
Pt-YAB3.1	51.07	71.69	61.50	**61.42±10.31**	0.40	0.42	0.35	**0.39±0.03**
Pt-YAB3.2	13.86	17.55	12.79	**14.74±2.50**	0.20	0.73	0.48	**0.47±0.26**
Pt-INO.1	0	0	0.02	**0.01±0.01**	0	0	0	**0**
Pt-INO.2	0	0	0.03	**0.01±0.02**	0	0	0	**0**
Pt-YAB5.1	29.55	67.89	45.29	**47.58±19.28**	0	0	0	**0**
Pt-YAB5.2	226.48	234.42	199.48	**220.13±18.32**	0	0	0	**0**
Pt-CRC.1	0	0	0	**0**	0	0	0	**0**
Pt-CRC.2	0	0	0	**0**	0	0	0	**0**
KANADI								
Pt-KAN.1	4.46	5.22	4.72	**4.80±0.39**	0.06	0	0.12	**0.06±0.06**
Pt-KAN.2	15.24	13.85	16.56	**15.22±1.36**	0.12	0.04	0.19	**0.12±0.08**
Pt-KAN.3	4.50	1.53	1.79	**2.61±1.64**	0.42	0.05	0.81	**0.43±0.38**
Pt-KAN.4	6.18	1.18	2.45	**3.27±2.60**	1.00	0	0.80	**0.60±0.53**
Pt-KAN2/3.1	8.12	7.54	9.35	**8.34±0.93**	0.51	0.08	0.51	**0.36±0.25**
Pt-KAN2/3.2	6.70	5.19	4.55	**5.48±1.10**	0.04	0.03	0.12	**0.06±0.05**
Pt-ATS.1	5.50	5.04	6.23	**5.59±0.60**	0.86	0.37	0.25	**0.49±0.32**
Pt-ATS.2	14.01	10.80	17.08	**19.96±3.14**	0	0.35	0.08	**0.14±0.18**
HD-ZIPIII								
Pt-PHB.1	32.32	21.59	27.58	**27.16±5.37**	75.43	59.62	86.87	**73.98±13.68**
Pt-PHB.2	36.29	16.79	23.97	**25.68±9.86**	152.05	131.60	140.63	**141.43±10.25**
Pt-HB1.7	7.57	3.52	7.03	**6.04±2.20**	12.75	13.37	16.52	**14.21±2.02**
Pt-HB1.8	33.36	16.15	28.24	**25.92±8.83**	47.19	69.28	64.12	**60.20±11.55**
Pt-HB1.5	9.07	4.30	6.91	**6.76±2.39**	59.51	52.75	69.80	**60.69±8.59**

Gene	Leaf RPKM expression				Xylem RPKM expression			
Pt-HB1.6	39.85	24.02	34.00	**32.29±7.56**	77.76	89.44	93.55	**86.92±8.19**
Pt-ATHB.11	16.74	8.81	16.16	**13.90±4.42**	75.64	80.15	76.92	**77.57±2.32**
Pt-ATHB.12	19.33	10.95	14.43	**14.90±4.21**	133.06	128.21	169.32	**143.53±22.47**

B.5 Comparison of gene expression between poplar leaf and xylem samples. P-values are presented with significant values ($p \leq 0.05$) underlined. N/A specifies where a comparison could not be made due to undetectable expression levels (or division by 0).

Gene family	Gene name	P-value
YABBY	*Pt-AFO.1*	0.009583726
	Pt-AFO.2	0.011832548
	Pt-YAB2.1	0.005665856
	Pt-YAB2.2	0.038294615
	Pt-YAB2.3	0.014482568
	Pt-YAB3.1	0.009353643
	Pt-YAB3.2	0.008681172
	Pt-INO.1	0.422649731
	Pt-INO.2	0.422649731
	Pt-YAB5.1	0.050596745
	Pt-YAB5.2	0.002300548
	Pt-CRC.1	N/A
	Pt-CRC.2	N/A
KANDI	*Pt-KAN.1*	0.002721648
	Pt-KAN.2	0.002388898
	Pt-KAN.3	0.151264622
	Pt-KAN.4	0.169011198
	Pt-KAN2/3.1	0.003016812
	Pt-KAN2/3.2	0.014346609
	Pt-ATS.1	0.007370281
	Pt-ATS.2	0.01821654
HD-ZIPIII	*Pt-PHB.1*	0.018228
	Pt-PHB.2	2.12558x10E-05
	Pt-HB1.5	0.006949278
	Pt-HB1.6	0.020972226
	Pt-HB1.7	0.0322138
	Pt-HB1.8	0.09465625
	Pt-ATHB.11	0.003678797
	Pt-ATHB.12	0.01032808

B.6 Ranked levels of expression of *YABBY*, *KANADI,* and *HD-ZIPIII* genes in *Populus trichocarpa* (v2.2). A value for each sample (as well as mean value) is presented as percent of total genes with detectable expression (RPKM > 0) and ranked in four quartiles. N/A specifies genes or samples where expression levels were undetectable.

Gene	**Leaf expression ranking**					**Xylem expression ranking**				
YABBY	PT 0033	PT 0034	PT 0035	**Mean leaf**	**Quartile rank**	PT 0005	PT 0006	PT 0010	**Mean xylem**	**Quartile rank**
Pt-AFO.1	3.94	3.99	4.45	**4.1277**	**1st**	96.76	96.23	97.53	**96.8394**	**4th**
Pt-AFO.2	3.17	3.14	3.60	**3.3058**	**1st**	N/A	96.89	N/A	**96.8945**	**4th**
Pt-YAB2.1	2.98	5.69	3.17	**3.9463**	**1st**	62.63	81.84	69.51	**71.3244**	**3rd**
Pt-YAB2.2	28.60	23.36	39.70	**30.5522**	**2nd**	N/A	N/A	N/A	**N/A**	**N/A**
Pt-YAB2.3	6.81	5.37	6.12	**6.1009**	**1st**	90.58	71.91	86.33	**82.9424**	**4th**
Pt-YAB3.1	8.47	7.52	7.54	**7.8419**	**1st**	80.67	80.82	80.91	**80.8008**	**4th**
Pt-YAB3.2	32.61	33.30	36.22	**34.0453**	**2nd**	86.43	75.98	78.06	**80.1582**	**4th**
Pt-INO.1	N/A	N/A	98.91	**98.9110**	**4th**	N/A	N/A	N/A	**N/A**	**N/A**
Pt-INO.2	N/A	N/A	97.61	**97.6117**	**4th**	N/A	N/A	N/A	**N/A**	**N/A**
Pt-YAB5.1	1.62	7.98	11.06	**6.8887**	**1st**	N/A	N/A	N/A	**N/A**	**N/A**
Pt-YAB5.2	0.63	1.34	1.20	**1.0555**	**1st**	N/A	N/A	N/A	**N/A**	**N/A**
Pt-CRC.1	N/A	N/A	N/A	**N/A**	**N/A**	N/A	N/A	N/A	**N/A**	**N/A**
Pt-CRC.2	N/A	N/A	N/A	**N/A**	**N/A**	N/A	N/A	N/A	**N/A**	**N/A**
KANADI										
Pt-KAN.1	56.54	53.90	57.20	**55.8782**	**3rd**	95.21	N/A	88.49	**91.8513**	**4th**
Pt-KAN.2	30.51	33.68	30.21	**31.4657**	**2nd**	90.33	96.53	85.47	**90.7768**	**4th**
Pt-KAN.3	56.43	70.72	70.08	**65.7402**	**3rd**	80.10	95.39	73.40	**82.9662**	**4th**
Pt-KAN.4	50.93	73.31	66.59	**63.6098**	**3rd**	71.84	N/A	73.50	**72.6718**	**3rd**
Pt-KAN2/3.1	45.16	46.73	43.88	**45.2563**	**2nd**	78.49	93.03	77.62	**83.0479**	**4th**
Pt-KAN2/3.2	49.30	54.04	57.90	**53.7480**	**3rd**	96.66	97.91	88.94	**94.5069**	**4th**
Pt-ATS.1	53.13	54.51	59.89	**55.8448**	**3rd**	73.36	81.84	83.63	**79.6111**	**4th**
Pt-ATS.2	32.34	39.08	29.50	**33.6425**	**2nd**	N/A	82.23	90.40	**86.3177**	**4th**
HD-ZIP III										
Pt-PHB.1	14.56	24.47	19.23	**19.4208**	**1st**	6.19	8.34	5.35	**6.6272**	**1st**
Pt-PHB.2	12.66	29.51	22.01	**21.3933**	**1st**	2.77	3.13	2.87	**2.9247**	**1st**
Pt-HB1.7	42.69	57.11	50.38	**50.0581**	**3rd**	8.10	9.64	6.85	**8.1963**	**1st**
Pt-HB1.8	11.73	22.48	15.42	**16.5415**	**1st**	6.01	5.14	4.87	**5.3419**	**1st**
Pt-HB1.5	46.83	60.31	49.97	**52.3710**	**3rd**	31.07	31.83	26.50	**29.8012**	**2nd**
Pt-HB1.6	13.96	30.38	18.74	**21.0251**	**1st**	10.56	7.01	7.56	**8.3758**	**1st**
Pt-ATHB.11	28.26	43.39	30.75	**34.1334**	**2nd**	6.17	5.90	6.19	**6.0895**	**1st**
Pt-ATHB.12	24.84	38.76	33.29	**32.2980**	**2nd**	3.27	3.24	2.22	**2.9087**	**1st**

B.7 Comparison of paralog expression values of poplar leaf polarity genes in leaf and xylem. P-values are presented with significant values (p≤0.05) underlined. N/A specifies where a comparison could not be made due to undetectable expression levels (or division by 0).

Gene family	Paralogous genes compared	p-value (≤0.05)	
		Xylem	Leaf
YABBY	*Pt-AFO*	0.137219967	0.030507758
	Pt-YAB2.1, 2.2	0.138974592	0.016909574
	Pt-YAB2.1, 2.3	0.28693716	0.225546744
	Pt-YAB2.2, 2.3	0.28693716	0.016679701
	Pt-YAB3	0.646619367	0.011231461
	Pt-INO	N/A	0.422649731
	Pt-YAB5	N/A	0.005375732
	Pt-CRC	N/A	N/A
KANADI	*Pt-KAN.1, .2*	0.016880044	0.008140052
	Pt-KAN.1, .3	0.181669822	0.193811402
	Pt-KAN.1, .4	0.194436556	0.463825613
	Pt-KAN.2, .3	0.219019364	0.008527241
	Pt-KAN.2, .4	0.221003576	0.015495484
	Pt-KAN.3, .4	0.486368495	0.37667691
	Pt-KAN2/3	0.142809839	0.105609236
	Pt-ATS	0.309839925	0.029478358
HD-ZIPIII	*Pt-PHB*	0.010527979	0.644338228
	Pt-HB1.5, 1.6	0.040743115	0.016782995
	Pt-HB1.7, 1.8	0.017963398	0.035593106
	Pt-ATHB.11, .12	0.03940367	0.541972635

B.8 FPKM expression values of *YABBY*, *KANADI*, and *HD-ZIPIII* gene families in *E. grandis* (mean values are in Fig. 3.3).

Gene	Leaf FPKM expression				Xylem FPKM expression			
YABBY	Leaf 1	Leaf 2	Leaf 3	**Mean leaf**	Xylem 1	Xylem 2	Xylem 3	**Mean xylem**
Eg-AFO/YAB3.1	174.10	257.30	168.07	**199.82±49.87**	0.055	0.08	0.27	**0.14±0.12**
Eg-AFO/YAB3.2	124.20	166.95	149.78	**146.98±21.51**	0.12	0.24	0.15	**0.17±0.06**
Eg-YAB2.1	113.30	76.97	90.27	**93.51±18.38**	0.06	0	0.062	**0.06±0.001**
Eg-INO.1	0	0	0	**0**	0	0	0	**0**
Eg-YAB5.1	38.17	46.40	64.39	**49.65±13.41**	0	0.12	0	**0.04**
Eg-CRC.1	0	0	0	**0**	0	0	0	**0**

Gene	Leaf FPKM expression				Xylem FPKM expression			
KANADI								
Eg-KAN.1	6.07	6.04	7.50	**6.54±0.83**	0	0	0	**0**
Eg-KAN.2	0.44	1.05	1.26	**0.92±0.42**	0.06	0	0	**0.02**
Eg-KAN2/3.1	15.81	18.68	17.41	**17.30±1.44**	0.20	0.03	0	**0.08±0.11**
Eg-KAN2/3.2	0.87	1.07	0.92	**0.95±0.11**	0	0	0.09	**0.03**
Eg-KAN2/3.3	1.84	2.42	2.44	**2.24±0.34**	0.14	0.033	0.05	**0.08±0.06**
Eg-ATS.1	4.09	3.04	3.51	**3.54±0.53**	0	0	0	**0**
HD-ZIPIII								
Eg-PHB/PHV.1	34.36	37.40	30.32	**34.03±3.55**	72.23	72.90	56.76	**67.29±9.13**
Eg-REV.1	17.95	11.42	12.88	**14.09±3.43**	104.66	157.94	144.90	**135.83±27.77**
Eg-ATHB8.1	13.34	18.25	16.91	**16.16±2.54**	197.31	196.59	172.01	**188.64±14.40**
Eg-CNA.1	33.22	30.81	29.10	**31.05±2.07**	114.44	121.957	130.9	**122.46±8.28**

B.9 Ranked levels of expression of *YABBY*, *KANADI*, and *HD-ZIPIII* genes in *Eucalyptus grandis* (v1.0). A value for each sample (as well as mean value) is presented as percent of total genes with detectable expression (FPKM > 0) and ranked in four quartiles. N/A specifies genes or samples where expression levels were undetectable.

Gene	Leaf expression ranking					Xylem expression ranking				
YABBY	Leaf 1	Leaf 2	Leaf 3	**Mean leaf**	**Quartile rank**	Xylem 1	Xylem 2	Xylem 3	**Mean xylem**	**Quartile rank**
Eg-AFO/YAB3.1	1.02	0.64	1.37	**1.0133**	**1st**	96.83	94.09	82.76	**91.2291**	**4th**
Eg-AFO/YAB3.2	1.91	1.51	1.66	**1.6935**	**1st**	91.01	84.18	88.78	**87.9907**	**4th**
Eg-YAB2.1	2.20	4.15	3.26	**3.2015**	**1st**	96.11	N/A	95.97	**96.0420**	**4th**
Eg-INO.1	N/A	N/A	N/A	**N/A**	**N/A**	N/A	N/A	N/A	**N/A**	**N/A**
Eg-YAB5.1	9.47	7.96	5.05	**7.4944**	**1st**	N/A	91.49	N/A	**91.4929**	**4th**
Eg-CRC.1	N/A	N/A	N/A	**N/A**	**N/A**	N/A	N/A	N/A	**N/A**	**N/A**
KANADI										
Eg-KAN.1	42.52	43.30	39.46	**41.7640**	**2nd**	N/A	N/A	N/A	**N/A**	**N/A**
Eg-KAN.2	79.20	68.52	65.70	**71.1413**	**3rd**	96.24	N/A	N/A	**96.2367**	**4th**
Eg-KAN2/3.1	24.15	21.18	22.25	**22.5264**	**1st**	85.22	99.22	N/A	**92.2215**	**4th**
Eg-KAN2/3.2	70.92	68.22	69.81	**69.6488**	**3rd**	N/A	N/A	93.14	**93.1407**	**4th**
Eg-KAN2/3.3	60.62	57.16	56.91	**58.2289**	**3rd**	88.96	99.04	97.17	**95.0568**	**4th**
Eg-ATS.1	48.89	54.06	51.65	**51.5316**	**3rd**	N/A	N/A	N/A	**N/A**	**N/A**
HD-ZIPIII										
Eg-PHB/PHV.1	10.80	10.24	12.74	**11.2581**	**1st**	5.70	5.41	7.42	**6.1749**	**1st**
Eg-REV.1	21.70	30.83	28.43	**26.9866**	**2nd**	3.73	1.72	2.03	**2.4917**	**1st**
Eg-ATHB8.1	27.64	21.66	22.88	**24.0613**	**1st**	1.45	1.22	1.58	**1.4166**	**1st**
Eg-CNA.1	11.25	12.62	13.30	**12.3897**	**1st**	3.27	2.64	2.33	**2.7479**	**1st**

B.10 Comparison of paralog expression values of eucalyptus leaf polarity genes in leaf and xylem. P-values are presented with significant values ($p \leq 0.05$) underlined. N/A denotes where paralogue expression values could not be compared due to undetectable levels of expression (or division by 0).

Gene family	Paralogous genes compared	p-value (≤0.05)	
		Xylem	Leaf
YABBY	*Eg-AFO*	0.659495712	0.115391604
KANADI	*Eg-KAN*	N/A	0.001205482
	Eg-KAN2/3.1, .2	N/A	0.004247438
	Eg-KAN2/3.1, .3	N/A	0.003671913
	Eg-KAN2/3.2, .3	N/A	0.020491952

B.11 Mean FPKM expression values comparing *E. grandis* and eucalyptus hybrid immature xylem and young leaf tissues (graphed in Fig. 3.4).

Gene family	*Eucalyptus grandis* FPKM values			*Eucalyptus* hybrid FPKM values		
	Gene name	Immature xylem	Young leaf	Contig name	Immature xylem	Young leaf
YABBY	*Eg-AFO/YAB3.2*	0.17±0.06	146.98±21.51	contig_92866	0	96.27
	Eg-YAB2.1	0.06±0.001	93.51±18.38	contig_94705	0	31.43
	Eg-YAB5.1	0.04	49.65±13.41	contig_82502	0	40.24
KANADI	*Eg-KAN2/3.1*	0.08±0.11	17.30±1.44	contig_19775	0	15.17
HD-ZIPIII	*Eg-PHB/PHV.1*	67.29±9.13	34.03±3.55	contig_3301	15.31	21.28
	Eg-REV.1	135.83±27.77	14.09±3.43	contig_22876	56.39	4.21
	Eg-ATHB8.1	188.64±14.40	16.16±2.54	contig_8660	162.51	17.85
	Eg-CNA.1	122.46±8.28	31.05±2.07	contig_2647	116.67	22.44

B.12 Mean FPKM expression values of eucalyptus hybrid (graphed in Fig. 3.5).

	E. grandis homologue	Hybrid contig name	Immature xylem	Xylem	Phloem	Shoot tip	Young leaf	Mature leaf
YABBY	*Eg-AFO/YAB3.2*	contig_82502	0	0	0	74.02	96.27	27.55
	Eg-YAB2.1	contig_94705	0	0	0	18.15	31.43	0
	Eg-YAB5.1	contig_92866	0	0	0	32.29	40.24	8.31
KANADI	*Eg-KAN2/3.1*	contig_19775	0	0	0	26.38	15.17	5.54

	***E. grandis* homologue**	**Hybrid contig name**	**Immature xylem**	**Xylem**	**Phloem**	**Shoot tip**	**Young leaf**	**Mature leaf**
HD-ZIPIII	*Eg-PHB/PHV.1*	contig_ 3301	28.4	15.31	41.28	16.17	21.28	0
	Eg-REV.1	contig_ 22876	47.3	56.39	69.99	10.15	4.21	11.26
	Eg-ATHB8.1	contig_ 8660	229.89	162.51	104.8	14.92	17.85	8.14
	Eg-CNA.1	contig_ 2647	87.96	116.67	55.3	26.32	22.44	25.16

B.13 *Populus trichocarpa* v2.2 gene names are compared to v1.1 names, showing the absence of several genes the in v1.1 version of the *Populus* genome, including *Pt-AFO.2, Pt-YAB2.1, Pt-INO.1, Pt-YAB5.2, Pt-KAN.2, Pt-KAN.3, Pt-KAN2/3.1*, and *Pt-ATS.1* (denoted as N/A in v1.1).

Gene family	**Gene names**	***Populus trichocarpa* gene id**	
		v2.2	**v1.1**
YABBY	*Pt-AFO.1*	POPTR_0014s06210	grail3.0035001101
	Pt-AFO.2	POPTR_0002s14600	N/A
	Pt-YAB2.1	POPTR_0001s22180	N/A
	Pt-YAB2.2	POPTR_0127s00201	gw1.257.2.1
	Pt-YAB2.3	POPTR_0016s06760	gw1.XVI.2137.1
	Pt-YAB3.1	POPTR_0003s11230	grail3.0018017701
	Pt-YAB3.2	POPTR_0001s00240	estExt_Genewise1_v1.C_1270153
	Pt-INO.1	POPTR_0008s19330	N/A
	Pt-INO.2	POPTR_0010s05220	eugene3.00100614
	Pt-YAB5.1	POPTR_0006s06700	grail3.0023002901
	Pt-YAB5.2	POPTR_0018s12990	N/A
	Pt-CRC.1	POPTR_0008s09740	fgenesh4_pg.C_LG_VIII000863
	Pt-CRC.2	POPTR_0010s16410	fgenesh4_pg.C_LG_X001405
KANADI	*Pt-KAN.1*	POPTR_0017s02220	fgenesh4_pg.C_LG_II002170
	Pt-KAN.2	POPTR_0004s08070	N/A
	Pt-KAN.3	POPTR_0015s05340	estExt_fgenesh4_pg.C_1220055
	Pt-KAN.4	POPTR_0012s03900	N/A
	Pt-KAN2/3.1	POPTR_0003s09490	N/A
	Pt-KAN2/3.2	POPTR_0001s02010	eugene3.00290237
	Pt-ATS.1	POPTR_0002s13170	N/A
	Pt-ATS.2	POPTR_0014s03650	gw1.40.547.1
HD-ZIPIII	*Pt-PHB.1*	POPTR_0011s10070	estExt_fgenesh4_pg.C_2360002
	Pt-PHB.2	POPTR_0001s38120	estExt_fgenesh4_pg.C_LG_I2905

Gene family	Gene names	*Populus trichocarpa* gene id	
		v2.2	**v1.1**
HD-ZIPIII	*Pt-HB1.7*	POPTR_0004s22090	estExt_Genewise1_v1.C_660759
	Pt-HB1.8	POPTR_0009s01990	gw1.IX.4748.1
	Pt-HB1.5	POPTR_0018s08110	fgenesh4_pg.C_LG_XVIII000250
	Pt-HB1.6	POPTR_0006s25390	estExt_fgenesh4_pm.C_LG_VI0713
	Pt-ATHB.11	POPTR_0003s04860	estExt_fgenesh4_pg.C_LG_III0436
	Pt-ATHB.12	POPTR_0001s18930	fgenesh4_pm.C_LG_I000560

B.14 Microarray data from (A) *Arabidopsis* (Schmid et al. 2005) and (B) balsam poplar (Wilkins et al. 2009) obtained from *Arabidopsis* eFP Browser (www.bar.utoronto.ca; Winter et al. 2007) and PopGenExpress (http://bar.utoronto.ca/efppop/cgi-bin/efpWeb.cgi; Wilkins et al. 2009), respectively. N/A indicates the genes for which the microarray data was not available.

(A) *Arabidopsis thaliana* transcript quantity				
Gene family	**Gene name**	**Mature leaf 8**	**Young leaf 2**	**Stem, 2nd internode**
YABBY	*AFO*	37.56±2.66	47.38±2.8	1.64±0.77
	YAB2	N/A	N/A	N/A
	YAB3	106.01±9.64	54.65±1.37	7.63±1.93
	INO	9.01±1.06	13.93±2.29	11.94±7.39
	YAB5	61.38±6.57	60±1.84	9.61±3.52
	CRC	0.81±0.28	0.58±0.10	1.01±0.12
KANADI	*KAN*	18.05±0.80	39.9±8.15	27.98±6,62
	KAN2	15.13±5.36	14.96±2.38	41.66±1.38
	KAN3	18.03±1.31	21.46±8.29	24±2.23
	ATS	8.54±1.97	5.4±0.97	10.38±1.78
HD-ZIPIII	*PHB*	59±5.48	44.95±5.35	176.18±5.86
	PHV	95.95±4.35	91.36±15.10	227.81±20.26
	REV	90.81±3.73	43.13±4.44	455.66±7.68
	ATHB8	44.53±6.66	14.56±2.77	187.88±15.64
	CNA	100±9.11	65.08±5.00	698.46±45.41
(B) *Populus balsamifera* transcript quantity				

Gene family	Gene name	Mature leaf	Young leaf 1	Xylem
YABBY	*Pt-AFO.1*	30.21±4.81	760.63±192.69	2.66±0.60
	Pt-AFO.2	N/A	N/A	N/A
	Pt-YAB2.1	N/A	N/A	N/A
	Pt-YAB2.2	48.56±9.92	310.3±57.59	60.43±18.20
	Pt-YAB2.3	114.77±47.27	107.63±86.89	5.73±2.25
	Pt-YAB3.1	72.55±9.88	275.59±68.25	167.36±97.13
	Pt-YAB3.2	N/A	N/A	N/A
	Pt-INO.2	1.76±0.93	8.2±1.95	33.69±5.00
	Pt-INO.1	N/A	N/A	N/A
	Pt-YAB5.1	183.54±22.38	2106.36±723.31	91.96±57.15
	Pt-YAB5.2	N/A	N/A	N/A
	Pt-CRC.1	10.67±2.03	12.63±9.06	27.13±17.30
	Pt-CRC.2	8.57±2.95	82.53±62.48	44±10.69
KANADI	*Pt-KAN.1*	26.11±4.97	83.93±27.73	41.33±29.55
	Pt-KAN.2	N/A	N/A	N/A
	Pt-KAN.3	10.62±3.15	129.43±9.57	113.80±34.99
	Pt-KAN.4	N/A	N/A	N/A
	Pt-KAN2/3.1	N/A	N/A	N/A
	Pt-KAN2/3.2	21.88±2.57	392.43±36.19	115.90±61.77
	Pt-ATS.1	N/A	N/A	N/A
	Pt-ATS.2	153.77±25.91	1469.93±171.01	53.79±21.58
HD-ZIPIII	*Pt-PHB.1*	105.76±6.56	506.73±380.12	970.06±707.74
	Pt-PHB.2	105.76±6.56	506.73±380.12	970.06±707.74
	Pt-HB1.7	87.63±8.81	665.43±104.21	1389.7±160.51
	Pt-HB1.8	87.63±8.81	665.43±104.21	1389.7±160.51
	Pt-HB1.5	4.37±1.39	16.9±9.76	178.86±127.92
	Pt-HB1.6	4.37±1.39	16.9±9.76	178.86±127.92
	Pt-ATHB.11	59.36±25.31	469.96±18.79	3686.19±807.95
	Pt-ATHB.12	49.76±15.18	279.93±66.18	1807.16±232.98

Appendix C : Supplementary data from Chapter 4.

C.1 Sequences of all of the genes used in this study showing primer locations and regions that were used in the final alignments. Available as supplementary data.

C.2 *Cad* alignment used in phylogenetic analysis. Available as supplementary data.

C.3 *Gly* alignment used in phylogenetic analysis. Available as supplementary data.

C.4 ITS alignment used in phylogenetic analysis. Available as supplementary data.

C.5 *Mip* alignment used in phylogenetic analysis. Available as supplementary data.

C.6 *Pcs* alignment used in phylogenetic analysis. Available as supplementary data.

C.7 *Sad* alignment used in phylogenetic analysis. Available as supplementary data.

C.8 Samples used for phylogenetic analysis.

Populus species	**Sample name**	**ITS**	**Gly**	**Cad**	**Pcs**	**Mip**	**Sad**
P. angustifolia *(Tacamahaca)*	11-2-6	x			x		
	11-2-8		x				
	203		x			x	x
P. balsamifera *(Tacamahaca)*	144					x	
	11-1-3	x			x	x	
	11-1-2	x					
	11-1-1	x		x	x		
	CHP10				x		

Populus species	**Sample name**	**ITS**	**Gly**	**Cad**	**Pcs**	**Mip**	**Sad**
P. balsamifera (Tacamahaca)	WHR10		x	x	x	x	x
	NWL13		x	x	x		
	CAR5		x	x	x	x	x
	GPR13				x	x	x
P. deltoides (Aigeiros)	125-3	x	x	x	x		
	125-4		x	x	x		x
	125-5	x		x			
	125-6	x	x	x			
	185		x	x	x	x	
	UGA		x	x	x	x	x
	181		x	x	x	x	
P. fremontii (Aigeiros)	126-1		x	x	x	x	
	186		x	x			
	11-2-2			x			
	11-2-3		x	x	x		
P. grandidentata (Populus)	UGA	x	x	x	x	x	x
	187	x		x		x	
P. guzmantlensis (Populus)	372	x	x		x		
P. heterophylla (Leucoides)	11-2-10			x			
P. mexicana (Abaso)	371	x	x		x	x	x
	370	x	x		x	x	
	376		x		x	x	x
P. tremuloides (Populus)	AUA	x					
	197	x		x	x	x	
	140	x		x			x
	UGA		x	x	x		
	11-2-5	x			x		
	196	x	x				
P. trichocarpa (Tacamahaca)	101-1	x	x			x	x
	Ptr2	x	x		x	x	x
	11-1-5			x			
	11-1-6			x	x		
	Ptr33		x	x		x	x
	Ptr34		x		x		
	QCI		x	x	x	x	x
S. arctica	N/A	x	x				
S. eleagnos	013854-0013-1976	x			x	x	x
S. lapponum	013859-0013-1976			x			
S. reticulata	N/A	x		x			
S. sitchensis	002538-0099-1971	x	x	x	x	x	

Appendix D : Supplementary data from Chapter 5.

D.1 Transcriptome data for xylem tissues comparing black cottonwood (Ptr) and hybrid aspen (Ptmx) expression levels (RPKM). A significant difference in expression levels between two species is determined with p-value < 0.05 (underlined). Bolded genes indicate RPKM > 5 in either species.

Gene id	Gene name	Ptr mean RPKM	Ptmx mean RPKM	Higher expression in:	Ptr-Ptm expression difference	p-value
POPTR_0008s06540	Pt-AE3.1	46.81±7.50	33.40±5.30	Ptr	13.40371142	0.038049554
POPTR_0008s06550	Pt-AE3.2	84.97±15.97	47.38±7.52	Ptr	37.58794523	0.008325602
POPTR_0001s01820	Pt-AE7.1	17.03±6.43	17.00±4.32	Ptr	0.026415973	0.995014291
POPTR_0003s09670	Pt-AE7.2	23.36±5.21	25.98±2.84	Ptm	-2.618820531	0.42611838
POPTR_0014s06210	Pt-AFO.1	0.04±0.01	0.08±0.03	Ptm	-0.039632949	0.111377046
POPTR_0002s14600	Pt-AFO.2	0.01±0.02	0.17±0.07	Ptm	-0.151802971	0.015026512
POPTR_0012s03410	Pt-AGO1.1	56.71±11.31	44.17±4.04	Ptr	12.54420696	0.089301134
POPTR_0015s05550	Pt-AGO1.2	52.02±5.24	48.61±6.84	Ptr	3.406936642	0.507257594
POPTR_0009s00660	Pt-AGO7.1	1.57±0.65	2.49±0.88	Ptm	-0.916631823	0.192321398
POPTR_0010s17100	Pt-AGO7.4	1.87±0.45	2.55±1.11	Ptm	-0.689275795	0.363675292
POPTR_0008s15860	Pt-AGO10.1	28.33±9.04	57.41±12.27	Ptm	-29.08054251	0.018581087
POPTR_0010s09150	Pt-AGO10.2	9.82±4.55	20.82±5.27	Ptr	-11.00401975	0.034292487
POPTR_0013s04090	Pt-AN3.1	9.20±3.59	8.06±2.55	Ptr	1.140568459	0.640911509
POPTR_0019s02320	Pt-AN3.2	14.13±3.14	7.65±1.97	Ptr	6.478104903	0.019600931
POPTR_0009s01700	Pt-ARF4.1	6.54±1.11	7.67±1.02	Ptm	-1.13652908	0.218705045
POPTR_0006s08610	Pt-AS1.1	0.98±0.90	1.20±0.36	Ptm	-0.219184413	0.669319702
POPTR_0004s10250	Pt-AS1.2	0.16±0.09	0.09±0.08	Ptr	0.07519898	0.298684876
POPTR_0017s13950	Pt-AS1.3	1.28±0.64	0.67±0.56	Ptr	0.614627869	0.23461869
POPTR_0010s18460	Pt-AS2.1	0.00	0.05±0.09	Ptm	-0.051425532	0.355125828

Gene id	Gene name	Ptr mean RPKM	Ptmx mean RPKM	Higher expression in:	Ptr-Ptm expression difference	p-value
POPTR_0008s07930	Pt-AS2.2	0.00	0.00	x	0	n/a
POPTR_0003s04860	**Pt-ATHB.11**	**77.57±2.32**	**171.02±14.99**	**Ptm**	**-93.44999349**	**0.000138292**
POPTR_0001s18930	**Pt-ATHB.12**	**143.53±22.47**	**101.77±19.10**	**Ptr**	**41.75813031**	**0.044595917**
POPTR_0002s13170	**Pt-ATS.1**	**0.49±0.32**	**0.04±0.04**	**Ptr**	**0.454825822**	**0.034810733**
POPTR_0014s03650	**Pt-ATS.2**	**0.14±0.18**	**0.49±0.28**	**Ptm**	**-0.345579289**	**0.126504845**
POPTR_0008s09740	Pt-CRC.1	0.00	0.00	x	0	n/a
POPTR_0010s16410	Pt-CRC.2	0.00	0.00	x	0	n/a
POPTR_0006s20310	Pt-DCL4.1	1.78±0.54	1.86±0.36	Ptm	-0.073012364	0.837822465
POPTR_0005s12480	**Pt-DUF59.1**	**35.40±1.78**	**45.91±9.40**	**Ptm**	**-10.5116589**	**0.120833883**
POPTR_0004s04970	**Pt-ETT.1**	**97.62±29.83**	**110.17±18.39**	**Ptm**	**-12.54755858**	**0.522392595**
POPTR_0011s05830	**Pt-ETT.2**	**5.56±0.63**	**3.57±0.61**	**Ptr**	**1.983228772**	**0.008527475**
POPTR_0018s08110	**Pt-HB1.5 (ATHB8)**	**60.69±8.59**	**31.33±2.23**	**Ptr**	**29.36079917**	**0.001086158**
POPTR_0006s25390	**Pt-HB1.6 (ATHB8)**	**86.92±8.19**	**79.40±4.87**	**Ptr**	**7.51945464**	**0.185104016**
POPTR_0004s22090	**Pt-HB1.7 (REV)**	**14.21±2.02**	**82.93±9.87**	**Ptm**	**-68.71481623**	**8.35028E-05**
POPTR_0009s01990	**Pt-HB1.8 (REV)**	**60.20±11.55**	**17.83±4.50**	**Ptr**	**42.36370595**	**0.001012508**
POPTR_0005s19650	**Pt-HYL1.1**	**6.89±0.23**	**5.48±0.84**	**Ptr**	**1.416647203**	**0.039601817**
POPTR_0002s11200	**Pt-HYL1.2**	**4.04±0.94**	**6.57±0.77**	**Ptm**	**-2.528783017**	**0.011181123**
POPTR_0008s19330	Pt-INO.1	0.00	0.07±0.15	Ptm	-0.074917003	0.436588061
POPTR_0010s05220	Pt-INO.2	0.00	0.00	x	0	n/a
POPTR_0017s02220	**Pt-KAN.1**	**0.06±0.06**	**0.56±0.12**	**Ptm**	**-0.496161777**	**0.001538932**
POPTR_0004s08070	**Pt-KAN.2**	**0.12±0.08**	**0.03±0.03**	**Ptr**	**0.085075067**	**0.097622281**
POPTR_0015s05340	**Pt-KAN.3**	**0.43±0.38**	**0.03±0.04**	**Ptr**	**0.397630303**	**0.084073748**
POPTR_0012s03900	Pt-KAN.4	0.60±0.53	0.08±0.04	Ptr	0.520923442	0.099429563
POPTR_0003s09490	**Pt-KAN2/3.1**	**0.37±0.25**	**0.09±0.05**	**Ptr**	**0.273382516**	**0.076898216**
POPTR_0001s02010	**Pt-KAN2/3.2**	**0.06±0.05**	**0.23±0.15**	**Ptm**	**-0.164801428**	**0.130475495**
POPTR_0011s10070	**Pt-PHB.1**	**73.98±13.68**	**93.74±19.41**	**Ptm**	**-19.76623999**	**0.19589451**

Gene id	Gene name	Ptr mean RPKM	Ptmx mean RPKM	Higher expression in:	Ptr-Ptm expression difference	p-value
POPTR_0001s38120	**Pt-PHB.2**	**141.43±10.25**	**52.24±8.27**	**Ptr**	**89.1905362**	**5.15227E-05**
POPTR_0007s11880	**Pt-PGY1.1**	**130.36±25.93**	**63.70±12.32**	**Ptr**	**66.65435783**	**0.005847476**
POPTR_0001s45810	**Pt-PGY2.1**	**92.32±13.39**	**37.40±8.37**	**Ptr**	**54.91260211**	**0.001089584**
POPTR_0011s15170	**Pt-PGY2.2**	**105.18±27.54**	**41.38±7.61**	**Ptr**	**63.79239758**	**0.006159331**
POPTR_0013s13220	**Pt-PGY3.1**	**426.40±76.75**	**279.47±59.15**	**Ptr**	**146.9221837**	**0.03451141**
POPTR_0006s26980	**Pt-RDR6.1**	**12.22±0.92**	**19.96±1.35**	**Ptm**	**-7.732121896**	**0.000381426**
POPTR_0018s01670	**Pt-RDR6.2**	**1.38±0.14**	**0.89±0.27**	**Ptr**	**0.487957008**	**0.03771733**
POPTR_0004s20730	**Pt-SE.1**	**11.51±0.06**	**11.29±0.49**	**Ptr**	**0.220722424**	**0.484522003**
POPTR_0009s16020	**Pt-SE.2**	**16.30±1.21**	**18.45±1.95**	**Ptm**	**-2.147553901**	**0.15829071**
POPTR_0019s00300	**Pt-SGS3.1**	**30.43±5.80**	**38.46±10,30**	**Ptm**	**-8.028220083**	**0.285115821**
POPTR_0001s07410	**Pt-SGS3.2**	**2.14±1.07**	**4.72±2.12**	**Ptm**	**-2.581300985**	**0.115556386**
POPTR_0001s07420	Pt-SGS3.3	0.06±0.06	0.18±0.08	Ptm	-0.118216705	0.086427292
POPTR_0003s18660	Pt-SGS3.4	0.43±0.43	0.03±0.04	Ptr	0.401216656	0.114850575
POPTR_0003s18670	Pt-SGS3.5	0.03±0.03	0.07±0.05	Ptm	-0.038478233	0.296980809
POPTR_0003s18680	Pt-SGS3.6	0.72±0.59	0.07±0.08	Ptr	0.653508411	0.074295656
POPTR_0003s18690	Pt-SGS3.7	0.03±0.03	0.00±0.01	Ptr	0.026825972	0.088075203
POPTR_0003s01530	**Pt-SGS3.8**	**0.42±0.20**	**3.46±2.53**	**Ptm**	**-3.039535443**	**0.098583373**
POPTR_0001s40870	**Pt-SPL4.1**	**0.03±.0.03**	**0.11±0.11**	**Ptm**	**-0.075391682**	**0.316944349**
POPTR_0011s11770	**Pt-SPL4.2**	**0.08±0.02**	**1.45±1.38**	**Ptm**	**-1.369655582**	**0.15374545**
POPTR_0004s04630	**Pt-SPL43.1**	**0.99±0.82**	**0.17±0.12**	**Ptr**	**0.819057373**	**0.097298442**
POPTR_0011s05480	**Pt-SPL43.2**	**2.71±2.45**	**1.20±0.85**	**Ptr**	**1.507554159**	**0.294200767**
POPTR_0016s04890	**Pt-SPL9.1**	**8.14±1.28**	**2.83±0.54**	**Ptr**	**5.304604039**	**0.000614029**
POPTR_0001s22180	**Pt-YAB2.1**	**1.26±0.91**	**1.72±1.15**	**Ptm**	**-0.462726764**	**0.593458195**
POPTR_0127s00201	**Pt-YAB2.2**	**0.00**	**0.04±0.07**	**Ptm**	**-0.036743718**	**0.436588061**
POPTR_0016s06760	**Pt-YAB2.3**	**0.47±0.57**	**0.05±0.10**	**Ptr**	**0.419034932**	**0.194677109**
POPTR_0003s11230	**Pt-YAB3.1**	**0.39±0.03**	**0.04±0.07**	**Ptr**	**0.352893241**	**0.000675462**

Gene id	Gene name	Ptr mean RPKM	Ptmx mean RPKM	Higher expression in:	Ptr-Ptm expression difference	p-value
POPTR_0001s00240	**Pt-YAB3.2**	**0.47±0.26**	**1.06±0.95**	**Ptm**	**-0.588706862**	**0.35492299**
POPTR_0006s06700	**Pt-YAB5.1**	**0.00**	**0.06±0.05**	**Ptm**	**-0.063081471**	**0.084879932**
POPTR_0018s12990	**Pt-YAB5.2**	**0.00**	**0.00**	**x**	**0**	**n/a**
POPTR_0006s26430	Pt-YUC.2	0.01±0.03	0.10±0.15	Ptm	-0.080137873	0.421126976
POPTR_0018s01210	Pt-YUC.1	0.00	0.00	x	0	n/a
POPTR_0006s26000	Pt-YUC2.1	1.22±0.23	2.14±2.02	Ptm	-0.92408915	0.47703667
POPTR_0018s00840	Pt-YUC2.2	0.60±0.23	0.13±0.04	Ptr	0.474012209	0.008746774
POPTR_0003s11710	Pt-ZPR1.1	61.25±3.08	117.11±21.20	Ptm	-55.86249727	0.006870161
POPTR_0001s08220	Pt-ZPR1.2	52.76±6.55	56.41±21.65	Ptm	-3.650098192	0.793158976
POPTR_0002s15060	Pt-ZPR2.1	3.46±0.96	4.90±3.91	Ptm	-1.43909985	0.568877891
POPTR_0014s06690	**Pt-ZPR2.2**	**4.81±2.11**	**0.33±0.49**	**Ptr**	**4.477458025**	**0.008306967**
POPTR_0006s08320	**Pt-ZPR3.1**	**30.45±4.06**	**13.31±5.00**	**Ptr**	**17.1435741**	**0.004759633**
POPTR_0010s24410	Pt-ZPR3.2	0.96±0.55	0.65±0.23	Ptr	0.311734118	0.343131316